UNIVERSITY OF CALIFORNIA

Los Angeles

Process Intensification of Reactive Separation Networks through Large-Scale Optimization

A dissertation submitted in partial satisfaction of the requirements for the degree of Doctor of Philosophy in Chemical Engineering

by

Flavio Eduardo Da Cruz

2018

ABSTRACT OF THE DISSERTATION

Process Intensification of Reactive Separation Networks

through Large-Scale Optimization

by

Flavio Eduardo Da Cruz

Doctor of Philosophy in Chemical Engineering

University of California, Los Angeles, 2018

Professor Vasilios Manousiouthakis, Chair

The chemical industry has historically favored increasingly larger plant designs to lower production costs for bulk chemicals and petrochemical products. The drawbacks of chemical plant scale-up, such as the growth in emissions and the treatment of by-products, have become more relevant due to tighter environmental regulations and more expensive energy resources. Process intensification (PI) is based on the search for radical improvements in chemical processing, substantially decreasing equipment volume, energy consumption or waste formation. Most of the developments in process intensification are based on experimental work, while the development of a systematic approach for process intensification is still in its incipient stages. This dissertation proposes to address this problem by applying the IDEAS framework as a systematic tool for process intensification. The search for intensified chemical processes

featuring nonlinear models is typically pursued through optimal synthesis procedures that stop in one of the possibly many locally optimal solutions. In the IDEAS approach, nonlinear chemical processes are linearized through the induction of an infinite number of states, forming a convex system that has a guaranteed global optimum. IDEAS based formulations generate an infinite linear program (ILP) which has its infimum value approximated by a series of finite-dimensional linear programs of ever increasing size. Reactive distillation systems are natural candidates for process intensification due to the prompt removal of the product from the reaction by the separation process, usually leading to higher conversion, smaller processing systems, and reduced volumetric footprint. The rigorous identification of the intensification limits for ternary reactive distillation systems through the application of the IDEAS framework is presented in chapter 1, featuring the tradeoff between the system's total capacity (a surrogate for size) and its total reactive holdup (a surrogate for catalyst use). In chapter 2, the tradeoff between the network size, captured by the total capacity variable, and the total utility consumption in a ternary reactive distillation system is investigated. The irreversibilities of reactive distillation systems are investigated in chapter 3 through the solution of the minimum entropy generation rate problem, subject to a network capacity constraint. In chapter 4, the potential benefits related to the use of multi-pressure reactive distillation systems are investigated for a ternary azeotropic mixture. The application of the IDEAS approach to higher dimensionality problems, such as the reactive separation of quaternary azeotropic mixtures, is presented in chapter 5, where a column generation procedure is applied to solve the resulting large-scale linear program.

The dissertation of Flavio Eduardo da Cruz is approved.

Jane Pei-Chen Chang

Dante A. Simonetti

Christina Panagio Fragouli

Vasilios Manousiouthakis, Committee Chair

University of California, Los Angeles

2018

DEDICATION

I dedicate this dissertation to my loving wife Rita, who said yes to me once again when I decided to move abroad to pursue my doctoral degree. This work would not be possible without your unconditional support, encouragement, and optimism along this journey. For all that, and for bringing joy to my life every day, you have my eternal love and gratitude.

TABLE OF CONTENTS

LIST OF FIGURES

LIST OF TABLES

ACKNOWLEDGMENTS

Financial support from CAPES – Brazilian Federal Agency for Support and Evaluation of Graduate Education within the Ministry of Education of Brazil, UCLA Graduate Division through the Dissertation Year Fellowship, NSF grant 1650574 "EAGER: Optimal Modular Process Synthesis," and Jorge Paulo Lemann Foundation are gratefully acknowledged.

Chapter 1 is a version of "Process Intensification of Reactive Separator Networks through the IDEAS Conceptual Framework. Computers and Chemical Engineering 2017, 105, 39–55. https://doi.org/10.1016/j.compchemeng.2016.12.006" by da Flavio Eduardo da Cruz & Vasilios Manousiouthakis. Chapter 4 is a version of "Process Intensification of Multi-Pressure Reactive Distillation Networks Using IDEAS," by Flavio Eduardo da Cruz & Vasilios Manousiouthakis, submitted to Industrial & Engineering Chemistry Research in September 2018 (currently in review). Chapters 2, 3 and 5 are in preparation for publication.

My research group members have my gratitude for their support and help during this venture. The invaluable guidance of Mr. Cameron Nimmo, while I was preparing to tackle the challenge of studying and living abroad is gratefully acknowledged. I would like to give a special thanks to Dr. Vasilios Manousiouthakis, for trusting in me to become his student, for the guidance and advise whenever needed, for the support in times of uncertainty, for all the countless insights (and for all the endless discussions), and for showing that friendship and mentorship can walk side by side.

Vita

2005 B.S. in Mechanical Engineering

University of São Paulo, Brazil

Areas of Concentration: "Energy systems and fluid dynamics."

2005-2014 Senior Mechanical Engineer, Supervisor

Promon Engenharia, Brazil

2010 M.S. in Mechanical Engineering

University of São Paulo, Brazil

Thesis: "Exergetic analysis and thermoeconomic evaluation of a hydrogen production unit."

2016 M.S. in Chemical Engineering

University of California, Los Angeles

Thesis: "Simulation of Reforming Reactor Tube: Quantifying Catalyst Pellet's Effectiveness Factor"

Publications and Presentations

da Cruz, F. E., Karagöz, S., Manousiouthakis V. I., Parametric study of porous catalyst for steam methane reforming using a multiscale reactor model. *Ind. Eng. Chem. Res.* (Submitted).

Karagöz, S., **da Cruz, F. E.**, Tsotsis, T. T., and Manousiouthakis, V.I., The multiscale (pellet-reactor scale) membrane reactor (MR) modeling and simulation: Molecular sieve MR for hydrogen production by low-temperature water gas shift reaction." *AIChE Journal* (Submitted).

da Cruz, F. E., Manousiouthakis, V. I., Process intensification of reactive separation networks through the IDEAS conceptual framework. *Comp. & Chem. Eng. Computers & Chemical Engineering*, **2017**, 105: 39-55. http://dx.doi.org/10.1016/j.compchemeng.2016.12.006

da Cruz, F. E., Oliveira Junior, S., Petroleum refinery hydrogen production unit: Exergy and production cost evaluation. *Int. J. of Thermodyn.* **2008**, 11 (4): 187–93. doi:10.5541/ijot.1034000227

da Cruz, F. E., Manousiouthakis, V. I., *Process Intensification of Reactive Separator Networks through the Ideas Conceptual Framework*. Oral presentation in the Computing and Systems Technology Division (CAST) at AIChE Annual Conference. **2017**.

da Cruz, F. E., *Multiscale Processes Intensification and Optimization of Process Systems*. Poster presentation in the Education Division (EDU) at AIChE Annual Conference. **2017**.

Karagöz, S., **da Cruz, F. E.**, Manousiouthakis, V. I., *Numerical Study of Hydrogen Production Via High-Temperature and Low-Temperature Water-Gas Shift Reactors' System: The Multi-Scale (Pellet-Reactor Scale) Modeling Approach and Simulation*. Oral presentation in the Transport and Energy Process Division (TEP) at AIChE Annual Conference. **2017**.

da Cruz, F. E., Karagöz, S., Manousiouthakis, V. I. *Parametric Studies of Steam Methane Reforming Using a Multiscale Reactor Model*. Oral presentation in the Catalysis and Reaction Engineering Division (CRE) at AIChE Annual Conference. **2017**.

da Cruz, F. E., Manousiouthakis, V. I. *Modeling and Simulation of Transport Effects to a Single Reactor Pellet*. Oral presentation in the Transport and Energy Process Division (TEP) at AIChE Annual Conference. **2016**.

da Cruz, F. E., Manousiouthakis, V. I. *Minimization of Entropy Generation in Multi-Pressure Reactive Distillation Networks*. Poster presentation in the Computing and Systems Technology Division (CAST) at AIChE Annual Conference. **2016**.

da Cruz, F. E., Manousiouthakis, V. I. *Energy Consumption Minimization in Multi-Pressure Reactive Distillation Networks*. Poster presentation in the Separations Division (SEP) at AIChE Annual Conference. **2016**.

da Cruz, F. E., *Optimization-Based Quantification of Performance Limits for Process Networks*. Poster presentation in the Education Division (EDU) at AIChE Annual Conference. **2016**.

da Cruz, F. E., Manousiouthakis, V. I. *Synthesis of Azeotropic Multi-Pressure Reactive Distillation Networks Involving Ternary Mixtures*. Oral presentation in the Separations Division (SEP) at AIChE Annual Conference. **2015**.

da Cruz, F. E., Manousiouthakis, V. I. *Synthesis of Azeotropic Reactive Distillation Networks Involving Quaternary Mixtures.* Oral presentation in the Computing and Systems Technology Division (CAST) at AIChE Annual Conference. **2015**.

CHAPTER 1

Process Intensification of Reactive Separator Networks through the IDEAS Conceptual Framework

1.1. Abstract

A method to rigorously identify the performance limits of a reactive separator network is presented in this paper. The quantification of the enhancement potential for a given technology can greatly benefit process intensification studies in the pursuit of radical improvements. The Infinite DimEnsionAl State-Space (IDEAS) conceptual framework is first reviewed and then shown to be capable of assessing the potential for process intensification of reactive separation processes. The IDEAS framework is employed to formulate an infinite linear program (ILP) that can synthesize optimal reactive separation networks, and establish rigorous tradeoffs between total network reactive holdup, and total network capacity. The proposed reactive separation process intensification method is demonstrated on a case study involving the metathesis of 2-pentene through reactive distillation. Significant intensification over prior designs is demonstrated.

1.2. Introduction

Process intensification (PI) is a major focus of current chemical engineering research. The concept encompasses any chemical engineering development that offers drastic improvements in chemical processing, substantially decreasing equipment volume, energy

consumption or waste formation [1,2]. More recently, process intensification was presented as a set of principles that are applicable to a broader spectrum of disciplines [3].

Process synthesis is the invention of chemical process designs to exploit chemical routes at the desired scale, safely, environmentally responsibly, efficiently, and economically in a manner superior to all other possible processes [4]. Often referred as a process intensification example, design of reactive distillation systems has been pursued using process synthesis methods [5]. Nevertheless, most of the developments in process intensification are based on experimental work [6], and pilot plant facilities [7], while the development of a systematic approach for process intensification is still in its incipient stages [8].

Considering this perspective, it is clear that PI can benefit from process synthesis tools that provide systematic approaches for the design and optimization of intensified processes. Moreover, synthesis tools that enable the thorough identification of the performance limit for a particular technology is an indispensable PI development since it would establish metrics to quantitatively evaluate intensified processes.

The Infinite DimEnsionAl State-Space (IDEAS) framework, a systematic approach for process synthesis, is applied in this work as a process intensification tool. IDEAS can rigorously identify the performance limits of a particular technology or combination of technologies, without establishing any a priori design. By finding performance limits on chemical process networks, IDEAS allows the detection of process intensification candidates, the comparison between different intensified approaches, and quantifies the potential for further improvements.

The IDEAS conceptual framework has been successfully applied to either globally optimize or to identify the attainable region of numerous process synthesis problems. Some examples of IDEAS application involve multicomponent mass exchange networks [9], ideal

distillation networks [10,11], separator networks [12], power cycles [13], heat/power integrated distillation networks [14,15], reactive distillation networks [16,17], reactor network attainable region construction [18–27], azeotropic distillation networks [28], reactor networks [29–31], batch reactor networks [32], and process network attainable region [33].

Derived by using simple physical concepts, IDEAS can be potentially applied to design and globally optimize virtually any chemical process. One of the key concepts behind the IDEAS framework can be visualized by considering, as a process operation example, a steady-state CSTR model as shown in Fig.1.1(a) and represented by Eq.(1.1). Usually, the design objective is to find an optimal H (variable) that can deliver a specified output C_i^{OUT} from a known input C_i^{IN} . This formulation is clearly nonlinear since the reaction rate $R_i(T)$ is also a variable.

$$FC_i^{IN} - FC_i^{OUT} + R_i(T)H = 0 \ , \ i = 1,n \quad ; \quad T \in D = \left\{ T \in \mathbb{R} \mid T^{lb} \le T \le T^{ub} \right\} \tag{1.1}$$

In the IDEAS approach, a part of the process output is considered to vary linearly with a part of the process input, when certain variables are considered constant. In the CSTR example, by converting the temperature domain D into a bounded series containing infinite elements, as shown in Eq.(1.2) , it is possible to calculate a unique reaction rate R_i^k for each CSTR according to the elements of the series.

$$FC_i^{IN} - FC_i^{OUT} + R_i^k(T)H = 0 \quad ; \quad T \in D = \left\{ T^k \right\}_{k=1}^{\infty} \wedge \left\{ T \mid T^{lb} \le T \le T^{ub} \right\} \tag{1.2}$$

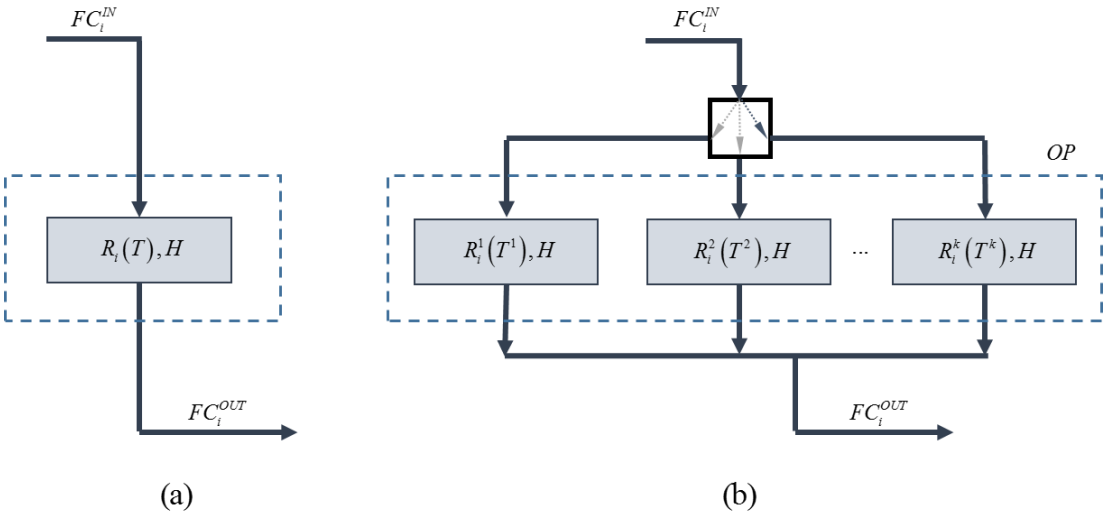

Figure 1.1 - Example of a steady-state CSTR design model: (a) Nonlinear traditional approach, (b) IDEAS linear process operator approach

As a result, IDEAS introduces several standalone units with different characteristics, covering the domain of the respective linearized variable as shown in Fig.1.1(b). The set of standalone units in the IDEAS framework is called process operator (OP). From the process synthesis point of view, considering that the OP set has an infinite number of standalone linear units and each unit can be individually activated by a distribution system, then any possible configuration taken by the standalone nonlinear unit in a synthesis procedure is contained in the IDEAS-OP. Despite the fact that IDEAS contemplates any design configuration obtained from a nonlinear unit, it is easy to verify that the infinite OP maintains its linearity feature for any chemical process.

In the IDEAS framework, all units in the OP can be used to reach the desired process objective. A flow operator structure, the IDEAS distribution network DN, is employed to connect all inlet-outlet possibilities (i.e., process inlets to process units, process inlets to process outlets, process units to process units and process units to process outlets). Considering that the DN operations (mixing, splitting, recycling, and bypass) are linear in the flow variables, the

IDEAS DN-OP representation is linear for any chemical process. The structure of IDEAS guarantees that all possible process flowsheets are taken into account in the network synthesis problem for an *a priori* given set of phenomena.

Due to IDEAS' innovative proposition for the process operations, which domain and range are considered to lie in an infinite (rather than finite) dimensional space, infinite dimensional linear programs (ILP) can be formulated for the synthesis of optimal process networks. In fact, since it is not possible to solve an ILP, its solution is approximated arbitrarily close by finite dimensional linear programs (LP) of ever-increasing size. The sequence formed by the LP optimal solutions converges to the global optimal solution of the ILP.

Even though the application of the IDEAS framework can lead to large LPs, in practice, IDEAS can generate very impressive results with relatively small LPs. Additionally, IDEAS features increase the possibility of finding a breakthrough in process synthesis. In this paper, the IDEAS framework is applied as a systematic design tool for reactive separation process intensification seeking minimum reactive holdup and minimum total capacity.

1.3. Mathematical formulation

1.3.1. Reactive flash separator model

The focus of this work is the synthesis of networks of reactive flash separators. In the work developed by Burri and Manousiouthakis [16], reactive flash separators were employed for the systematic synthesis of reactive distillation networks. Other models have also been proposed to design and optimize reactive distillation systems. Procedures based on geometrical approaches, such as the residue curve maps and the fixed point method have been heavily

utilized to attack the problem [34–43]. In addition to the graphical approach, optimization-based methods using mixed-integer nonlinear programming (MINPL) formulations [44–51] or infinite linear programming (ILP) formulations [16] have also contributed to the advancement of the reactive distillation process synthesis.

Focused on process intensification concepts, in this work we present a series of improvements in the general approach presented by Burri and Manousiouthakis [16] for the systematic synthesis of reactive distillation networks. In this improved model, an isothermal, isobaric, reactive flash separator is considered, as shown in Fig.1.2. The reactive flash separator's vapor and liquid exit streams are considered to be in phase equilibrium with one another, and reactions may occur in the liquid phase, depending on the reactive volume H (the reactive holdup) of the flash separator. In addition, a capacity variable C, associated with the total liquid holdup, is also considered.

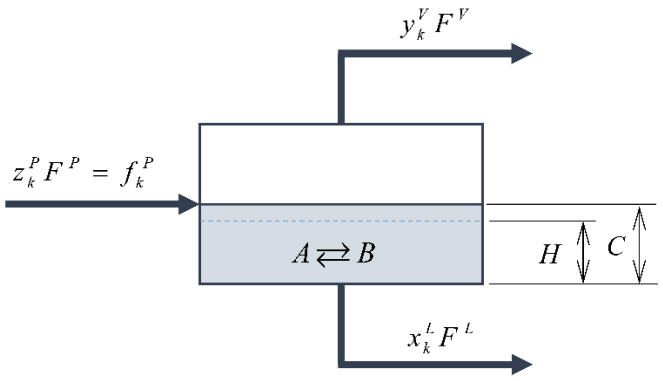

Figure 1.2 - Representation of the reactive flash separator

This approach gives to the reactive flash the ability to account for several phenomena that can act together or in isolation, depending on the needs of the synthesis process. A fully operational reactive flash will simultaneously act as both a reactor and VLE separator. Moreover,

if the reactive holdup is zero, the process acts only as a VLE flash separator; and if no separation takes place, the process assumes the behavior of an isolated CSTR reactor, with only one liquid flow as output. The component balance formulation for the reactive flash separator model is shown in Eq.(1.3):

$$f_k^P + R_k\left(\left\{x_j^L\right\}_{j=1}^n, T, P\right)H - x_k^L F^L - y_k^V F^V = 0 \qquad ; \qquad \forall k = 1,...,n \tag{1.3}$$

The general formulation for the phase equilibrium condition of each k^{th}-component in the mixture uses the Gamma-Phi model to relate the liquid molar fraction x_k^L with the correspondent vapor molar fraction y_k^V inside the reactive flash separator, as shown in Eq.(1.4):

$$y_k^V \phi_k\left(\left\{y_l^V\right\}_{l=1}^n, T, P\right)P = x_k^L \gamma_k\left(\left\{x_l^L\right\}_{l=1}^n, T\right)P_k^{sat}(T) \qquad \forall k = 1,...,n \tag{1.4}$$

The k^{th}-component's generation rate R_k in the reactive flash is usually given by a kinetic rate expression in the form of Eq.(1.5), although other rate forms are also possible.

$$R_k = k_f(T)\left(\prod_{reactants} a_r\left(\gamma_r, x_r\right)^{\nu_r} - \frac{1}{K_{eq}(T)}\prod_{products} a_p\left(\gamma_p, x_p\right)^{\nu_p}\right) \tag{1.5}$$

The species i activity in a multicomponent mixture is related to the activity coefficient in the liquid phase and the liquid molar fraction for the respective component as shown in Eq.(1.6).

$$a_i = \gamma_i\left(\left\{x_l^L\right\}_{l=1}^n, T\right)x_i \tag{1.6}$$

In order to solve the vapor-liquid equilibrium model shown in Eq. (1.4), a variety of thermodynamic models can be utilized to describe the behavior of the fugacity coefficient function $\phi_k\left(\left\{y_l^V\right\}_{l=1}^n, T, P\right)$, the activity coefficient function $\gamma_k\left(\left\{x_l^L\right\}_{l=1}^n, T\right)$ and the saturated pressure $P_k^{sat}(T)$ for the k^{th}-component in the mixture. Since vapor-liquid equilibrium is assumed in the reactive flash and considering ideal gas behavior, for each specified composition in the liquid output the specified thermodynamic models can be iteratively calculated for different temperatures until the vapor fractions sum up to unity. This procedure was successfully applied by Burri and Manousiouthakis [16] and by Ghougassian and Manousiouthakis [28], in which the Wilson and the Antoine equation were used to express the components' non-ideal liquid activity coefficients and partial pressures respectively. Since the selection of these models depends on the information available, which can vary from each case, the models used will be presented in the application example.

In the IDEAS ILP formulation, an infinite number of the aforementioned reactive flash separators are presented in the process operator (OP). The ILP formulation is presented in the next section.

1.3.2. IDEAS ILP for the reactive distillation synthesis problem

In order to consider all possible flowsheets for the reactive flash separator network, the process operator OP is interfaced with a distribution network (DN) where all stream splitting, mixing and pressure adjustment occurs. Fig. 1.3 shows the resulting IDEAS framework for the reactive flash separator synthesis problem.

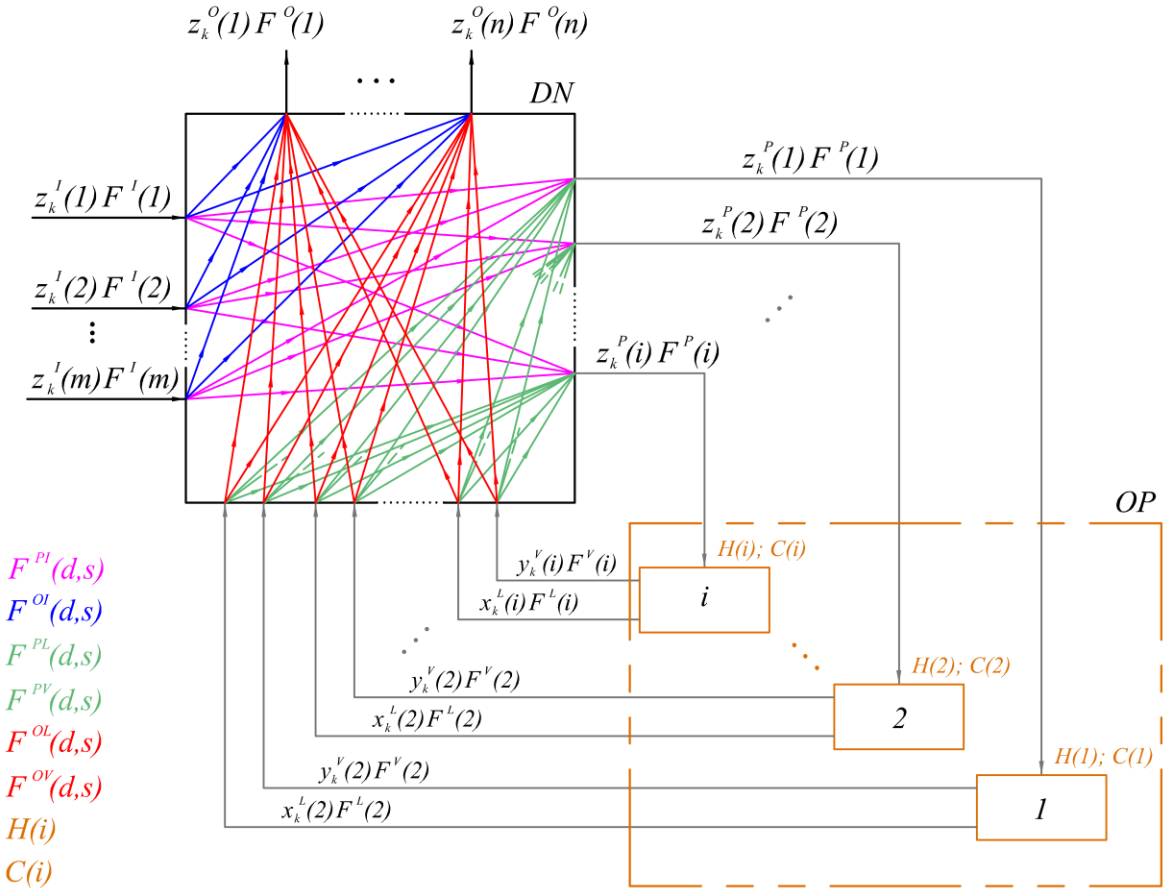

Figure 1.3 - IDEAS representation for a reactive flash separator network.

Each of the cross-flow streams in the DN is characterized by a flow rate variable, which has fixed origin molar fraction conditions. The flow variables are identified by a superscript that indicates their destination and source respectively: the DN inlet is identified as I, the DN outlet as O, the OP inlet as P, the liquid and vapor outputs from the OP as L and V respectively. The flow variables also feature indices designating the destination-source pair structure. The reactive holdups and the capacity are both variables associated with the elements of the OP.

Several infinite LP formulations can be derived using the IDEAS framework. In order to simplify the application on the case study, a general ILP formulation is developed can be modified for any specific case. A generic linear objective function is proposed at this point as

$$c^T F \tag{1.7}$$

where the vector F includes all flows of the DN, the inlet flows, the reactive holdups for the reactive flashes and their respective capacity. The above objective function can be used to realize a wide array of objectives, through appropriate selection of the elements of the cost vector c^T.

The development of the constraints for the ILP general formulation uses mass and component balances on the DN, and the proposed reactive flash separator model for the OP. For each inlet flow $F^I(j)$ associated with one of the M inlets of the DN, a splitting balance is written as shown in Eq.(1.8).

$$F^I(j) - \sum_{i=1}^{N} F^{OI}(i,j) - \sum_{i=1}^{\infty} F^{PI}(i,j) = 0 \quad ; \quad \forall j = 1,...,M \tag{1.8}$$

For each outlet flow $F^O(i)$ leaving the DN from one of its N outlets, a mixing balance as shown in Eq.(1.9) is considered.

$$F^O(i) - \sum_{j=1}^{M} F^{OI}(i,j) - \sum_{j=1}^{\infty} F^{OL}(i,j) - \sum_{j=1}^{\infty} F^{OV}(i,j) = 0 \quad ; \quad \forall i = 1,...,N \tag{1.9}$$

The component flow $f_k^P(i)$ that feeds the i^{th} reactive flash separator can be considered as the sum of component flows feeding that specific mixing point of the DN (component balance).

$$f_k^P(i) - \sum_{j=1}^{M} z_k^I(j) F^{PI}(i,j) - \sum_{j=1}^{\infty} x_k^L(j) F^{PL}(i,j) - \sum_{j=1}^{\infty} y_k^V(j) F^{PV}(i,j) = 0 \qquad \forall i = 1,...,\infty \ ; \ \forall k = 1,...,n \tag{1.10}$$

Thus, the total mass flow in this mixing node is represented by Eq.(1.11) below.

$$F^P(i) - \sum_{j=1}^{M} F^{PI}(i,j) - \sum_{j=1}^{\infty} F^{PL}(i,j) - \sum_{j=1}^{\infty} F^{PV}(i,j) = 0 \quad ; \quad \forall i = 1,...,\infty \tag{1.11}$$

For each $F^L(j)$ liquid and $F^V(j)$ vapor input flow entering the DN's after being processed in the OP, a splitting balance is written as:

$$F^L(j) - \sum_{i=1}^{N} F^{OL}(i,j) - \sum_{i=1}^{\infty} F^{PL}(i,j) = 0 \quad ; \quad \forall j = 1,...,\infty \tag{1.12}$$

$$F^V(j) - \sum_{i=1}^{N} F^{OV}(i,j) - \sum_{i=1}^{\infty} F^{PV}(i,j) = 0 \quad ; \quad \forall j = 1,...,\infty \tag{1.13}$$

The final products from the reactive distillation process can be found in the DN outlets. Lower and upper bounds constraints are introduced on each of the N flow variables $F^O(i)$ as design parameters. The total balance for each flow exiting the DN is shown in Eq.(1.14).

$$\left(F^O(i)\right)^l \le \sum_{j=1}^{M} F^{OI}(i,j) + \sum_{j=1}^{\infty} F^{OL}(i,j) + \sum_{j=1}^{\infty} F^{OV}(i,j) \le \left(F^O(i)\right)^u \quad ; \quad \forall i = 1,...,N \tag{1.14}$$

Equations (1.14) can also be expressed by two independent as shown below:

$$\left[\sum_{j=1}^{M} F^{OI}(i,j) + \sum_{j=1}^{\infty} F^{OL}(i,j) + \sum_{j=1}^{\infty} F^{OV}(i,j)\right] - \left(F^O(i)\right)^l \ge 0 \quad ; \quad \forall i = 1,...,N \tag{1.15}$$

$$\left[\sum_{j=1}^{M} F^{OI}(i,j) + \sum_{j=1}^{\infty} F^{OL}(i,j) + \sum_{j=1}^{\infty} F^{OV}(i,j)\right] - \left(F^O(i)\right)^u \le 0 \quad ; \quad \forall i = 1,...,N \tag{1.16}$$

The component balance at the DN's outputs, including upper and lower bounds for the product's molar fractions are represented by Eq.(1.17).

$$\left(z_k^O(i)\right)^l F^O(i) \le \left\{ \begin{array}{l} \sum_{j=1}^{M} z_k^I(j) F^{OI}(i,j) \\ + \sum_{j=1}^{\infty} x_k^L(j) F^{OL}(i,j) \\ + \sum_{j=1}^{\infty} y_k^V(j) F^{OV}(i,j) \end{array} \right\} \le \left(z_k^O(i)\right)^u F^O(i) \quad ; \quad \begin{array}{l} \forall i = 1,...,N \\ \forall k = 1,...,n \end{array} \tag{1.17}$$

Finally, the balances for the reactive flash separators in the OP are expressed as shown in Eq.(1.18).

$$f_k^P(i) + R_k(i) H(i) - x_k^L(i) F^L(i) - y_k^V(i) F^V(i) = 0 \quad ; \quad \begin{array}{l} \forall i = 1,...,\infty \\ \forall k = 1,...,n \end{array} \tag{1.18}$$

A minimum residence time τ is proposed for the feasible reactive flash separators in the network. The capacity of each reactive flash in the OP is determined by either the reactive holdup, Eq.(1.19), or the residence time times the reactive flash inlet flow, Eq.(1.20), whichever is greater.

$$C(i) \ge H(i) \quad ; \quad \forall i = 1,...,\infty \tag{1.19}$$

$$C(i) \ge \tau F^P(i) \quad ; \quad \forall i = 1,...,\infty \tag{1.20}$$

By substituting Eq.(1.11) in Eq.(1.20), the capacity is then calculated as follows:

$$C(i) \ge \tau \left[\sum_{j=1}^{M} F^{PI}(i,j) + \sum_{j=1}^{\infty} F^{PL}(i,j) + \sum_{j=1}^{\infty} F^{PV}(i,j) \right] \quad ; \quad \forall i = 1,...,\infty \tag{1.21}$$

The number of variables can be reduced by substituting Eq.(1.8) to Eq.(1.10) in Eq.(1.18) :

$$
\begin{aligned}
& R_k(i)H(i) - x_k^L(i)\left[\sum_{j=1}^{N} F^{OL}(j,i) + \sum_{j=1}^{\infty} F^{PL}(j,i)\right] \\
& \quad - y_k^V(i)\left[\sum_{j=1}^{N} F^{OV}(j,i) + \sum_{j=1}^{\infty} F^{PV}(j,i)\right] + \sum_{j=1}^{M} z_k^I(j) F^{PI}(i,j) \quad ; \quad \begin{matrix} \forall i = 1,\ldots,\infty \\ \forall k = 1,\ldots,n \end{matrix} \\
& \quad + \sum_{j=1}^{\infty} x_k^L(j) F^{PL}(i,j) + \sum_{j=1}^{\infty} y_k^V(j) F^{PV}(i,j) = 0
\end{aligned}
\tag{1.22}
$$

From Eq.(1.22), self-recycling flows are naturally eliminated from the system. This fact can lead to further simplifications as shown in Eq.(1.23):

$$
\begin{aligned}
& R_k(i)H(i) + \sum_{j=1}^{M} z_k^I(j) F^{PI}(i,j) \\
& - \sum_{j=1}^{N} x_k^L(i) F^{OL}(j,i) - \sum_{j=1}^{N} y_k^V(i) F^{OV}(j,i) \\
& \quad + \sum_{\substack{j=1 \\ j\neq i}}^{\infty} \left[x_k^L(j) F^{PL}(i,j) - x_k^L(i) F^{PL}(j,i) \right] \quad ; \quad \begin{matrix} \forall i = 1,\ldots,\infty \\ \forall k = 1,\ldots,n \end{matrix} \\
& \quad + \sum_{\substack{j=1 \\ j\neq i}}^{\infty} \left[y_k^V(j) F^{PV}(i,j) - y_k^V(i) F^{PV}(j,i) \right] = 0
\end{aligned}
\tag{1.23}
$$

Some variables in the component outlet bounds equations can be eliminated substituting Eq. (1.9) in Eq.(1.17):

$$
\left(z_k^O(i)\right)^l \begin{bmatrix} \sum_{j=1}^{M} F^{OI}(i,j) \\ + \sum_{j=1}^{\infty} F^{OL}(i,j) \\ + \sum_{j=1}^{\infty} F^{OV}(i,j) \end{bmatrix} \leq \begin{bmatrix} \sum_{j=1}^{M} z_k^I(j) F^{OI}(i,j) \\ + \sum_{j=1}^{\infty} x_k^L(j) F^{OL}(i,j) \\ + \sum_{j=1}^{\infty} y_k^V(j) F^{OV}(i,j) \end{bmatrix} \leq \left(z_k^O(i)\right)^u \begin{bmatrix} \sum_{j=1}^{M} F^{OI}(i,j) \\ + \sum_{j=1}^{\infty} F^{OL}(i,j) \\ + \sum_{j=1}^{\infty} F^{OV}(i,j) \end{bmatrix} ; \begin{matrix} \forall i = 1,\ldots,N \\ \forall k = 1,\ldots,n \end{matrix}
\tag{1.24}
$$

Moreover, Eq.(1.24) can then be split into two inequalities:

$$\begin{aligned}
&\sum_{j=1}^{M}\left[\left(\left(z_k^O(i)\right)^l - z_k^I(j)\right)F^{OI}(i,j)\right] \\
&+\sum_{j=1}^{\infty}\left[\left(\left(z_k^O(i)\right)^l - x_k^L(j)\right)F^{OL}(i,j)\right] \qquad ; \quad \begin{matrix}\forall i=1,...,N \\ \forall k=1,...,n\end{matrix} \\
&+\sum_{j=1}^{\infty}\left[\left(\left(z_k^O(i)\right)^l - y_k^V(j)\right)F^{OV}(i,j)\right] \le 0
\end{aligned} \tag{1.25}$$

$$\begin{aligned}
&\sum_{j=1}^{M}\left[\left(\left(z_k^O(i)\right)^u - z_k^I(j)\right)F^{OI}(i,j)\right] \\
&+\sum_{j=1}^{\infty}\left[\left(\left(z_k^O(i)\right)^u - x_k^L(j)\right)F^{OL}(i,j)\right] \qquad ; \quad \begin{matrix}\forall i=1,...,N \\ \forall k=1,...,n\end{matrix} \\
&+\sum_{j=1}^{\infty}\left[\left(\left(z_k^O(i)\right)^u - y_k^V(j)\right)F^{OV}(i,j)\right] \ge 0
\end{aligned} \tag{1.26}$$

In order to make it easier to calculate and restrict the total size of the network, a total capacity constraint with upper bound C^{ub} was modeled. This constraint is used in the intensification procedure to enable the search for the smallest feasible network size for the specified problem and are presented in Eq.(1.27).

$$\sum_{i=1}^{\infty} C(i) \le C^{ub} \tag{1.27}$$

The final general ILP formulation for the reactive distillation network synthesis has a general objective function as showed in Eq. (1.7) subject to the constraints represented by Eqs. (1.8), (1.15), (1.16), (1.19), (1.21), (1.23), (1.25), (1.26) and (1.27), summarized below:

$$\nu \triangleq \inf \; c^T F$$

s.t.

$$F^I(j) - \sum_{i=1}^{N} F^{OI}(i,j) - \sum_{i=1}^{\infty} F^{PI}(i,j) = 0 \qquad \forall j = 1,...,M$$

$$\left[\sum_{j=1}^{M} F^{OI}(i,j)+\sum_{j=1}^{\infty} F^{OL}(i,j)+\sum_{j=1}^{\infty} F^{OV}(i,j)\right]-\left(F^{O}(i)\right)^{l}\geq 0 \qquad \forall i=1,...,N$$

$$\left[\sum_{j=1}^{M} F^{OI}(i,j)+\sum_{j=1}^{\infty} F^{OL}(i,j)+\sum_{j=1}^{\infty} F^{OV}(i,j)\right]-\left(F^{O}(i)\right)^{u}\leq 0 \qquad \forall i=1,...,N$$

$$C(i)\geq H(i) \qquad \forall i=1,...,\infty$$

$$C(i)\geq \tau\left[\sum_{j=1}^{M} F^{PI}(i,j)+\sum_{j=1}^{\infty} F^{PL}(i,j)+\sum_{j=1}^{\infty} F^{PV}(i,j)\right] \qquad \forall i=1,...,\infty$$

$$R_k(i)H(i)+\sum_{j=1}^{M} z_k^I(j)F^{PI}(i,j)-\sum_{j=1}^{N} x_k^L(i)F^{OL}(j,i)-\sum_{j=1}^{N} y_k^V(i)F^{OV}(j,i)+$$
$$+\sum_{\substack{j=1\\ j\neq i}}^{\infty}\left[x_k^L(j)F^{PL}(i,j)-x_k^L(i)F^{PL}(j,i)\right]+\sum_{\substack{j=1\\ j\neq i}}^{\infty}\left[y_k^V(j)F^{PV}(i,j)-y_k^V(i)F^{PV}(j,i)\right]=0 \qquad \forall i=1,...,\infty \quad \forall k=1,...,n$$

$$\sum_{j=1}^{M}\left[\left(\left(z_k^O(i)\right)^{l}-z_k^I(j)\right)F^{OI}(i,j)\right]+\sum_{j=1}^{\infty}\left[\left(\left(z_k^O(i)\right)^{l}-x_k^L(j)\right)F^{OL}(i,j)\right]+$$
$$+\sum_{j=1}^{\infty}\left[\left(\left(z_k^O(i)\right)^{l}-y_k^V(j)\right)F^{OV}(i,j)\right]\leq 0 \qquad \forall i=1,...,N \quad \forall k=1,...,n$$

$$\sum_{j=1}^{M}\left[\left(\left(z_k^O(i)\right)^{u}-z_k^I(j)\right)F^{OI}(i,j)\right]+\sum_{j=1}^{\infty}\left[\left(\left(z_k^O(i)\right)^{u}-x_k^L(j)\right)F^{OL}(i,j)\right]$$
$$+\sum_{j=1}^{\infty}\left[\left(\left(z_k^O(i)\right)^{u}-y_k^V(j)\right)F^{OV}(i,j)\right]\geq 0 \qquad \forall i=1,...,N \quad \forall k=1,...,n$$

$$\sum_{i=1}^{\infty} C(i)\leq C^{ub}$$

$$F^I\geq 0\,;F^O\geq 0\,;F^{OI}\geq 0\,;F^{PI}\geq 0\,;F^{OL}\geq 0\,;F^{OV}\geq 0\,;F^{PL}\geq 0\,;F^{PV}\geq 0\,;H\geq 0\,;C\geq 0$$

1.3.3. ILP infimum approximation by finite LPs

An infinite dimensional linear program cannot be explicitly solved. However, its solution can be approximated by a series of finite linear programs of increasing size, whose sequence of optimum values converges to the infinite dimensional problem's infimum. In particular, instead

of an infinite number, consider a finite set containing G of reactive flash separators in the OP. Consequently, the aforementioned IDEAS infinite LP formulation becomes a finite LP, which is a convex problem and can be solved by any LP solver.

Considering that the finite LP can now be solved η times using an ever-increasing number G of reactive flash separators, i.e. $G(1) < G(2) < ... < G(\eta)$, the resulting finite linear programs form a non-increasing sequence of optimal values $\nu(1) > \nu(2) > ... > \nu(\eta)$, which converges to the infimum of the ILP when $\eta \to \infty$. This evolution of the optimal solution is shown in the case study.

1.4. Case study: Olefin metathesis

1.4.1. Thermodynamic data and problem specifications

In this section, the proposed IDEAS framework formulation is applied in the design of an intensified reactive distillation network for the metathesis of 2-pentene to form 2-butene and 3-hexene as shown in Eq.(1.28).

$$2C_5H_{10} \rightleftarrows C_4H_8 + C_6H_{12} \tag{1.28}$$

Metathesis reactions are important for rebalancing the light olefins in both catalytic and steam cracking. The interest in applying reactive distillation systems on the metathesis of 2-pentene is reflected in the recent literature [37,39,46,49,51–54].

Considering 2-pentene as the reference component, the temperature dependent rate expression is given by Eq.(1.29) [39]:

$$R = k_f \left(a_{C_5H_{10}}^2 - \frac{a_{C_4H_8}\, a_{C_6H_{12}}}{K_{eq}} \right) \tag{1.29}$$

The reaction equilibrium constant K_{eq} and the kinetic rate constant k_f $\left(h^{-1}\right)$ are shown in Eq.(1.30) and Eq.(1.31) respectively.

$$K_{eq} = 0.25 \tag{1.30}$$

$$k_f = 1.0661 \times 10^5 \; e^{\left(-3321.2/T(K)\right)} \tag{1.31}$$

This system is a candidate for reactive distillation because butane is the low boiling component, whose removal from the liquid reacting mixture as vapor favors conversion since it is readily separated away from the reactive zone. This reaction occurs at atmospheric pressure and has negligible heat of reaction. Moreover, since this system shows ideal vapor-liquid equilibrium, both the fugacity $\phi_k\left(\left\{y_l^V\right\}_{l=1}^n, T, P\right)$ and the activity $\gamma_k\left(\left\{x_l^L\right\}_{l=1}^n, T\right)$ coefficient functions showed in Eq.(1.4) are equal the unity and Raoult's law is assumed. In addition, the species activities in Eq.(1.29) take the values of the respective molar fractions. The saturated pressure of the mixture is calculated by using Antoine's equation, the coefficients of which can be found in Table 1.1 for T in K and P in Pa. Thus, for a fixed operational pressure P and for the specified liquid outlet composition of each i reactive flash separator, the respective bubble point temperature, reaction rate, and vapor outlet composition is iteratively changing $T(i)$ in Eq.(1.32) until the condition specified in Eq.(1.35) is reached.

$$\ln P_k^{sat}(i) = A_{1,k} + \frac{A_{2,k}}{\left(T(i) + A_{3,k}\right)} \quad ; \quad \forall k = C_5H_{10},\, C_8H_8,\, C_6H_{12} \tag{1.32}$$

$$y_k^V(i) = \frac{x_k^L(i)\; P_k^{sat}\left(T(i)\right)}{P} \quad ; \quad \forall k = C_5H_{10},\, C_8H_8,\, C_6H_{12} \tag{1.33}$$

$$R(i) = 1.0661 \times 10^5 \; e^{\left(-3321.2/T(i)\right)} \left[\left(x_{C_5H_{10}}(i)\right)^2 - \frac{x_{C_4H_8}(i)\; x_{C_6H_{12}}(i)}{0.25} \right] \tag{1.34}$$

$$y_{C_5H_{10}}^V(i) + y_{C_4H_8}^V(i) + y_{C_6H_{12}}^V(i) - 1 = 0 \tag{1.35}$$

Table 1.1. Antoine coefficients for 2-butene, 2-pentene, 3-hexene[37].

	$k = C_4H_8$	$k = C_5H_{10}$	$k = C_6H_{12}$
$A_{1,k}$	20.6909	20.723	20.7312
$A_{2,k}$	−2202.188	−2462.02	−2680.52
$A_{3,k}$	−36.578	−42.391	−48.401

In order to perform the reactive distillation process, the distribution network of IDEAS is set to have one inlet stream, containing pure pentene, and two outlet streams according to the specifications for the final products as shown in Table 1.2.

Table 1.2. Specifications for the 2-pentene metathesis problem example.

Feed Flow	100
Outlet Flow 1 (Distillate) (kmol/h)	50
Outlet Flow 2 (Bottom) (kmol/h)	50
Residence Time (s)	60
Operating pressure (bar)	1
Inlet molar fractions	
C4H8	0.0000
C5H10	1.0000
C6H12	0.0000
Purity target (lower - upper bounds)	
Outlet Flow 1	
C4H8	0.9800 - 1.0000
C5H10	0.0000 - 0.2000
C6H12	0.0000 - 0.2000
Outlet Flow 2	
C4H8	0.0000 - 0.2000
C5H10	0.0000 - 0.2000
C6H12	0.9800 - 1.0000

1.4.2. Objective function

This work focuses on reactive separation systems, quantifying rigorous tradeoffs between the network's total reactive holdup and its total capacity. In doing so it can assess what is the potential for process intensification compared to designs proposed in the literature. The tradeoff is quantified rigorously by repeatedly minimizing the reactive holdup (objective function) while constraining the system's total capacity to be lower than an ever decreasing sequence of upper bounds C^{ub}, Eq.(1.27). The total reactive holdup is a surrogate for capital costs associated with reactors, in particular the amount of catalyst used to carry out the reaction [55,56]. The system's total capacity is a surrogate for capital costs associated with vessels (e.g. flashes), and is also a surrogate for operating costs, as it is proportional to the network's total flowrate, which in turn is a surrogate for the reactive separation system's energy consumption, as higher energy consumption results in higher material flows within the network [55,56].

The resulting IDEAS' finite LP formulation is shown in Eq.(1.36).

$$\begin{aligned} &\min \sum_{i=1}^{G} H(i) \\ &\text{s.t.} \\ &\text{Eqs. (8), (15), (16), (19), (21), (23), (25), (26) and (27)} \\ &\text{All variables} \geq 0 \end{aligned} \tag{1.36}$$

The LP problem in Eq.(1.36) is solved several times with an ever smaller value for the capacity upper bound until it reaches the feasibility limit, which allows the identification of the minimum capacity needed to deliver the desired purity specifications for the reactive distillation network.

1.4.3. Discretization strategy and IDEAS convergence

To generate the set of reactive flash separators, establishing the IDEAS OP for the finite LP problem, the ternary mixture's liquid composition (molar fraction) domain is discretized.

The impact of a non-uniform discretization in the generation of the IDEAS OP is investigated in this work. For a three-component system, such as the metathesis of 2-pentene, the liquid molar fraction domain can be represented by a traditional triangular diagram, where each vertex represents a pure substance and the sum of the species molar fractions is equal to unity, for any point inside the triangle. The ternary mixture's liquid molar fraction domain was divided into three regions as shown in Fig.1.4. Different discretization steps are allowed in each of the proposed regions, which edges specified by the molar fractions α and β.

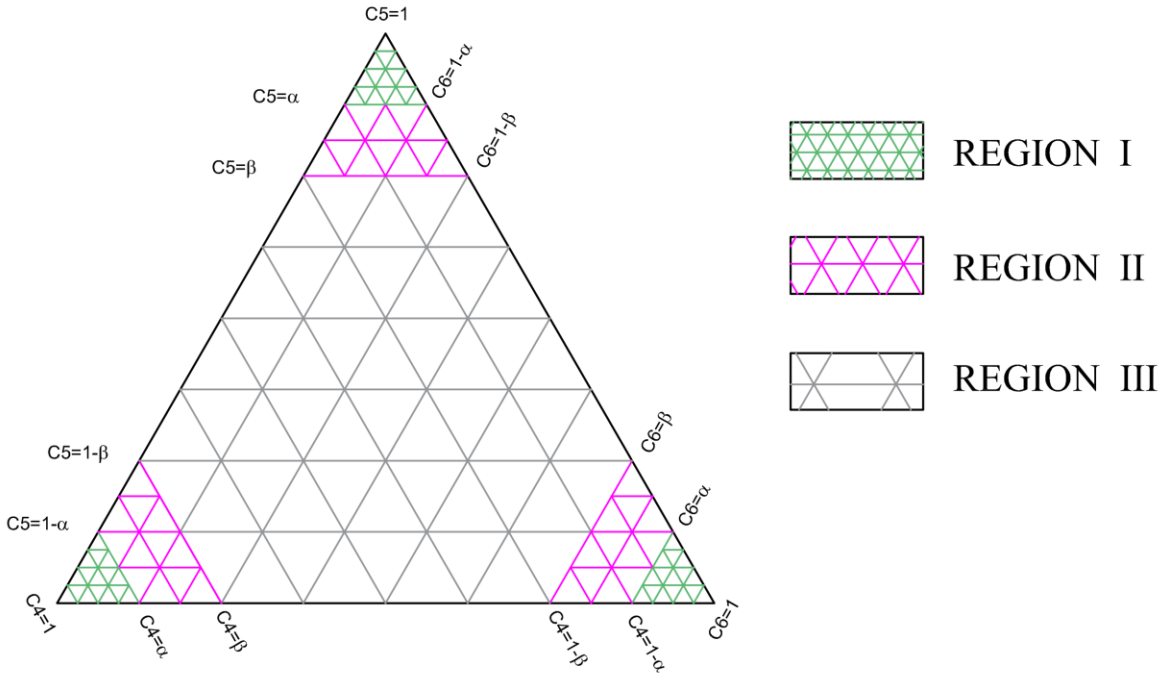

Figure 1.4 - Discretization of ternary mixture's liquid molar fraction domain.

This procedure allows the generation of more reactive flash separators in regions where the separation is more difficult, such as close to the high purity points, controlling the growth of the cardinality G of the universe of considered reactive flash separators. The minimization of the total reactive holdup H was performed for a variety of discretization steps, as shown in Table 1.3. Results were obtained for $\alpha = 0.875$ and $\beta = 0.75$ as the region edges, and minimum purity of 87.5% for both butane and hexene to facilitate convergence.

Table 1.3. Optimal total reactive holdup (87.5% purity) per discretized set in regions I, II and III.

Discretized step size			Optimum total reactive holdup
Region I	Region II	Region III	
1/8	1/8	1/8	Infeasible
1/16	1/8	1/8	Infeasible
1/32	1/8	1/8	Infeasible
1/64	1/8	1/8	596.74
1/128	1/8	1/8	378.66
1/16	1/16	1/8	416.99
1/32	1/16	1/8	394.15
1/64	1/16	1/8	381.46
1/128	1/16	1/8	376.79
1/16	1/16	1/16	65.44
1/32	1/16	1/16	61.6
1/64	1/16	1/16	42.24
1/128	1/16	1/16	39.64
1/32	1/32	1/16	48.31
1/64	1/32	1/16	42.24
1/128	1/32	1/16	39.64
1/32	1/32	1/32	48.31
1/64	1/32	1/32	42.24
1/128	1/32	1/32	39.64
1/64	1/64	1/16	42.24
1/128	1/64	1/16	39.64
1/64	1/64	1/32	42.24
1/128	1/64	1/32	39.64

This assessment reveals that, for this minimization problem, the optimal value depends strongly on the discretization of region I, which is related to the set of reactive flash separators used to obtain each of the components in the mixture at high purity. Beyond some discretization level, the size of the discretized steps in regions II and III did not change the optimal value of the total reactive holdup.

As indicated in section 2.3, the infimum of the IDEAS ILP is approximated through a convergent series composed by the solutions of the finite LP for an ever smaller discretized step size, i.e., an ever increasing number of reactive separator flash units G. For the conditions specified in this assessment, a convergence plot of IDEAS framework for the discretized set in Table 1.4 is shown in Fig.1.5.

Table 1.4. Discretized set in regions I, II and III utilized in the IDEAS convergence plot.

	Region I	Region II	Region III	Number of reactive separator flashes in G
Set 1	*1/16*	*1/16*	*1/8*	*60*
Set 2	*1/16*	*1/16*	*1/16*	*154*
Set 3	*1/32*	*1/32*	*1/32*	*561*
Set 4	*1/64*	*1/64*	*1/32*	*627*
Set 5	*1/128*	*1/64*	*1/32*	*903*

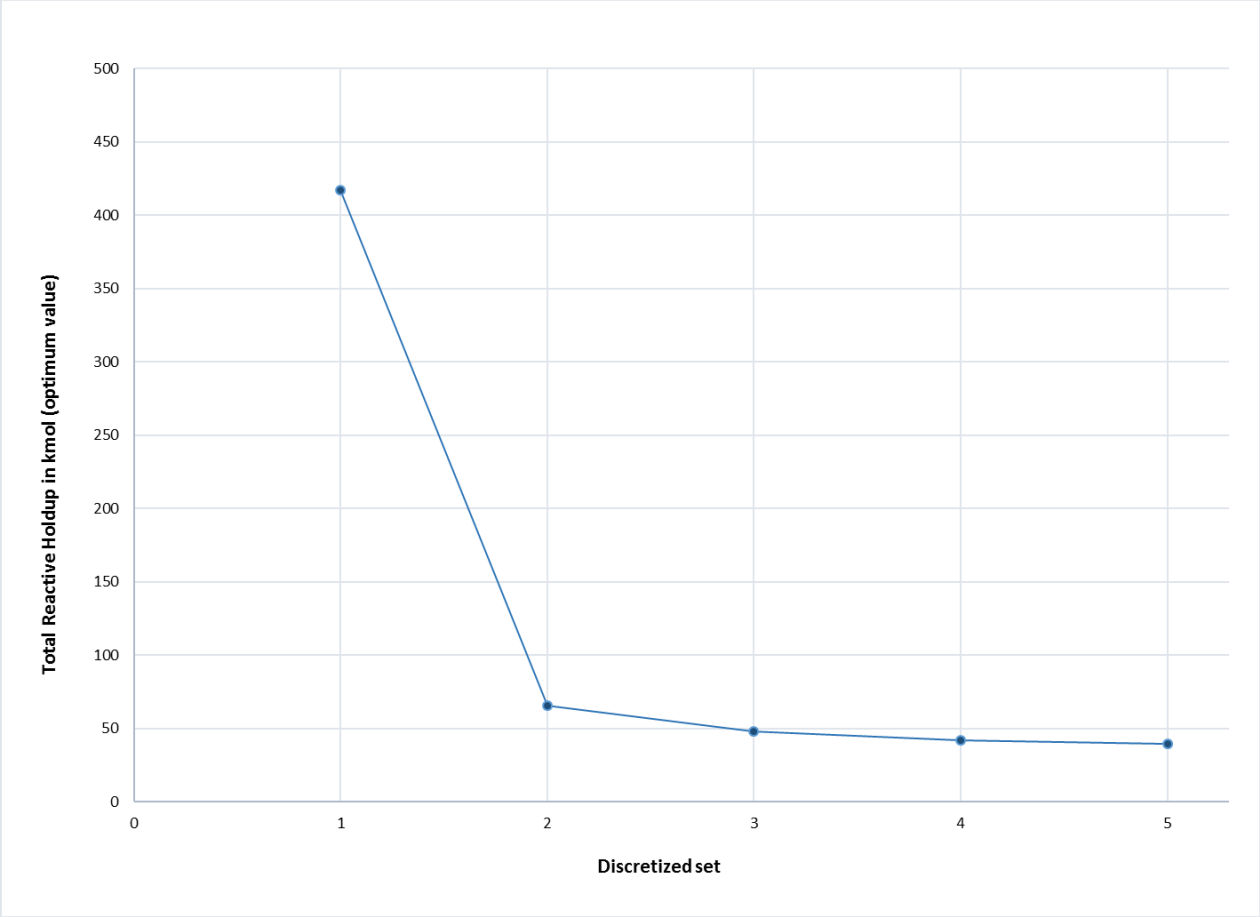

Figure 1.5 - IDEAS convergence for the metathesis of 2-Pentene with 87.5% purity, for minimum total reactive holdup

1.4.4. IDEAS process intensification results

The performance limits of the reactive distillation network are investigated by solving the optimization problem described in Eq.(1.36). Based on the previous section, a discretization level of 1/256, 1/128 and 1/32, for regions I, II and III respectively, is used to establish the IDEAS OP. Specifying $\alpha = 0.96875$ and $\beta = 0.0875$ as the region's edges, the 969 reactive flash separators are contained in the OP.

A reactor followed by an optimized separation system is used as a baseline to compare the results. The reactor outputs close to the equilibrium conversion, which is equal to 50% conversion of pentene for this reaction. The separation system is an IDEAS based network of flash separators (nonreactive). This baseline design is shown in Fig.1.6.

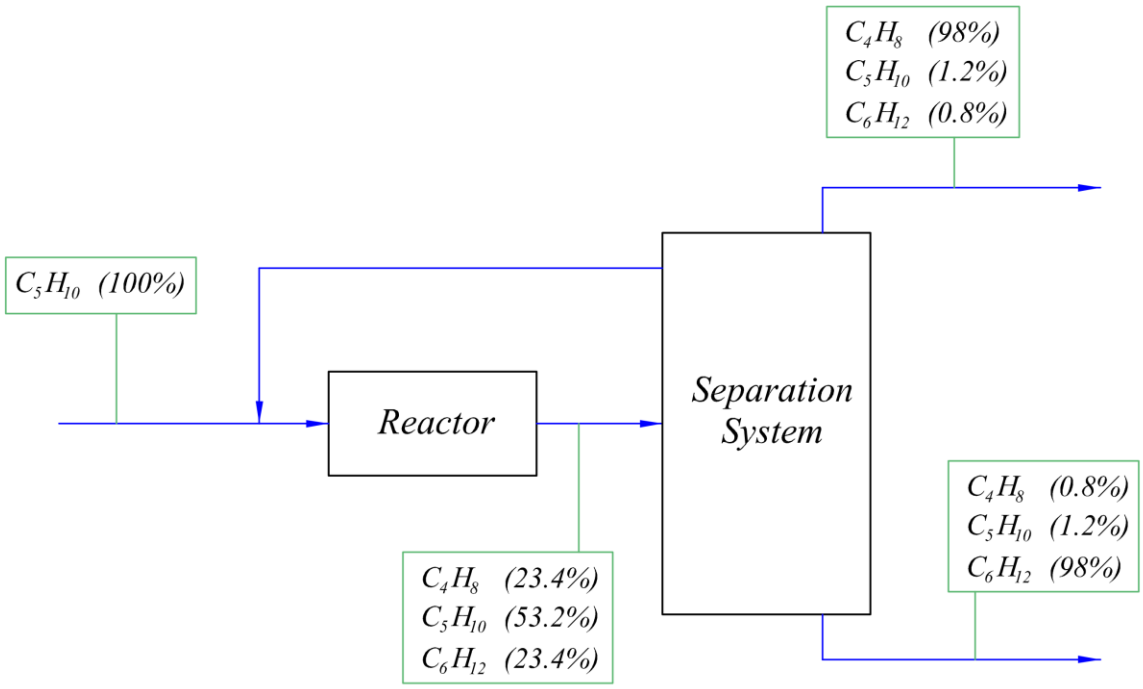

Figure 1.6 – A reactor followed by separation system used as baseline design for the metathesis of 2-pentene

The IDEAS results for different bounds in the total capacity, as well as the baseline value, are plotted in Fig.1.7. The intensified reactive distillation network works with 5.5% of the baseline total reactive holdup for the same capacity value. The IDEAS based solution can also deliver a network with 15.7% of the baseline capacity for the same production rate and purity.

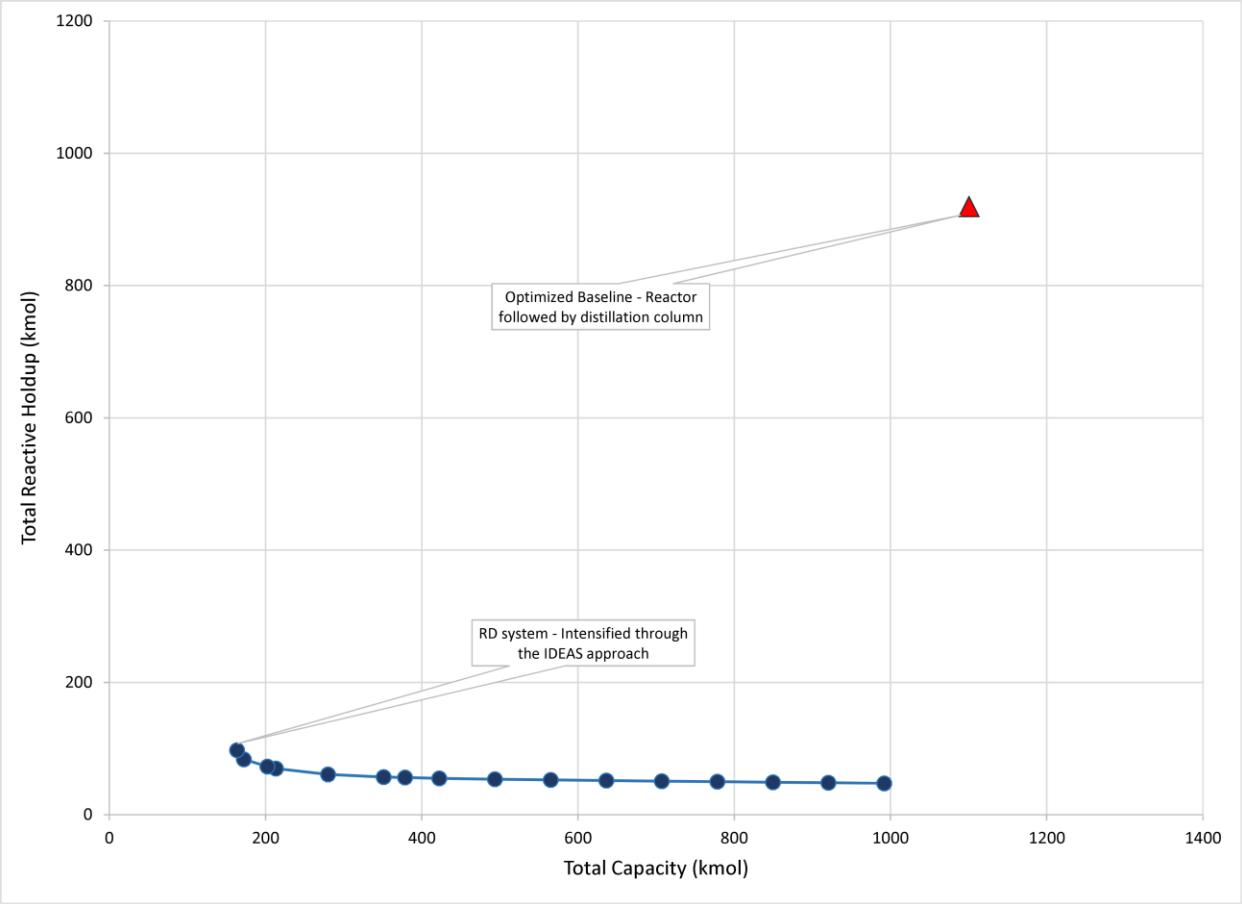

Figure 1.7 - Reactive holdup comparison between baseline and IDEAS designs as a function of total capacity

The IDEAS reactive distillation network results can also be compared with some of the reactive distillation solutions proposed in the literature. Nevertheless, values must be converted from the format originally presented to the total reactive holdup-total capacity space used in this work. Hoffmaster and Hauan [49] presented two optimized reactive distillation columns, using single and multi-feed respectively. They presented both columns in a 20-stage design, detailed enough to convert the reactive holdup to kmol and to calculate the equivalent total capacity of the column. The Damköhler number was used to represent the dimensionless amount of reactive

holdup. Hoffmaster and Hauan [49] correlate the total amount of reactive liquid holdup H_T and the total Damköhler number Da_T according to the following equation:

$$\mathrm{Da}_T = \frac{k_{f,ref}}{F} H_T \tag{1.37}$$

The normal boiling point of 2-Pentene (310.08 K) is reported in the literature [37,39,49] as the reference temperature used in the calculation of the reference rate constant $k_{f,ref}$ for the metathesis case. Following the specifications of the study case, the system's total flowrate F is considered to be 100 kmol/h. The procedure and respective values used in the calculation of the equivalent reactive holdups and equivalent capacities for the referenced literature are detailed in the Appendix.

The residence time of 60 seconds (same as used in the IDEAS solution) was used to calculate the equivalent capacity of the non-reactive stages. Okasinski and Doherty's [37] design is also presented in Hoffmaster and Hauan's the paper for comparison. Since the pieces of information required to calculate the solution's capacity are not available, for the sake of comparison Okasinski and Doherty's design is considered to have the equal reactive holdup and capacity, which is the lowest possible value for the capacity variable. Finally, a design proposed by Jackson and Grossmann [46], developed for minimum annualized cost, is also considered for comparison. This design has a slightly different purity target (95%) and inlet flow (120 kmol/h). Considering the conditions mentioned in this paragraph, the comparison is presented in Fig.1.8.

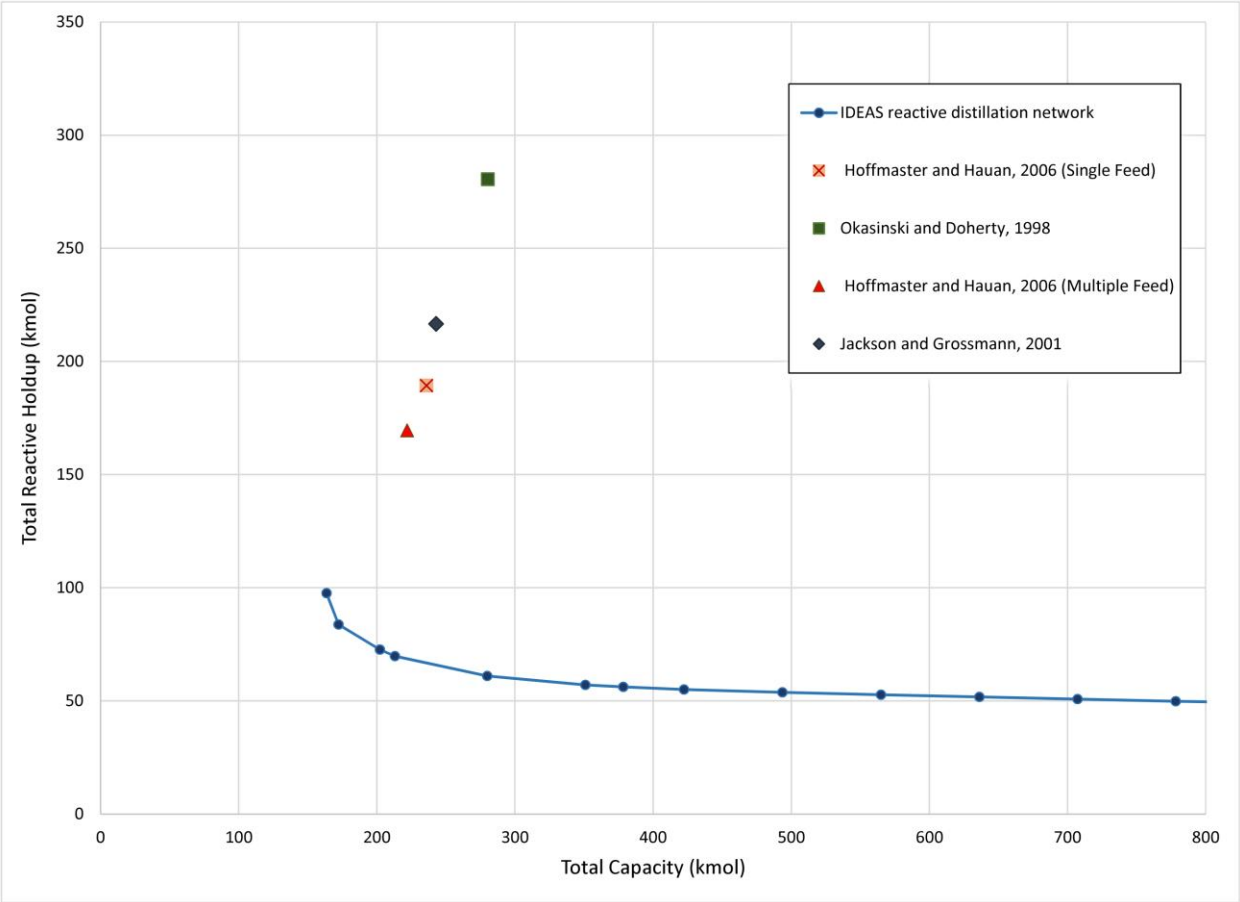

Figure 1.8 - IDEAS based performance limit for 2-Pentane metathesis (P = 1 bar) and comparison with other solutions in the literature

Based on the identified performance limits, one can quantitatively assess the available design options with respect to this limit. For example, the reactor-followed-by-separation-system, used as a baseline design, has a reactive holdup of 919.53 kmol, while the IDEAS based value for the same capacity is 47.48 kmol. Similarly, while the baseline utilizes 1,100.71 kmol as total capacity, the best IDEAS based value total capacity is 163.63 kmol. Thus, based on this baseline design, it is easy to verify that all proposed design solutions can be considered intensified. Moreover, optimized design solutions are evolving towards the IDEAS performance limits for this technology. Nevertheless, the results obtained from the application of the IDEAS

framework shows improvement opportunities in both total reactive holdup (amount of catalyst used) and total capacity (equipment size) directions.

1.5. Conclusions

The Infinite DimEnsionAl State-Space (IDEAS) framework is proposed as a process intensification tool in order to identify the performance limits of reactive separation processes. A model for the study of reactive distillation is developed using the IDEAS approach. The procedure leads to a linear programming problem formulation, in which the optimal solution is guaranteed to be global over all possible network configurations. The model was applied to investigate the use of reactive distillation for olefin metathesis. The case study features the metathesis of 2-pentene to form 2-butene and 3-hexene, an important chemical process for the oil industry. Total reactive holdup and total capacity, surrogates for the amount of catalyst used and capital cost respectively, were selected as the system's variables of interest for process intensification. Using a traditional reactor-followed-by-separation-system scheme as a baseline, an intensified IDEAS based reactive distillation network can reduce the total reactive holdup and total capacity by 94.5% and 84.3% respectively. Results available in the literature were converted to the total holdup-total capacity space to the extent possible and compared with the IDEAS results. The comparison shows the existence of improvement potential, indicating that process intensification opportunities can be further explored in this reactive distillation system.

1.6. Notation

Thermodynamic Variables*:*

P	Reactive flash separator pressure (Pa)
T	Reactive flash separator temperature (K)
$y_k^V(i)$	k^{th} Species equilibrium vapor composition leaving the i^{th} unit $(\dim)$
$x_k^L(i)$	k^{th} Species equilibrium liquid composition leaving the i^{th} unit $(\dim)$
$P_k^{sat}(T)$	k^{th} Species temperature dependent saturated vapor pressure (Pa)
$\phi_k\left(\left\{y_l^V\right\}_{l=1}^n, T, P\right)$	k^{th} Species non-ideal fugacity coefficient
$\gamma_k\left(\left\{x_l^L\right\}_{l=1}^n, T\right)$	k^{th} Species non-ideal liquid activity coefficient
a_k	Activity of the k^{th} species $(\dim)$
$A_{j,k}$	Antoine equation j^{th} parameter of the k^{th} species $(\dim)$
K_{eq}	Reaction equilibrium constant $(\dim)$
k_f	Forward reaction rate constant $(1/\mathrm{h})$

IDEAS Variables*:*

$F^I(i)$	i^{th} DN inlet stream
$F^O(i)$	i^{th} DN outlet stream
$F^L(i)$	i^{th} OP liquid outlet
$F^V(i)$	i^{th} OP vapor outlet
$F^{OI}(i,j)$	j^{th} DN inlet stream to i^{th} DN outlet
$F^{PI}(i,j)$	i^{th} OP inlet stream from j^{th} DN network inlet
$F^{OL}(i,j)$	i^{th} DN outlet stream from j^{th} OP liquid outlet
$F^{OV}(i,j)$	i^{th} DN outlet stream from j^{th} OP vapor outlet
$F^{PL}(i,j)$	i^{th} OP inlet stream from j^{th} OP liquid outlet
$F^{PV}(i,j)$	i^{th} OP inlet stream from j^{th} OP vapor outlet
$H(i)$	Reactive holdup of the i^{th} reactive flash separator unit in the OP
$C(i)$	Capacity of the i^{th} reactive flash separator unit in the OP
$z_k^I(i)$	k^{th} species, i^{th} DN inlet stream composition
$z_k^O(i)$	k^{th} species, i^{th} DN outlet stream composition

$\left(z_k^O(i)\right)^l$ k^{th} species, i^{th} DN outlet stream composition vector, lower bound

$\left(z_k^O(i)\right)^u$ k^{th} species, i^{th} DN outlet stream composition vector, upper bound

$x_k^L(i)$ k^{th} species, i^{th} OP liquid outlet composition

$y_k^V(i)$ k^{th} species, i^{th} OP vapor outlet composition

G Total number of reactive flashes in the OP

M Number of IDEAS network inlets

N Number of IDEAS network outlets

1.7. Appendix

The detailed procedure and respective values used in the calculation of the equivalent reactive holdups and equivalent capacities for the referenced literature, represented in Fig.1.8, are presented in this appendix. From Hoffmaster and Hauan (2006), the total amount of reactive liquid holdup H_T and the total Damköhler number Da_T are correlated by:

$$\mathrm{Da}_T = \frac{k_{f,ref}}{F} H_T \tag{1.38}$$

Since the kinetic model for the problem is already defined, if the temperature in which the reference rate constant $k_{f,ref}$ was calculated is known, it is possible to determine the total reactive holdup from the value of the total Damköhler number, for a given feed F.

According to Hoffmaster and Hauan, their results for the metathesis of 2-pentane were obtained using the same conditions as the design presented by Okasinski and Doherty (1998). Chen et al. (2000) also used the same specifications as Okasinski and Doherty (1998), explicitly declaring that the reference temperature used to calculate $k_{f,ref}$ is the normal boiling point of 2-Pentene (310.08 K).

The feed F used in this work's case study is equal to 100 kmol/h, as shown in Table 1.2. Considering this information, the total reactive holdup is determined from the Da_T presented in each of the reactive distillation systems presented in Fig.1.8.

The value of the reactive holdup in each stage is calculated by using the total reactive holdup and the reaction distribution per stage, as shown in the referenced papers. The capacity for the specified residence time in each stage is also calculated, assuming constant molar overflow and considering the data presented in each of the cited references. For the reactive stages, the final value of the stage's capacity is either the capacity for the specified residence time or the reactive holdup for the stage, whichever is greater. This procedure is the same as adopted by the IDEAS methodology in the manuscript.

The values used in the reactive holdup and capacity calculations, in each of the referenced systems, are presented in Table 1.5. The distribution per stage of the reactive holdup and the stage's capacity based on the residence time are shown in Table 1.6 to Table 1.9. In all these tables the roman characters represent the following systems:

I. Hoffmaster and Hauan (2006) – Single Feed

II. Hoffmaster and Hauan (2006) – Multiple Feed

III. Okasinski and Doherty (1998)

IV. Jackson and Grossmann (2001)

Table 1.5. Values for the calculation of the referenced system's reactive holdup and capacities

	I	II	III	IV*
Reflux ratio (dim)				
r	2	2	4	0.516
Flows (kmol/h)				
D	50	50	50	60*
F	100	100	100	120*
B	50	50	50	60*
Number of stages (dim)				
n	20	20	13	29
Feed stage (dim)				
Feed 1	11 (100%)	9 (75%)	7 (100%)	12 (28.6%)
Feed 2	-	14 (25%)		13 (30.6%)
Feed 3	-			17 (20.8%)
Feed 4	-			19 (20.0%)
Residence time (h)				
Tau	0.0166667	0.0166667	0.0166667	0.0166667
Total Reactive Holdup calculation - Eq.(A.1)				
Holdup (Da)	4.49	4.02	6.65	-
T_ref (C5) (K)	310.08	310.08	310.08	-
kf_ref (1/h)	2.3777348	2.3777348	2.3777348	-
Total Reactive Holdup (kmol)	***188.84***	***169.07***	***279.68***	***216.66****

* This design has a purity target and inlet flow values of 95% and 120 kmol/h, respectively.

Table 1.6. Calculated capacity (per stage and total) for reactive distillation system I

Stage	rxn/st	H	Tau*F	**Capacity**
1	0%	0.00	4.17	**4.17**
2	0%	0.00	4.17	**4.17**
3	0%	0.00	4.17	**4.17**
4	0%	0.00	4.17	**4.17**
5	1%	1.89	4.17	**4.17**
6	2%	3.79	4.17	**4.17**
12	10%	18.94	5.83	**18.94**
13	10%	18.94	5.83	**18.94**
14	9%	17.04	5.83	**17.04**
15	6%	11.36	5.83	**11.36**
16	1%	1.89	5.83	**5.83**
17	0%	0.00	5.83	**5.83**
18	0%	0.00	5.83	**5.83**
19	0%	0.00	5.83	**5.83**
20	0%	0.00	5.83	**5.83**

Total Capacity =	**235.95**

Table 1.7. Calculated capacity (per stage and total) for reactive distillation system II

Stage	rxn/st	H	Tau*F	**Capacity**
1	0%	0.00	4.17	**4.17**
2	0%	0.00	4.17	**4.17**
3	0%	0.00	4.17	**4.17**
4	0%	0.00	4.17	**4.17**
5	0%	0.00	4.17	**4.17**
6	1%	1.70	4.17	**4.17**
12	16%	27.13	6.25	**27.13**
13	15%	25.43	6.25	**25.43**
14	10%	16.95	6.25	**16.95**
15	4%	6.78	5.83	**6.78**
16	0%	0.00	5.83	**5.83**
17	0%	0.00	5.83	**5.83**
18	0%	0.00	5.83	**5.83**
19	0%	0.00	5.83	**5.83**
20	0%	0.00	5.83	**5.83**

Total Capacity =	**222.01**

Table 1.8. Calculated capacity (per stage and total) for reactive distillation system III

Stage	rxn/st	H	Tau*F	**Capacity**
1	7.69%	21.57	7.50	**21.57**
2	7.69%	21.57	7.50	**21.57**
3	7.69%	21.57	7.50	**21.57**
4	7.69%	21.57	7.50	**21.57**
5	7.69%	21.57	7.50	**21.57**
6	7.69%	21.57	7.50	**21.57**
12	7.69%	21.57	9.17	**21.57**
13	7.69%	21.57	9.17	**21.57**

Total Capacity =	**280.45**

Table 1.9. Calculated capacity (per stage and total) for reactive distillation system IV

Stage	rxn/st	H	Tau*F	**Capacity**
Cond.	0%	0.00	2.03	**2.03**
27	0%	0.00	2.03	**2.03**
26	0%	0.00	2.03	**2.03**
25	6.25%	10.32	2.03	**10.32**
24	6.25%	10.32	2.03	**10.32**
23	6.25%	10.32	2.03	**10.32**
17	6.25%	10.32	2.85	**10.32**
16	6.25%	10.32	2.85	**10.32**
15	6.25%	10.32	2.85	**10.32**
14	6.25%	10.32	2.85	**10.32**
13	6.25%	10.32	3.46	**10.32**
12	6.25%	10.32	4.03	**10.32**
11	6.25%	10.32	4.03	**10.32**
10	6.25%	10.32	4.03	**10.32**
9	6.25%	10.32	4.03	**10.32**
8	6.25%	10.32	4.03	**10.32**
7	6.25%	10.32	4.03	**10.32**
6	6.25%	10.32	4.03	**10.32**
5	6.25%	10.32	4.03	**10.32**
4	0%	0.00	4.03	**4.03**
3	0%	0.00	4.03	**4.03**
2	0%	0.00	4.03	**4.03**
1	0%	0.00	4.03	**4.03**
Reb.	0%	0.00	4.03	**4.03**

Total Capacity =	**242.92**

1.8. References

(1) Stankiewicz, A. I.; Moulijn, J. A. Process Intensification: Transforming Chemical Engineering. *Chem. Eng. Prog.* **2000**, *96* (1), 22–34.

(2) Stankiewicz, A. Reactive Separations for Process Intensification: An Industrial Perspective. *Chem. Eng. Process. Process Intensif.* **2003**, *42* (3), 137–144. https://doi.org/10.1016/S0255-2701(02)00084-3.

(3) Van Gerven, T.; Stankiewicz, A. Structure, Energy, Synergy, Time—The Fundamentals of Process Intensification. *Ind. Eng. Chem. Res.* **2009**, *48* (5), 2465–2474. https://doi.org/10.1021/ie801501y.

(4) Barnicki, S. D.; Siirola, J. J. Process Synthesis Prospective. *Comput. Chem. Eng*. **2004**, *28* (4), 441–446. https://doi.org/10.1016/j.compchemeng.2003.09.030.

(5) Harmsen, G. J. Industrial Best Practices of Conceptual Process Design. *Chem. Eng. Process. Process Intensif.* **2004**, *43* (5), 671–675. https://doi.org/10.1016/j.cep.2003.02.003.

(6) Moulijn, J. A.; Stankiewicz, A.; Grievink, J.; Górak, A. Process Intensification and Process Systems Engineering: A Friendly Symbiosis. *Comput. Chem. Eng.* **2008**, *32* (1–2), 3–11. https://doi.org/10.1016/j.compchemeng.2007.05.014.

(7) Harmsen, G. J. Reactive Distillation: The Front-Runner of Industrial Process Intensification: A Full Review of Commercial Applications, Research, Scale-up, Design and Operation. *Chem. Eng. Process. Process Intensif.* **2007**, *46* (9), 774–780. https://doi.org/10.1016/j.cep.2007.06.005.

(8) Baldea, M. From Process Integration to Process Intensification. *Comput. Chem. Eng.* **2015**, *81*, 104–114. https://doi.org/10.1016/j.compchemeng.2015.03.011.

(9) Wilson, S.; Manousiouthakis, V. IDEAS Approach to Process Network Synthesis: Application to Multicomponent MEN. *AIChE J.* **2000**, *46* (12), 2408–2416. https://doi.org/10.1002/aic.690461209.

(10) Drake, J. E.; Manousiouthakis, V. IDEAS Approach to Process Network Synthesis: Minimum Utility Cost for Complex Distillation Networks. *Chem. Eng. Sci.* **2002**, *57* (15), 3095–3106. https://doi.org/10.1016/S0009-2509(02)00159-8.

(11) Drake, J. E.; Manousiouthakis, V. IDEAS Approach to Process Network Synthesis: Minimum Plate Area for Complex Distillation Networks with Fixed Utility Cost. *Ind. Eng. Chem. Res.* **2002**, *41* (20), 4984–4992. https://doi.org/10.1021/ie010735s.

(12) Justanieah, A. M.; Manousiouthakis, V. IDEAS Approach to the Synthesis of Globally Optimal Separation Networks: Application to Chromium Recovery from Wastewater. *Adv. Environ. Res.* **2003**, *7* (2), 549–562. https://doi.org/10.1016/S1093-0191(02)00026-6.

(13) Martin, L. L.; Manousiouthakis, V. I. Globally Optimal Power Cycle Synthesis via the Infinite-DimEnsionAl State-Space (IDEAS) Approach Featuring Minimum Area with Fixed Utility. *Chem. Eng. Sci.* **2003**, *58* (18), 4291–4305. https://doi.org/10.1016/S0009-2509(02)00526-2.

(14) Holiastos, K.; Manousiouthakis, V. Infinite-Dimensional State-Space (IDEAS) Approach to Globally Optimal Design of Distillation Networks Featuring Heat and Power Integration. *Ind. Eng. Chem. Res.* **2004**, *43* (24), 7826–7842. https://doi.org/10.1021/ie010434i.

(15) Takase, H.; Hasebe, S. Synthesis of Ternary Distillation Process Structures Featuring Minimum Utility Cost Using the IDEAS Approach. *AIChE J.* **2018**, *64* (4), 1285–1294. https://doi.org/10.1002/aic.16023.

(16) Burri, J. F.; Manousiouthakis, V. I. Global Optimization of Reactive Distillation Networks Using IDEAS. *Comput. Chem. Eng.* **2004**, *28* (12), 2509–2521. https://doi.org/10.1016/j.compchemeng.2004.06.014.

(17) da Cruz, F. E.; Manousiouthakis, V. I. Process Intensification of Reactive Separator Networks through the IDEAS Conceptual Framework. *Comput. Chem. Eng.* **2017**, *105*, 39–55. https://doi.org/10.1016/j.compchemeng.2016.12.006.

(18) Burri, J. F.; Wilson, S. D.; Manousiouthakis, V. I. Infinite DimEnsionAl State-Space Approach to Reactor Network Synthesis: Application to Attainable Region Construction. *Comput. Chem. Eng.* **2002**, *26* (6), 849–862. https://doi.org/10.1016/S0098-1354(02)00008-X.

(19) Manousiouthakis, V. I.; Justanieah, A. M.; Taylor, L. A. The Shrink–Wrap Algorithm for the Construction of the Attainable Region: An Application of the IDEAS Framework. *Comput. Chem. Eng.* **2004**, *28* (9), 1563–1575. https://doi.org/10.1016/j.compchemeng.2003.12.005.

(20) Zhou, W.; Manousiouthakis, V. I. Non-Ideal Reactor Network Synthesis through IDEAS: Attainable Region Construction. *Chem. Eng. Sci.* **2006**, *61* (21), 6936–6945. https://doi.org/10.1016/j.ces.2006.07.002.

(21) Zhou, W.; Manousiouthakis, V. I. Variable Density Fluid Reactor Network Synthesis—Construction of the Attainable Region through the IDEAS Approach. *Chem. Eng. J.* **2007**, *129* (1–3), 91–103. https://doi.org/10.1016/j.cej.2006.11.004.

(22) Zhou, W.; Manousiouthakis, V. I. Pollution Prevention through Reactor Network Synthesis: The IDEAS Approach. *Int. J. Environ. Pollut.* **2007**, *29* (1–3), 206–231. https://doi.org/10.1504/IJEP.2007.012804.

(23) Posada, A.; Manousiouthakis, V. Multi-Feed Attainable Region Construction Using the Shrink–Wrap Algorithm. *Chem. Eng. Sci.* **2008**, *63* (23), 5571–5592. https://doi.org/10.1016/j.ces.2008.07.026.

(24) Zhou, W.; Manousiouthakis, V. I. Global Capital/Total Annualized Cost Minimization of Homogeneous and Isothermal Reactor Networks. *Ind. Eng. Chem. Res.* **2008**, *47* (10), 3771–3782. https://doi.org/10.1021/ie060653+.

(25) Zhou, W.; Manousiouthakis, V. I. On Dimensionality of Attainable Region Construction for Isothermal Reactor Networks. *Comput. Chem. Eng.* **2008**, *32* (3), 439–450. https://doi.org/10.1016/j.compchemeng.2007.02.013.

(26) Zhou, W.; Manousiouthakis, V. I. Automating the AR Construction for Non-Isothermal Reactor Networks. *Comput. Chem. Eng.* **2009**, *33* (1), 176–180. https://doi.org/10.1016/j.compchemeng.2008.07.011.

(27) Ghougassian, P. G.; Manousiouthakis, V. Attainable Composition, Energy Consumption, and Entropy Generation Properties for Isothermal/Isobaric Reactor Networks. *Ind. Eng. Chem. Res.* **2013**, *52* (9), 3225–3238. https://doi.org/10.1021/ie301158m.

(28) Ghougassian, P. G.; Manousiouthakis, V. Globally Optimal Networks for Multipressure Distillation of Homogeneous Azeotropic Mixtures. *Ind. Eng. Chem. Res.* **2012**, *51* (34), 11183–11200. https://doi.org/10.1021/ie300423q.

(29) Al-Husseini, Z.; Manousiouthakis, V. I. IDEAS Based Synthesis of Minimum Volume Reactor Networks Featuring Residence Time Density/Distribution Models. *Comput. Chem. Eng.* **2014**, *60*, 124–142. https://doi.org/10.1016/j.compchemeng.2013.07.005.

(30) Ghougassian, P. G.; Manousiouthakis, V. Minimum Entropy Generation for Isothermal Endothermic/Exothermic Reactor Networks. *AIChE J.* **2015**, *61* (1), 103–117. https://doi.org/10.1002/aic.14598.

(31) Pichardo, P.; Manousiouthakis, V. I. Infinite DimEnsionAl State-Space as a Systematic Process Intensification Tool: Energetic Intensification of Hydrogen Production. *Chem. Eng. Res. Des.* **2017**, *120*, 372–395. https://doi.org/10.1016/j.cherd.2017.01.026.

(32) Davis, B. J.; Taylor, L. A.; Manousiouthakis, V. I. Identification of the Attainable Region for Batch Reactor Networks. *Ind. Eng. Chem. Res.* **2008**, *47* (10), 3388–3400. https://doi.org/10.1021/ie071664l.

(33) Conner, J. A.; Manousiouthakis, V. I. On the Attainable Region for Process Networks. *AIChE J.* **2014**, *60* (1), 193–212. https://doi.org/10.1002/aic.14257.

(34) Barbosa, D.; Doherty, M. F. The Simple Distillation of Homogeneous Reactive Mixtures. *Chem. Eng. Sci.* **1988**, *43* (3), 541–550. https://doi.org/10.1016/0009-2509(88)87015-5.

(35) Venimadhavan, G.; Buzad, G.; Doherty, M. F.; Malone, M. F. Effect of Kinetics on Residue Curve Maps for Reactive Distillation. *AIChE J.* **1994**, *40* (11), 1814–1824. https://doi.org/10.1002/aic.690401106.

(36) Siirola, J. J. Industrial Applications of Chemical Process Synthesis. In Advances in Chemical Engineering; Anderson, J. L., Ed.; Academic Press, **1996**; Vol. 23, pp 1–62.

(37) Okasinski, M. J.; Doherty, M. F. Design Method for Kinetically Controlled, Staged Reactive Distillation Columns. *Ind. Eng. Chem. Res.* **1998**, *37* (7), 2821–2834. https://doi.org/10.1021/ie9708788.

(38) Malone, M. F.; Doherty, M. F. Reactive Distillation. *Ind. Eng. Chem. Res.* **2000**, *39* (11), 3953–3957. https://doi.org/10.1021/ie000633m.

(39) Chen, F.; Huss, R. S.; Malone, M. F.; Doherty, M. F. Simulation of Kinetic Effects in Reactive Distillation. *Comput. Chem. Eng.* **2000**, *24* (11), 2457–2472. https://doi.org/10.1016/S0098-1354(00)00609-8.

(40) Barnicki, S. D.; Hoyme, C. A.; Siirola, J. J. Separations Process Synthesis. In Kirk-Othmer Encyclopedia of Chemical Technology; John Wiley & Sons, Inc., **2000**.

(41) Jiménez, L.; Wanhschafft, O. M.; Julka, V. Analysis of Residue Curve Maps of Reactive and Extractive Distillation Units. *Comput. Chem. Eng.* **2001**, *25* (4–6), 635–642. https://doi.org/10.1016/S0098-1354(01)00644-5.

(42) Huss, R. S.; Chen, F.; Malone, M. F.; Doherty, M. F. Reactive Distillation for Methyl Acetate Production. *Comput. Chem. Eng.* **2003**, *27* (12), 1855–1866. https://doi.org/10.1016/S0098-1354(03)00156-X.

(43) Li, H.; Meng, Y.; Li, X.; Gao, X. A Fixed Point Methodology for the Design of Reactive Distillation Columns. *Chem. Eng. Res. Des.* **2016**, *111*, 479–491. https://doi.org/10.1016/j.cherd.2016.05.015.

(44) Ciric, A. R.; Gu, D. Synthesis of Nonequilibrium Reactive Distillation Processes by MINLP Optimization. *AIChE J.* **1994**, *40* (9), 1479–1487. https://doi.org/10.1002/aic.690400907.

(45) Papalexandri, K. P.; Pistikopoulos, E. N. Generalized Modular Representation Framework for Process Synthesis. *AIChE J.* **1996**, *42* (4), 1010–1032. https://doi.org/10.1002/aic.690420413.

(46) Jackson, J. R.; Grossmann, I. E. A Disjunctive Programming Approach for the Optimal Design of Reactive Distillation Columns. *Comput. Chem. Eng.* **2001**, *25* (11–12), 1661–1673. https://doi.org/10.1016/S0098-1354(01)00730-X.

(47) Georgiadis, M. C.; Schenk, M.; Pistikopoulos, E. N.; Gani, R. The Interactions of Design Control and Operability in Reactive Distillation Systems. *Comput. Chem. Eng.* **2002**, *26* (4–5), 735–746. https://doi.org/10.1016/S0098-1354(01)00774-8.

(48) Cardoso, M. F.; Salcedo, R. L.; de Azevedo, S. F.; Barbosa, D. Optimization of Reactive Distillation Processes with Simulated Annealing. *Chem. Eng. Sci.* **2000**, *55* (21), 5059–5078. https://doi.org/10.1016/S0009-2509(00)00119-6.

(49) Hoffmaster, W. R.; Hauan, S. Using Feasible Regions to Design and Optimize Reactive Distillation Columns with Ideal VLE. *AIChE J.* **2006**, *52* (5), 1744–1753. https://doi.org/10.1002/aic.10765.

(50) Avami, A.; Marquardt, W.; Saboohi, Y.; Kraemer, K. Shortcut Design of Reactive Distillation Columns. *Chem. Eng. Sci.* **2012**, *71*, 166–177. https://doi.org/10.1016/j.ces.2011.12.021.

(51) Urselmann, M.; Engell, S. Design of Memetic Algorithms for the Efficient Optimization of Chemical Process Synthesis Problems with Structural Restrictions. *Comput. Chem. Eng.* **2015**, *72*, 87–108. https://doi.org/10.1016/j.compchemeng.2014.08.006.

(52) Al-Arfaj, M. A.; Luyben, W. L. Design and Control of an Olefin Metathesis Reactive Distillation Column. *Chem. Eng. Sci.* **2002**, *57* (5), 715–733. https://doi.org/10.1016/S0009-2509(01)00442-0.

(53) Chadda, N.; Malone, M. F.; Doherty, M. F. Feasible Products for Kinetically Controlled Reactive Distillation of Ternary Mixtures. *AIChE J.* **2000**, *46* (5), 923–936. https://doi.org/10.1002/aic.690460507.

(54) Li, P.; Huang, K.; Lin, Q. A Generalized Method for the Synthesis and Design of Reactive Distillation Columns. *Chem. Eng. Res. Des.* **2012**, *90* (2), 173–184. https://doi.org/10.1016/j.cherd.2011.06.020.

(55) Biegler, L. T.; Grossmann, I. E.; Westerberg, A. W. Systematic Methods for Chemical Process Design. **1997**.

(56) Towler, G.; Sinnott, R. K. Chemical Engineering Design: Principles, Practice and Economics of Plant and Process Design; Elsevier, **2012**.

CHAPTER 2

Energy Consumption Minimization of Intensified Reactive Separator Networks through the IDEAS Conceptual Framework

2.1. Abstract

The energy minimization problem of reactive separation network systems is performed in this work through the application of the IDEAS framework. For reactive distillation systems, energy consumption and utility cost are directly correlated, which may determine the viability of intensified designs. A rigorous quantification of the energy performance limit for reactive-separative systems in relation to its size footprint can further advance process intensification studies in the pursuit of radical improvements. The application of the IDEAS framework allows the establishment of rigorous tradeoffs energy consumption (utility cost), total network reactive holdup, and total capacity. IDEAS generates an infinite linear program (ILP) that contains all possible reactive distillation flash units (a surrogate for distillation trays), and all possible mixing and splitting connections among them, resulting in a formulation that encompasses all possible process flowsheets for the reactive-separative process. The application of the IDEAS framework in the model formulation is first presented and then used in a case study involving the metathesis of 2-pentene through reactive distillation. A tradeoff curve showing the feasible region for different sizes of reactive distillation systems in relation to energy/utility consumption demonstrates larger energy requirements for smaller systems at the globally optimal feasible boundary.

2.2. Introduction

Distillation is the most widely used method to separate and increase purity of chemicals. In 2014, over 40,000 distillation columns were in operation worldwide [1], consuming over 230 gigawatts (GW)[2], which is equivalent to the total energy consumption of the United Kingdom in the same year. Distillation systems have been a major focus in process intensification (PI) studies[3,4]. Process intensification encompasses any chemical engineering development that offers drastic improvements in chemical processing, substantially decreasing equipment volume, and energy consumption [5,3]. Major achievements in the design of intensified distillation systems came through the adoption of reactive distillation systems. One example is the Eastman Chemical Company's methyl acetate reactive distillation unit, that replaced an entire plant with eight conventional distillation columns, and is reported to cost one-fifth of the capital investment of the conventional process and consume one-fifth of the energy [6].

Process synthesis is the invention of chemical process designs exploiting chemical routes at the desired scale, safely, environmentally responsibly, efficiently, and economically in a manner superior to all other possible processes [7]. Given the potential of reactive distillation systems in delivering chemical separation with reduced energy consumption and material/land footprint, RD designs have been pursued using process synthesis methods [8]. However, developments in process intensification are mostly based on experimental work [9], and pilot plant facilities [4], while the use of systematic computational/mathematical approaches is still rare [10].

In this context, a systematic approach for the synthesis of optimized process flowsheets can support the development of PI design options. Process synthesis tools, such as the Infinite

Dimensional Steady State (IDEAS) framework, can establish metrics to quantitatively evaluate current intensified processes by rigorously defining the process performance limits of a particular technology, or combination of technologies, without establishing any a priori design. IDEAS enables the detection of process intensification candidates and quantifies the potential for further improvements.

The IDEAS conceptual framework has been successfully applied to either globally optimize or to identify the attainable region of numerous process synthesis problems. Some examples of IDEAS application involve multicomponent mass exchange networks [11], ideal distillation networks [12,13], separator networks [14], power cycles [15], heat/power integrated distillation networks [16,17], reactive distillation networks [18,19], reactor network attainable region construction [20–29], azeotropic distillation networks [30], reactor networks [31–33], batch reactor networks [36], and process network attainable region [37].

In the IDEAS framework, all units in the OP can be used to reach the desired process objective. A flow operator structure, the IDEAS distribution network DN, is employed to connect all inlet-outlet possibilities (i.e., process inlets to process units, process inlets to process outlets, process units to process units and process units to process outlets). Considering that the DN operations (mixing, splitting, recycling, and bypass) are linear in the flow variables, the IDEAS DN-OP representation is linear for any chemical process. The structure of IDEAS guarantees that all possible process flowsheets are taken into account in the network synthesis problem for an *a priori* given set of phenomena.

Due to IDEAS' innovative proposition for the process operations, whose domain and range is considered to lie in an infinite (rather than finite) dimensional space, infinite dimensional linear programs (ILP) can be formulated for the synthesis of optimal process

networks. In fact, since it is not possible to solve an ILP, its solution is approximated arbitrarily close by finite dimensional LP of ever increasing size. The sequence formed by the LP optimal solutions converges to the global optimal solution of the ILP.

In this paper, the IDEAS framework is applied as a systematic tool to identify the minimum total energy required by reactive separation networks for different values of total capacity, a variable that directs correlate to intensified process designs.

2.3. Mathematical formulation for the energy minimization problem

2.3.1. Reactive flash separator model

A variety of models have been proposed to design and optimize reactive distillation systems. Geometrical approaches, such as the residue curve maps and the fixed-point method, have been heavily utilized to attack the problem [6,38–46]. Another approach is the application of optimization methods using mixed-integer nonlinear programming (MINPL) formulations [47–54] or infinite linear programming (ILP) formulations [17,18,55]. These have all contributed to the advancement of reactive distillation process synthesis.

In this work, the reactive flash separator model presented by da Cruz and Manousiouthakis [55] is improved by the consideration of heat transferring from/to the reactive flash (Fig.2.1). In the synthesis process, this feature gives flexibility to the network to meet the energy requirements of each flash, which functions as a reactive distillation tray: the reactive flash separator's vapor and liquid exit streams are considered to be in phase equilibrium with one another, and reactions may occur in the liquid phase, depending on the reactive volume H (the

reactive holdup) of the flash separator. A capacity variable C associated with the total liquid holdup is also considered.

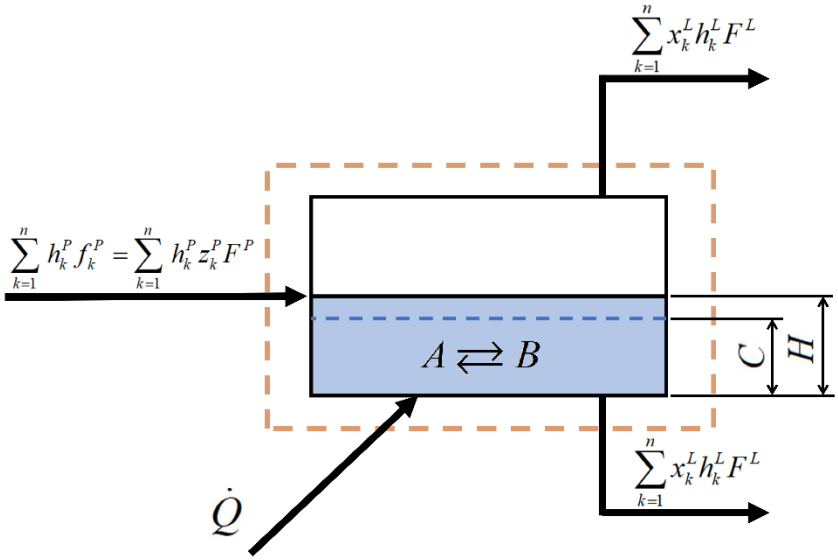

Figure 2.1 – Representation of the improved reactive flash separator

In terms of mass and component balances, the reactive flash separator used in this work follows the formulation and assumptions presented in da Cruz and Manousiouthakis [55]: the Gamma-Phi model to relate the liquid and vapor molar fractions, Eq.(2.1), a general kinetic rate expression, Eq.(2.2), where the i^{th} species activity in a multicomponent mixture is related to the activity coefficient in the liquid phase and the liquid molar fraction for the respective component as shown in Eq.(2.3).

$$y_k^V \phi_k\left(\left\{y_l^V\right\}_{l=1}^n, T, P\right) P = x_k^L \gamma_k\left(\left\{x_l^L\right\}_{l=1}^n, T\right) P_k^{sat}(T) \qquad \forall k = 1,\ldots,n \tag{2.1}$$

$$R_k = k_f(T)\left(\prod_{reactants} a_r\left(\gamma_r, x_r\right)^{\nu_r} - \frac{1}{K_{eq}(T)} \prod_{products} a_p\left(\gamma_p, x_p\right)^{\nu_p}\right) \tag{2.2}$$

$$a_i = \gamma_i \left(\left\{ x_l^L \right\}_{l=1}^{n}, T \right) x_i \tag{2.3}$$

An important feature of this reactive flash separator model is the ability to account for several different phenomena. In the case where the flash has reactive holdup, vapor, and liquid streams greater than zero, the unit is fully operational and will simultaneously act as both a reactor and VLE separator. On the other hand, if the reactive holdup is zero, the process acts only as a VLE flash separator; and if no separation takes place, the process assumes the behavior of an isolated CSTR reactor, with only one liquid flow as output.

The improved reactive flash separator model was employed in the systematic synthesis of reactive distillation networks through IDEAS, aiming to find the global minimum energy consumption in the network.

2.3.2. IDEAS formulation

During the synthesis process, the IDEAS framework enables the consideration of all possible flowsheets for a reactive flash separator network. The IDEAS framework allows each operational unit in the process operator OP to interface with all other possible operating – network inlets, network outlets, and other operational units – by using mixing and splitting operations through the distribution network (DN). Figure 2.2 shows the resulting IDEAS framework for the reactive flash separator synthesis problem featuring a distributed energy system.

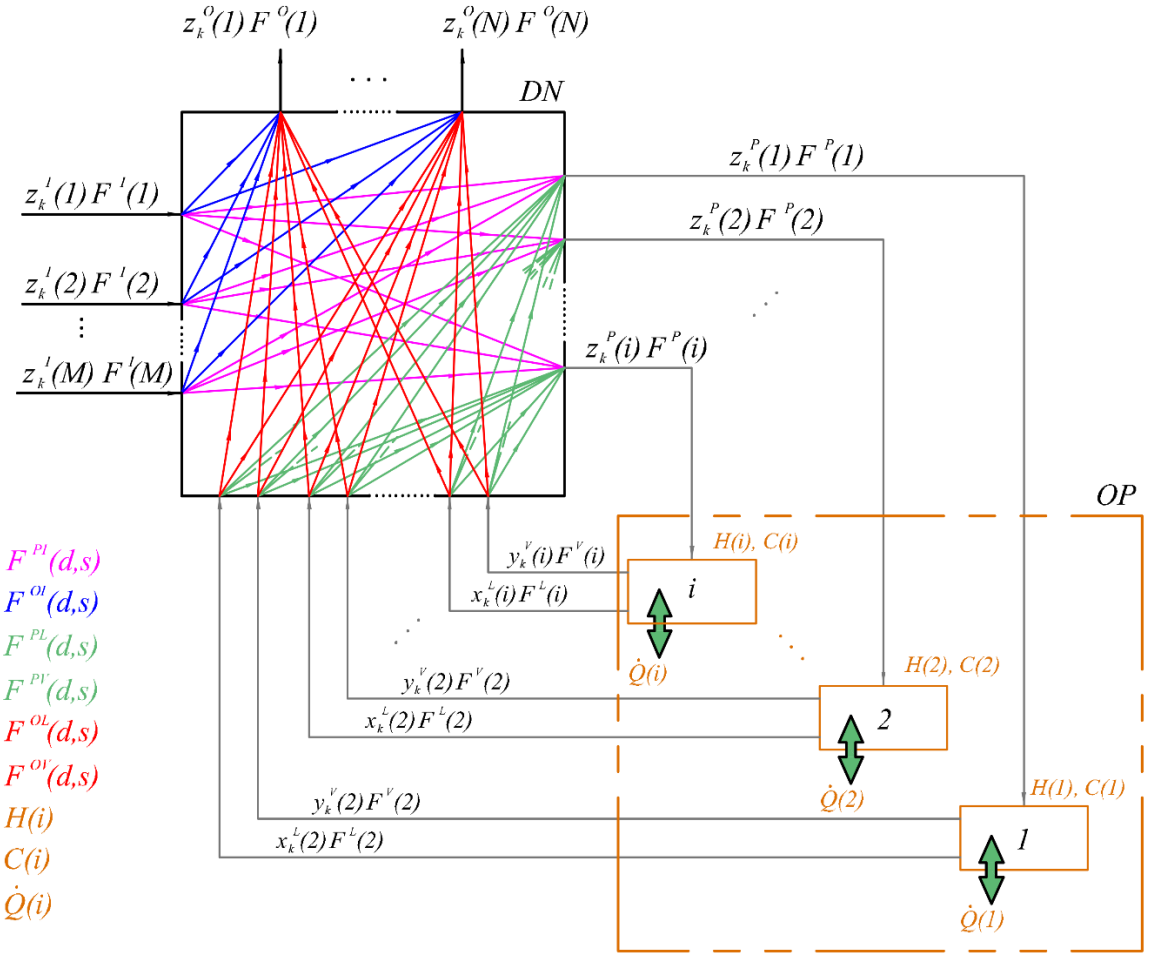

Figure 2.2 - IDEAS representation for a reactive flash separator network featuring a distributed energy system

Each cross-flow streams in the DN are characterized by a flow rate variable, which has fixed molar fraction conditions at the origin. The flow variables are identified by a superscript that indicates their destination and source respectively: the DN inlet is identified as I, the DN outlet as O, the OP inlet as P, the liquid and vapor outputs from the OP as L and V respectively. The flow variables also feature indices designating their destination and source, respectively. The reactive holdups, capacities, and heat transferred from/to the reactive flash are variables associated with the elements of the OP.

The distribution network (DN) is considered adiabatic, therefore the development of the constraints for the IDEAS ILP general formulation uses only mass and component balances on the DN. On the other hand, for the process units in the OP, mass, component and energy balances are developed. Starting with the mass and component balances, for each inlet flow $F^I(j)$ associated with one of the M inlets of the DN, a splitting balance is written as shown in Eq.(2.4).

$$F^I(j) - \sum_{i=1}^{N} F^{OI}(i,j) - \sum_{i=1}^{\infty} F^{PI}(i,j) = 0 \quad ; \quad \forall j = 1,...,M \tag{2.4}$$

For each outlet flow $F^O(i)$ leaving the DN from one of its N outlets, a mixing balance as shown in Eq.(2.5) is considered.

$$F^O(i) - \sum_{j=1}^{M} F^{OI}(i,j) - \sum_{j=1}^{\infty} F^{OL}(i,j) - \sum_{j=1}^{\infty} F^{OV}(i,j) = 0 \quad ; \quad \forall i = 1,...,N \tag{2.5}$$

The component flow $f_k^P(i)$ that feeds the i^{th} reactive flash separator can be considered as the sum of component flows feeding that specific mixing point of the DN (component balance).

$$f_k^P(i) - \sum_{j=1}^{M} z_k^I(j) F^{PI}(i,j) - \sum_{j=1}^{\infty} x_k^L(j) F^{PL}(i,j) - \sum_{j=1}^{\infty} y_k^V(j) F^{PV}(i,j) = 0 \qquad \forall i = 1,...,\infty \ ; \ \forall k = 1,...,n \tag{2.6}$$

Thus, the total mass flow in this mixing node is represented by Eq.(2.7) below.

$$F^P(i) - \sum_{j=1}^{M} F^{PI}(i,j) - \sum_{j=1}^{\infty} F^{PL}(i,j) - \sum_{j=1}^{\infty} F^{PV}(i,j) = 0 \quad ; \quad \forall i = 1,...,\infty \tag{2.7}$$

For each $F^L(j)$ liquid and $F^V(j)$ vapor input flow entering the DN's after being processed in the OP, a splitting balance is written as:

$$F^{L}(j)-\sum_{i=1}^{N}F^{OL}(i,j)-\sum_{i=1}^{\infty}F^{PL}(i,j)=0 \quad ; \quad \forall j=1,...,\infty \tag{2.8}$$

$$F^{V}(j)-\sum_{i=1}^{N}F^{OV}(i,j)-\sum_{i=1}^{\infty}F^{PV}(i,j)=0 \quad ; \quad \forall j=1,...,\infty \tag{2.9}$$

The final products from the reactive distillation process can be found in the DN outlets. Lower and upper bound constraints are introduced on each of the N flow variables $F^{O}(i)$ as design parameters. The total balance for each flow exiting the DN is shown in Eq.(2.10).

$$\left(F^{O}(i)\right)^{l} \le \sum_{j=1}^{M}F^{OI}(i,j)+\sum_{j=1}^{\infty}F^{OL}(i,j)+\sum_{j=1}^{\infty}F^{OV}(i,j) \le \left(F^{O}(i)\right)^{u} \quad ; \quad \forall i=1,...,N \tag{2.10}$$

Equations (2.10) can also be expressed by two independent inequalities as shown below:

$$\left[\sum_{j=1}^{M}F^{OI}(i,j)+\sum_{j=1}^{\infty}F^{OL}(i,j)+\sum_{j=1}^{\infty}F^{OV}(i,j)\right]-\left(F^{O}(i)\right)^{l} \ge 0 \quad ; \quad \forall i=1,...,N \tag{2.11}$$

$$\left[\sum_{j=1}^{M}F^{OI}(i,j)+\sum_{j=1}^{\infty}F^{OL}(i,j)+\sum_{j=1}^{\infty}F^{OV}(i,j)\right]-\left(F^{O}(i)\right)^{u} \le 0 \quad ; \quad \forall i=1,...,N \tag{2.12}$$

The component balances at the DN's outputs, including upper and lower bounds for the product's molar fractions are represented by Eq.(2.13).

$$\left(z_k^{O}(i)\right)^{l} F^{O}(i) \le \left\{ \begin{array}{l} \sum_{j=1}^{M} z_k^{I}(j) F^{OI}(i,j) \\ +\sum_{j=1}^{\infty} x_k^{L}(j) F^{OL}(i,j) \\ +\sum_{j=1}^{\infty} y_k^{V}(j) F^{OV}(i,j) \end{array} \right\} \le \left(z_k^{O}(i)\right)^{u} F^{O}(i) \quad ; \quad \begin{array}{l} \forall i=1,...,N \\ \forall k=1,...,n \end{array} \tag{2.13}$$

Finally, the component balances for the reactive flash separators in the OP are expressed as shown in Eq.(2.14).

$$f_k^P(i) + R_k(i)H(i) - x_k^L(i)F^L(i) - y_k^V(i)F^V(i) = 0 \quad ; \quad \begin{matrix} \forall i = 1,...,\infty \\ \forall k = 1,...,n \end{matrix} \tag{2.14}$$

A minimum residence time τ is proposed for the feasible reactive flash separators in the network. The capacity of each reactive flash in the OP is determined by either the reactive holdup, Eq.(2.15), or the residence time times the reactive flash inlet flow, Eq.(2.16), whichever is greater.

$$C(i) \geq H(i) \quad ; \quad \forall i = 1,...,\infty \tag{2.15}$$

$$C(i) \geq \tau F^P(i) \quad ; \quad \forall i = 1,...,\infty \tag{2.16}$$

By substituting Eq.(2.7) in Eq.(2.16), the capacity must then satisfy:

$$C(i) \geq \tau \left[\sum_{j=1}^{M} F^{PI}(i,j) + \sum_{j=1}^{\infty} F^{PL}(i,j) + \sum_{j=1}^{\infty} F^{PV}(i,j) \right] \quad ; \quad \forall i = 1,...,\infty \tag{2.17}$$

The number of variables can be reduced by substituting Eq.(2.4) to Eq.(2.6) in Eq.(2.14):

$$\begin{aligned} & R_k(i)H(i) - x_k^L(i)\left[\sum_{j=1}^{N} F^{OL}(j,i) + \sum_{j=1}^{\infty} F^{PL}(j,i) \right] \\ & - y_k^V(i)\left[\sum_{j=1}^{N} F^{OV}(j,i) + \sum_{j=1}^{\infty} F^{PV}(j,i) \right] + \sum_{j=1}^{M} z_k^I(j) F^{PI}(i,j) \quad ; \quad \begin{matrix} \forall i = 1,...,\infty \\ \forall k = 1,...,n \end{matrix} \\ & + \sum_{j=1}^{\infty} x_k^L(j) F^{PL}(i,j) + \sum_{j=1}^{\infty} y_k^V(j) F^{PV}(i,j) = 0 \end{aligned} \tag{2.18}$$

From Eq.(2.18), self-recycling flows are naturally eliminated from the system. This fact can lead to further simplifications as shown in Eq.(2.19):

$$
\begin{aligned}
& R_k(i)H(i)+\sum_{j=1}^{M} z_k^I(j)F^{PI}(i,j) \\
& -\sum_{j=1}^{N} x_k^L(i)F^{OL}(j,i)-\sum_{j=1}^{N} y_k^V(i)F^{OV}(j,i) \\
& +\sum_{\substack{j=1 \\ j\neq i}}^{\infty}\left[x_k^L(j)F^{PL}(i,j)-x_k^L(i)F^{PL}(j,i)\right] \qquad ; \quad \begin{matrix}\forall i=1,\ldots,\infty \\ \forall k=1,\ldots,n\end{matrix} \\
& +\sum_{\substack{j=1 \\ j\neq i}}^{\infty}\left[y_k^V(j)F^{PV}(i,j)-y_k^V(i)F^{PV}(j,i)\right]=0
\end{aligned}
\tag{2.19}
$$

Some variables in the component outlet bounds equations can be eliminated substituting Eq.(2.5) in Eq.(2.13):

$$
\left(z_k^O(i)\right)^l \begin{bmatrix} \sum_{j=1}^{M} F^{OI}(i,j) \\ +\sum_{j=1}^{\infty} F^{OL}(i,j) \\ +\sum_{j=1}^{\infty} F^{OV}(i,j) \end{bmatrix} \le \begin{bmatrix} \sum_{j=1}^{M} z_k^I(j)F^{OI}(i,j) \\ +\sum_{j=1}^{\infty} x_k^L(j)F^{OL}(i,j) \\ +\sum_{j=1}^{\infty} y_k^V(j)F^{OV}(i,j) \end{bmatrix} \le \left(z_k^O(i)\right)^u \begin{bmatrix} \sum_{j=1}^{M} F^{OI}(i,j) \\ +\sum_{j=1}^{\infty} F^{OL}(i,j) \\ +\sum_{j=1}^{\infty} F^{OV}(i,j) \end{bmatrix} ; \begin{matrix}\forall i=1,\ldots,N \\ \forall k=1,\ldots,n\end{matrix} \tag{2.20}
$$

Moreover, Eq.(2.20) can then be split into two inequalities:

$$
\begin{aligned}
& \sum_{j=1}^{M}\left[\left(\left(z_k^O(i)\right)^l - z_k^I(j)\right)F^{OI}(i,j)\right] \\
& +\sum_{j=1}^{\infty}\left[\left(\left(z_k^O(i)\right)^l - x_k^L(j)\right)F^{OL}(i,j)\right] \qquad ; \quad \begin{matrix}\forall i=1,\ldots,N \\ \forall k=1,\ldots,n\end{matrix} \\
& +\sum_{j=1}^{\infty}\left[\left(\left(z_k^O(i)\right)^l - y_k^V(j)\right)F^{OV}(i,j)\right] \le 0
\end{aligned}
\tag{2.21}
$$

$$
\begin{aligned}
& \sum_{j=1}^{M}\left[\left(\left(z_k^O(i)\right)^u - z_k^I(j)\right)F^{OI}(i,j)\right] \\
& +\sum_{j=1}^{\infty}\left[\left(\left(z_k^O(i)\right)^u - x_k^L(j)\right)F^{OL}(i,j)\right] \qquad ; \quad \begin{matrix}\forall i=1,\ldots,N \\ \forall k=1,\ldots,n\end{matrix} \\
& +\sum_{j=1}^{\infty}\left[\left(\left(z_k^O(i)\right)^u - y_k^V(j)\right)F^{OV}(i,j)\right] \ge 0
\end{aligned}
\tag{2.22}
$$

In order to make it easier to calculate and restrict the total size of the network, a total capacity constraint with upper bound C^{ub} was modeled. This constraint, Eq.(2.23), is used to investigate process intensification opportunities in the network, enabling the search for the smallest feasible network for the specified problem.

$$\sum_{i=1}^{\infty} C(i) \leq C^{ub} \tag{2.23}$$

As mentioned before, a distributed heat system is considered so that each reactive flash separator has the ability to exchange heat with an external source that provides the necessary load for the reactive-separative operation. Therefore, for the isobaric, isothermal, steady-state reactive flash separator i in the network, the energy balance is presented in Eq.(2.24).

$$\dot{Q}(i) + h^{P}(i) F^{P}(i) = h^{L}(i) F^{L}(i) + h^{V}(i) F^{V}(i) + \dot{W}(i) \quad ; \quad \forall i = 1, ..., \infty \tag{2.24}$$

In the equation above, $\dot{Q}$ is the heat transferred from or to the system, while h^{P}, h^{L} and h^{V} correspond to the total molar enthalpy of the reactive flash inlet, liquid outlet, and vapor outlet, respectively. The use of total enthalpy instead of partial enthalpies allows a more general formulation since the relation between the total enthalpy of the mixture and the enthalpy of each of the mixture component can be treated later through ideal or non-ideal enthalpy models. Moreover, since no work is done or received by the flash separator and the system is considered isobaric, $\dot{W}$ is zero for all reactive flashes in the network, and all energy effects are captured through heat transfer and enthalpy changes.

According to the distribution network, $F^P(i)$ and $h^P(i)$ are determined by summing up the streams originated in other points of the network that feed the reactive flash i. Thus, the energy flow entering the reactive flash separator i control volume is shown in Eq.(2.25).

$$h^P(i)F^P(i)=\left\{\begin{array}{l}\sum_{j=1}^{M}h^I(j)F^{PI}(i,j)\\ +\sum_{\substack{j=1\\ j\neq i}}^{\infty}h^L(j)F^{PL}(i,j)\\ +\sum_{\substack{j=1\\ j\neq i}}^{\infty}h^V(j)F^{PV}(i,j)\end{array}\right\}\quad;\quad \forall i=1,...,\infty \tag{2.25}$$

In Eq.(2.25), $h^I(j)$ represents the total enthalpy of the j^{th} inlet stream and M represents the number of network inlets. Also, self-recycling flows were eliminated from this system as shown in Eq.(2.18). Thus, the energy balance in each reactive flash separator in the OP has the form shown in Eq.(2.26).

$$\dot{Q}(i)=\left\{\begin{array}{l}h^L(i)F^L(i)+h^V(i)F^V(i)\\ -\sum_{j=1}^{M}h^I(j)F^{PI}(i,j)\\ -\sum_{\substack{j=1\\ j\neq i}}^{\infty}h^L(j)F^{PL}(i,j)\\ -\sum_{\substack{j=1\\ j\neq i}}^{\infty}h^V(j)F^{PV}(i,j)\end{array}\right\}\quad;\quad \forall i=1,...,\infty \tag{2.26}$$

Equations (2.8) and (2.9) show the splitting balance when the $F^L(i)$ liquid and $F^V(i)$ vapor flows enter the DN's after being processed in the OP. Thus, Eq.(2.26) can be rewritten as:

$$\dot{Q}(i)=\left\{\begin{array}{l}\left[\sum_{j=1}^{N}h^{L}(i)F^{OL}(j,i)+\sum_{\substack{j=1\\ j\neq i}}^{\infty}h^{L}(i)F^{PL}(j,i)\right]\\ +\left[\sum_{j=1}^{N}h^{V}(i)F^{OV}(j,i)+\sum_{\substack{j=1\\ j\neq i}}^{\infty}h^{V}(i)F^{PV}(j,i)\right]\\ -\sum_{j=1}^{M}h^{I}(j)F^{PI}(i,j)-\sum_{\substack{j=1\\ j\neq i}}^{\infty}h^{L}(j)F^{PL}(i,j)\\ -\sum_{\substack{j=1\\ j\neq i}}^{\infty}h^{V}(j)F^{PV}(i,j)\end{array}\right\}\quad;\quad\forall i=1,...,\infty \qquad (2.27)$$

The value of the heat transferred to each reactive flash can have negative or positive values, indicating that heat is either released by the system or given to the system, respectively. This value depends on the energetic needs of each given unit during the synthesis process, so the identification of either endothermicity or exothermicity in each reactive flash is established by the optimization process.

2.3.3. IDEAS ILP approximation by finite LPs

The IDEAS framework creates an infinite linear programming (ILP), which cannot be solved explicitly. Nevertheless, its solution can be approximated by a series of finite linear programming of increasing size, whose sequence of optimum values converges to the infinite dimensional problem's infimum. Thus, if one considers a finite number G instead of an infinite number of dimensions, where G corresponds to the number of reactive flash separators available for the synthesis problem, the problem becomes an LP which in turn is convex and can be solved by a variety of different LP solvers.

The ILP approximation occurs when one allows G to contain an ever-increasing number of reactive flash-separator units, such that the optimum objective function values of each LP solved forms a non-increasing sequence that converges to the ILP infimum. Thus, considering that the optimal value for the corresponding finite LP is ν^*, and that the finite LP can be solved η times using an ever-increasing number G of reactive flash separators, i.e. $G(1) < G(2) < ... < G(\eta)$, the resulting optimal values of each finite LP form a non-increasing sequence $\nu^*(1) > \nu^*(2) > ... > \nu^*(\eta)$, which converges to the infimum of the ILP when $\eta \to \infty$. The convergence to the infimum is shown in the case study presented in this work.

2.3.4. Objective function and final IDEAS LP formulation

For the total energy minimization problem, the objective function has the format shown in Eq.(2.28), where G corresponds to the number of reactive flash separators in the OP for the finite LP formulation and IDEAS ILP procedure infimum approximation.

$$\min \sum_{i=1}^{G} \left| \dot{Q}(i) \right| \tag{2.28}$$

This objective function captures the least amount of energy needed by the reactive separation process network. This task is performed by minimizing the sum of the absolute value of the heat needed in each reactive flash separator, where $\dot{Q}(i)$ can be either a positive or negative number, i.e., $-\infty \le \dot{Q}(i) \le \infty$, which in turn shows if the reactive flash is being cooled or heated.

The nonlinearity given by the absolute value function can be overcome by using a transformation strategy. First, $\dot{Q}(i)$ is defined as the difference of two non-negative variables, as shown in Eq.(2.29).

$$\dot{Q}(i) = \dot{Q}_H(i) - \dot{Q}_C(i) \quad ; \quad \forall i = 1,...,G \tag{2.29}$$

The physical meaning of $\dot{Q}_H$ and $\dot{Q}_C$ are consistent with common design variables used in defining heat or cooling needs of a process unit, and represents the heat consumed or discarded by the system, respectively. The resulting objective function and respective impacted constraints is shown in Eq.(2.30) to (2.32).

$$\min \sum_{i=1}^{G} \left| \dot{Q}_H(i) - \dot{Q}_C(i) \right| \tag{2.30}$$

$$\left\{ \begin{array}{l} \dot{Q}_H(i) - \dot{Q}_C(i) - \left[\sum_{j=1}^{N} h^L(i) F^{OL}(j,i) + \sum_{j=1}^{G} h^L(i) F^{PL}(j,i) \right] \\ \quad - \left[\sum_{j=1}^{N} h^V(i) F^{OV}(j,i) + \sum_{j=1}^{G} h^V(i) F^{PV}(j,i) \right] \\ \quad + \sum_{j=1}^{M} h^I(j) F^{PI}(i,j) + \sum_{j=1}^{G} h^L(j) F^{PL}(i,j) \\ \quad + \sum_{j=1}^{G} h^V(j) F^{PV}(i,j) \end{array} \right\} = 0 \quad ; \quad \forall i = 1,...,G \tag{2.31}$$

$$\dot{Q}_H(i) \geq 0; \dot{Q}_C(i) \geq 0 \tag{2.32}$$

This problem is still nonlinear because of the absolute value term on Eq.(2.30). Nevertheless, whenever either $\dot{Q}_H(i)$ or $\dot{Q}_C(i)$ is equal zero, the absolute value expression reduces to zero plus a positive term and can be eliminated. This condition is naturally satisfied by the minimization problem, i.e., at least one of the two variables representing the absolute value of $\dot{Q}(i)$ are equal zero at the optimal solution. This makes sense intuitively because, even though a

given value of $\dot{Q}(i)$ can be expressed by $\dot{Q}_H(i)$ and $\dot{Q}_L(i)$ in infinite different forms, the only case where $\dot{Q}(i)$ is either equal to $\dot{Q}_H(i)$ and $\dot{Q}_C(i)$ is when $\dot{Q}_H(i)+\dot{Q}_C(i)$ reaches their minimum value, which happens only when one of the two is zero. Thus, the absolute value expression in the objective function can be simplified as the sum of the two variables, as shown in Eq.(2.33).

$$\left|\dot{Q}_H(i)-\dot{Q}_C(i)\right|=\left|\dot{Q}_H(i)\right|+\left|\dot{Q}_C(i)\right|=\dot{Q}_H(i)+\dot{Q}_C(i) \quad ; \quad \begin{cases}\dot{Q}_H(i)=0 \vee \dot{Q}_C(i)=0 \\ \forall i=1,...,G\end{cases} \tag{2.33}$$

Thus, the objective function of the total energy minimization problem has the form shown in Eq.(2.34).

$$\min \sum_{i=1}^{G}\left[\dot{Q}_H(i)+\dot{Q}_C(i)\right] \tag{2.34}$$

An alternative way to deal with the presence of summations of absolute values in infinite dimensional optimization problems is presented by Sourlas and Manousiouthakis [34], who have employed it in identifying the best achievable performance over all linear time-invariant decentralized controllers. Considering that, the final IDEAS finite LP formulation for the total energy minimization problem in a reactive distillation network has the objective function shown in Eq.(2.34), subject to the constraints presented in Eq.(2.4), (2.11), (2.12), (2.15), (2.17), (2.19), (2.21), (2.22), (2.23), (2.31) and (2.32), all summarized in Eq.(2.35), where $\dot{Q}_{\text{tot}}$ is used to store the value of optimal solution.

$$\dot{Q}_{\text{tot}}=\min \sum_{i=1}^{G}\left[\dot{Q}_H(i)+\dot{Q}_C(i)\right] \tag{2.35}$$

s.t.

$$\left\{\begin{array}{l}\dot{Q}_H(i)-\dot{Q}_C(i)-\left[\sum_{j=1}^{N}h^L(i)F^{OL}(j,i)+\sum_{j=1}^{G}h^L(i)F^{PL}(j,i)\right]\\ \quad-\left[\sum_{j=1}^{N}h^V(i)F^{OV}(j,i)+\sum_{j=1}^{G}h^V(i)F^{PV}(j,i)\right]\\ \quad+\sum_{j=1}^{M}\sum_{k=1}^{n}z_k^I(j)h_k^I(j)F^{PI}(i,j)+\sum_{j=1}^{G}h^L(j)F^{PL}(i,j)\\ \quad+\sum_{j=1}^{G}h^V(j)F^{PV}(i,j)\end{array}\right\}=0 \qquad \forall i=1,\ldots,G$$

$$F^I(j)-\sum_{i=1}^{N}F^{OI}(i,j)-\sum_{i=1}^{G}F^{PI}(i,j)=0 \qquad \forall j=1,\ldots,M$$

$$\left[\sum_{j=1}^{M}F^{OI}(i,j)+\sum_{j=1}^{G}F^{OL}(i,j)+\sum_{j=1}^{G}F^{OV}(i,j)\right]-\left(F^O(i)\right)^l\geq 0 \qquad \forall i=1,\ldots,N$$

$$\left[\sum_{j=1}^{M}F^{OI}(i,j)+\sum_{j=1}^{G}F^{OL}(i,j)+\sum_{j=1}^{G}F^{OV}(i,j)\right]-\left(F^O(i)\right)^u\leq 0 \qquad \forall i=1,\ldots,N$$

$$C(i)\geq H(i) \qquad \forall i=1,\ldots,G$$

$$C(i)\geq \tau\left[\sum_{j=1}^{M}F^{PI}(i,j)+\sum_{j=1}^{G}F^{PL}(i,j)+\sum_{j=1}^{G}F^{PV}(i,j)\right] \qquad \forall i=1,\ldots,G$$

$$\begin{array}{l}R_k(i)H(i)+\sum_{j=1}^{M}z_k^I(j)F^{PI}(i,j)-\sum_{j=1}^{N}x_k^L(i)F^{OL}(j,i)-\sum_{j=1}^{N}y_k^V(i)F^{OV}(j,i)+\\ +\sum_{\substack{j=1\\ j\neq i}}^{G}\left[x_k^L(j)F^{PL}(i,j)-x_k^L(i)F^{PL}(j,i)\right]+\sum_{\substack{j=1\\ j\neq i}}^{G}\left[y_k^V(j)F^{PV}(i,j)-y_k^V(i)F^{PV}(j,i)\right]=0\end{array} \qquad \begin{array}{l}\forall i=1,\ldots,G\\ \forall k=1,\ldots,n\end{array}$$

$$\begin{array}{l}\sum_{j=1}^{M}\left[\left(\left(z_k^O(i)\right)^l-z_k^I(j)\right)F^{OI}(i,j)\right]+\sum_{j=1}^{G}\left[\left(\left(z_k^O(i)\right)^l-x_k^L(j)\right)F^{OL}(i,j)\right]+\\ \qquad+\sum_{j=1}^{G}\left[\left(\left(z_k^O(i)\right)^l-y_k^V(j)\right)F^{OV}(i,j)\right]\leq 0\end{array} \qquad \begin{array}{l}\forall i=1,\ldots,N\\ \forall k=1,\ldots,n\end{array}$$

$$\begin{array}{l}\sum_{j=1}^{M}\left[\left(\left(z_k^O(i)\right)^u-z_k^I(j)\right)F^{OI}(i,j)\right]+\sum_{j=1}^{G}\left[\left(\left(z_k^O(i)\right)^u-x_k^L(j)\right)F^{OL}(i,j)\right]\\ \qquad+\sum_{j=1}^{G}\left[\left(\left(z_k^O(i)\right)^u-y_k^V(j)\right)F^{OV}(i,j)\right]\geq 0\end{array} \qquad \begin{array}{l}\forall i=1,\ldots,N\\ \forall k=1,\ldots,n\end{array}$$

$$C^{tot} = \sum_{i=1}^{G} C(i)$$

$$H^{tot} = \sum_{i=1}^{G} H(i)$$

$$\left(F^{P}\right)^{tot} = \left\{ \begin{array}{l} \sum_{i=1}^{G}\sum_{j=1}^{M} F^{PI}(i,j) + \sum_{i=1}^{G}\sum_{\substack{j=1 \\ j\neq i}}^{G} F^{PL}(i,j) \\ \quad + \sum_{i=1}^{G}\sum_{\substack{j=1 \\ j\neq i}}^{G} F^{PV}(i,j) \end{array} \right\}$$

$$Q^{tot} = \sum_{i=1}^{G} Q_H(i) + \sum_{i=1}^{G} Q_C(i)$$

$$Q_H \geq 0; Q_C \geq 0; F^{I} \geq 0;\ F^{OI} \geq 0; F^{PI} \geq 0; F^{OL} \geq 0; F^{OV} \geq 0; F^{PL} \geq 0; F^{PV} \geq 0; H \geq 0; C \geq 0;$$

$$0 \leq C^{tot} \leq C^{ub};\ 0 \leq H^{tot} \leq H^{ub};\ 0 \leq \left(F^{P}\right)^{tot} \leq \left(F^{P}\right)^{ub};\ 0 \leq Q^{tot} \leq Q^{ub};$$

Since all variables represent physical quantities (flowrate, catalyst amount, stage volume, stage duty), they can have only non-negative values. In addition to that, the total reactive holdup, total capacity, total flow, and total energy can have their upper bound specified in the synthesis process.

2.3.5. Enthalpy model discussion

In general, for a multicomponent mixture of n species and component molar fraction z_i, the molar enthalpy is quantified by summing its ideal value h^{id} with its excess value h^{E} [56], as shown in Eq.(2.36).

$$h\left(T, P, \{z_k\}_{k=1}^{n}\right) = h^{id}\left(T, \{z_k\}_{k=1}^{n}\right) + h^{E}\left(T, P, \{z_k\}_{k=1}^{n}\right) \tag{2.36}$$

Since the ideal model is independent of pressure, each component enthalpy can be evaluated at the mixture pressure instead of its correspondent component partial pressure [56]. Therefore, due to the summability relation of the partial properties, the ideal mixture molar enthalpy can be calculated as shown in Eq.(2.36).

$$h^{id}\left(T,\{z_k\}_{k=1}^{n}\right)=\sum_{k=1}^{n} z_k h_k\left(T\right) \tag{2.37}$$

The excess molar enthalpy h^E can be evaluated from the excess Gibbs free energy G^E, which is a function of the mixture temperature, pressure, and composition. Moreover, the excess Gibbs free energy can be expressed in terms of the components' fugacity pressure [56]. In this case study presented in this work, the mixture is considered to be ideal. Thus, the excess molar enthalpy h^E is considered zero and the molar enthalpy of the multicomponent mixture h is equal to its ideal value h^{id}, as shown in Eq.(2.38).

$$h\left(T,\{z_k\}_{k=1}^{n}\right)=h^{id}\left(T,\{z_k\}_{k=1}^{n}\right)=\sum_{k=1}^{n} z_k h_k\left(T\right) \tag{2.38}$$

Any applicable model can provide enthalpy values. The choice depends primarily on the nature of the fluids. For a reactive flash separator operating at constant pressure, the total molar enthalpy h is a function of temperature, and composition only. Therefore, one can write the liquid and vapor enthalpies of the k^{th} component in the i^{th} reactive flash as shown in Eq.(2.39) and (2.40) below:

$$h_k^L\left(i\right)=h_k^L\left(T\left(i\right),x_k\left(i\right)\right) \quad ; \quad \begin{matrix}\forall k\in\{1,...,\,n\}\\ \forall i\in\{1,...,G\}\end{matrix} \tag{2.39}$$

$$h_k^V\left(i\right)=h_k^V\left(T\left(i\right),y_k\left(i\right)\right) \quad ; \quad \begin{matrix}\forall k\in\{1,...,\,n\}\\ \forall i\in\{1,...,G\}\end{matrix} \tag{2.40}$$

Let the heat capacity be denoted $C_k^{p,L}$ and $C_k^{p,V}$ for the liquid and vapor of component k, respectively. Then the k^{th} component molar liquid and vapor enthalpy is given by Eq.(2.41) and (2.42).

$$h_k^L(T) = \int C_k^{p,L} dT \tag{2.41}$$

$$h_k^V(T) = \int C_k^{p,V} dT \tag{2.42}$$

The k^{th} component enthalpy of formation h_k^0 is by definition the enthalpy of the pure component at the standard reference state, i.e., temperature equals 25°C and pressure equals 1 atm. Thus, assuming a 3rd order polynomial that correlates both liquid and vapor heat capacities of species k, as shown in Eq.(2.43) below,

$$\frac{C_k^P}{R} = c_{k,1} + c_{k,2}T + c_{k,3}T^2 + c_{k,4}T^3 \tag{2.43}$$

the enthalpy from the temperature of the reference state T^0 to the operating temperature T one can be solved as shown in Eq.(2.44).

$$\begin{aligned}
&h_k(T) - h_k^0(T^0) = \int_{T^0}^{T} R\left(c_{k,1} + c_{k,2}T + c_{k,3}T^2 + c_{k,4}T^3\right)dT = \\
&= R\left[\int_{T^0}^{T} c_{k,1}\,dT + \int_{T^0}^{T} c_{k,2}T\,dT + \int_{T^0}^{T} c_{k,3}T^2 dT + \int_{T^0}^{T} c_{k,4}T^3 dT\right] = \\
&= \left(Rc_{k,1}T + \frac{R}{2}c_{k,2}T^2 + \frac{R}{3}c_{k,3}T^3 + \frac{R}{4}c_{k,4}T^4\right)\Bigg|_{T^0}^{T} = \\
&= Rc_{k,1}\left[T - T^0\right] + \frac{R}{2}c_{k,2}\left[T^2 - \left(T^0\right)^2\right] + \frac{R}{3}c_{k,3}\left[T^3 - \left(T^0\right)^3\right] + \frac{R}{4}c_{k,4}\left[T^4 - \left(T^0\right)^4\right]
\end{aligned} \tag{2.44}$$

In the reactive flash separator outlets, the multicomponent mixture streams exit the system in saturated forms, either liquid or vapor, depending on the flash separator outlet. If pure species k is liquid at the standard condition, i.e., T^0 is lower than the species normal boiling

point T_k^b, the fraction of k that appears in the mixture at the vapor outlet must consider its the heat of vaporization regardless of the flash temperature. The same approach is valid when pure species k is in vapor phase at standard condition $\left(T^0 \geq T_k^b\right)$ and shows up in the liquid output of a multicomponent list at VLE conditions. In the latest case, the component k enthalpy at the mixture liquid stream should consider the heat necessary for its liquefaction. By defining λ_k^b as the dimensionless heat of vaporization of species k, this approach is described below by Eq.(2.45) and (2.46) for the liquid and vapor enthalpic contribution of species k in a mixture, respectively.

$$\begin{cases} h_k^L = h_k\left(T\right) & ; \quad if \quad T^0 \leq T_k^b \\ h_k^L = h_k\left(T\right) - \lambda_k^b R T_k^b & ; \quad if \quad T^0 \geq T_k^b \end{cases} \tag{2.45}$$

$$\begin{cases} h_k^V = h_k\left(T\right) + \lambda_k^b R T_k^b & ; \quad if \quad T^0 \leq T_k^b \\ h_k^V = h_k\left(T\right) & ; \quad if \quad T^0 \geq T_k^b \end{cases} \tag{2.46}$$

Separations of different species in both reactive and non-reactive flashes rely on vapor-liquid equilibrium (VLE) conditions to occur. Thus, once species composition is specified in a flash liquid outlet for example, the vapor molar fractions at the flash's operating temperature are also fixed due to the equilibrium conditions and can be calculated iteratively. This procedure was successfully used in several applications featuring reactive and non-reactive distillation systems [18,30,55]. Considering that the reactive flash's temperature, pressure, and outlet compositions are fixed by the VLE condition, so are the specific total molar enthalpies at the outlets, regardless of the enthalpy model used. Thus, by recalling Eq.(2.38) for the reactive flash separator presented in this work, the total molar enthalpy for the vapor and liquid mixture streams exiting each flash

have the form shown in Eq.(2.47) and (2.48) , respectively, under the conditions presented in Eq.(2.45) and (2.46).

$$h^L(i) = \sum_{k=1}^{n} x_k(i) h_k^L(i) \qquad ; \qquad \forall i \in \{1,...,G\} \tag{2.47}$$

$$h^V(i) = \sum_{k=1}^{n} y_k(i) h_k^V(i) \qquad ; \qquad \forall i \in \{1,...,G\} \tag{2.48}$$

The formulation described in this session, based on the IDEAS framework and applicable thermodynamic concepts, was applied in a study case featuring the metathesis of 2-pentene.

2.4. Case study: Olefin metathesis

2.4.1. Thermodynamic data and problem specifications

Metathesis reactions are used in the petrochemical industry to rebalance the light olefins originated during the catalytic and steam cracking processes. In this case study, the formulation based on the IDEAS framework is applied in the intensification of a reactive separation network for 2-butene and 3-hexene production through metathesis of 2-pentene, as shown in Eq.(2.49).

$$2C_5H_{10} \rightleftarrows C_4H_8 + C_6H_{12} \tag{2.49}$$

The hydrocarbons involved in this system are similar in chemical structure, and deviations from ideality are negligible. Moreover, the components in the mixture have normal boiling points temperatures that are far from each other – 2-pentene at 310 K, 2-butene at 277 K, and 3-hexene at 340 K – allowing an easy separation through distillation process.

This reactive distillation system has negligible heat of reaction and, due to this fact, the system can run at atmospheric pressure or other low-pressure operating values without

significant changes on the value of the equilibrium constant. Considering 2-pentene as the reference component, the temperature dependent rate expression is given by Eq.(2.50) (Chen et al. 2000), while the reaction equilibrium constant K_{eq} and the kinetic rate constant $k_f\left(h^{-1}\right)$ are shown in Eq.(2.51) and Eq.(2.52) respectively:

$$R = k_f\left(a_{C_5H_{10}}^2 - \frac{a_{C_4H_8}\, a_{C_6H_{12}}}{K_{eq}}\right) \tag{2.50}$$

$$K_{eq} = 0.25 \tag{2.51}$$

$$k_f = 1.0661 \times 10^5\ e^{\left(-3321.2/T(K)\right)}\left(h^{-1}\right) \tag{2.52}$$

Since this system behaves as ideal, both the fugacity and the activity coefficient functions are equal the unity and Raoult's law is assumed. Moreover, the values of the species' molar fractions can be used in place of the respective activity coefficient in Eq.(2.3). Antoine's model is used to calculate the saturated pressure of each component in the mixture, and coefficients can be found in Table 2.1 for T in K and P in Pa.

Table 2.1. Antoine coefficients for 2-butene, 2-pentene, 3-hexene (Okasinski and Doherty 1998).

	$k = C_4H_8$	$k = C_5H_{10}$	$k = C_6H_{12}$
$A_{1,k}$	20.6909	20.723	20.7312
$A_{2,k}$	−2202.188	−2462.02	−2680.52
$A_{3,k}$	−36.578	−42.391	−48.401

As demonstrated in previous works[18,30,55], for a fixed value of the operating pressure P and for an specified liquid outlet composition, the respective bubble point temperature, reaction rate, and vapor outlet composition can be calculated iteratively by changing $T\left(i\right)$ in Eq.(2.53) until the sum of the molar fractions in the vapor phase is equal to unity, as specified in Eq.(2.56).

$$\ln P_k^{sat}(i) = A_{1,k} + \frac{A_{2,k}}{\left(T(i) + A_{3,k}\right)} \quad ; \quad \forall k = C_5H_{10},\, C_8H_8,\, C_6H_{12} \tag{2.53}$$

$$y_k^V(i) = \frac{x_k^L(i)\; P_k^{sat}\left(T(i)\right)}{P} \quad ; \quad \forall k = C_5H_{10},\, C_8H_8,\, C_6H_{12} \tag{2.54}$$

$$R(i) = 1.0661 \times 10^5 \; e^{\left(-3321.2/T(i)\right)} \left[\left(x_{C_5H_{10}}(i)\right)^2 - \frac{x_{C_4H_8}(i)\; x_{C_6H_{12}}(i)}{0.25} \right] \tag{2.55}$$

$$y^V_{C_5H_{10}}(i) + y^V_{C_4H_8}(i) + y^V_{C_6H_{12}}(i) - 1 = 0 \tag{2.56}$$

The coefficient values of the third order polynomial shown in Eq.(2.43), applied in the calculation of both liquid and vapor heat capacities, as well as the value of the dimensionless heat of vaporization for the 2-pentene metathesis system, are shown in Table 2.2.

Table 2.2. Thermodynamic data for the metathesis of 2-pentene (Okasinski and Doherty 1998).

Component:	$k = C_4H_8$	$k = C_5H_{10}$	$k = C_6H_{12}$
Liquid Heat Capacity			
$c_{1,k}$	13.357	21.224	19.897
$c_{2,k}$	−3.9752E−03	−6.9842E−02	−1.4182E−02
$c_{3,k}$	3.3249E−05	2.5206E−04	8.2626E−05
$c_{4,k}$	0.0	−1.7167E−07	0.0
Vapor Heat Capacity			
$c_{1,k}$	−6.256E−01	−1.8739	−2.9336
$c_{2,k}$	3.8721E−02	5.6102E−02	7.1697E−02
$c_{3,k}$	−1.6763E−05	−3.1656E−05	−4.3559E−05
$c_{4,k}$	1.877E−09	6.9946E−09	1.0609E−08
Normal Boiling Point (K)	276.87	310.08	339.60
Dimensionless Heat of Vaporization	10.178	10.294	10.166

Enthalpy calculations are based on the values shown in the table above, employed in the calculation method shown in Eq.(2.36) to Eq.(2.48).

For the reactive distillation process in this case study, the distribution network of IDEAS is set to have one inlet stream of pure 2-pentene at saturated liquid state, i.e., feed quality $q = 1$ as defined by Doherty and Malone [35], and two outlets streams: the first rich in 2-butene at saturated vapor state and the second rich in 3-hexene at saturated liquid state. Simulations were performed for the operating conditions specified in Table 2.3.

Table 2.3. Specifications for the 2-pentene metathesis problem example.

Feed Flow (kmol/h)	100
Outlet Flow 1 (Distillate) (kmol/h)	50
Outlet Flow 2 (Bottom) (kmol/h)	50
Residence Time (s)	60
Operating pressure (bar)	1
Feed quality	1
Inlet molar fractions	
C4H8	0.0000
C5H10	1.0000
C6H12	0.0000
Outlet molar fraction target bounds	
Outlet Flow 1	
C4H8	0.9800 - 1.0000
C5H10	0.0000 - 0.2000
C6H12	0.0000 - 0.2000
Outlet Flow 2	
C4H8	0.0000 - 0.2000
C5H10	0.0000 - 0.2000
C6H12	0.9800 - 1.0000

2.4.2. Discretization strategy and IDEAS convergence

The strategy developed to discretize the ternary liquid composition space follows the concept presented in a previous work [55], where different discretization steps were used in different regions of the composition domain to generate a finite set of reactive flash separators. In this work, three different regions are considered in the discretization strategy, whose limits are specified by the molar fractions α and β, as shown schematically in Fig. 2.3.

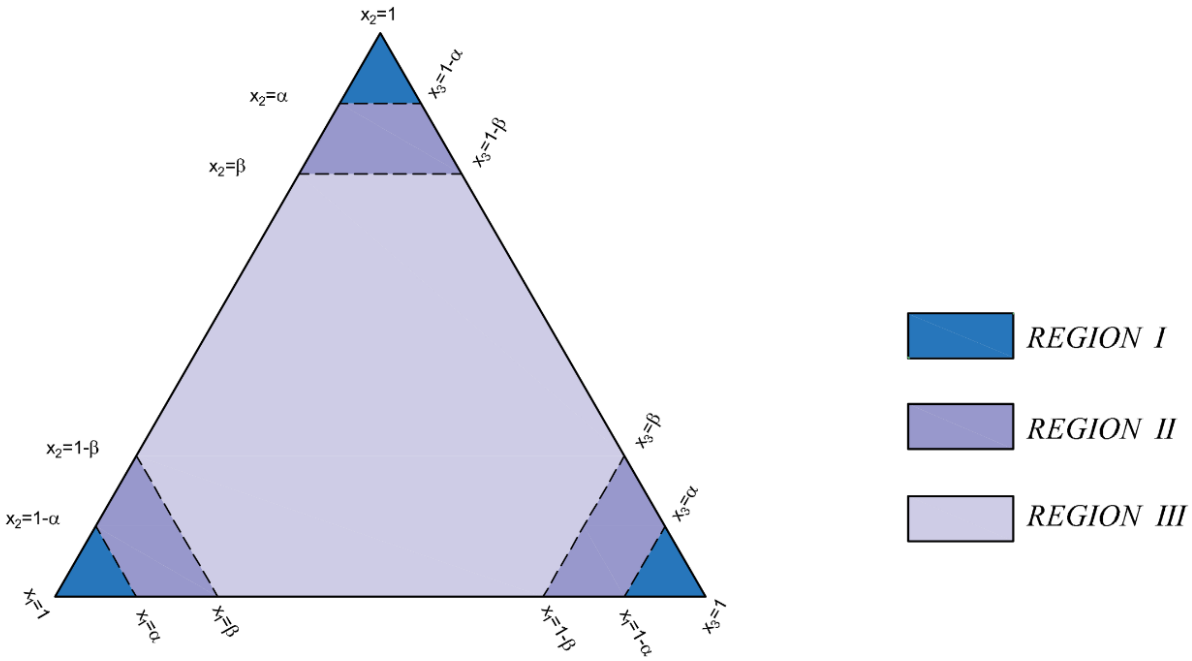

Figure 2.3 - Discretization strategy for the ternary liquid molar fraction domain

The procedure to accurately identify the discretization impact in a given region of the domain, which translates to the number of process units available for the optimization problem, consists in reducing the discretization step size (which increases the size of the reactive flash separator set G) until the impact of that in the optimization solution is negligible. As pointed out

in the referenced work, the feasibility of the problem and the optimization result is highly dependent on the discretization of region I, where separation is more difficult to obtain. For the total energy minimization problem, an additional assessment was performed in order to identify the impact that the growth of the cardinality G, specifically on regions I, II and III, had on the optimal solution. For this assessment the minimization of the total energy in the network was performed for a variety of discretization steps, as shown in Table 2.4. Results were obtained for $\alpha = 0.6665$ and $\beta = 0.5286$ as the region edges, which gives roughly the same number of flashes in each region. Moreover, a minimum purity of 87.5% was set for both butane and hexene.

Table 2.4. Optimal value for the energy minimization (87.5% purity, $\alpha = 0.6665$, $\beta = 0.5286$) per discretized set in regions I, II and III

Discretized step size			Number of Flashes in G	Minimum total energy (kW)
Region I	Region II	Region III		
1/16	1/16	1/8	124	5651.24
1/16	1/8	1/16	121	4962.36
1/16	1/16	1/16	153	3687.01
1/16	1/16	1/32	262	2910.60
1/16	1/32	1/16	319	2218.21
1/32	1/16	1/16	289	2196.30
1/16	1/32	1/32	427	1875.23
1/32	1/16	1/32	397	1327.56
1/32	1/32	1/16	454	1269.91
1/16	1/16	1/64	766	2214.22
1/16	1/64	1/16	838	1479.18
1/64	1/16	1/16	850	1265.77

To create a better understanding of the values shown in Table 2.4, results were plotted and grouped by discretization changes in each region and is shown in Fig.2.4. Once again, the imposition of smaller discretization (larger number of reactive flashes) in regions I and II results

in a much lower optimum value when compared to region III, showing that the set of reactive flash separators used to obtain each of the components in the mixture at high purity has a stronger influence in reducing the network energy consumption during the synthesis procedure.

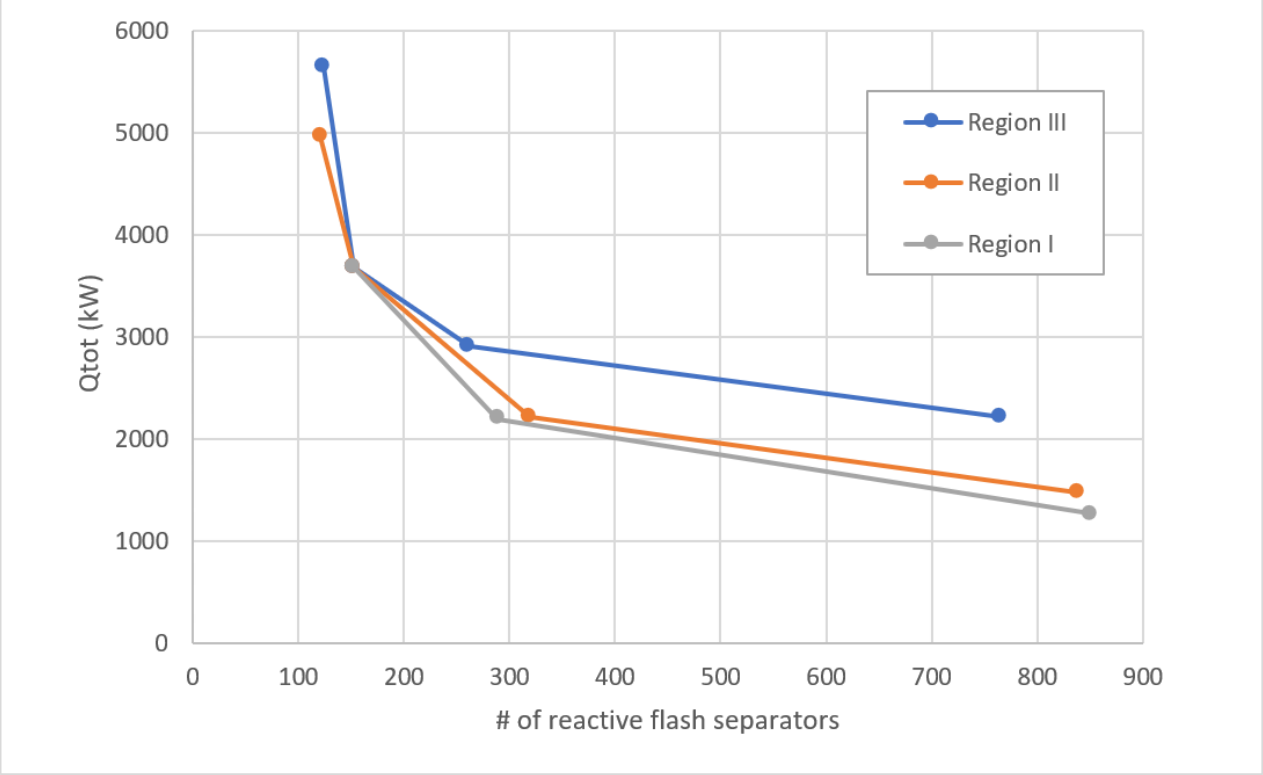

Figure 2.4 - Effect of smaller discretization steps in each region for the minimum total energy problem

The results also show three different convergence curves, which means that the approximation of the LP to the rate of approximation to the ILP infimum is faster depending not only on the number of reactive flashes in G, but also on the location of those flashes in the liquid molar fraction space.

The IDEAS full convergence plot for a minimum purity of 87.5% in the separation products is shown in Fig. 2.5. This result was obtained by setting $\alpha = 0.75$ and $\beta = 0.875$ as the region edges, and for the discretization shown in Table 2.5.

Table 2.5. Optimal value for the minimum energy problem (87.5% purity, $\alpha = 0.75$, $\beta = 0.875$) per discretized set in regions I, II and III

Discretized step size			Number of Flashes in G	Minimum total energy (kW)
Region I	Region II	Region III		
1/16	1/16	1/8	92	24249.8
1/16	1/16	1/16	153	3687.01
1/32	1/32	1/16	244	2222.71
1/32	1/32	1/32	561	1026.81
1/64	1/64	1/32	885	814.23
1/128	1/64	1/32	1209	803.61
1/256	1/64	1/32	2433	767.22

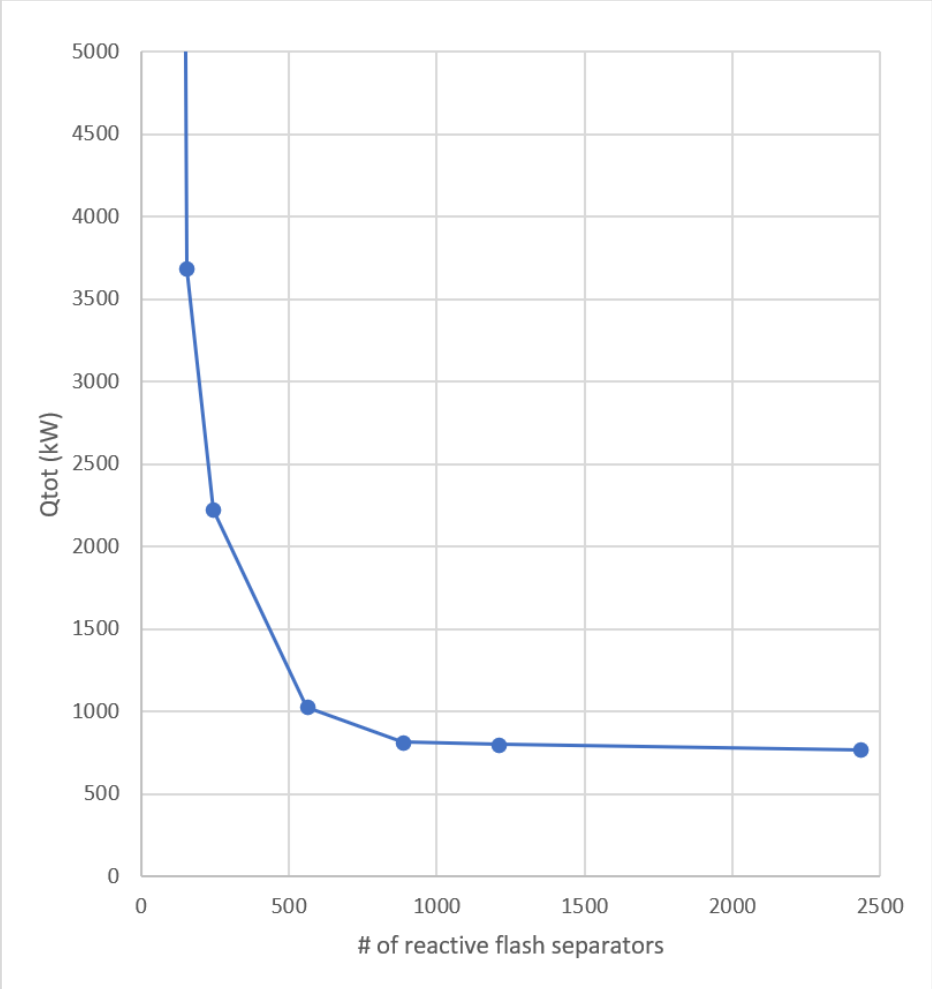

Figure 2.5 - IDEAS convergence plot for the energy minimization problem in the metathesis of 2-pentene (87.5% purity in the products).

2.4.3. IDEAS minimum energy consumption results

The optimization problem presented in Eq.(2.35) is used to solve the total energy minimization problem for the metathesis of 2-pentene through reactive separation. To define the finite set used by the IDEAS OP, a discretization level of 1/256, 1/128, and 1/64 was employed in regions I, II, and III, respectively. The total number of reactive flash separators in the set G is 2559, which is the result obtained when $\alpha = 0.96875$ and $\beta = 0.875$ are specified as the edges of the regions inside the liquid molar fraction domain.

A 2-pentene metathesis system simulated in UniSim® Design, featuring a reactor followed by sequence of distillation columns (Fig.2.6), is considered the baseline for comparison with the results obtained by the IDEAS approach. The system consists of a reactor operating with 48% conversion, which is close to the equilibrium conversion of 50%. The effluent from the reactor is sent to a distillation column (T-101) that separates the ternary mixture into a 2-butene stream with 98% purity at the distillate (saturated vapor state), and a binary mixtures of 2-pentene and 3-hexene at the bottom. Following that, the bottoms from the T-101 are sent to the distillation column T-102, where 3-hexene is separated at the bottom with a 98% purity. The distillate stream rich in 2-pentene from T-102 is recycled to the reactor. The input conditions, output production, and purity target of this baseline design are the same used in the IDEAS simulation, as listed in Table 2.3. The total amount of energy used by this reactor followed by distillation system baseline design is 6616.67 kW.

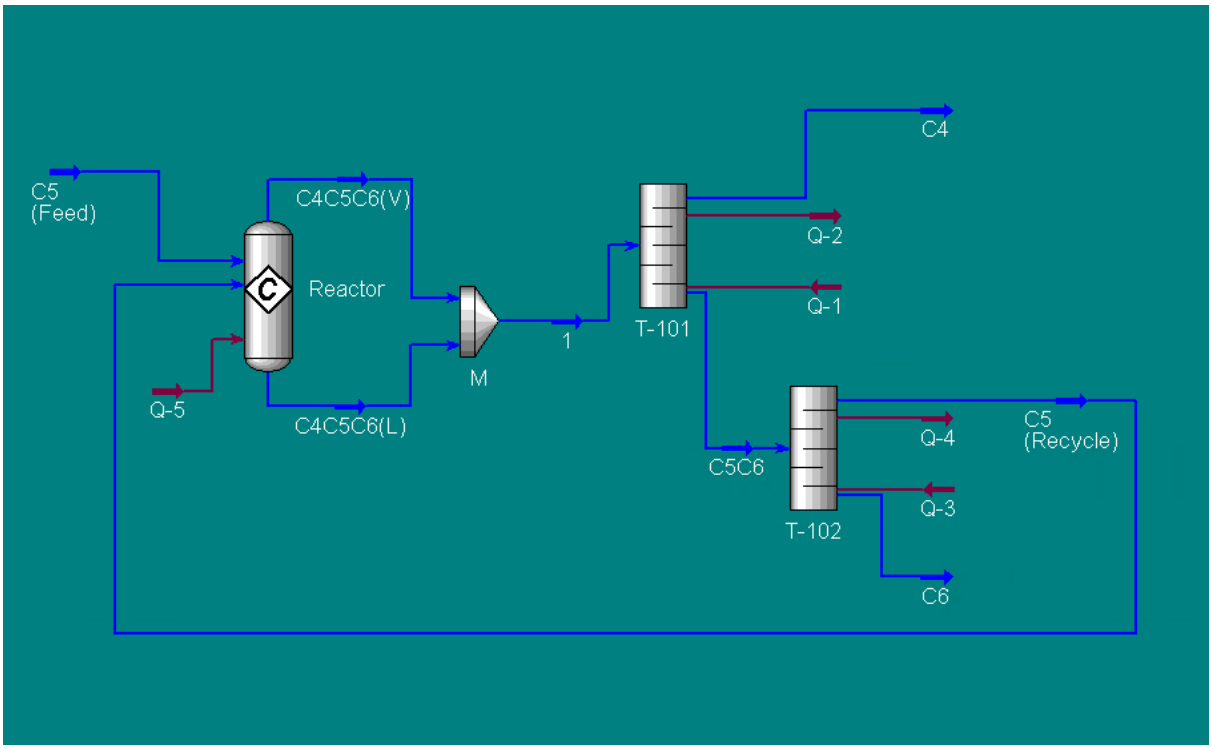

Figure 2.6 – UniSim® baseline for the Metathesis of 2-Pentene

The unbounded IDEAS result is 832.17 kW, which can be considered a close approximation to the global minimum that this technology can achieve for the conditions specified in Table 2.3. The results obtained by the IDEAS reactive separation network shows that the optimized system works with 12.58% of the energy required by the proposed baseline design. The results are shown in Fig.2.7 for comparison.

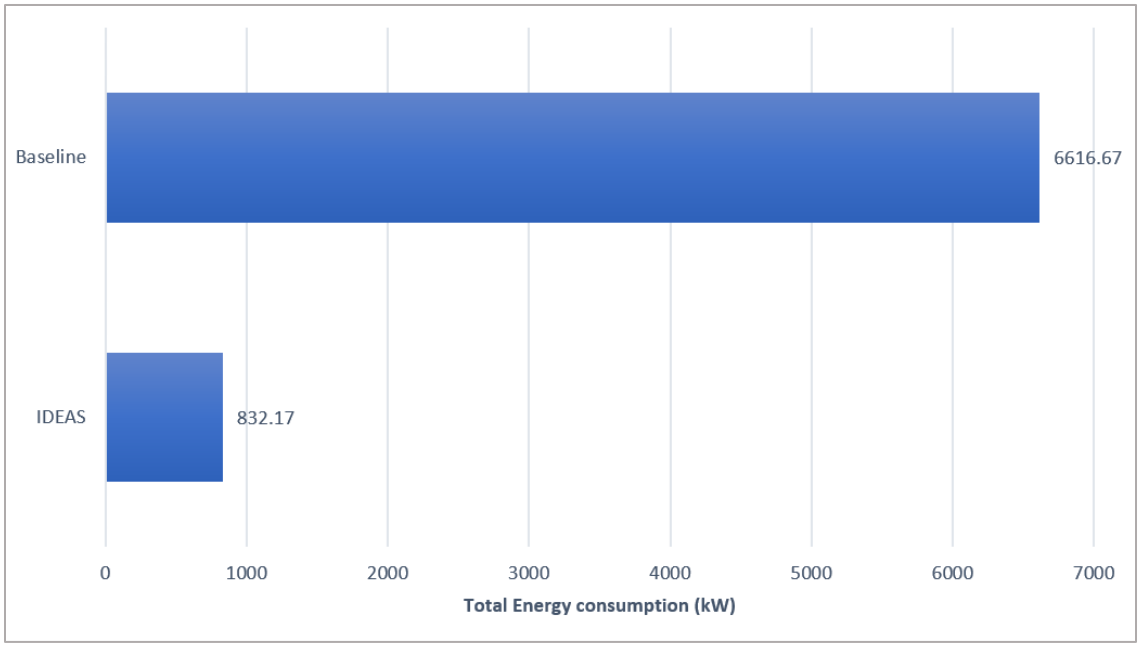

Figure 2.7 - Comparison between IDEAS results and Baseline

The investigation of the reactive separation network performance limit in regards to energy minimization is performed with a special interest in the relation to their corresponding intensified designs. The goal is to rigorously quantify tradeoffs between the network's total energy consumption and its total capacity. The identification of this relationship allows the assessment of energy-related impacts in intensified process designs using reactive distillation schemes. The LP problem presented in Eq.(2.35) is solved several times with an increasingly smaller value for the capacity upper bound until it reaches the feasibility limit, which allows the identification of the minimum energy requirements for each feasible capacity value needed to deliver the desired purity specifications. The tradeoff curve for the metathesis case study and the indication of the feasible region are presented in Fig.2.8.

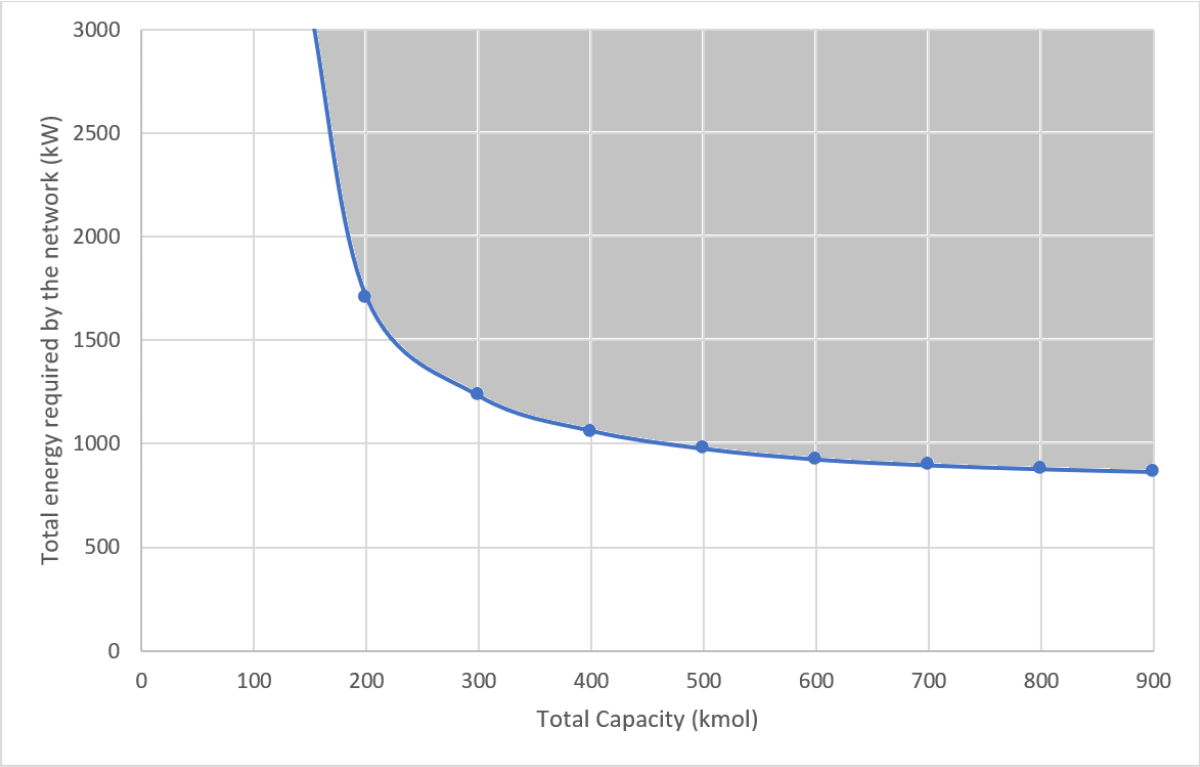

Figure 2.8 - Minimum energy performance limit for the 2-pentene metathesis problem for different network capacity values (feasible region in gray).

The tradeoff curve shows that the minimum total energy required by the reactive separation system increases for reductions in the capacity value. This is an indication that reactive distillation processes that have their size further intensified may require more energy, if they are already at the minimum energy consumption for a given total capacity. Systems that are located far from the performance limit curve can pursue reductions in both energy consumption and size through process intensification.

The fact that the minimum energy required by the reactive separation system increases for smaller network sizes is conceptually consistent with the idea of minimum reflux and minimum number of stages for distillation columns. The energy required by a separation system reduces for smaller values of reflux ratios, which in turns increase the number of stages in the

column, i.e., the size/capacity of the system has to be larger to meet the separation goals. On the other hand, for smaller number of stages (smaller sizes/capacities) the reflux ratio and consequently the energy required is larger. This indicates that the underlying conceptual base of distillation systems and separations is included in the approach used in the development of the IDEAS model. Nevertheless, it is important to point out that the system presented in the case study has negligible heat of reaction. Therefore, the impact of highly endothermic or exothermic reactions in reactive distillation systems may impact the shape of the tradeoff curve, although the general format may be unaltered due to the reasons mentioned in this paragraph.

2.5. Conclusions

The Infinite DimEnsionAl State-Space (IDEAS) framework is used as a tool to identify the performance limits of reactive separation systems featuring the minimum total energy required by the reactive separation process network. A model for the study of the energy effects in reactive separation systems is developed and applied through the IDEAS approach. The procedure leads to a linear program problem formulation, in which the optimal solution is guaranteed to be global over all possible network configurations. The model was used in the investigation of reactive separation for olefin metathesis. The case study features the metathesis of 2-pentene to form 2-butene and 3-hexene, an important chemical process for the oil industry. A distributed heat network system was considered in this work and was responsible to supply heating or cooling to individual process units (reactive flash separators) according to the system energetic needs. The minimum total energy required by the system was considered as the problem's objective, and results were obtained for unbounded systems and for increasingly

smaller capacity values, a variable of interest for process intensification. The goal is to rigorously quantify tradeoffs between the network's total energy consumption and its total capacity. The identification of this relationship allows the assessment of energy-related impacts in intensified process designs using reactive distillation schemes.

The globally minimized total energy required by the IDEAS based reactive separation metathesis system was 832.17 kW. Using a traditional reactor-followed-by-separation-system scheme as a baseline, an intensified IDEAS based reactive separation network uses 12.58% of the energy required by the baseline design. The tradeoff curve for minimum total energy consumption shows that the energy required by the reactive separation system increases for reductions in the capacity value. This result is consistent with the energy implications of a minimum reflux system – which corresponds to increases in size (number of trays) and energy demand reduction – and minimum number of stages (larger reflux ration and energy demand) for distillation columns. It is important to point out that systems located far from the performance limit curve in the minimum energy-capacity space can pursue further reductions in both energy consumption and size through process intensification.

2.6. Notation

Thermodynamic Variables*:*

P	Reactive flash separator pressure (Pa)
T	Reactive flash separator temperature (K)
$y_k^V(i)$	k^{th} Species equilibrium vapor composition leaving the i^{th} unit $(\dim)$
$x_k^L(i)$	k^{th} Species equilibrium liquid composition leaving the i^{th} unit $(\dim)$
$P_k^{sat}(T)$	k^{th} Species temperature dependent saturated vapor pressure (Pa)
$\phi_k\left(\left\{y_l^V\right\}_{l=1}^n, T, P\right)$	k^{th} Species non-ideal fugacity coefficient
$\gamma_k\left(\left\{x_l^L\right\}_{l=1}^n, T\right)$	k^{th} Species non-ideal liquid activity coefficient
a_k	Activity of the k^{th} species $(\dim)$
$A_{j,k}$	Antoine equation j^{th} parameter of the k^{th} species $(\dim)$
K_{eq}	Reaction equilibrium constant $(\dim)$
k_f	Forward reaction rate constant $(1/\mathrm{h})$

IDEAS Variables*:*

$F^{I}(i)$	i^{th} DN inlet stream
$F^{O}(i)$	i^{th} DN outlet stream
$F^{L}(i)$	i^{th} OP liquid outlet
$F^{V}(i)$	i^{th} OP vapor outlet
$F^{OI}(i,j)$	j^{th} DN inlet stream to i^{th} DN outlet
$F^{PI}(i,j)$	i^{th} OP inlet stream from j^{th} DN network inlet
$F^{OL}(i,j)$	i^{th} DN outlet stream from j^{th} OP liquid outlet
$F^{OV}(i,j)$	i^{th} DN outlet stream from j^{th} OP vapor outlet
$F^{PL}(i,j)$	i^{th} OP inlet stream from j^{th} OP liquid outlet
$F^{PV}(i,j)$	i^{th} OP inlet stream from j^{th} OP vapor outlet
$H(i)$	Reactive holdup of the i^{th} reactive flash separator unit in the OP
$C(i)$	Capacity of the i^{th} reactive flash separator unit in the OP
$\dot{Q}_H(i)$	Heat transferre to the i^{th} reactive flash separator unit in the OP

$\dot{Q}_L(i)$	Heat released by the i^{th} reactive flash separator unit in the OP
$z_k^I(i)$	k^{th} species, i^{th} DN inlet stream composition
$z_k^O(i)$	k^{th} species, i^{th} DN outlet stream composition
$\left(z_k^O(i)\right)^l$	k^{th} species, i^{th} DN outlet stream composition vector, lower bound
$\left(z_k^O(i)\right)^u$	k^{th} species, i^{th} DN outlet stream composition vector, upper bound
$x_k^L(i)$	k^{th} species, i^{th} OP liquid outlet composition
$y_k^V(i)$	k^{th} species, i^{th} OP vapor outlet composition
G	Total number of reactive flashes in the OP
M	Number of IDEAS network inlets
N	Number of IDEAS network outlets

2.7. References

(1) Kiss, A. A. Distillation Technology – Still Young and Full of Breakthrough Opportunities. *J. Chem. Technol. Biotechnol.* **2014**, *89* (4), 479–498. https://doi.org/10.1002/jctb.4262.

(2) Sholl, D. S.; Lively, R. P. Seven Chemical Separations to Change the World. *Nat. News* **2016**, *532* (7600), 435. https://doi.org/10.1038/532435a.

(3) Stankiewicz, A. Reactive Separations for Process Intensification: An Industrial Perspective. *Chem. Eng. Process. Process Intensif.* **2003**, *42* (3), 137–144. https://doi.org/10.1016/S0255-2701(02)00084-3.

(4) Harmsen, G. J. Reactive Distillation: The Front-Runner of Industrial Process Intensification: A Full Review of Commercial Applications, Research, Scale-up, Design and Operation. *Chem. Eng. Process. Process Intensif.* **2007**, *46* (9), 774–780. https://doi.org/10.1016/j.cep.2007.06.005.

(5) Stankiewicz, A. I.; Moulijn, J. A. Process Intensification: Transforming Chemical Engineering. *Chem. Eng. Prog.* **2000**, *96* (1), 22–34.

(6) Siirola, J. J. Industrial Applications of Chemical Process Synthesis. In *Advances in Chemical Engineering*; Anderson, J. L., Ed.; Academic Press, 1996; Vol. 23, pp 1–62.

(7) Barnicki, S. D.; Siirola, J. J. Process Synthesis Prospective. *Comput. Chem. Eng.* **2004**, *28* (4), 441–446. https://doi.org/10.1016/j.compchemeng.2003.09.030.

(8) Harmsen, G. J. Industrial Best Practices of Conceptual Process Design. *Chem. Eng. Process. Process Intensif.* **2004**, *43* (5), 671–675. https://doi.org/10.1016/j.cep.2003.02.003.

(9) Moulijn, J. A.; Stankiewicz, A.; Grievink, J.; Górak, A. Process Intensification and Process Systems Engineering: A Friendly Symbiosis. *Comput. Chem. Eng.* **2008**, *32* (1–2), 3–11. https://doi.org/10.1016/j.compchemeng.2007.05.014.

(10) Baldea, M. From Process Integration to Process Intensification. *Comput. Chem. Eng.* **2015**, *81*, 104–114. https://doi.org/10.1016/j.compchemeng.2015.03.011.

(11) Wilson, S.; Manousiouthakis, V. IDEAS Approach to Process Network Synthesis: Application to Multicomponent MEN. *AIChE J.* **2000**, *46* (12), 2408–2416. https://doi.org/10.1002/aic.690461209.

(12) Drake, J. E.; Manousiouthakis, V. IDEAS Approach to Process Network Synthesis: Minimum Utility Cost for Complex Distillation Networks. *Chem. Eng. Sci.* **2002**, *57* (15), 3095–3106. https://doi.org/10.1016/S0009-2509(02)00159-8.

(13) Drake, J. E.; Manousiouthakis, V. IDEAS Approach to Process Network Synthesis: Minimum Plate Area for Complex Distillation Networks with Fixed Utility Cost. *Ind. Eng. Chem. Res.* **2002**, *41* (20), 4984–4992. https://doi.org/10.1021/ie010735s.

(14) Justanieah, A. M.; Manousiouthakis, V. IDEAS Approach to the Synthesis of Globally Optimal Separation Networks: Application to Chromium Recovery from Wastewater. *Adv. Environ. Res.* **2003**, *7* (2), 549–562. https://doi.org/10.1016/S1093-0191(02)00026-6.

(15) Martin, L. L.; Manousiouthakis, V. I. Globally Optimal Power Cycle Synthesis via the Infinite-DimEnsionAl State-Space (IDEAS) Approach Featuring Minimum Area with Fixed Utility. *Chem. Eng. Sci.* **2003**, *58* (18), 4291–4305. https://doi.org/10.1016/S0009-2509(02)00526-2.

(16) Holiastos, K.; Manousiouthakis, V. Infinite-Dimensional State-Space (IDEAS) Approach to Globally Optimal Design of Distillation Networks Featuring Heat and Power Integration. *Ind. Eng. Chem. Res.* **2004**, *43* (24), 7826–7842. https://doi.org/10.1021/ie010434i.

(17) Takase, H.; Hasebe, S. Synthesis of Ternary Distillation Process Structures Featuring Minimum Utility Cost Using the IDEAS Approach. *AIChE J.* **2018**, *64* (4), 1285–1294. https://doi.org/10.1002/aic.16023.

(18) Burri, J. F.; Manousiouthakis, V. I. Global Optimization of Reactive Distillation Networks Using IDEAS. *Comput. Chem. Eng.* **2004**, *28* (12), 2509–2521. https://doi.org/10.1016/j.compchemeng.2004.06.014.

(19) da Cruz, F. E.; Manousiouthakis, V. I. Process Intensification of Reactive Separator Networks through the IDEAS Conceptual Framework. *Comput. Chem. Eng.* **2017**, *105*, 39–55. https://doi.org/10.1016/j.compchemeng.2016.12.006.

(20) Burri, J. F.; Wilson, S. D.; Manousiouthakis, V. I. Infinite DimEnsionAl State-Space Approach to Reactor Network Synthesis: Application to Attainable Region Construction. *Comput. Chem. Eng.* **2002**, *26* (6), 849–862. https://doi.org/10.1016/S0098-1354(02)00008-X.

(21) Manousiouthakis, V. I.; Justanieah, A. M.; Taylor, L. A. The Shrink–Wrap Algorithm for the Construction of the Attainable Region: An Application of the IDEAS Framework. *Comput. Chem. Eng.* **2004**, *28* (9), 1563–1575. https://doi.org/10.1016/j.compchemeng.2003.12.005.

(22) Zhou, W.; Manousiouthakis, V. I. Non-Ideal Reactor Network Synthesis through IDEAS: Attainable Region Construction. *Chem. Eng. Sci.* **2006**, *61* (21), 6936–6945. https://doi.org/10.1016/j.ces.2006.07.002.

(23) Zhou, W.; Manousiouthakis, V. I. Variable Density Fluid Reactor Network Synthesis—Construction of the Attainable Region through the IDEAS Approach. *Chem. Eng. J.* **2007**, *129* (1–3), 91–103. https://doi.org/10.1016/j.cej.2006.11.004.

(24) Zhou, W.; Manousiouthakis, V. I. Pollution Prevention through Reactor Network Synthesis: The IDEAS Approach. *Int. J. Environ. Pollut.* **2007**, *29* (1–3), 206–231. https://doi.org/10.1504/IJEP.2007.012804.

(25) Posada, A.; Manousiouthakis, V. Multi-Feed Attainable Region Construction Using the Shrink–Wrap Algorithm. *Chem. Eng. Sci.* **2008**, *63* (23), 5571–5592. https://doi.org/10.1016/j.ces.2008.07.026.

(26) Zhou, W.; Manousiouthakis, V. I. Global Capital/Total Annualized Cost Minimization of Homogeneous and Isothermal Reactor Networks. *Ind. Eng. Chem. Res.* **2008**, *47* (10), 3771–3782. https://doi.org/10.1021/ie060653+.

(27) Zhou, W.; Manousiouthakis, V. I. On Dimensionality of Attainable Region Construction for Isothermal Reactor Networks. *Comput. Chem. Eng.* **2008**, *32* (3), 439–450. https://doi.org/10.1016/j.compchemeng.2007.02.013.

(28) Zhou, W.; Manousiouthakis, V. I. Automating the AR Construction for Non-Isothermal Reactor Networks. *Comput. Chem. Eng.* **2009**, *33* (1), 176–180. https://doi.org/10.1016/j.compchemeng.2008.07.011.

(29) Ghougassian, P. G.; Manousiouthakis, V. Attainable Composition, Energy Consumption, and Entropy Generation Properties for Isothermal/Isobaric Reactor Networks. *Ind. Eng. Chem. Res.* **2013**, *52* (9), 3225–3238. https://doi.org/10.1021/ie301158m.

(30) Ghougassian, P. G.; Manousiouthakis, V. Globally Optimal Networks for Multipressure Distillation of Homogeneous Azeotropic Mixtures. *Ind. Eng. Chem. Res.* **2012**, *51* (34), 11183–11200. https://doi.org/10.1021/ie300423q.

(31) Al-Husseini, Z.; Manousiouthakis, V. I. IDEAS Based Synthesis of Minimum Volume Reactor Networks Featuring Residence Time Density/Distribution Models. *Comput. Chem. Eng.* **2014**, *60*, 124–142. https://doi.org/10.1016/j.compchemeng.2013.07.005.

(32) Ghougassian, P. G.; Manousiouthakis, V. Minimum Entropy Generation for Isothermal Endothermic/Exothermic Reactor Networks. *AIChE J.* **2015**, *61* (1), 103–117. https://doi.org/10.1002/aic.14598.

(33) Pichardo, P.; Manousiouthakis, V. I. Infinite DimEnsionAl State-Space as a Systematic Process Intensification Tool: Energetic Intensification of Hydrogen Production. *Chem. Eng. Res. Des.* **2017**, *120*, 372–395. https://doi.org/10.1016/j.cherd.2017.01.026.

(34) Sourlas, D. D.; Manousiouthakis, V. Best Achievable Decentralized Performance. *IEEE Trans. Autom. Control* **1995**, *40* (11), 1858–1871. https://doi.org/10.1109/9.471207.

(35) Doherty, M. F.; Malone, M. F. *Conceptual Design of Distillation Systems*; McGraw-Hill, 2001.

(36) Davis, B. J.; Taylor, L. A.; Manousiouthakis, V. I. Identification of the Attainable Region for Batch Reactor Networks. *Ind. Eng. Chem. Res.* **2008**, *47* (10), 3388–3400. https://doi.org/10.1021/ie071664l.

(37) Conner, J. A.; Manousiouthakis, V. I. On the Attainable Region for Process Networks. *AIChE J.* **2014**, *60* (1), 193–212. https://doi.org/10.1002/aic.14257.

(38) Barbosa, D.; Doherty, M. F. Design and Minimum-Reflux Calculations for Single-Feed Multicomponent Reactive Distillation Columns. *Chem. Eng. Sci.* **1988**, *43* (7), 1523–1537. https://doi.org/10.1016/0009-2509(88)85144-3.

(39) Venimadhavan, G.; Buzad, G.; Doherty, M. F.; Malone, M. F. Effect of Kinetics on Residue Curve Maps for Reactive Distillation. *AIChE J.* **1994**, *40* (11), 1814–1824. https://doi.org/10.1002/aic.690401106.

(40) Okasinski, M. J.; Doherty, M. F. Design Method for Kinetically Controlled, Staged Reactive Distillation Columns. *Ind. Eng. Chem. Res.* **1998**, *37* (7), 2821–2834. https://doi.org/10.1021/ie9708788.

(41) Malone, M. F.; Doherty, M. F. Reactive Distillation. *Ind. Eng. Chem. Res.* **2000**, *39* (11), 3953–3957. https://doi.org/10.1021/ie000633m.

(42) Chen, F.; Huss, R. S.; Malone, M. F.; Doherty, M. F. Simulation of Kinetic Effects in Reactive Distillation. *Comput. Chem. Eng.* **2000**, *24* (11), 2457–2472. https://doi.org/10.1016/S0098-1354(00)00609-8.

(43) Barnicki, S. D.; Hoyme, C. A.; Siirola, J. J. Separations Process Synthesis. In *Kirk-Othmer Encyclopedia of Chemical Technology*; John Wiley & Sons, Inc., 2000.

(44) Jiménez, L.; Wanhschafft, O. M.; Julka, V. Analysis of Residue Curve Maps of Reactive and Extractive Distillation Units. *Comput. Chem. Eng.* **2001**, *25* (4–6), 635–642. https://doi.org/10.1016/S0098-1354(01)00644-5.

(45) Huss, R. S.; Chen, F.; Malone, M. F.; Doherty, M. F. Reactive Distillation for Methyl Acetate Production. *Comput. Chem. Eng.* **2003**, *27* (12), 1855–1866. https://doi.org/10.1016/S0098-1354(03)00156-X.

(46) Li, H.; Meng, Y.; Li, X.; Gao, X. A Fixed Point Methodology for the Design of Reactive Distillation Columns. *Chem. Eng. Res. Des.* **2016**, *111*, 479–491. https://doi.org/10.1016/j.cherd.2016.05.015.

(47) Ciric, A. R.; Gu, D. Synthesis of Nonequilibrium Reactive Distillation Processes by MINLP Optimization. *AIChE J.* **1994**, *40* (9), 1479–1487. https://doi.org/10.1002/aic.690400907.

(48) Papalexandri, K. P.; Pistikopoulos, E. N. Generalized Modular Representation Framework for Process Synthesis. *AIChE J.* **1996**, *42* (4), 1010–1032. https://doi.org/10.1002/aic.690420413.

(49) Jackson, J. R.; Grossmann, I. E. A Disjunctive Programming Approach for the Optimal Design of Reactive Distillation Columns. *Comput. Chem. Eng.* **2001**, *25* (11–12), 1661–1673. https://doi.org/10.1016/S0098-1354(01)00730-X.

(50) Georgiadis, M. C.; Schenk, M.; Pistikopoulos, E. N.; Gani, R. The Interactions of Design Control and Operability in Reactive Distillation Systems. *Comput. Chem. Eng.* **2002**, *26* (4–5), 735–746. https://doi.org/10.1016/S0098-1354(01)00774-8.

(51) Cardoso, M. F.; Salcedo, R. L.; de Azevedo, S. F.; Barbosa, D. Optimization of Reactive Distillation Processes with Simulated Annealing. *Chem. Eng. Sci.* **2000**, *55* (21), 5059–5078. https://doi.org/10.1016/S0009-2509(00)00119-6.

(52) Hoffmaster, W. R.; Hauan, S. Using Feasible Regions to Design and Optimize Reactive Distillation Columns with Ideal VLE. *AIChE J.* **2006**, *52* (5), 1744–1753. https://doi.org/10.1002/aic.10765.

(53) Avami, A.; Marquardt, W.; Saboohi, Y.; Kraemer, K. Shortcut Design of Reactive Distillation Columns. *Chem. Eng. Sci.* **2012**, *71*, 166–177. https://doi.org/10.1016/j.ces.2011.12.021.

(54) Urselmann, M.; Engell, S. Design of Memetic Algorithms for the Efficient Optimization of Chemical Process Synthesis Problems with Structural Restrictions. *Comput. Chem. Eng.* **2015**, *72*, 87–108. https://doi.org/10.1016/j.compchemeng.2014.08.006.

(55) da Cruz, F. E.; Manousiouthakis, V. I. Process Intensification of Reactive Separator Networks through the IDEAS Conceptual Framework. *Comput. Chem. Eng.* **2017**, *105*, 39–55. https://doi.org/10.1016/j.compchemeng.2016.12.006.

(56) Smith, J. M.; Van Ness, H. C.; Abbott, M. *Introduction to Chemical Engineering Thermodynamics*, 7 edition.; McGraw-Hill Education: Boston, 2004.

CHAPTER 3

Minimum Entropy Generation in Reactive Distillation Networks through the IDEAS Conceptual Framework

3.1. Abstract

This paper presents a continuation on the investigation of reactive distillation (RD) processes through an entropy generation analysis. The rate of entropy generation measures the amount of irreversibilities in a given process, indicating by how much a system is far from its ideal configuration, and serving as a comparison tool between different process configurations. A minimum entropy generation formulation for reactive distillation systems is rigorously obtained through the application of the IDEAS framework. A unit operation model is proposed for reactive vapor-liquid equilibrium flash separators employed as network building blocks, and the concepts of reactive holdup, and capacity are introduced as network performance metrics so the tradeoff between minimum entropy generation and those two variables can be developed. The proposed reactive separation process intensification method is demonstrated on a case study involving the metathesis of 2-pentene through reactive distillation.

3.2. Introduction

A common strategy to reduce energy costs in the chemical process industry is to increase process reversibility through improved equipment design [1]. This strategy may be compatible to the process intensification concept, which encompasses any chemical engineering development

that offers drastic improvements in chemical processing, substantially decreasing equipment volume, energy consumption or waste formation [2,3].

Entropy change is a natural process that any system is subject to when changing states, due to the fact that not all states in the immediate neighborhood of every state of a system are accessible through adiabatic processes [4]. Entropy generation minimization (EGM) is the method of thermodynamic optimization of real systems that owe their thermodynamic imperfection to heat transfer, fluid flow, and mass-transfer irreversibility [5]. Tolman and Fine concluded in 1948 that an increase in the internal entropy of a system reduced the maximum available work [6]. Thus, loss of available work can be measured in units of entropy generation [7].

If one considers the product and feed streams, the separation by distillation generally requires a decrease of the entropy so addition of heat is used in practice to make this process thermodynamically possible. Still, the overall efficiency of distillation is rather low due to irreversible losses related to pressure drop, mass transfer, and irreversible heat transfer [8]. Studies about entropy minimization on distillation columns based on non-equilibrium thermodynamics with Cauchy-Lagrange optimization procedures resulted in a process design technique called principle of equipartition of forces [1,9,10]. Nevertheless, this equipartition of forces optimization methodology is still to be proven applicable to reactive distillation systems.

The Infinite DimEnsionAl State-Space (IDEAS) framework, a systematic approach for process synthesis, is applied in this work as a process intensification tool. IDEAS can rigorously identify the performance limits of a particular technology or combination of technologies, without establishing any a priori design. By finding performance limits on chemical process networks, IDEAS allows the detection of prospective intensified designs and supports the quantification of potential improvements.

Derived by using simple physical concepts, IDEAS can be potentially applied to design and globally optimize virtually any chemical process. The IDEAS conceptual framework has been successfully applied to either globally optimize, or to identify the attainable region for, various types of process networks. Some IDEAS applications include the synthesis of multicomponent mass exchange networks [11], ideal distillation networks [12,13], separator networks [14,15], power cycles [16], heat/power integrated distillation networks [17], reactive distillation networks [18,19], reactor network attainable region [20–28], azeotropic distillation networks [29], reactor networks [30–32], batch reactor networks [33], and process network attainable region [34].

Due to IDEAS' innovative proposition for the process operations, whose domain and range is considered to lie in an infinite (rather than finite) dimensional space, infinite dimensional linear programs (ILP) can be formulated for the synthesis of optimal process networks. In fact, since it is not possible to solve an ILP, its solution is approximated arbitrarily close by finite dimensional linear programs (LP) of ever-increasing size. The sequence formed by the LP optimal solutions converges to the global optimal solution of the ILP.

In this paper, the IDEAS framework is applied as a systematic tool to identify the minimum total entropy required by reactive separation networks for different values of total capacity, and minimum total reactive holdup, variables that can be considered surrogates for volumetric size and catalyst use, respectively.

3.3. Mathematical formulation for the entropy minimization problem

3.3.1. Reactive flash separator model

The design and optimization of reactive distillation systems have been studied through the application of a variety of models. Geometrical approaches, such as the residue curve maps

and the fixed-point method, have been consistently utilized to attack the problem [35–44]. Optimization methods using mixed-integer nonlinear programming (MINPL) formulations [45–52] or infinite linear programming (ILP) formulations [15,18,19] have also contributed to the advancement of reactive distillation design by addressing the problem from the perspective of process synthesis.

This work uses the reactive flash separator model previously presented by da Cruz and Manousiouthakis [19], which was improved to quantify entropy generation in the reactive flash (Fig.3.1) as well as in the network. By pursuing a minimum entropy generation reactive distillation design through the synthesis process, one expects to obtain a network of reactive flash separators with the least amount of irreversible processes. This feature gives flexibility to the network to completely meet the thermodynamic requirements of each flash, which is a surrogate for a reactive distillation tray. In this reactive flash model, vapor and liquid exit streams are considered to be in phase equilibrium with one another, and reactions may occur in the liquid phase, depending on the reactive volume H (the reactive holdup) of the flash separator. A capacity variable C associated with the total liquid holdup is also considered. Ghougassian and Manousiouthakis [32] have shown that while net energy consumption is only a function of the inlet/outlet compositions, entropy generation and hot (or cold) utility are strong functions of the network's internal structure. Therefore, the quantification of the minimum entropy generation is meaningful and desirable to organize the distillation network structure when pursuing pre-defined separation purity goals.

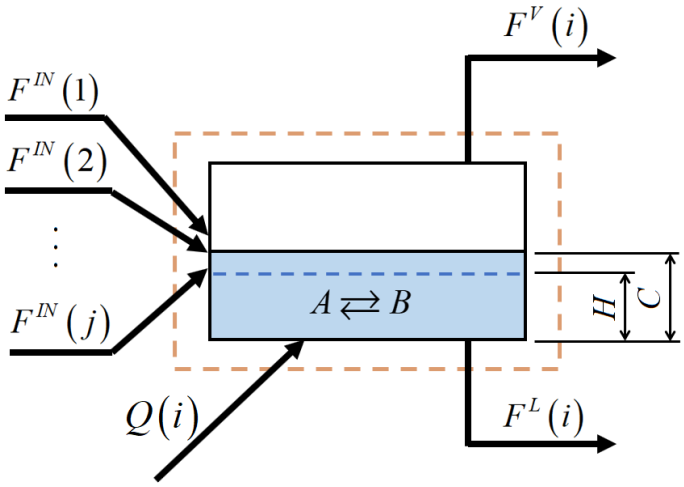

Figure 3.1 – Representation of the improved reactive flash separator

For mass and component balances in the reactive flash separator, the Gamma-Phi model is used to correlate the liquid and vapor molar fractions, as shown i. Eq.(3.1).

$$y_k^V \phi_k\left(\left\{y_l^V\right\}_{l=1}^n, T, P\right) P = x_k^L \gamma_k\left(\left\{x_l^L\right\}_{l=1}^n, T\right) P_k^{sat}(T) \qquad \forall k = 1,\ldots,n \tag{3.1}$$

The model also make use of a general kinetic rate expression, Eq.(3.2), where the i^{th} species activity in a multicomponent mixture is related to the activity coefficient in the liquid phase and the liquid molar fraction for the respective component as shown in Eq.(3.3).

$$R_k = k_f(T)\left(\prod_{reactants} a_r\left(\gamma_r, x_r\right)^{\nu_r} - \frac{1}{K_{eq}(T)} \prod_{products} a_p\left(\gamma_p, x_p\right)^{\nu_p}\right) \tag{3.2}$$

$$a_i = \gamma_i\left(\left\{x_l^L\right\}_{l=1}^n, T\right) x_i \tag{3.3}$$

As mentioned in other works, one important feature of this reactive flash separator model is the ability to account for several different phenomena. In the case where the flash has reactive holdup, vapor, and liquid streams greater than zero, the unit is fully operational and will simultaneously act as both a reactor and VLE separator. Conversely, if the reactive holdup is zero, the process acts only as a VLE flash separator; and if no separation takes place, the process assumes the behavior of an isolated CSTR reactor, with only one liquid flow as output.

As for the energy transferred from or released by the reactive flash separator, two infinite reservoirs at temperature T^H and T^C are available for the process synthesis to perform the heating or cooling, depending on each reactive flash separator energetic needs. A distributed heat transfer system is considered to provide heat at T^H and cooling T^C at to each reactive flash in the network individually, according to its respective endo or exothermicity.

The improved reactive flash separator model was employed in the systematic synthesis of reactive distillation networks through IDEAS, aiming to find the global minimum value for the entropy generated by the separation network.

3.3.2. IDEAS formulation

The IDEAS framework allows each operational unit in the process operator OP to interface with all other possible operating – network inlets, network outlets, and other operational units – by using mixing and splitting operations through the distribution network (DN), enabling the consideration of all possible flowsheets for a reactive flash separator network during the synthesis process. The resulting IDEAS framework for the reactive flash separator

synthesis problem featuring a distributed heating/cooling system and the respective infinite reservoirs operating at T^H and T^C is shown in Fig.3.2.

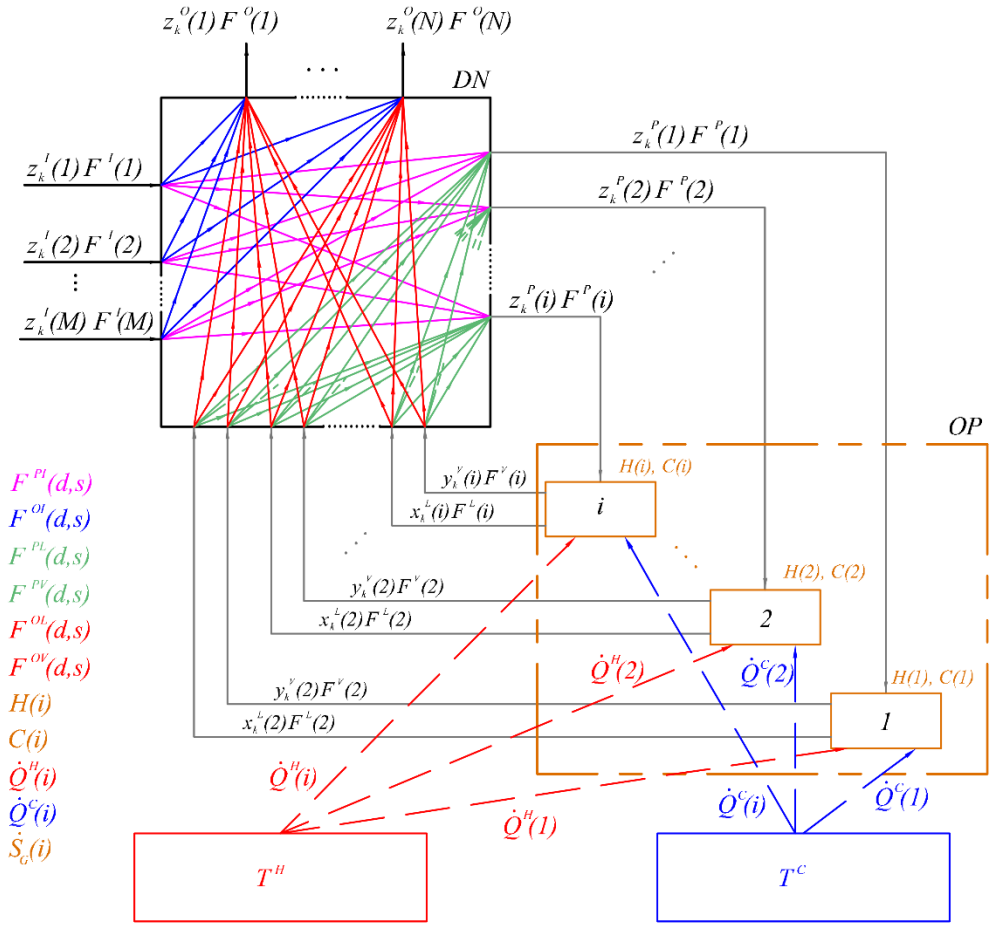

Figure 3.2 - IDEAS representation for a reactive flash separator network featuring a distributed energy system coming from either a hot or a cold infinite reservoir

Flow rate variables are represented by the cross-flow streams in the DN, which has molar fraction conditions fixed at the origin. Each flow variables are identified superscripts that indicate its destination and source, respectively. The notation used in previous works is maintained in this formulation: the DN inlet is identified as I, the DN outlet as O, the OP inlet as P, the liquid and vapor outputs from the OP as L and V respectively. Indexes designating

source and destination, respectively, are also used to identify each flow variable in the DN. Reactive holdups, capacities, the amount of heat transferred from/to the reactive flash, and entropy generated are variables associated with the process units within the process operator.

The IDEAS ILP general formulation uses only mass and component balances on the distribution network (DN), since it is considered adiabatic in this work. Conversely, for the process units in the OP, mass, component and energy balances are developed. Starting with the mass and component balances, for each inlet flow $F^I(j)$ associated with one of the M inlets of the DN, a splitting balance is written as shown in Eq.(3.4).

$$F^I(j) - \sum_{i=1}^{N} F^{OI}(i,j) - \sum_{i=1}^{\infty} F^{PI}(i,j) = 0 \quad ; \quad \forall j = 1,...,M \tag{3.4}$$

A mixing balances for each outlet flow $F^O(i)$ leaving the DN from one of its N outlets is shown in Eq.(3.5).

$$F^O(i) - \sum_{j=1}^{M} F^{OI}(i,j) - \sum_{j=1}^{\infty} F^{OL}(i,j) - \sum_{j=1}^{\infty} F^{OV}(i,j) = 0 \quad ; \quad \forall i = 1,...,N \tag{3.5}$$

The component flow $f_k^P(i)$ that feeds the i^{th} reactive flash separator can be considered as the sum of component flows feeding that specific mixing point of the DN (component balance).

$$f_k^P(i) - \sum_{j=1}^{M} z_k^I(j) F^{PI}(i,j) - \sum_{j=1}^{\infty} x_k^L(j) F^{PL}(i,j) - \sum_{j=1}^{\infty} y_k^V(j) F^{PV}(i,j) = 0 \qquad \forall i = 1,...,\infty \; ; \quad \forall k = 1,...,n \tag{3.6}$$

Thus, the total mass flow in this mixing node is represented by Eq.(3.7) below.

$$F^P(i) - \sum_{j=1}^{M} F^{PI}(i,j) - \sum_{j=1}^{\infty} F^{PL}(i,j) - \sum_{j=1}^{\infty} F^{PV}(i,j) = 0 \quad ; \quad \forall i = 1,...,\infty \tag{3.7}$$

After being processed in the OP, each liquid flow $F^L(j)$ and vapor flow $F^V(j)$ entering the DN have a splitting balance as shown in Eq.(3.8) and (3.9), respectively.

$$F^L(j) - \sum_{i=1}^{N} F^{OL}(i,j) - \sum_{i=1}^{\infty} F^{PL}(i,j) = 0 \quad ; \quad \forall j = 1,\ldots,\infty \tag{3.8}$$

$$F^V(j) - \sum_{i=1}^{N} F^{OV}(i,j) - \sum_{i=1}^{\infty} F^{PV}(i,j) = 0 \quad ; \quad \forall j = 1,\ldots,\infty \tag{3.9}$$

Lower and upper bound constraints are introduced on each of the N flow variables $F^O(i)$ as design parameters. The total balance for each flow exiting the DN is shown in Eq.(3.10).

$$\left(F^O(i)\right)^l \le \sum_{j=1}^{M} F^{OI}(i,j) + \sum_{j=1}^{\infty} F^{OL}(i,j) + \sum_{j=1}^{\infty} F^{OV}(i,j) \le \left(F^O(i)\right)^u \quad ; \quad \forall i = 1,\ldots,N \tag{3.10}$$

Equation (3.10) can also be expressed by two independent inequalities as shown below:

$$\left[\sum_{j=1}^{M} F^{OI}(i,j) + \sum_{j=1}^{\infty} F^{OL}(i,j) + \sum_{j=1}^{\infty} F^{OV}(i,j)\right] - \left(F^O(i)\right)^l \ge 0 \quad ; \quad \forall i = 1,\ldots,N \tag{3.11}$$

$$\left[\sum_{j=1}^{M} F^{OI}(i,j) + \sum_{j=1}^{\infty} F^{OL}(i,j) + \sum_{j=1}^{\infty} F^{OV}(i,j)\right] - \left(F^O(i)\right)^u \le 0 \quad ; \quad \forall i = 1,\ldots,N \tag{3.12}$$

The component balances at the DN's outputs, including upper and lower bounds for the product's molar fractions are represented by Eq.(3.13).

$$\left(z_k^O(i)\right)^l F^O(i) \le \left\{ \begin{array}{l} \sum_{j=1}^{M} z_k^I(j) F^{OI}(i,j) \\ + \sum_{j=1}^{\infty} x_k^L(j) F^{OL}(i,j) \\ + \sum_{j=1}^{\infty} y_k^V(j) F^{OV}(i,j) \end{array} \right\} \le \left(z_k^O(i)\right)^u F^O(i) \quad ; \quad \begin{array}{l} \forall i = 1,\ldots,N \\ \forall k = 1,\ldots,n \end{array} \tag{3.13}$$

The component balance for each reactive flash separators in the OP is expressed as shown in Eq.(3.14).

$$f_k^P(i) + R_k(i)H(i) - x_k^L(i)F^L(i) - y_k^V(i)F^V(i) = 0 \quad ; \quad \begin{matrix}\forall i = 1,\ldots,\infty \\ \forall k = 1,\ldots,n\end{matrix} \tag{3.14}$$

Each feasible reactive flash separator in the network has a minimum residence time (τ). The capacity of each reactive flash in the OP is determined by either the reactive holdup, Eq.(3.15), or the residence time times the reactive flash inlet flow, Eq.(3.16), whichever is greater.

$$C(i) \geq H(i) \quad ; \quad \forall i = 1,\ldots,\infty \tag{3.15}$$

$$C(i) \geq \tau F^P(i) \quad ; \quad \forall i = 1,\ldots,\infty \tag{3.16}$$

By substituting Eq.(3.7) in Eq.(3.16), the capacity must then satisfy:

$$C(i) \geq \tau\left[\sum_{j=1}^{M} F^{PI}(i,j) + \sum_{j=1}^{\infty} F^{PL}(i,j) + \sum_{j=1}^{\infty} F^{PV}(i,j)\right] \quad ; \quad \forall i = 1,\ldots,\infty \tag{3.17}$$

The number of variables can be reduced by substituting Eq.(3.6) to Eq.(3.9) in Eq.(3.14):

$$\begin{aligned} & R_k(i)H(i) - x_k^L(i)\left[\sum_{j=1}^{N} F^{OL}(j,i) + \sum_{j=1}^{\infty} F^{PL}(j,i)\right] \\ & - y_k^V(i)\left[\sum_{j=1}^{N} F^{OV}(j,i) + \sum_{j=1}^{\infty} F^{PV}(j,i)\right] + \sum_{j=1}^{M} z_k^I(j)F^{PI}(i,j) \quad ; \quad \begin{matrix}\forall i = 1,\ldots,\infty \\ \forall k = 1,\ldots,n\end{matrix} \\ & + \sum_{j=1}^{\infty} x_k^L(j)F^{PL}(i,j) + \sum_{j=1}^{\infty} y_k^V(j)F^{PV}(i,j) = 0 \end{aligned} \tag{3.18}$$

From Eq.(3.18), self-recycling flows are naturally eliminated from the system. This fact can lead to further simplifications as shown in Eq.(3.19):

$$
\begin{aligned}
& R_k(i)H(i)+\sum_{j=1}^{M} z_k^I(j)F^{PI}(i,j) \\
& -\sum_{j=1}^{N} x_k^L(i)F^{OL}(j,i)-\sum_{j=1}^{N} y_k^V(i)F^{OV}(j,i) \\
& \quad +\sum_{\substack{j=1 \\ j\neq i}}^{\infty}\left[x_k^L(j)F^{PL}(i,j)-x_k^L(i)F^{PL}(j,i)\right] \qquad ; \quad \begin{matrix}\forall i=1,\ldots,\infty \\ \forall k=1,\ldots,n\end{matrix} \\
& \quad +\sum_{\substack{j=1 \\ j\neq i}}^{\infty}\left[y_k^V(j)F^{PV}(i,j)-y_k^V(i)F^{PV}(j,i)\right]=0
\end{aligned}
\tag{3.19}
$$

By substituting Eq.(3.10) in (3.11), some variables in the component outlet bounds equations can be eliminated, as shown in Eq.(3.20).

$$
\left(z_k^O(i)\right)^l \begin{bmatrix} \sum_{j=1}^{M} F^{OI}(i,j) \\ +\sum_{j=1}^{\infty} F^{OL}(i,j) \\ +\sum_{j=1}^{\infty} F^{OV}(i,j) \end{bmatrix} \le \begin{bmatrix} \sum_{j=1}^{M} z_k^I(j)F^{OI}(i,j) \\ +\sum_{j=1}^{\infty} x_k^L(j)F^{OL}(i,j) \\ +\sum_{j=1}^{\infty} y_k^V(j)F^{OV}(i,j) \end{bmatrix} \le \left(z_k^O(i)\right)^u \begin{bmatrix} \sum_{j=1}^{M} F^{OI}(i,j) \\ +\sum_{j=1}^{\infty} F^{OL}(i,j) \\ +\sum_{j=1}^{\infty} F^{OV}(i,j) \end{bmatrix} ; \begin{matrix}\forall i=1,\ldots,N \\ \forall k=1,\ldots,n\end{matrix} \tag{3.20}
$$

One can split Eq.(3.20) into two inequalities, facilitating the implementation that will be carried on later:

$$
\begin{aligned}
& \sum_{j=1}^{M}\left[\left(\left(z_k^O(i)\right)^l - z_k^I(j)\right)F^{OI}(i,j)\right] \\
& +\sum_{j=1}^{\infty}\left[\left(\left(z_k^O(i)\right)^l - x_k^L(j)\right)F^{OL}(i,j)\right] \qquad ; \quad \begin{matrix}\forall i=1,\ldots,N \\ \forall k=1,\ldots,n\end{matrix} \\
& +\sum_{j=1}^{\infty}\left[\left(\left(z_k^O(i)\right)^l - y_k^V(j)\right)F^{OV}(i,j)\right]\le 0
\end{aligned}
\tag{3.21}
$$

$$\sum_{j=1}^{M}\left[\left(\left(z_k^O(i)\right)^u - z_k^I(j)\right)F^{OI}(i,j)\right] + \sum_{j=1}^{\infty}\left[\left(\left(z_k^O(i)\right)^u - x_k^L(j)\right)F^{OL}(i,j)\right] + \sum_{j=1}^{\infty}\left[\left(\left(z_k^O(i)\right)^u - y_k^V(j)\right)F^{OV}(i,j)\right] \geq 0 \quad ; \quad \begin{matrix}\forall i = 1,\ldots,N \\ \forall k = 1,\ldots,n\end{matrix} \tag{3.22}$$

A total capacity constraint with upper bound C^{ub} is also considered in this formulation. This constraint, Eq.(3.23), is used to investigate process intensification opportunities in the network, enabling the search for the smallest feasible network for the specified problem.

$$C^{tot} = \sum_{i=1}^{\infty} C(i) \leq C^{ub} \tag{3.23}$$

Similarly, a total reactive holdup H^{tot} has been added to the model with an upper bound constraint H^{ub}, as shown in Eq.(3.24), so that the total reactive holdup in the system can be controlled during the synthesis process.

$$H^{tot} = \sum_{i=1}^{\infty} H(i) \leq H^{ub} \tag{3.24}$$

A constraint for the total flow circulating in the network $\left(F^P\right)^{tot}$ has also been considered in this work, as shown in Eq.(3.25). This variable takes in account all flows entering the OP and has its upper bound constrained by $\left(F^P\right)^{ub}$.

$$\left(F^P\right)^{tot} = \sum_{i=1}^{\infty} F^P(i) = \sum_{i=1}^{\infty}\sum_{j=1}^{M} F^{PI}(i,j) + \sum_{i=1}^{\infty}\sum_{\substack{j=1 \\ j\neq i}}^{\infty} F^{PL}(i,j) + \sum_{i=1}^{\infty}\sum_{\substack{j=1 \\ j\neq i}}^{\infty} F^{PV}(i,j) \leq \left(F^P\right)^{ub} \tag{3.25}$$

A distributed heat system is considered so that each reactive flash separator has the ability to exchange heat with either one of the two heat reservoirs available to the system, providing the necessary load for the reactive-separative operation. Therefore, for the isobaric, isothermal, steady-state reactive flash separator i in the network, the energy balance is presented in Eq.(3.26).

$$\dot{Q}(i)+h^{P}(i)F^{P}(i)=h^{L}(i)F^{L}(i)+h^{V}(i)F^{V}(i)+\dot{W}(i) \qquad ; \qquad \forall i=1,...,\infty \qquad (3.26)$$

In the equation above, $\dot{Q}$ is the heat transferred from or to the system, while h^{P}, h^{L} and h^{V} correspond to the total molar enthalpy of the reactive flash inlet, liquid outlet, and vapor outlet, respectively. The use of total enthalpy instead of partial enthalpies allows a more general formulation since the relation between the total enthalpy of the mixture and the enthalpy of each of the mixture component can be treated later through ideal or non-ideal enthalpy models. Moreover, since no work is done or received by the flash separator and the system is considered isobaric, $\dot{W}$ is zero for all reactive flashes in the network, and all energy effects are captured through heat transfer and enthalpy changes.

An entropy balance for an open system shows that the rate of entropy generation in a system $\dot{S}_{G}$ accounts for the second-law requirement that the total entropy change associated with any process must be positive. The limiting case where the rate of entropy generation is zero occurs only for completely reversible processes, thus, entropy generation measures the irreversibility of processes that are taking place on a given system. There are two sources of irreversibility, the ones that occur within the control volume, called internal irreversibilities, and those occurring at the outside limit of the control volume such as heat transfer across finite temperature differences between system and surroundings, called external irreversibilities.

In the presence of heat-transfer irreversibility between the i^{th} reactive flash separator, which is operating at $T(i)$, and either one of the infinite reservoirs available, where the high and low-temperature reservoirs operate at T^H and T^C, respectively, an entropy balance for the same process is presented in Eq.(3.27). Heat given to (released by) the system is represented by $\dot{Q}^H$ ($\dot{Q}^C$).

$$\dot{S}_G(i) = \begin{bmatrix} s^L(i)F^L(i) \\ +s^V(i)F^V(i) \\ -s^P(i)F^P(i) \end{bmatrix} - \frac{\dot{Q}^H(i)}{T^H} + \frac{\dot{Q}^C(i)}{T^C} \geq 0;\ \dot{Q}^H(i) \geq 0,\ \dot{Q}^C(i) \geq 0,\ \forall i = 1,...,\infty \quad (3.27)$$

The IDEAS distribution network for this problem indicates that $F^P(i)$, $h^P(i)$, and $s^P(i)$ can be determined by mixing the streams originated in all other points of the network that feed the reactive flash i, excluding any self-recycling flow as shown in the component balance presented in Eq.(3.18). Thus, the equivalent energy flow entering the control volume of the i^{th} reactive flash separator is shown in Eq.(3.28).

$$h^P(i)F^P(i) = \left\{ \begin{array}{l} \sum_{j=1}^{M} h^I(j)F^{PI}(i,j) \\ +\sum_{\substack{j=1 \\ j\neq i}}^{\infty} h^L(j)F^{PL}(i,j) \\ +\sum_{\substack{j=1 \\ j\neq i}}^{\infty} h^V(j)F^{PV}(i,j) \end{array} \right\} \quad ; \quad \forall i = 1,...,\infty \quad (3.28)$$

For the enthalpic flow entering the control volume an important assumption is that the control volume encompasses the mixing point in the DN. Therefore, the rate of entropy generation due to mixing is considered an internal irreversibility and its occurrence is accounted

in $\dot{S}_G$. Considering this fact, the entropic flow entering the control volume of the i^{th} reactive flash separator is presented in Eq.(3.29).

$$s^P(i)F^P(i) = \left\{ \begin{array}{l} \sum_{j=1}^{M} s^I(j)F^{PI}(i,j) \\ +\sum_{\substack{j=1 \\ j\neq i}}^{\infty} s^L(j)F^{PL}(i,j) \\ +\sum_{\substack{j=1 \\ j\neq i}}^{\infty} s^V(j)F^{PV}(i,j) \end{array} \right\} \quad ; \quad \forall i = 1,...,\infty \tag{3.29}$$

In Eq.(3.28) and (3.29), M represents the number of network inlets while $h^I(j)$ and $s^I(j)$ represent the total enthalpy and total entropy of the j^{th} inlet stream, respectively.

Considering that, the energy and entropy balances in each reactive flash separator in the OP can be rewritten as shown in Eq.(3.30) and (3.31).

$$\dot{Q}(i) = \left\{ \begin{array}{l} h^L(i)F^L(i) + h^V(i)F^V(i) \\ -\sum_{j=1}^{M} h^I(j)F^{PI}(i,j) \\ -\sum_{\substack{j=1 \\ j\neq i}}^{\infty} h^L(j)F^{PL}(i,j) \\ -\sum_{\substack{j=1 \\ j\neq i}}^{\infty} h^V(j)F^{PV}(i,j) \end{array} \right\} \quad ; \quad \forall i = 1,...,\infty \tag{3.30}$$

$$\dot{S}_G(i)=\left[\begin{array}{l} s^L(i)F^L(i)+ \\ +s^V(i)F^V(i) \\ \quad -\sum_{j=1}^{M} s^I(j)F^{PI}(i,j) \\ \quad -\sum_{\substack{j=1 \\ j\neq i}}^{\infty} s^L(j)F^{PL}(i,j) \\ \quad -\sum_{\substack{j=1 \\ j\neq i}}^{\infty} s^V(j)F^{PV}(i,j) \end{array}\right] - \frac{\dot{Q}^H(i)}{T^H} + \frac{\dot{Q}^C(i)}{T^C} \geq 0;\ \dot{Q}^H(i) \geq 0,\ \dot{Q}^C(i) \geq 0,\ \forall i = 1,...,\infty \quad (3.31)$$

Equations (3.8) and (3.9) show the splitting balance when the $F^L(i)$ liquid and $F^V(i)$ vapor flows enter the DN's after being processed in the OP. Thus, Eq.(3.30) and (3.31) can be rewritten as a function of all the flows present in the DN, as presented in Eq.(3.32) and .

$$\dot{Q}(i)=\left\{\begin{array}{l} \left[\sum_{j=1}^{N} h^L(i)F^{OL}(j,i)+\sum_{\substack{j=1 \\ j\neq i}}^{\infty} h^L(i)F^{PL}(j,i)\right] \\ +\left[\sum_{j=1}^{N} h^V(i)F^{OV}(j,i)+\sum_{\substack{j=1 \\ j\neq i}}^{\infty} h^V(i)F^{PV}(j,i)\right] \\ -\sum_{j=1}^{M} h^I(j)F^{PI}(i,j)-\sum_{\substack{j=1 \\ j\neq i}}^{\infty} h^L(j)F^{PL}(i,j) \\ \quad -\sum_{\substack{j=1 \\ j\neq i}}^{\infty} h^V(j)F^{PV}(i,j) \end{array}\right\} \quad ; \quad \forall i = 1,...,\infty \qquad (3.32)$$

$$\dot{S}_G(i)=\left\{\begin{array}{l}\left[\begin{array}{l}\sum_{j=1}^{N} s^L(i)F^{OL}(j,i)+\\ +\sum_{\substack{j=1\\ j\neq i}}^{\infty} s^L(i)F^{PL}(j,i)\end{array}\right]\\ +\left[\begin{array}{l}\sum_{j=1}^{N} s^V(i)F^{OV}(j,i)+\\ +\sum_{\substack{j=1\\ j\neq i}}^{\infty} s^V(i)F^{PV}(j,i)\end{array}\right]\\ -\sum_{j=1}^{M} s^I(j)F^{PI}(i,j)\\ -\sum_{\substack{j=1\\ j\neq i}}^{\infty} s^L(j)F^{PL}(i,j)\\ -\sum_{\substack{j=1\\ j\neq i}}^{\infty} s^V(j)F^{PV}(i,j)\end{array}\right\}-\frac{\dot{Q}^H(i)}{T^H}+\frac{\dot{Q}^C(i)}{T^C};\dot{Q}^H(i)\geq 0,\ \dot{Q}^C(i)\geq 0,\quad \forall i=1,...,\infty \tag{3.33}$$

The value of the heat transferred to each reactive flash can have negative or positive values, indicating that heat is either released by the system or given to the system, respectively. This value depending on the energy needs of each given unit during the synthesis process, so the identification of either endothermicity or exothermicity in each reactive flash is established by the optimization process. The calculation of the entropy generation rate follows the energetic needs of the reactive flash, transferring (rejecting) heat to (from) the system using the infinite reservoir at $\left(T^C\right)$ accordingly.

A variable that accounts for the total rate of entropy generation in the system, $\dot{S}_G^{tot}$, has been added to the model with an upper bound constraint $\left(\dot{S}_G^{tot}\right)^{ub}$, as shown in Eq.(3.34), so that the total reactive holdup in the system can be controlled during the synthesis process.

$$\dot{S}_G^{tot} = \sum_{i=1}^{\infty} \dot{S}_G(i) \leq \left(\dot{S}_G^{tot}\right)^{ub} \tag{3.34}$$

The ability to bound the total rate of entropy generation is a key element on the minimization problem pursued in this work.

3.3.3. IDEAS ILP approximation by finite LPs

The IDEAS framework creates an infinite linear programming (ILP), which cannot be solved explicitly. Nevertheless, its solution can be approximated by a series of finite linear programming of increasing size, whose sequence of optimum values converges to the infinite dimensional problem's infimum. Thus, if one considers a finite number G instead of an infinite number of dimensions, where G corresponds to the number of reactive flash separators available for the synthesis problem, the problem becomes an LP which in turns is convex and can be solved by a variety of different LP solvers.

The ILP approximation occurs when one allows G to contain an ever-increasing number of reactive flash-separator units, such that the optimum objective function values of each LP solved forms a non-increasing sequence that converges to the ILP infimum. Thus, considering that the optimal value for the corresponding finite LP is ν, and that the finite LP can be solved η times using an ever-increasing number G of reactive flash separators, i.e. $G(1) < G(2) < ... < G(\eta)$, the resulting optimal values of each finite LP form a non-increasing sequence $\nu(1) > \nu(2) > ... > \nu(\eta)$, which converges to the infimum of the ILP when $\eta \to \infty$. The convergence to the infimum is shown in the case study presented in this work.

3.3.4. Objective function and final IDEAS LP formulation

In order to find a solution for the total entropy generation minimization problem, the external irreversibility caused by the heat transfer term must be calculated. The objective function presented in Eq.(3.35) has been used in this work, where G corresponds to the number of reactive flash separators in the OP for the finite LP formulation and IDEAS ILP procedure infimum approximation.

$$\min \sum_{i=1}^{G} \left[\dot{Q}^{H}(i) + \dot{Q}^{C}(i) \right] \tag{3.35}$$

The physical meaning of $\dot{Q}^{H}$ and $\dot{Q}^{C}$ are consistent with common design variables used in defining heat or cooling needs of a process unit, and represents the heat consumed or discarded by the system, respectively. The energy balance and entropy balance constraints are shown in Eq.(3.36) to (3.38).

$$\left\{ \begin{array}{l} \dot{Q}^{H}(i) - \dot{Q}^{C}(i) - \left[\sum_{j=1}^{N} h^{L}(i) F^{OL}(j,i) + \sum_{j=1}^{G} h^{L}(i) F^{PL}(j,i) \right] \\ \quad - \left[\sum_{j=1}^{N} h^{V}(i) F^{OV}(j,i) + \sum_{j=1}^{G} h^{V}(i) F^{PV}(j,i) \right] \\ \quad + \sum_{j=1}^{M} h^{I}(j) F^{PI}(i,j) + \sum_{j=1}^{G} h^{L}(j) F^{PL}(i,j) \\ \quad + \sum_{j=1}^{G} h^{V}(j) F^{PV}(i,j) \end{array} \right\} = 0 \quad ; \quad \forall i = 1,\ldots,G \tag{3.36}$$

$$\dot{Q}^{H}(i) \geq 0; \; \dot{Q}^{C}(i) \geq 0 \tag{3.37}$$

$$\dot{S}_G(i)=\left\{\begin{array}{l}\left[\sum_{j=1}^{N} s^L(i)F^{OL}(j,i)+\sum_{\substack{j=1\\ j\neq i}}^{\infty} s^L(i)F^{PL}(j,i)\right]\\ +\left[\sum_{j=1}^{N} s^V(i)F^{OV}(j,i)+\sum_{\substack{j=1\\ j\neq i}}^{\infty} s^V(i)F^{PV}(j,i)\right]\\ -\sum_{j=1}^{M} s^I(j)F^{PI}(i,j)-\sum_{\substack{j=1\\ j\neq i}}^{\infty} s^L(j)F^{PL}(i,j)\\ -\sum_{\substack{j=1\\ j\neq i}}^{\infty} s^V(j)F^{PV}(i,j)\end{array}\right\}-\frac{\dot{Q}^H(i)}{T^H}+\frac{\dot{Q}^C(i)}{T^C} \quad ; \quad \forall i=1,...,G \quad (3.38)$$

Thus, the final IDEAS finite LP formulation for the total energy minimization problem in a reactive distillation network has the objective function shown in Eq.(3.39), subject to the constraints presented in Eqs.(3.4), (3.11), (3.12), (3.15), (3.17), (3.19), (3.21), (3.22), (3.23), (3.24), (3.25), (3.34), (3.36), (3.37) and (3.38), all summarized in Eq.(3.39), where $\dot{Q}_{\text{tot}}$ is used to store the value of optimal solution.

$$\dot{Q}_{\text{tot}}=\min \sum_{i=1}^{G}\left[\dot{Q}_H(i)+\dot{Q}_C(i)\right] \quad (3.39)$$

s.t.

$$\left\{\begin{array}{l}\dot{Q}_H(i)-\dot{Q}_C(i)-\left[\sum_{j=1}^{N} h^L(i)F^{OL}(j,i)+\sum_{j=1}^{G} h^L(i)F^{PL}(j,i)\right]\\ -\left[\sum_{j=1}^{N} h^V(i)F^{OV}(j,i)+\sum_{j=1}^{G} h^V(i)F^{PV}(j,i)\right]\\ +\sum_{j=1}^{M}\sum_{k=1}^{n} z_k^I(j)h_k^I(j)F^{PI}(i,j)+\sum_{j=1}^{G} h^L(j)F^{PL}(i,j)\\ +\sum_{j=1}^{G} h^V(j)F^{PV}(i,j)\end{array}\right\}=0 \qquad \forall i=1,...,G$$

$$\left\{\begin{array}{l}\dot{S}_G(i)+\dfrac{\dot{Q}^H(i)}{T^H}-\dfrac{\dot{Q}^C(i)}{T^C}-\left[\displaystyle\sum_{j=1}^{N}s^L(i)F^{OL}(j,i)+\sum_{\substack{j=1\\ j\neq i}}^{\infty}s^L(i)F^{PL}(j,i)\right]\\ -\left[\displaystyle\sum_{j=1}^{N}s^V(i)F^{OV}(j,i)+\sum_{\substack{j=1\\ j\neq i}}^{\infty}s^V(i)F^{PV}(j,i)\right]\\ +\displaystyle\sum_{j=1}^{M}s^I(j)F^{PI}(i,j)+\sum_{\substack{j=1\\ j\neq i}}^{\infty}s^L(j)F^{PL}(i,j)+\sum_{\substack{j=1\\ j\neq i}}^{\infty}s^V(j)F^{PV}(i,j)\end{array}\right\}=0 \qquad \forall i=1,\ldots,G$$

$$F^I(j)-\sum_{i=1}^{N}F^{OI}(i,j)-\sum_{i=1}^{G}F^{PI}(i,j)=0 \qquad \forall j=1,\ldots,M$$

$$\left[\sum_{j=1}^{M}F^{OI}(i,j)+\sum_{j=1}^{G}F^{OL}(i,j)+\sum_{j=1}^{G}F^{OV}(i,j)\right]-\left(F^O(i)\right)^l\geq 0 \qquad \forall i=1,\ldots,N$$

$$\left[\sum_{j=1}^{M}F^{OI}(i,j)+\sum_{j=1}^{G}F^{OL}(i,j)+\sum_{j=1}^{G}F^{OV}(i,j)\right]-\left(F^O(i)\right)^u\leq 0 \qquad \forall i=1,\ldots,N$$

$$C(i)\geq H(i) \qquad \forall i=1,\ldots,G$$

$$C(i)\geq \tau\left[\sum_{j=1}^{M}F^{PI}(i,j)+\sum_{j=1}^{G}F^{PL}(i,j)+\sum_{j=1}^{G}F^{PV}(i,j)\right] \qquad \forall i=1,\ldots,G$$

$$\begin{array}{l}R_k(i)H(i)+\displaystyle\sum_{j=1}^{M}z_k^I(j)F^{PI}(i,j)-\sum_{j=1}^{N}x_k^L(i)F^{OL}(j,i)-\sum_{j=1}^{N}y_k^V(i)F^{OV}(j,i)+ \qquad \forall i=1,\ldots,G\\ +\displaystyle\sum_{\substack{j=1\\ j\neq i}}^{G}\left[x_k^L(j)F^{PL}(i,j)-x_k^L(i)F^{PL}(j,i)\right]+\sum_{\substack{j=1\\ j\neq i}}^{G}\left[y_k^V(j)F^{PV}(i,j)-y_k^V(i)F^{PV}(j,i)\right]=0 \qquad \forall k=1,\ldots,n\end{array}$$

$$\begin{array}{l}\displaystyle\sum_{j=1}^{M}\left[\left(\left(z_k^O(i)\right)^l-z_k^I(j)\right)F^{OI}(i,j)\right]+\sum_{j=1}^{G}\left[\left(\left(z_k^O(i)\right)^l-x_k^L(j)\right)F^{OL}(i,j)\right]+ \qquad \forall i=1,\ldots,N\\ \qquad +\displaystyle\sum_{j=1}^{G}\left[\left(\left(z_k^O(i)\right)^l-y_k^V(j)\right)F^{OV}(i,j)\right]\leq 0 \qquad \forall k=1,\ldots,n\end{array}$$

$$\sum_{j=1}^{M}\left[\left(\left(z_k^O(i)\right)^u - z_k^I(j)\right)F^{OI}(i,j)\right] + \sum_{j=1}^{G}\left[\left(\left(z_k^O(i)\right)^u - x_k^L(j)\right)F^{OL}(i,j)\right] + \sum_{j=1}^{G}\left[\left(\left(z_k^O(i)\right)^u - y_k^V(j)\right)F^{OV}(i,j)\right] \geq 0 \qquad \forall i = 1,\ldots,N \quad \forall k = 1,\ldots,n$$

$$C^{tot} = \sum_{i=1}^{G} C(i)$$

$$H^{tot} = \sum_{i=1}^{G} H(i)$$

$$\left(F^P\right)^{tot} = \left\{ \sum_{i=1}^{G}\sum_{j=1}^{M} F^{PI}(i,j) + \sum_{i=1}^{G}\sum_{\substack{j=1 \\ j\neq i}}^{G} F^{PL}(i,j) + \sum_{i=1}^{G}\sum_{\substack{j=1 \\ j\neq i}}^{G} F^{PV}(i,j) \right\}$$

$$Q^{tot} = \sum_{i=1}^{G} Q_H(i) + \sum_{i=1}^{G} Q_C(i)$$

$$\dot{S}_G^{tot} = \sum_{i=1}^{\infty} \dot{S}_G(i)$$

$$Q_H \geq 0; Q_C \geq 0; F^I \geq 0;\ F^{OI} \geq 0; F^{PI} \geq 0; F^{OL} \geq 0; F^{OV} \geq 0; F^{PL} \geq 0; F^{PV} \geq 0; H \geq 0; C \geq 0;$$
$$0 \leq C^{tot} \leq C^{ub};\ 0 \leq H^{tot} \leq H^{ub};\ 0 \leq \left(F^P\right)^{tot} \leq \left(F^P\right)^{ub};\ 0 \leq Q^{tot} \leq Q^{ub}; 0 \leq \dot{S}_G^{tot} \leq \left(\dot{S}_G^{tot}\right)^{ub}$$

Since all variables represent physical quantities (flowrate, catalyst amount, stage volume, stage duty), they can have only non-negative values. In addition to that, the total reactive holdup, total capacity, total flow, total energy consumption, and total entropy generated can have their upper bound specified in the synthesis process.

Since the objective function is being used to identify the correct direction of the heat transferring in each flash, the minimum rate of entropy generation in the reactive separation process is identified by tightening the value of $\left(\dot{S}_G^{tot}\right)^{ub}$ in the LP presented in Eq.(3.39), until the system becomes infeasible.

3.3.5. Enthalpy and entropy model discussion

In general, for a multicomponent mixture of n species and component molar fraction z_i, the molar enthalpy is quantified by summing its ideal value h^{id} with its excess value h^E [53], as shown in Eq.(3.40).

$$h\left(T,P,\{z_k\}_{k=1}^{n}\right)=h^{id}\left(T,\{z_k\}_{k=1}^{n}\right)+h^{E}\left(T,P,\{z_k\}_{k=1}^{n}\right) \tag{3.40}$$

Since the ideal model is independent of pressure, each component enthalpy can be evaluated at the mixture pressure instead of its correspondent component partial pressure [53]. Therefore, due to the summability relation of the partial properties, the ideal mixture molar enthalpy can be calculated as shown in Eq.(3.41).

$$h^{id}\left(T,\{z_k\}_{k=1}^{n}\right)=\sum_{k=1}^{n}z_k h_k\left(T\right) \tag{3.41}$$

The excess molar enthalpy h^E can be evaluated from the excess Gibbs free energy G^E, which is a function of the mixture temperature, pressure, and composition. Moreover, the excess Gibbs free energy can be expressed in terms of the components' fugacity pressure [53]. In this case study present in this work, the mixture is considered to be ideal. Thus, the excess molar enthalpy h^E is considered zero and the molar enthalpy of the multicomponent mixture h is equal to its ideal value h^{id}, as shown in Eq.(3.42).

$$h\left(T,\{z_k\}_{k=1}^{n}\right)=h^{id}\left(T,\{z_k\}_{k=1}^{n}\right)=\sum_{k=1}^{n}z_k h_k\left(T\right) \tag{3.42}$$

Any applicable model can provide enthalpy values. The choice depends primarily on the nature of the fluids. For a reactive flash separator operating at constant pressure, the total molar enthalpy h is a function of temperature, and composition only. Therefore, one can write the liquid and vapor enthalpies of the k^{th} component in the i^{th} reactive flash as shown in Eq.(3.43) and (3.44) below:

$$h_k^L(i) = h_k^L\left(T(i), x_k(i)\right) \quad ; \quad \begin{matrix}\forall k \in \{1,..., n\} \\ \forall i \in \{1,..., G\}\end{matrix} \tag{3.43}$$

$$h_k^V(i) = h_k^V\left(T(i), y_k(i)\right) \quad ; \quad \begin{matrix}\forall k \in \{1,..., n\} \\ \forall i \in \{1,..., G\}\end{matrix} \tag{3.44}$$

Let the heat capacity be denoted $C_k^{p,L}$ and $C_k^{p,V}$ for the liquid and vapor of component k, respectively. Then the k^{th} component molar liquid and vapor enthalpy is given by Eq.(3.45) and (3.46).

$$h_k^L(T) = \int C_k^{p,L} dT \tag{3.45}$$

$$h_k^V(T) = \int C_k^{p,V} dT \tag{3.46}$$

The k^{th} component enthalpy of formation h_k^0 is by definition the enthalpy of the pure component at the standard reference state, i.e., temperature equals 25°C and pressure equals 1 atm. Thus, assuming a 3rd order polynomial that correlates both liquid and vapor heat capacities of species k, as shown in Eq.(3.47) below,

$$\frac{C_k^P}{R} = c_{k,1} + c_{k,2}T + c_{k,3}T^2 + c_{k,4}T^3 \tag{3.47}$$

the enthalpy from the temperature of the reference state T^0 to the operating temperature T one can be solved as shown in Eq.(3.48).

$$
\begin{aligned}
&h_k(T) - h_k^0(T^0) = \int_{T^0}^{T} R\left(c_{k,1} + c_{k,2}T + c_{k,3}T^2 + c_{k,4}T^3\right)dT = \\
&= R\left[\int_{T^0}^{T} c_{k,1}\,dT + \int_{T^0}^{T} c_{k,2}T\,dT + \int_{T^0}^{T} c_{k,3}T^2 dT + \int_{T^0}^{T} c_{k,4}T^3 dT\right] = \\
&= \left(Rc_{k,1}T + \frac{R}{2}c_{k,2}T^2 + \frac{R}{3}c_{k,3}T^3 + \frac{R}{4}c_{k,4}T^4\right)\Bigg|_{T^0}^{T} = \\
&= Rc_{k,1}\left[T - T^0\right] + \frac{R}{2}c_{k,2}\left[T^2 - \left(T^0\right)^2\right] + \frac{R}{3}c_{k,3}\left[T^3 - \left(T^0\right)^3\right] + \frac{R}{4}c_{k,4}\left[T^4 - \left(T^0\right)^4\right]
\end{aligned}
\tag{3.48}
$$

In the reactive flash separator outlets, the multicomponent mixture streams exit the system in saturated forms, either liquid or vapor, depending on the flash separator outlet. If pure species k is liquid at the standard condition, i.e., T^0 is lower than the species normal boiling point T_k^b, the fraction of k that appears in the mixture at the vapor outlet must consider its the heat of vaporization regardless of the flash temperature. The same approach is valid when pure species k is in vapor phase at standard condition $\left(T^0 \geq T_k^b\right)$ and shows up in the liquid output of a multicomponent list at VLE conditions. In the latest case, the component k enthalpy at the mixture liquid stream should consider the heat necessary for its liquefaction. By defining λ_k^b as the dimensionless heat of vaporization of species k, this approach is described below by Eq.(3.49) and (3.50) for the liquid and vapor enthalpic contribution of species k in a mixture, respectively.

$$
\begin{cases}
h_k^L = h_k(T) & ; \quad if \quad T^0 \leq T_k^b \\
h_k^L = h_k(T) - \lambda_k^b R T_k^b & ; \quad if \quad T^0 \geq T_k^b
\end{cases}
\tag{3.49}
$$

$$
\begin{cases}
h_k^V = h_k(T) + \lambda_k^b R T_k^b & ; \quad if \quad T^0 \leq T_k^b \\
h_k^V = h_k(T) & ; \quad if \quad T^0 \geq T_k^b
\end{cases}
\tag{3.50}
$$

Separations of different species in both reactive and non-reactive flashes rely on vapor-liquid equilibrium (VLE) conditions to occur. Thus, once species composition is specified in a flash liquid outlet for example, the vapor molar fractions the flash's operating temperature are also fixed due to the equilibrium conditions and can be calculated iteratively. This procedure was successfully used in several applications featuring reactive and non-reactive distillation systems [18,19,29]. Considering that the reactive flash's temperature, pressure, and outlet compositions are fixed by the VLE condition, so are the specific total molar enthalpies at the outlets, regardless of the enthalpy model used. Thus, by recalling Eq.(3.42) for the reactive flash separator presented in this work, the total molar enthalpy for the vapor and liquid mixture streams exiting each flash have the form shown in Eq.(3.51) and (3.52) , respectively, under the conditions presented in Eq.(3.49) and (3.50).

$$h^L(i) = \sum_{k=1}^{n} x_k(i)\, h_k^L(i) \qquad ; \qquad \forall i \in \{1,...,G\} \tag{3.51}$$

$$h^V(i) = \sum_{k=1}^{n} y_k(i)\, h_k^V(i) \qquad ; \qquad \forall i \in \{1,...,G\} \tag{3.52}$$

The entropy model used in this work follows the assumptions and procedure presented above for the enthalpy model. Let the heat capacity of the pure substance k be denoted C_k^p. Then, for an isobaric system, the infinitesimal variation of the entropy for the k^{th} substance is only a function of the temperature, as shown in Eq.(3.53).

$$ds_k = C_k^p \frac{dT}{T} - R\frac{dP}{P} \overset{\text{Isobaric System}}{\Rightarrow} s_k(T) = \int C_k^p \frac{dT}{T} \tag{3.53}$$

Thus, considering that the heat capacity of the liquid $C_k^{p,L}$ and vapor $C_k^{p,V}$ phases of the k^{th} pure substance can be described by a continuous function for example, the k^{th} component molar liquid and vapor entropy for an isobaric system is given by Eq.(3.54) and (3.55).

$$s_k^L(T) = \int C_k^{p,L} \frac{dT}{T} \tag{3.54}$$

$$s_k^V(T) = \int C_k^{p,V} \frac{dT}{T} \tag{3.55}$$

Considering the 3rd order polynomial shown in Eq.(3.47), the entropy variation for pure component k from the temperature of the reference state T^0 to the operating temperature T can be calculated as shown in Eq.(3.48). Considering the assumptions presented, although entropy variation depends only on temperature, the value of the entropy at the reference state depends on the pressure of the reference state p^0.

$$\begin{aligned} s_k(T, p^0) - s_k^0(T^0, p^0) &= \int_{T^0}^{T} \left[R\left(\frac{c_{k,1}}{T} + c_{k,2} + c_{k,3}T + c_{k,4}T^2 \right) \right] dT = \\ &= \left(Rc_{k,1}\ln(T) + Rc_{k,2}T + \frac{R}{2}c_{k,3}T^2 + \frac{R}{3}c_{k,4}T^3 \right)\Bigg|_{T^0}^{T} = \\ &= Rc_{k,1}\ln\left(\frac{T}{T^0}\right) + Rc_{k,2}\left(T - T^0\right) + \frac{R}{2}c_{k,3}\left[T^2 - \left(T^0\right)^2\right] + \frac{R}{3}c_{k,4}\left[T^3 - \left(T^0\right)^3\right] \end{aligned} \tag{3.56}$$

The liquid and vapor entropy values for each component in the mixture follows the approach presented previously for enthalpy calculations, i.e., for liquid (vapor) entropy of a component in the mixture in which the temperature is above (below) the component's boiling point, latent heat is considered as presented in Eq.(3.57) and (3.58).

$$\begin{cases} s_k^L = s_k\left(T\right) & ; \quad if \quad T^0 \le T_k^b \\ s_k^L = s_k\left(T\right) - \dfrac{\lambda_k^b R}{T_k^b} & ; \quad if \quad T^0 \ge T_k^b \end{cases} \tag{3.57}$$

$$\begin{cases} s_k^V = s_k\left(T\right) + \dfrac{\lambda_k^b R}{T_k^b} & ; \quad if \quad T^0 \le T_k^b \\ s_k^V = s_k\left(T\right) & ; \quad if \quad T^0 \ge T_k^b \end{cases} \tag{3.58}$$

Thus, the total entropy for the liquid and vapor phases of an ideal mixture of pure component k exiting each flash have the form shown in Eq.(3.59) and (3.60), respectively, where the individual species entropy value are calculated using Eq.(3.57) and (3.58).

$$s^L\left(i\right) = \sum_{k=1}^{n} x_k\left(i\right) s_k^L\left(i\right) - R\sum_{k=1}^{n} x_k\left(i\right) \ln x_k\left(i\right) \quad ; \quad \forall i \in \left\{1,...,G\right\} \tag{3.59}$$

$$s^V\left(i\right) = \sum_{k=1}^{n} y_k\left(i\right) s_k^V\left(i\right) - R\sum_{k=1}^{n} y_k\left(i\right) \ln y_k\left(i\right) \quad ; \quad \forall i \in \left\{1,...,G\right\} \tag{3.60}$$

The equations above show that even for ideal substances the relation between pure substance's entropy and the entropy of mixtures has a component that accounts for the entropy generated in the mixing process. The formulation described in this session, based on the IDEAS framework and applicable thermodynamic concepts, was applied in a study case featuring the metathesis of 2-pentene.

3.4. Case study: Olefin metathesis

3.4.1. Thermodynamic data and problem specifications

The study case shows a continuation of the work done previously involving the metathesis reaction, a process commonly used in the petrochemical industry to rebalance the light olefins originated during the catalytic and steam cracking processes. In this case study, the minimization of the rate of entropy generated is investigated through the IDEAS framework. The metathesis of 2-pentene is assessed in this intensification study of reactive separation networks. The overall metathesis reaction is shown in Eq.(3.61).

$$2C_5H_{10} \rightleftarrows C_4H_8 + C_6H_{12} \tag{3.61}$$

The hydrocarbons involved in this system are similar in chemical structure, and deviations from ideality are negligible. Moreover, the components in the mixture have normal boiling points temperatures that are far from each other – 2-pentene at 310 K, 2-butene at 277 K, and 3-hexene at 340 K – allowing an easy separation through distillation process.

This reactive distillation system has negligible heat of reaction and, due to this fact, the system can run at atmospheric pressure or other low-pressure operating values without significant changes on the value of the equilibrium constant. Considering 2-pentene as the reference component, the temperature dependent rate expression is given by Eq.(3.62) (Chen et al. 2000), while the reaction equilibrium constant K_{eq} and the kinetic rate constant $k_f\ \left(h^{-1}\right)$ are shown in Eq.(3.63) and Eq.(3.64), respectively:

$$R = k_f \left(a_{C_5H_{10}}^2 - \frac{a_{C_4H_8}\, a_{C_6H_{12}}}{K_{eq}} \right) \tag{3.62}$$

$$K_{eq} = 0.25 \tag{3.63}$$

$$k_f = 1.0661 \times 10^5 \; e^{\left(-3321.2/T(K)\right)} \; \left(h^{-1}\right) \tag{3.64}$$

The ideal behavior of this system allows the consideration of both the fugacity and the activity coefficient functions are equal the unity and Raoult's law is assumed. Moreover, the values of the species' molar fractions can be used in place of the respective activity coefficient in Eq.(3.62). Antoine's model is used to calculate the saturated pressure of each component in the mixture, and coefficients can be found in Table 3.1 for T in K and P in Pa.

Table 3.1. Antoine coefficients for 2-butene, 2-pentene, 3-hexene (Okasinski and Doherty 1998).

	$k = C_4H_8$	$k = C_5H_{10}$	$k = C_6H_{12}$
$A_{1,k}$	20.6909	20.723	20.7312
$A_{2,k}$	−2202.188	−2462.02	−2680.52
$A_{3,k}$	−36.578	−42.391	−48.401

As demonstrated in previous works[18,19,29], for a fixed value of the operating pressure P and for an specified liquid outlet composition, the respective bubble point temperature, reaction rate, and vapor outlet composition can be calculated iteratively by changing $T(i)$ in Eq.(3.65) until the sum of the molar fractions in the vapor phase is equal to unity, as specified in Eq.(3.68).

$$\ln P_k^{sat}(i) = A_{1,k} + \frac{A_{2,k}}{\left(T(i) + A_{3,k}\right)} \quad ; \quad \forall k = C_5H_{10},\, C_8H_8,\, C_6H_{12} \tag{3.65}$$

$$y_k^V(i) = \frac{x_k^L(i)\; P_k^{sat}\left(T(i)\right)}{P} \quad ; \quad \forall k = C_5H_{10},\, C_8H_8,\, C_6H_{12} \tag{3.66}$$

$$R(i) = 1.0661 \times 10^5 \; e^{\left(-3321.2/T(i)\right)} \left[\left(x_{C_5H_{10}}(i)\right)^2 - \frac{x_{C_4H_8}(i)\; x_{C_6H_{12}}(i)}{0.25} \right] \tag{3.67}$$

$$y^V_{C_5H_{10}}(i) + y^V_{C_4H_8}(i) + y^V_{C_6H_{12}}(i) - 1 = 0 \tag{3.68}$$

The coefficient values of the third order polynomial shown in Eq.(3.47), applied in the calculation of both liquid and vapor heat capacities, as well as the value of the dimensionless heat of vaporization for the 2-pentene metathesis system, are shown in Table 3.2.

Table 3.2. Thermodynamic data for the metathesis of 2-pentene (Okasinski and Doherty 1998).

Component:	$k = C_4H_8$	$k = C_5H_{10}$	$k = C_6H_{12}$
Liquid Heat Capacity			
$c_{1,k}$	13.357	21.224	19.897
$c_{2,k}$	−3.9752E−03	−6.9842E−02	−1.4182E−02
$c_{3,k}$	3.3249E−05	2.5206E−04	8.2626E−05
$c_{4,k}$	0.0	−1.7167E−07	0.0
Vapor Heat Capacity			
$c_{1,k}$	−6.256E−01	−1.8739	−2.9336
$c_{2,k}$	3.8721E−02	5.6102E−02	7.1697E−02
$c_{3,k}$	−1.6763E−05	−3.1656E−05	−4.3559E−05
$c_{4,k}$	1.877E−09	6.9946E−09	1.0609E−08
Normal Boiling Point (K)	276.87	310.08	339.60
Dimensionless Heat of Vaporization	10.178	10.294	10.166

Enthalpy and entropy calculations are based in the values shown in the table above, employed using Eq.(3.49) to (3.52), and (3.57) to (3.60), respectively.

For the reactive distillation process in this case study, the distribution network of IDEAS is set to have one inlet stream of pure 2-pentene at saturated liquid state, i.e., feed quality $q = 1$ as defined by Doherty and Malone [54], and two outlets streams: the first rich in 2-butene at saturated vapor state and the second rich in 3-hexene at saturated liquid state. Simulations were performed for the operating conditions specified in Table 3.3.

Table 3.3. Specifications for the 2-pentene metathesis problem example.

Feed Flow (kmol/h)	100
Outlet Flow 1 (Distillate) (kmol/h)	50
Outlet Flow 2 (Bottom) (kmol/h)	50
Residence Time (s)	60
Operating pressure (bar)	1
Feed quality	1
Inlet molar fractions	
C4H8	0.0000
C5H10	1.0000
C6H12	0.0000
Outlet molar fraction target bounds	
Outlet Flow 1	
C4H8	0.9800 - 1.0000
C5H10	0.0000 - 0.2000
C6H12	0.0000 - 0.2000
Outlet Flow 2	
C4H8	0.0000 - 0.2000
C5H10	0.0000 - 0.2000
C6H12	0.9800 - 1.0000

3.4.2. Discretization strategy and IDEAS convergence

The strategy developed to discretize the ternary liquid composition space follows the concept presented in a previous works [19], where different discretization steps were used in

different regions of the composition domain to generate a finite set of reactive flash separators. In this work, three different regions are considered in the discretization strategy, whose limits are specified by the molar fractions α and β, as shown schematically in Fig. 3.3.

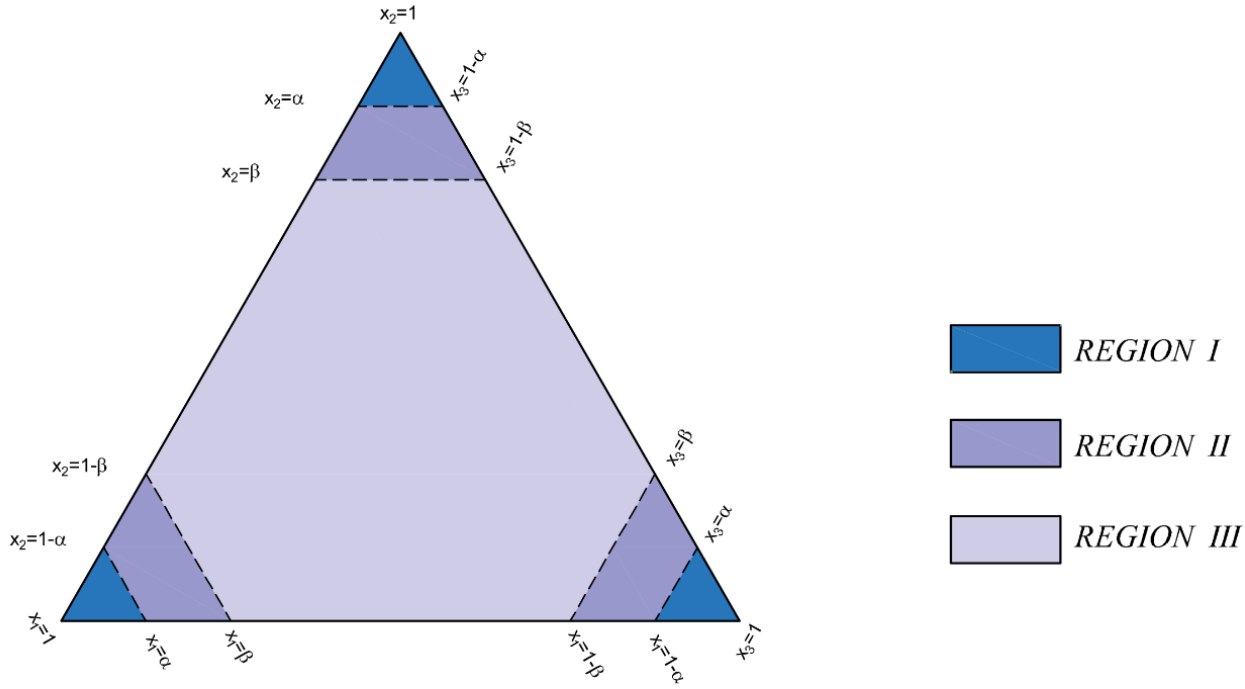

Figure 3.3 - Discretization strategy for the ternary liquid molar fraction domain

Considering that the total energy minimization and the entropy generation minimization have similar behavior in relation to the impact of the discretization in each region, the discretization sets used in this work follows the sets used in the total energy minimization problem for the same system.

The IDEAS full convergence plot for a minimum purity of 87.5% in the separation products is shown in Fig. 3.4. This result was obtained by setting $\alpha = 0.75$ and $\beta = 0.875$ as the region edges, and for the discretization shown in Table 3.4.

Table 3.4. Optimal value for the minimum entropy generation problem (87.5% purity, $\alpha = 0.75$, $\beta = 0.875$) per discretized set in regions I, II and III

Discretized step size			Number of Flashes in G	Minimum total entropy generation (kJ/K.s)
Region I	Region II	Region III		
1/16	1/8	1/8	92	14555.70
1/16	1/16	1/8	120	5650.86
1/16	1/16	1/16	153	7813.20
1/32	1/32	1/16	243	6655.22
1/32	1/32	1/32	561	5740.74
1/64	1/64	1/32	885	5572.83
1/128	1/64	1/32	1209	5503.05

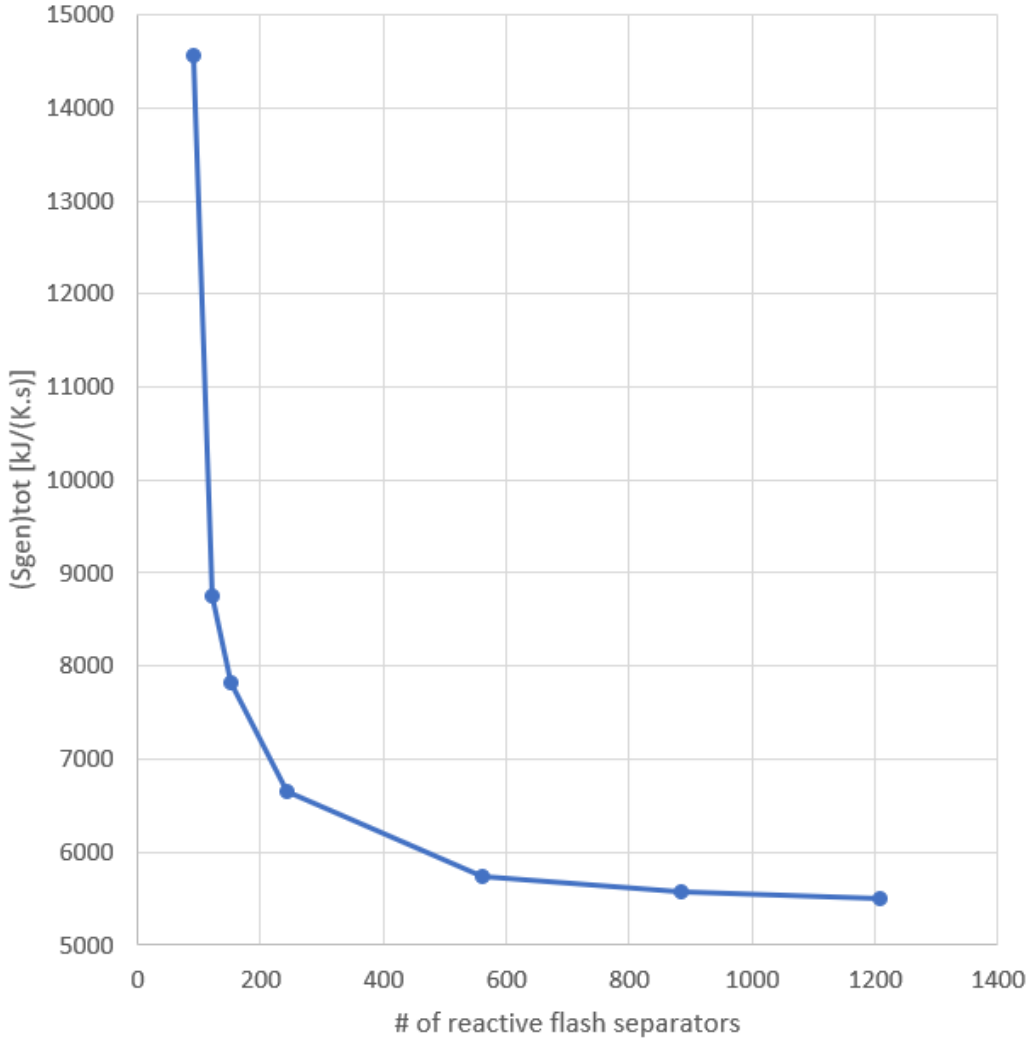

Figure 3.4 - IDEAS convergence plot for the minimum entropy generation problem in the metathesis of 2-pentene (87.5% purity in the products).

3.4.3. IDEAS minimum entropy generation results

The optimization problem presented in Eq.(3.43) is used to find the minimum total entropy generated by reactive separation systems performing the 2-pentene metathesis process. To define the finite set used by the IDEAS OP, a discretization level of 1/256, 1/128, and 1/32 was employed in regions I, II, and III, respectively. The total number of reactive flash separators in the set G is 1065, which is the result obtained when $\alpha = 0.96875$ and $\beta = 0.875$ are specified as the edges of the regions inside the liquid molar fraction domain.

A 2-pentene metathesis system simulated in UniSim® Design, featuring a reactor followed by sequence of distillation columns (Fig.2.6), is considered the baseline for comparison with the results obtained by the IDEAS approach. The system consists of a reactor operating with 48% conversion, which is close to the equilibrium conversion of 50%. The effluent from the reactor is sent to a distillation column (T-101) that separates the ternary mixture into a 2-butene stream with 98% purity at the distillate (saturated vapor state), and a binary mixtures of 2-pentene and 3-hexene at the bottom. Following that, the bottoms from the T-101 are sent to the distillation column T-102, where 3-hexene is separated at the bottom with a 98% purity. The distillate stream rich in 2-pentene from T-102 is recycled to the reactor. The input conditions, output production, and purity target of this baseline design are the same used in the IDEAS simulation, as listed in Table 3.3. The total entropy generated by the baseline configuration system is 17,788.73 kJ/(h.K).

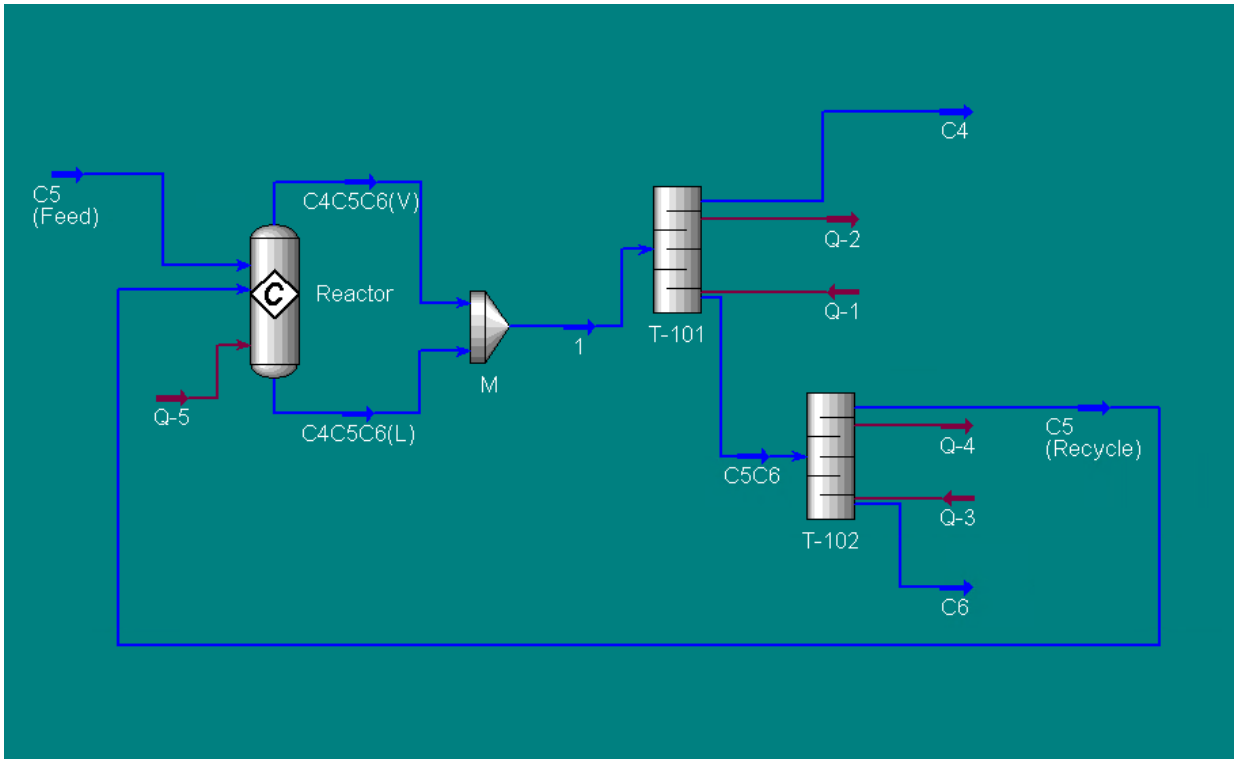

Figure 3.5 – UniSim® baseline for the Metathesis of 2-Pentene

The minimum entropy generation rate obtained through IDEAS was 7,480.91 kJ/(h.K), which can be considered a close approximation to the global minimum that this technology can achieve for the conditions specified in Table 3.3. The results obtained by the IDEAS reactive separation network shows that the optimized system generates 57.94% less entropy than proposed baseline design. The results are shown in Fig.3.6 for comparison.

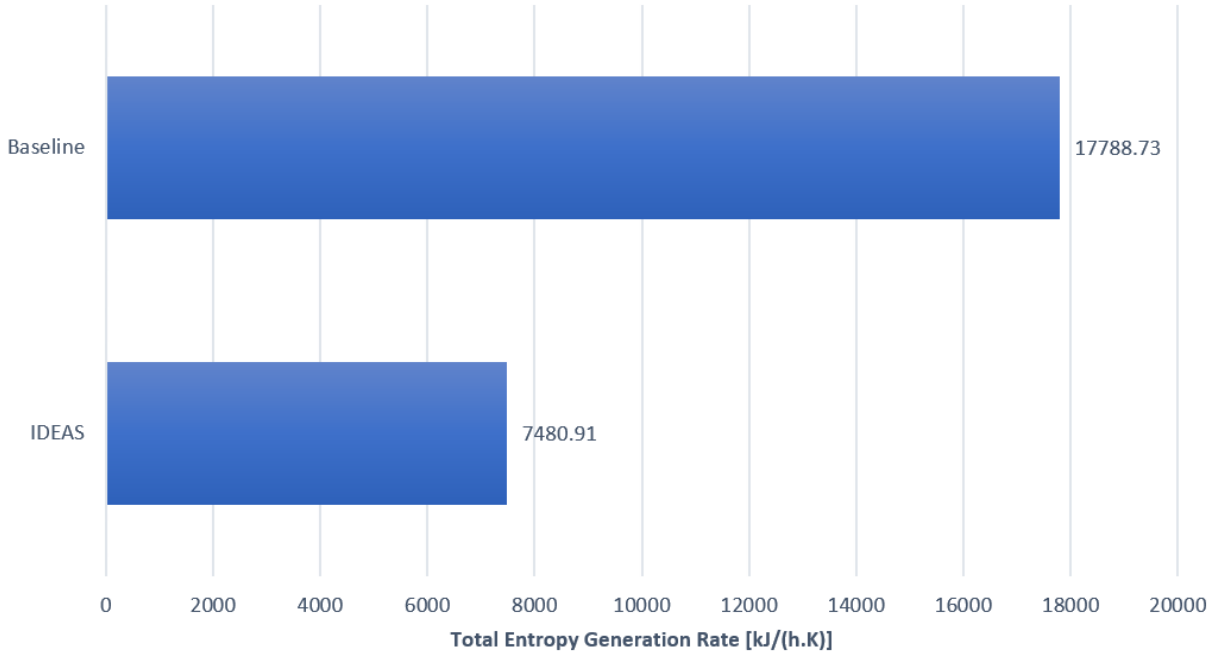

Figure 3.6 - Comparison between IDEAS results and Baseline

The connection between the amount of irreversibilities in reactive distillation systems and the design of corresponding intensified system is assessed in this work. The goal is to rigorously quantify tradeoffs between the network's total entropy generation and its total capacity. The LP problem presented in Eq.(3.39) is solved several times with an increasingly smaller value for the capacity upper bound until it reaches the feasibility limit, which allows the identification of the minimum entropy generation rate for each feasible capacity value needed to deliver the desired purity specifications. The tradeoff curve for the metathesis study case and the indication of the feasible region are presented in Fig.3.7.

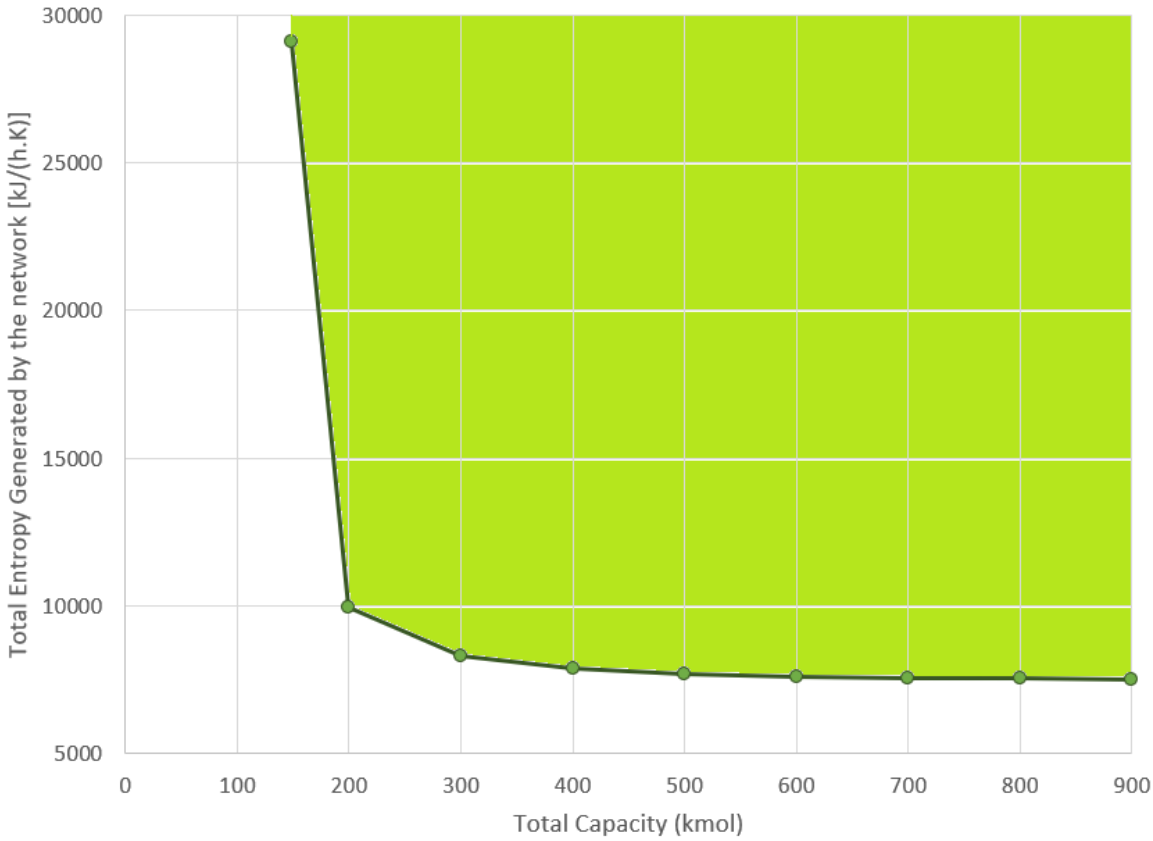

Figure 3.7 - Minimum entropy generation rate limit for the 2-pentene metathesis problem for different network capacity values (feasible region in green).

As expected for a globally optimal synthesis problem, the minimum entropy generation rate and the minimum energy consumption, presented in another work, have a similar pattern. The indication, that size-intensified reactive distillation processes may require more energy, seems more meaningful when considered in the light of entropy generation: an intensified system close to the feasible limit will inevitably be more irreversible if further intensified. Nevertheless, systems that are located far from the performance limit curve can possibly enjoy energy, size, and irreversibility reductions through process intensification.

3.5. Conclusions

The Infinite DimEnsionAl State-Space (IDEAS) framework is used as a tool to identify the performance limits of reactive separation systems featuring the minimization of the total entropy generation rate of the system. The rate of entropy generation measures the amount of irreversibilities in a given process, indicating by how much a system is far from its ideal configuration, and serving as a comparison tool between different process configurations. A model for the evaluation of entropy generation using an isobaric reactive vapor-liquid equilibrium flash separator, with liquid holdup, capacity, and a distributed heat (cooling) system. Kinetically and/or equilibrium limited reactions are assumed to occur in the liquid phase. A formulation of the mass, energy and entropy balances is then developed through the IDEAS approach. The procedure leads to a linear convex problem formulation, in which the optimal solution is guaranteed to be global over all possible network configurations. The model was used in the investigation of reactive separation for olefin metathesis. The case study features the metathesis of 2-pentene to form 2-butene and 3-hexene, an important chemical process for the oil industry. The minimum total energy required by the system was considered as the problem's objective while the minimum total entropy generation rate was obtained through tightening the respective variable during the solution process. Results were obtained for unbounded systems and for increasingly smaller capacity values, a variable of interest for process intensification. The goal is to rigorously quantify tradeoffs between the network's irreversibilities and its total capacity.

The globally minimized total entropy generation rate found through the application of IDEAS in the reactive-separative metathesis system was 7513.62 kJ/(K.s). Using a traditional

reactor-followed-by-separation-system scheme as a baseline, the optimized IDEAS based reactive separation network generates 57.94% less entropy than proposed baseline design.

The tradeoff curve for minimum total entropy generation rate shows that the amount of irreversibility connected to reactive separation systems increases for reductions in the capacity value. This result is consistent with the energy implications shown in other works, and implicates that not only energy consumption increases, but also the irreversibility of the system increases with the system's intensification. Nevertheless, systems located far from the performance limit curve in the minimum entropy generated-capacity space can pursue further reductions in both energy consumption, size, and irreversibility of processes through process intensification.

3.6. Notation

Thermodynamic Variables*:*

P	Reactive flash separator pressure (Pa)
T	Reactive flash separator temperature (K)
$y_k^V(i)$	k^{th} Species equilibrium vapor composition leaving the i^{th} unit $(\dim)$
$x_k^L(i)$	k^{th} Species equilibrium liquid composition leaving the i^{th} unit $(\dim)$
$P_k^{sat}(T)$	k^{th} Species temperature dependent saturated vapor pressure (Pa)
$\phi_k\left(\left\{y_l^V\right\}_{l=1}^n, T, P\right)$	k^{th} Species non-ideal fugacity coefficient

$\gamma_k\left(\left\{x_l^L\right\}_{l=1}^n, T\right)$	k^{th} Species non-ideal liquid activity coefficient
a_k	Activity of the k^{th} species $(\dim)$
$A_{j,k}$	Antoine equation j^{th} parameter of the k^{th} species $(\dim)$
K_{eq}	Reaction equilibrium constant $(\dim)$
k_f	Forward reaction rate constant $(1/\mathrm{h})$

IDEAS Variables*:*

$F^I(i)$	i^{th} DN inlet stream
$F^O(i)$	i^{th} DN outlet stream
$F^L(i)$	i^{th} OP liquid outlet
$F^V(i)$	i^{th} OP vapor outlet
$F^{OI}(i,j)$	j^{th} DN inlet stream to i^{th} DN outlet
$F^{PI}(i,j)$	i^{th} OP inlet stream from j^{th} DN network inlet
$F^{OL}(i,j)$	i^{th} DN outlet stream from j^{th} OP liquid outlet
$F^{OV}(i,j)$	i^{th} DN outlet stream from j^{th} OP vapor outlet

$F^{PL}(i,j)$	i^{th} OP inlet stream from j^{th} OP liquid outlet
$F^{PV}(i,j)$	i^{th} OP inlet stream from j^{th} OP vapor outlet
$H(i)$	Reactive holdup of the i^{th} reactive flash separator unit in the OP
$C(i)$	Capacity of the i^{th} reactive flash separator unit in the OP
$\dot{Q}_H(i)$	Heat transferred to the i^{th} reactive flash separator unit in the OP
$\dot{Q}_L(i)$	Heat released by the i^{th} reactive flash separator unit in the OP
$z_k^I(i)$	k^{th} species, i^{th} DN inlet stream composition
$z_k^O(i)$	k^{th} species, i^{th} DN outlet stream composition
$\left(z_k^O(i)\right)^l$	k^{th} species, i^{th} DN outlet stream composition vector, lower bound
$\left(z_k^O(i)\right)^u$	k^{th} species, i^{th} DN outlet stream composition vector, upper bound
$x_k^L(i)$	k^{th} species, i^{th} OP liquid outlet composition
$y_k^V(i)$	k^{th} species, i^{th} OP vapor outlet composition
G	Total number of reactive flashes in the OP
M	Number of IDEAS network inlets
N	Number of IDEAS network outlets

3.7. References

(1) Sauar, E.; Kjelstrup, S.; Lien, K. M. Equipartition of Forces — Extension to Chemical Reactors. *Comput. Chem. Eng.* **1997**, *21*, S29–S34. https://doi.org/10.1016/S0098-1354(97)87474-1.

(2) Stankiewicz, A. I.; Moulijn, J. A. Process Intensification: Transforming Chemical Engineering. *Chem. Eng. Prog.* **2000**, *96* (1), 22–34.

(3) Stankiewicz, A. Reactive Separations for Process Intensification: An Industrial Perspective. *Chem. Eng. Process. Process Intensif.* **2003**, *42* (3), 137–144. https://doi.org/10.1016/S0255-2701(02)00084-3.

(4) Carathéodory, C. Untersuchungen Über Die Grundlagen Der Thermodynamik. *Math. Ann.* **1909**, *67* (3), 355–386.

(5) Bejan, A. *Entropy Generation Minimization: The Method of Thermodynamic Optimization of Finite-Size Systems and Finite-Time Processes*; CRC press, 2013.

(6) Tolman, R. C.; Fine, P. C. On the Irreversible Production of Entropy. *Rev. Mod. Phys.* **1948**, *20* (1), 51–77. https://doi.org/10.1103/RevModPhys.20.51.

(7) Bejan, A. *Advanced Engineering Thermodynamics*; John Wiley & Sons, 2016.

(8) Kiss, A. A. Distillation Technology – Still Young and Full of Breakthrough Opportunities. *J. Chem. Technol. Biotechnol.* **2014**, *89* (4), 479–498. https://doi.org/10.1002/jctb.4262.

(9) Sauar, E.; Kjelstrup Ratkje, S.; Lien, K. M. Equipartition of Forces: A New Principle for Process Design and Optimization. *Ind. Eng. Chem. Res.* **1996**, *35* (11), 4147–4153. https://doi.org/10.1021/ie9507078.

(10) Ratkje, S. K.; Sauar, E.; Hansen, E. M.; Lien, K. M.; Hafskjold, B. Analysis of Entropy Production Rates for Design of Distillation Columns. *Ind. Eng. Chem. Res.* **1995**, *34* (9), 3001–3007.

(11) Wilson, S.; Manousiouthakis, V. IDEAS Approach to Process Network Synthesis: Application to Multicomponent MEN. *AIChE J.* **2000**, *46* (12), 2408–2416. https://doi.org/10.1002/aic.690461209.

(12) Drake, J. E.; Manousiouthakis, V. IDEAS Approach to Process Network Synthesis: Minimum Utility Cost for Complex Distillation Networks. *Chem. Eng. Sci.* **2002**, *57* (15), 3095–3106. https://doi.org/10.1016/S0009-2509(02)00159-8.

(13) Drake, J. E.; Manousiouthakis, V. IDEAS Approach to Process Network Synthesis: Minimum Plate Area for Complex Distillation Networks with Fixed Utility Cost. *Ind. Eng. Chem. Res.* **2002**, *41* (20), 4984–4992. https://doi.org/10.1021/ie010735s.

(14) Justanieah, A. M.; Manousiouthakis, V. IDEAS Approach to the Synthesis of Globally Optimal Separation Networks: Application to Chromium Recovery from Wastewater. *Adv. Environ. Res.* **2003**, *7* (2), 549–562. https://doi.org/10.1016/S1093-0191(02)00026-6.

(15) Takase, H.; Hasebe, S. Synthesis of Ternary Distillation Process Structures Featuring Minimum Utility Cost Using the IDEAS Approach. *AIChE J.* **2018**, *64* (4), 1285–1294. https://doi.org/10.1002/aic.16023.

(16) Martin, L. L.; Manousiouthakis, V. I. Globally Optimal Power Cycle Synthesis via the Infinite-DimEnsionAl State-Space (IDEAS) Approach Featuring Minimum Area with Fixed Utility. *Chem. Eng. Sci.* **2003**, *58* (18), 4291–4305. https://doi.org/10.1016/S0009-2509(02)00526-2.

(17) Holiastos, K.; Manousiouthakis, V. Infinite-Dimensional State-Space (IDEAS) Approach to Globally Optimal Design of Distillation Networks Featuring Heat and Power Integration. *Ind. Eng. Chem. Res.* **2004**, *43* (24), 7826–7842. https://doi.org/10.1021/ie010434i.

(18) Burri, J. F.; Manousiouthakis, V. I. Global Optimization of Reactive Distillation Networks Using IDEAS. *Comput. Chem. Eng.* **2004**, *28* (12), 2509–2521. https://doi.org/10.1016/j.compchemeng.2004.06.014.

(19) da Cruz, F. E.; Manousiouthakis, V. I. Process Intensification of Reactive Separator Networks through the IDEAS Conceptual Framework. *Comput. Chem. Eng.* **2017**, *105*, 39–55. https://doi.org/10.1016/j.compchemeng.2016.12.006.

(20) Burri, J. F.; Wilson, S. D.; Manousiouthakis, V. I. Infinite DimEnsionAl State-Space Approach to Reactor Network Synthesis: Application to Attainable Region Construction. *Comput. Chem. Eng.* **2002**, *26* (6), 849–862. https://doi.org/10.1016/S0098-1354(02)00008-X.

(21) Manousiouthakis, V. I.; Justanieah, A. M.; Taylor, L. A. The Shrink–Wrap Algorithm for the Construction of the Attainable Region: An Application of the IDEAS Framework. *Comput. Chem. Eng.* **2004**, *28* (9), 1563–1575. https://doi.org/10.1016/j.compchemeng.2003.12.005.

(22) Zhou, W.; Manousiouthakis, V. I. Non-Ideal Reactor Network Synthesis through IDEAS: Attainable Region Construction. *Chem. Eng. Sci.* **2006**, *61* (21), 6936–6945. https://doi.org/10.1016/j.ces.2006.07.002.

(23) Zhou, W.; Manousiouthakis, V. I. Pollution Prevention through Reactor Network Synthesis: The IDEAS Approach. *Int. J. Environ. Pollut.* **2007**, *29* (1–3), 206–231. https://doi.org/10.1504/IJEP.2007.012804.

(24) Zhou, W.; Manousiouthakis, V. I. Variable Density Fluid Reactor Network Synthesis—Construction of the Attainable Region through the IDEAS Approach. *Chem. Eng. J.* **2007**, *129* (1–3), 91–103. https://doi.org/10.1016/j.cej.2006.11.004.

(25) Posada, A.; Manousiouthakis, V. Multi-Feed Attainable Region Construction Using the Shrink–Wrap Algorithm. *Chem. Eng. Sci.* **2008**, *63* (23), 5571–5592. https://doi.org/10.1016/j.ces.2008.07.026.

(26) Zhou, W.; Manousiouthakis, V. I. On Dimensionality of Attainable Region Construction for Isothermal Reactor Networks. *Comput. Chem. Eng.* **2008**, *32* (3), 439–450. https://doi.org/10.1016/j.compchemeng.2007.02.013.

(27) Zhou, W.; Manousiouthakis, V. I. Automating the AR Construction for Non-Isothermal Reactor Networks. *Comput. Chem. Eng.* **2009**, *33* (1), 176–180. https://doi.org/10.1016/j.compchemeng.2008.07.011.

(28) Ghougassian, P. G.; Manousiouthakis, V. Attainable Composition, Energy Consumption, and Entropy Generation Properties for Isothermal/Isobaric Reactor Networks. *Ind. Eng. Chem. Res.* **2013**, *52* (9), 3225–3238. https://doi.org/10.1021/ie301158m.

(29) Ghougassian, P. G.; Manousiouthakis, V. Globally Optimal Networks for Multipressure Distillation of Homogeneous Azeotropic Mixtures. *Ind. Eng. Chem. Res.* **2012**, *51* (34), 11183–11200. https://doi.org/10.1021/ie300423q.

(30) Zhou, W.; Manousiouthakis, V. I. Global Capital/Total Annualized Cost Minimization of Homogeneous and Isothermal Reactor Networks. *Ind. Eng. Chem. Res.* **2008**, *47* (10), 3771–3782. https://doi.org/10.1021/ie060653+.

(31) Al-Husseini, Z.; Manousiouthakis, V. I. IDEAS Based Synthesis of Minimum Volume Reactor Networks Featuring Residence Time Density/Distribution Models. *Comput. Chem. Eng.* **2014**, *60*, 124–142. https://doi.org/10.1016/j.compchemeng.2013.07.005.

(32) Ghougassian, P. G.; Manousiouthakis, V. Minimum Entropy Generation for Isothermal Endothermic/Exothermic Reactor Networks. *AIChE J.* **2015**, *61* (1), 103–117. https://doi.org/10.1002/aic.14598.

(33) Davis, B. J.; Taylor, L. A.; Manousiouthakis, V. I. Identification of the Attainable Region for Batch Reactor Networks. *Ind. Eng. Chem. Res.* **2008**, *47* (10), 3388–3400. https://doi.org/10.1021/ie071664l.

(34) Conner, J. A.; Manousiouthakis, V. I. On the Attainable Region for Process Networks. *AIChE J.* **2014**, *60* (1), 193–212. https://doi.org/10.1002/aic.14257.

(35) Barbosa, D.; Doherty, M. F. Design and Minimum-Reflux Calculations for Single-Feed Multicomponent Reactive Distillation Columns. *Chem. Eng. Sci.* **1988**, *43* (7), 1523–1537. https://doi.org/10.1016/0009-2509(88)85144-3.

(36) Venimadhavan, G.; Buzad, G.; Doherty, M. F.; Malone, M. F. Effect of Kinetics on Residue Curve Maps for Reactive Distillation. *AIChE J.* **1994**, *40* (11), 1814–1824. https://doi.org/10.1002/aic.690401106.

(37) Siirola, J. J. Industrial Applications of Chemical Process Synthesis. In *Advances in Chemical Engineering*; Anderson, J. L., Ed.; Academic Press, 1996; Vol. 23, pp 1–62.

(38) Okasinski, M. J.; Doherty, M. F. Design Method for Kinetically Controlled, Staged Reactive Distillation Columns. *Ind. Eng. Chem. Res.* **1998**, *37* (7), 2821–2834. https://doi.org/10.1021/ie9708788.

(39) Malone, M. F.; Doherty, M. F. Reactive Distillation. *Ind. Eng. Chem. Res.* **2000**, *39* (11), 3953–3957. https://doi.org/10.1021/ie000633m.

(40) Chen, F.; Huss, R. S.; Malone, M. F.; Doherty, M. F. Simulation of Kinetic Effects in Reactive Distillation. *Comput. Chem. Eng.* **2000**, *24* (11), 2457–2472. https://doi.org/10.1016/S0098-1354(00)00609-8.

(41) Barnicki, S. D.; Hoyme, C. A.; Siirola, J. J. Separations Process Synthesis. In *Kirk-Othmer Encyclopedia of Chemical Technology*; John Wiley & Sons, Inc., 2000.

(42) Jiménez, L.; Wanhschafft, O. M.; Julka, V. Analysis of Residue Curve Maps of Reactive and Extractive Distillation Units. *Comput. Chem. Eng.* **2001**, *25* (4–6), 635–642. https://doi.org/10.1016/S0098-1354(01)00644-5.

(43) Huss, R. S.; Chen, F.; Malone, M. F.; Doherty, M. F. Reactive Distillation for Methyl Acetate Production. *Comput. Chem. Eng.* **2003**, *27* (12), 1855–1866. https://doi.org/10.1016/S0098-1354(03)00156-X.

(44) Li, H.; Meng, Y.; Li, X.; Gao, X. A Fixed Point Methodology for the Design of Reactive Distillation Columns. *Chem. Eng. Res. Des.* **2016**, *111*, 479–491. https://doi.org/10.1016/j.cherd.2016.05.015.

(45) Ciric, A. R.; Gu, D. Synthesis of Nonequilibrium Reactive Distillation Processes by MINLP Optimization. *AIChE J.* **1994**, *40* (9), 1479–1487. https://doi.org/10.1002/aic.690400907.

(46) Papalexandri, K. P.; Pistikopoulos, E. N. Generalized Modular Representation Framework for Process Synthesis. *AIChE J.* **1996**, *42* (4), 1010–1032. https://doi.org/10.1002/aic.690420413.

(47) Jackson, J. R.; Grossmann, I. E. A Disjunctive Programming Approach for the Optimal Design of Reactive Distillation Columns. *Comput. Chem. Eng.* **2001**, *25* (11–12), 1661–1673. https://doi.org/10.1016/S0098-1354(01)00730-X.

(48) Georgiadis, M. C.; Schenk, M.; Pistikopoulos, E. N.; Gani, R. The Interactions of Design Control and Operability in Reactive Distillation Systems. *Comput. Chem. Eng.* **2002**, *26* (4–5), 735–746. https://doi.org/10.1016/S0098-1354(01)00774-8.

(49) Cardoso, M. F.; Salcedo, R. L.; de Azevedo, S. F.; Barbosa, D. Optimization of Reactive Distillation Processes with Simulated Annealing. *Chem. Eng. Sci.* **2000**, *55* (21), 5059–5078. https://doi.org/10.1016/S0009-2509(00)00119-6.

(50) Hoffmaster, W. R.; Hauan, S. Using Feasible Regions to Design and Optimize Reactive Distillation Columns with Ideal VLE. *AIChE J.* **2006**, *52* (5), 1744–1753. https://doi.org/10.1002/aic.10765.

(51) Avami, A.; Marquardt, W.; Saboohi, Y.; Kraemer, K. Shortcut Design of Reactive Distillation Columns. *Chem. Eng. Sci.* **2012**, *71*, 166–177. https://doi.org/10.1016/j.ces.2011.12.021.

(52) Urselmann, M.; Engell, S. Design of Memetic Algorithms for the Efficient Optimization of Chemical Process Synthesis Problems with Structural Restrictions. *Comput. Chem. Eng.* **2015**, *72*, 87–108. https://doi.org/10.1016/j.compchemeng.2014.08.006.

(53) Smith, J. M.; Van Ness, H. C.; Abbott, M. *Introduction to Chemical Engineering Thermodynamics*, 7 edition.; McGraw-Hill Education: Boston, 2004.

(54) Doherty, M. F.; Malone, M. F. *Conceptual Design of Distillation Systems*; McGraw-Hill, 2001.

(55) Sourlas, D. D.; Manousiouthakis, V. Best Achievable Decentralized Performance. *IEEE Trans. Autom. Control* **1995**, *40* (11), 1858–1871. https://doi.org/10.1109/9.471207.

CHAPTER 4

Process Intensification of Multi-Pressure Reactive Distillation Networks Using IDEAS

4.1. Abstract

The Infinite DimEnsionAl State-Space (IDEAS) conceptual framework is put forward as an intensification tool for the synthesis of globally optimal, multi-pressure, reactive, azeotropic, distillation networks. To this end, a unit operation model is proposed for reactive vapor-liquid equilibrium flash separators employed as network building blocks, and the concepts of reactive holdup, and capacity are introduced as network performance metrics. The method is demonstrated on a case study involving MTBE production using multi-pressure reactive distillation of methanol/isobutene/MTBE azeotropic mixtures. The globally optimal solutions for the minimum total reactive holdup, minimum total flow, and minimum capacity problems are obtained for a dual-pressure reactive distillation process operating simultaneously at 1.0 atm and 5.0 atm. For the problem of minimum capacity, the global optimum is found to have both reaction and pressure swing features, indicating those are complementary rather than competing technologies for process intensification purposes.

4.2. Introduction

Process intensification (PI) is a concept that encompasses any drastic improvement in chemical processing, substantially decreasing equipment volume, energy consumption and/or waste formation [1,2], aiming to maximize the effectiveness of chemical processes from molecular

to macro-scale level [3]. Reactive distillation (RD) systems employ simultaneous reaction and distillative separation, offering a distinct set of advantages over conventional processes employing separate reactor and distillation units: improvements of selectivity and conversion, ability to overcome azeotropes, energy savings, and capital cost savings from the elimination of unit operations [4]. A successful industrial implementation of reactive distillation is the methyl acetate production process by the Eastman Chemical Company, where a single reactive distillation column replaced eleven major operational units along with heat exchangers, pumps and controllers, reducing by five times the capital investment and energy consumption over a conventional design for methyl acetate production [5,6].

The separation of azeotropic mixtures can often benefit from the use of pressure swing distillation (PSD) [7]. Multiple columns at different pressures are used in the PSD process to bypass pressure-dependent azeotropic pinch points and to recover high purity products. Although RD and PSD are usually considered competing technologies [8], the implications of multiple operating pressures in reactive distillation processes are rarely explored. Indeed, the fact that only one of these technologies is sufficient to separate azeotropic mixtures discourages the exploration of synergies between those technologies. Nevertheless, from a PI perspective, the association or those two technologies is justified if the resulting system has advantages over all solutions that use those technologies separately.

Different approaches have been proposed to assess and design reactive distillation systems [9–16], including the residue curve maps approach [17,18], driving-force based design methods[19,20], and mixed integer nonlinear programs (MINLP) numerical approaches [21–23]. Those methods can be applied in the design of reactive distillation columns to rapidly provide feasible solutions, although none of them guarantees global optimality. [21–23]The MINLP methods, for

instance, can lead to nonconvex optimization formulations, which also do not guarantee global optimality for typical optimization problem sizes. In addition, none of these methods takes allows for the occurrence of different operating pressure levels in the process network.

In this paper, the Infinite DimEnsionAl State space (IDEAS) framework is applied to the synthesis of reactive distillation networks operating at different pressures. The networks are compound by reactive flash separators, which are surrogates for trays in distillation columns. The application of IDEAS framework to the synthesis problem can overcome the non-linearity of previous approaches and can lead to a globally optimum solution over all possible networks.

The IDEAS conceptual framework has been successfully applied to the globally optimal synthesis of various types of process networks. Some IDEAS applications include the synthesis of multicomponent mass exchange networks [24], ideal distillation networks [25,26], separator networks [27], power cycles [28], heat/power integrated distillation networks [29,30], reactive distillation networks [31,32], reactor network attainable region construction [33–42], azeotropic distillation networks [43], reactor networks [44–46], compressor sequences [47,48], batch reactor networks [49], and process network attainable region [50].

4.3. IDEAS framework review

In any process network synthesis task, a feasible network design is sought that can deliver a product from given raw materials using available process technologies. Many researchers have pursued process network synthesis over the years [51–54]. One of the frameworks for this task is the Infinite DimEnsionAl State space (IDEAS) approach to process network synthesis, which has been developed in numerous publications over the years [24–50]. IDEAS

organizes the flow of information in the network, leading to a simple and elegant formulation of the generalized process synthesis problem. The IDEAS framework can be explained by first exploring its structure, and then introducing the chemical properties that lead to important features such as linearity and convexity.

The process network in IDEAS is decomposed into two blocks of operations (figure 4.1). The first is called the distribution network (DN). It is here that all mixing, splitting, recycling, and bypassing of process flow streams occurs. The second is called the process operator (OP). Here, all other process unit operations take place. The process input streams feed into and the process outlet streams emerge from the DN. The OP is fed by a set of streams from the DN and in turn feeds the DN. Additionally to this block organization, IDEAS framework uses a process operator whose domain and range lie in infinite dimensional spaces. This process representation allows the consideration of all possible process networks for an a priori given set of technologies.

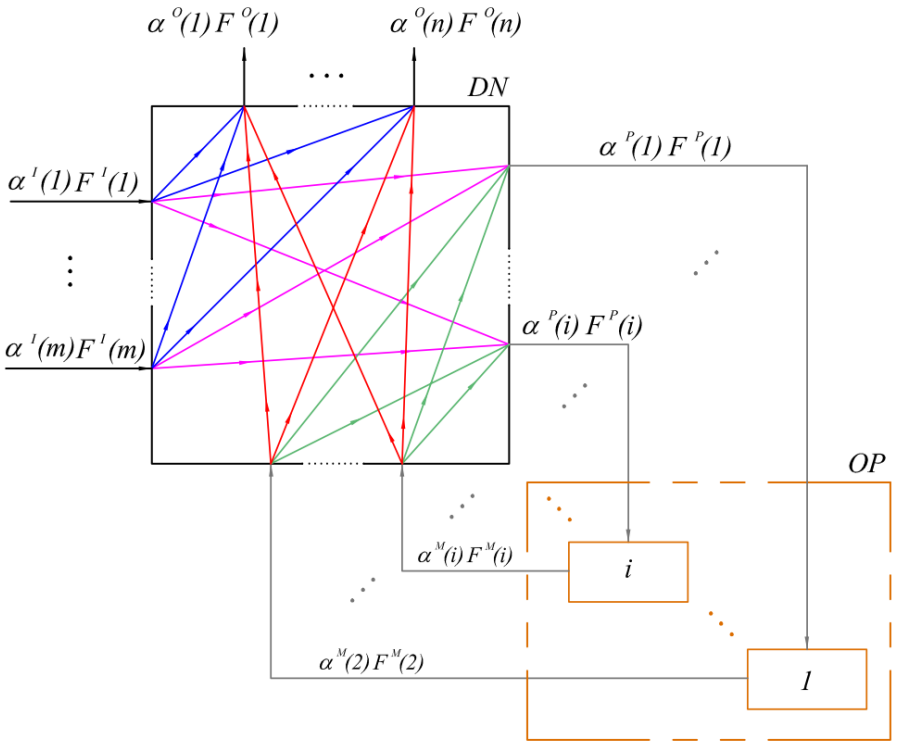

Figure 4.1 - IDEAS structure representation

Traditionally, process operations have been considered to take inlet stream information (such as flows, component concentration, enthalpies, and so on) and transform it to similar outlet stream information. The resulting process operators were nonlinear, giving rise to nonconvex optimal network synthesis formulations. The IDEAS framework provides a radical departure from this approach. It considers that the process operator takes extensive (quantity) inlet stream information, represented by $F^P(i)$ in Fig.4.1 (where $i = 1,...,\infty$), available at its respective $\alpha^P(i)$ intensive (quality) stream condition (that is, the i^{th} component concentration, enthalpy, and so on) and unit operation parameter conditions (that is, the i^{th} residence time, number of transfer units, and so on) and transforms it to extensive outlet stream information, represented by flow $F^M(i)$, available at the corresponding intensive outlet stream condition $\alpha^M(i)$ provided by the unit operation model.

When viewed in this manner, it is easy for the reader to verify that the resulting IDEAS process operator OP is linear for any chemical process. This is the direct result of the following property of chemical processes: When their inlet flow rates are increased proportionally (without altering the other intensive inlet conditions), their outlet flow rates are also increased by the same proportion, while their intensive outlet conditions remain unaltered, as long as appropriately defined design parameters are kept constant. Heat exchangers, mass exchangers, reactors and reactive systems, distillation columns, flash drums, and all other chemical processes satisfy this property.

The structure of IDEAS guarantees that all possible process networks are taken into account in the synthesis problem. Additionally, considering the linearity of the IDEAS process operator OP, a claim that the IDEAS representation gives rise to convex (linear) problem formulations can be made. Indeed, since the constraints in the DN are solely mixing and splitting

operations, the intensive (quality) information concerning any flow entering or leaving the DN is now fixed, resulting in DN constraints that are linear in the extensive (flow) variables. This fact, combined with the linear OP, results in a convex (linear) feasible region. Therefore, the IDEAS framework allows the formulation of convex (linear) process network synthesis problems that guarantee global optimality of the obtained solutions.

The applicability of IDEAS to the reactive distillation problem can be assessed by checking the properties of both the DN and the OP for the chemical process model used to solve the design problem. In the DN, the model requisites are conservation of mass and conservation of quality related entities (component balances and energy balances, for instance). In chemical process, mass conservation is easily verified since it must hold throughout the flow distribution process, but if a spontaneous reaction can occur in the mixing process for instance, component balances may not hold in the DN. Nevertheless, even in such case, IDEAS can be applicable with a review of the proposed model that contemplates this reaction, transferring it to the OP or adding mixture constraints to the DN. In the OP, besides the application of the conservation laws for any chemical system, the model formulation of the process unit must guarantee the linearity of the OP with the mass flow.

In this work, the reactive distillation process is modeled by using reactive flash separators as process units in the OP. Reactions can occur when catalyst is present, and no catalyst is used outside the process units. As a result, the DN conditions for IDEAS application hold for the proposed model. For the case study presented, energy balances are not incorporated in the reactive flash separator model since any cooling/heating required by the process can always be met after the network synthesis is carried out. In the IDEAS framework, changes in the flow

properties are carried by an infinite number of process units in the OP. In the next sections, the process unit model equations are presented, and the linearity of the OP is illustrated.

4.4. Mathematical formulation

4.4.1. Process unit model: Reactive flash separator

In this work, the isothermal, isobaric reactive flash separator shown in Fig.4.2 is considered. The separator's vapor and liquid output streams are in phase equilibrium with one another and depending on the reactive holdup H – a surrogate for the amount of catalyst in the system – reactions may occur. A capacity variable C, which is associated to the liquid holdup, is considered in this flash separator model.

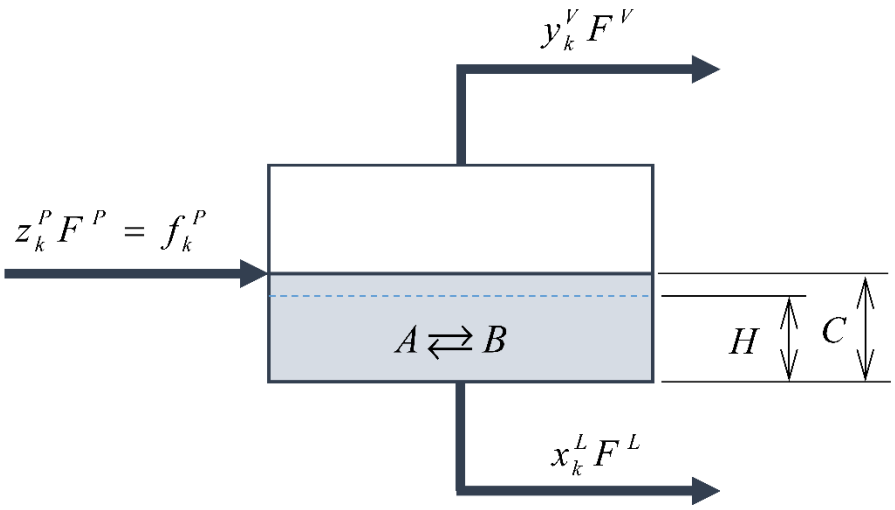

Figure 4.2 - Representation of the reactive flash separator

This approach not only gives to the flash the capability to act as a reactor and VLE separator simultaneously, but also has the flexibility to induce isolated process behavior, if

necessary. This induced behavior can be expressed as follows: if the reactive holdup is zero, the reactive flash separator acts as a VLE flash separator only; and if the synthesis process results in zero vapor stream from a specific flash, the separator behaves as a CSTR reactor only and delivers only a liquid exit stream.

The reactive flash separator model is shown in Eq.(4.1). It employs a CSTR component balance formulation with no accumulation and vapor-liquid equilibrium at the outlets.

$$f_k^P + R_k\left(\left\{x_j^L\right\}_{j=1}^n, T, P\right)H - x_k^L F^L - y_k^V F^V = 0 \qquad ; \qquad \forall k = 1,...,n \tag{4.1}$$

Phase equilibrium condition for each k^{th}-component in the mixture is obtained from the Gamma-Phi vapor-liquid equilibrium formulation as shown in Eq.(4.2), creating a correlation between the liquid molar fraction x_k^L with the vapor molar fraction y_k^V for each reactive flash separator.

$$y_k^V \phi_k\left(\left\{y_l^V\right\}_{l=1}^n, T, P\right)P = x_k^L \gamma_k\left(\left\{x_l^L\right\}_{l=1}^n, T\right)P_k^{sat}(T) \qquad \forall k = 1,...,n \tag{4.2}$$

For a given a reaction that is going to be carried out inside the reactive flash, the production or consumption rate R_k of the k^{th}-component is usually defined by a kinetic rate expression, which is a function of the reaction rate constant $k_f(T)$, the equilibrium constant $K_{eq}(T)$, the species activities $a_i(\gamma_i, x_i)$ and the species stoichiometric coefficients ν_i, as shown in Eq.(4.3).

$$R_k = k_f(T)\left(\prod_{reactants} a_r\left(\gamma_r, x_r\right)^{\nu_r} - \frac{1}{K_{eq}(T)}\prod_{products} a_p\left(\gamma_p, x_p\right)^{\nu_p}\right) \tag{4.3}$$

The species activity for the i^{th}-component in the mixture is related to the activity coefficient in the liquid phase and the liquid molar fraction as shown in Eq.(4.4).

$$a_i = \gamma_i \left(\left\{ x_l^L \right\}_{l=1}^{n}, T \right) x_i \tag{4.4}$$

Total balances are calculated from the molar fraction definition, Eq.(4.5) and Eq.(4.6), for the liquid and the vapor phases respectively, and Eq.(4.7) for the k^{th}-component inlet flow f_k^P. The component inlet flow f_k^P is equal to the total molar inlet flow F^P times z_k^P, which is the molar fraction of the k^{th}-component in the flash separator inlet stream.

$$\sum_{k=1}^{n} x_k^L = 1 \tag{4.5}$$

$$\sum_{k=1}^{n} y_k^V = 1 \tag{4.6}$$

$$\sum_{k=1}^{n} f_k^P = \sum_{k=1}^{n} \left(z_k^P F^P \right) = F^P \left(\sum_{k=1}^{n} z_k^P \right) = F^P \qquad \forall k = 1, ..., n \tag{4.7}$$

For a mixture containing n different chemical species, a variety of thermodynamic models can be used to calculate the fugacity coefficient function $\phi_k \left(\left\{ y_l^V \right\}_{l=1}^{n}, T, P \right)$, the activity coefficient function $\gamma_k \left(\left\{ x_l^L \right\}_{l=1}^{n}, T \right)$ and the saturated pressure $P_k^{sat}(T)$ for the k^{th} species in the mixture.

In this work, ideal gas behavior is assumed in the gas phase of the reactive flash separators, therefore $\phi_k \left(\left\{ y_l^V \right\}_{l=1}^{n}, T, P \right)$ is unitary for all species. The Wilson model is considered

in the calculation of the k^{th}-component activity coefficient γ_k in the non-ideal liquid mixture, as shown in Eq.(4.8) and Eq.(4.9).

$$\ln\left(\gamma_k\left(\left\{x_l^L\right\}_{l=1}^n, T\right)\right) = 1 - \ln\left(\sum_{j=1}^n x_j^L \Lambda_{k,j}(T)\right) - \sum_{i=1}^n \left(\frac{x_i^L \Lambda_{i,k}(T)}{\sum_{j=1}^n x_j^L \Lambda_{i,j}(T)} \right) \qquad \forall k = 1, n \qquad (4.8)$$

$$\Lambda_{k,j}(T) = \frac{V_j^L}{V_k^L} \exp\left(\frac{-A_{k,j}}{RT}\right) \qquad \forall k = 1, n; \quad \forall j = 1, n \qquad (4.9)$$

The Antoine equation, Eq.(4.10), is used to calculate the vapor pressure $P_k^{sat}(T)$ of the k^{th} component in the mixture.

$$\ln\left(P_k^{sat}(T)\right) = A_k + \frac{B_k}{T + C_k} \qquad \forall k = 1, n \qquad (4.10)$$

Given the thermodynamic model presented, Eq.(4.2) can be solved iteratively for a specified operational pressure P of the reactive flash separator. As part of this procedure, for any given liquid molar fraction vector $\left\{x_k^L\right\}_{k=1}^n$, an initial temperature T is chosen to solve Eq.(4.8) to Eq.(4.10) for all components in the mixture. Then, Eq.(4.2) is solved for all y_k^V and the condition given by Eq.(4.4) is checked. If the condition holds, the vapor molar fraction vector $\left\{y_k^V\right\}_{k=1}^n$ is considered to be in phase equilibrium and the respective activity coefficients vector $\left\{\gamma_k\right\}_{k=1}^n$ is considered valid. If the check fails, the initial temperature is slightly modified in the next iteration, until the condition returns true. Since uniqueness of the solution of Eq.(4.2) is not

guaranteed, a wide enough temperature interval is considered, so that all physically meaningful solutions can be identified.

4.4.2. IDEAS ILP formulation for the multi-pressure RD synthesis problem

To account for all possible multi-pressure reactive distillation network combinations, the process operator OP is connected with a distribution network (DN), which manages all flow-related functions (splitting, mixing, origin, destination). The resulting IDEAS framework for the reactive distillation synthesis problem is shown in Fig.4.3. Each stream in the DN has a flowrate variable and fixed process conditions in the origin, which in the multi-pressure case are molar fractions and pressure. The identification of the destination/source pair for each flow variable is carried by superscripts: the DN inlet is identified as I, the DN outlet as O, the OP inlet as P, the liquid and vapor outputs from the OP as L and V respectively. In addition, the flow variables use a 4-tuple index to identify the elements of the OP that are being connected and their respective operating pressures. Variables representing the flash separator reactive holdup H and capacity C carry no superscript and are identified by the respective element of the OP and its operating pressure.

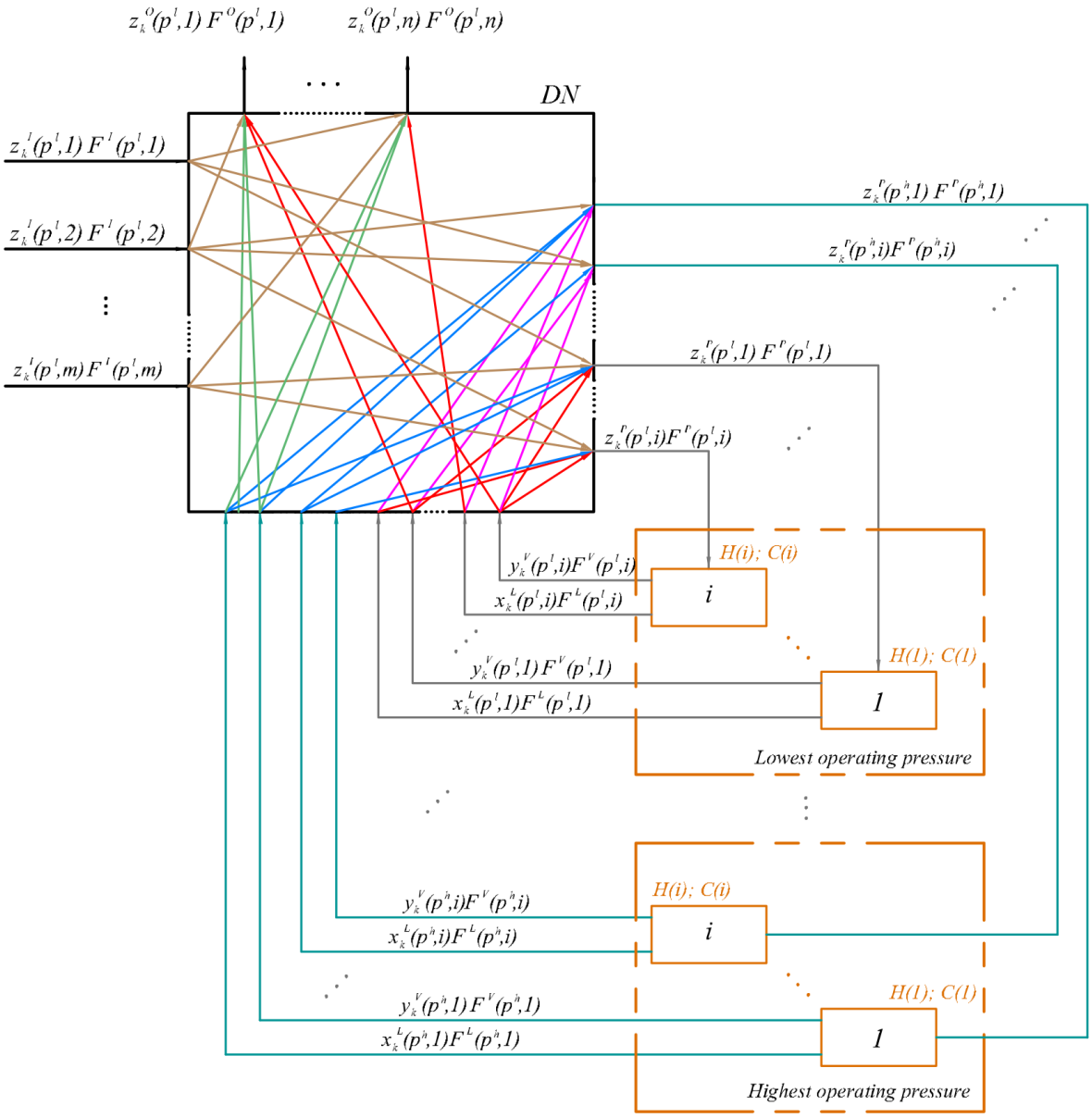

Figure 4.3 - : IDEAS representation for the multi-pressure reactive flash separator system

A variety of infinite LP (ILP) formulations can be derived using the IDEAS framework. To simplify the application on the case study, a general ILP formulation is presented can be modified for any specific case. This formulation considers a system with M inlets, N outlets, S different operating pressures, and a n different species. At this point, one can define a generic

linear objective function as shown in Eq.(4.11) , where the vector X includes all flows from the DN, all inlet flows, all reactive holdups and capacities for the reactive flashes in the OP.

$$c^T X \tag{4.11}$$

The above objective function can compute a wide array of objectives through appropriate selection of the coefficients of c^T associated with each of the problem's variables. Such objectives may include total reactive holdup, total capacity, operating cost, capital cost, energy cost, pumping/compression cost, among many other options.

The development of the constraints for the ILP general formulation uses mass and component balances on the DN, and the reactor model in the OP. For each $F^I(j)$ inlet flow entering the DN a splitting balance is considered, as shown in Eq.(4.12).

$$F^I(j) - \sum_{i=1}^{N} F^{OI}(i,j) - \sum_{p^P=1}^{S} \sum_{i=1}^{\infty} F^{PI}(p^P,i,j) = 0 \quad ; \quad \forall j = 1,...,M \tag{4.12}$$

A mixing balance, Eq.(4.13), is also considered for each $F^O(i)$ output flow (final product) leaving the DN:

$$F^O(i) - \sum_{j=1}^{M} F^{OI}(i,j) - \sum_{p^L=1}^{S} \sum_{j=1}^{\infty} F^{OL}(p^L,i,j) - \sum_{p^V=1}^{S} \sum_{j=1}^{\infty} F^{OV}(p^V,i,j) = 0 \quad \forall i = 1,...,N \tag{4.13}$$

The component flow $f_k^P(p^P,i)$ that feeds the i^{th} reactive flash operating at pressure p^P is calculated as the sum of the species flows feeding that specific the mixing point of the DN (component balance), as shown in Eq.(4.14).

$$f_k^P\left(p^P,i\right)-\sum_{j=1}^{M} z_k^I(j)F^{PI}\left(p^P,i,j\right) - \sum_{p^L=1}^{S}\sum_{j=1}^{\infty} x_k^L\left(p^L,j\right)F^{PL}\left(p^P,p^L,i,j\right) - \sum_{p^V=1}^{S}\sum_{j=1}^{\infty} y_k^V\left(p^V,j\right)F^{PV}\left(p^P,p^V,i,j\right)=0 \quad ; \quad \begin{matrix}\forall i=1,\ldots,\infty \\ \forall k=1,\ldots,n \\ \forall p^P=1,\ldots,S\end{matrix} \tag{4.14}$$

Therefore, the total mass flow in this mixing node is represented by Eq(4.15).

$$F^P\left(p^P,i\right)-\sum_{j=1}^{M} F^{PI}\left(p^P,i,j\right) - \sum_{p^L=1}^{S}\sum_{j=1}^{\infty} F^{PL}\left(p^P,p^L,i,j\right) - \sum_{p^V=1}^{S}\sum_{j=1}^{\infty} F^{PV}\left(p^P,p^V,i,j\right)=0 \quad ; \quad \begin{matrix}\forall i=1,\ldots,\infty \\ \forall p^P=1,\ldots,S\end{matrix} \tag{4.15}$$

A splitting balance is implemented for each $F^L\left(p^L,j\right)$ liquid and $F^V\left(p^V,j\right)$ vapor input flow entering the DN's after being processed in the OP, as shown in Eq.(4.16) and Eq.(4.17).

$$F^L\left(p^L,j\right)-\sum_{i=1}^{N} F^{OL}\left(p^L,i,j\right)-\sum_{p^P=1}^{S}\sum_{i=1}^{\infty} F^{PL}\left(p^P,p^L,i,j\right)=0 \; ; \quad \begin{matrix}\forall j=1,\ldots,\infty \\ \forall p^L=1,\ldots,S\end{matrix} \tag{4.16}$$

$$F^V\left(p^V,j\right)-\sum_{i=1}^{N} F^{OV}\left(p^V,i,j\right)-\sum_{p^P=1}^{S}\sum_{i=1}^{\infty} F^{PV}\left(p^P,p^V,i,j\right)=0 \; ; \quad \begin{matrix}\forall j=1,\ldots,\infty \\ \forall p^V=1,\ldots,S\end{matrix} \tag{4.17}$$

The reactive distillation process output is found on the DN outlet flows $F^O\left(i\right)$. Lower and upper bounds are introduced for these variables as design parameters, allowing the specification of the desired product in each DN exit. The mass balance for each flow variable exiting the DN is shown in Eq.(4.18).

$$\left(F^{O}(i)\right)^{l} \le \sum_{j=1}^{M} F^{OI}(i,j) + \sum_{p^{L}=1}^{S}\sum_{j=1}^{\infty} F^{OL}\left(p^{L},i,j\right) + \sum_{p^{V}=1}^{S}\sum_{j=1}^{\infty} F^{OV}\left(p^{V},i,j\right) \le \left(F^{O}(i)\right)^{u} \quad \forall i=1,.....,N \tag{4.18}$$

The constraint presented in Eq.(4.18) can be rewritten as two independent constraints, Eq.(4.19) and Eq.(4.20):

$$\left[\sum_{j=1}^{M} F^{OI}(i,j) + \sum_{p^{L}=1}^{S}\sum_{j=1}^{\infty} F^{OL}\left(p^{L},i,j\right) + \sum_{p^{V}=1}^{S}\sum_{j=1}^{\infty} F^{OV}\left(p^{V},i,j\right)\right] - \left(F^{O}(i)\right)^{l} \ge 0 \quad \forall i=1,.....,N \tag{4.19}$$

$$\left[\sum_{j=1}^{M} F^{OI}(i,j) + \sum_{p^{L}=1}^{S}\sum_{j=1}^{\infty} F^{OL}\left(p^{L},i,j\right) + \sum_{p^{V}=1}^{S}\sum_{j=1}^{\infty} F^{OV}\left(p^{V},i,j\right)\right] - \left(F^{O}(i)\right)^{u} \le 0 \quad \forall i=1,.....,N \tag{4.20}$$

The specification of the final product in each exit is done by the definition of lower and upper bounds for each individual component at each of the DN's outlets, as shown in Eq.(4.21).

$$\left(z_{k}^{O}(i)\right)^{l} F^{O}(i) \le \left\{ \begin{array}{l} \sum_{j=1}^{M} z_{k}^{I}(j) F^{OI}(i,j) \\ + \sum_{p^{L}=1}^{S}\sum_{j=1}^{\infty} x_{k}^{L}\left(p^{L},j\right) F^{OL}\left(p^{L},i,j\right) \\ + \sum_{p^{V}=1}^{S}\sum_{j=1}^{\infty} y_{k}^{V}\left(p^{V},j\right) F^{OV}\left(p^{V},i,j\right) \end{array} \right\} \le \left(z_{k}^{O}(i)\right)^{u} F^{O}(i) \quad ; \quad \begin{array}{l} \forall i=1,...,N \\ \forall k=1,...,n \end{array} \tag{4.21}$$

The reactive-separative functionality of the process units are carried through a component balance constraint for each reactive flash separator presented in the OP, as presented in Eq.(4.22).

$$f_k^P\left(p^P,i\right)+R_k\left(p^P,i\right)H\left(p^P,i\right) - x_k^L\left(p^L,i\right)F^L\left(p^L,i\right)-y_k^V\left(p^V,i\right)F^V\left(p^V,i\right)=0 \quad ; \quad \begin{matrix}\forall i=1,...,\infty \\ \forall k=1,...,n \\ \forall p^P=1,...,S \\ \forall p^L=1,...,S \\ \forall p^V=1,...,S\end{matrix} \tag{4.22}$$

For any reactive flash separator presented in Eq.(4.22), the process occurs at its respective operating pressure. To reflect this fact in the notation, the pressure superscript that identifies the origin of a given stream is adjusted to p^F, indicating the operating pressure of the flash actually carrying the process at that point, as shown in Eq.(4.23).

$$f_k^P\left(p^F,i\right)+R_k\left(p^F,i\right)H\left(p^F,i\right) - x_k^L\left(p^F,i\right)F^L\left(p^F,i\right)-y_k^V\left(p^F,i\right)F^V\left(p^F,i\right)=0 \quad ; \quad \begin{matrix}\forall i=1,...,\infty \\ \forall k=1,...,n \\ \forall p^F=1,...,S\end{matrix} \tag{4.23}$$

The set of equations presented can be combined to reduce the number of variables substituting Eq.(4.14), Eq.(4.16), and Eq.(4.17) in Eq.(4.23):

$$\begin{aligned}&\sum_{j=1}^{M} z_k^I(j)F^{PI}\left(p^F,i,j\right)+\sum_{p^L=1}^{S}\sum_{j=1}^{\infty}x_k^L\left(p^L,j\right)F^{PL}\left(p^F,p^L,i,j\right) \\ &+\sum_{p^V=1}^{S}\sum_{j=1}^{\infty}y_k^V\left(p^V,j\right)F^{PV}\left(p^F,p^V,i,j\right)+R_k\left(p^F,i\right)H\left(p^F,i\right) \\ &-x_k^L\left(p^F,i\right)\left[\sum_{j=1}^{N}F^{OL}\left(p^F,j,i\right)+\sum_{p^P=1}^{S}\sum_{j=1}^{\infty}F^{PL}\left(p^P,p^F,j,i\right)\right] \\ &-y_k^V\left(p^F,i\right)\left[\sum_{j=1}^{N}F^{OV}\left(p^F,j,i\right)+\sum_{p^P=1}^{S}\sum_{j=1}^{\infty}F^{PV}\left(p^P,p^F,j,i\right)\right]=0\end{aligned} \quad ; \quad \begin{matrix}\forall i=1,...,\infty \\ \forall k=1,...,n \\ \forall p^F=1,...,S\end{matrix} \tag{4.24}$$

One can verify that self-recycling flows, i.e., flows in which the origin and destination reference the same reactive flash operating at the same pressure, are naturally eliminated from Eq.(4.24).

A minimum residence time τ is proposed for the feasible reactive flash separators in the network. The capacity of each reactive flash in the OP is determined by either the reactive holdup, Eq.(4.25) or the residence time times the reactive flash inlet flow, Eq.(4.26), whichever is greater.

$$C\left(p^F,i\right)\geq H\left(p^F,i\right) \quad ; \quad \begin{matrix}\forall i=1,...,\infty \\ \forall p^F=1,...,S\end{matrix} \tag{4.25}$$

$$C\left(p^F,i\right)\geq \tau F^P\left(p^F,i\right) \quad ; \quad \begin{matrix}\forall i=1,...,\infty \\ \forall p^F=1,...,S\end{matrix} \tag{4.26}$$

By substituting Eq.(4.15) in Eq.(4.26), the capacity constraint must satisfy:

$$C\left(p^F,i\right)\geq \tau\left[\begin{matrix}\sum_{j=1}^{M}F^{PI}\left(p^F,i,j\right) \\ +\sum_{p^L=1}^{S}\sum_{j=1}^{\infty}F^{PL}\left(p^F,p^L,i,j\right) \\ +\sum_{p^V=1}^{S}\sum_{j=1}^{\infty}F^{PV}\left(p^F,p^V,i,j\right)\end{matrix}\right] \quad ; \quad \begin{matrix}\forall i=1,...,\infty \\ \forall p^F=1,...,S\end{matrix} \tag{4.27}$$

Some variables in the component outlet bounds equations can be eliminated substituting Eq.(4.13) in Eq.(4.21):

$$\begin{aligned}&\left(z_k^O(i)\right)^l\left[\sum_{j=1}^{M}F^{OI}(i,j)+\sum_{p^L=1}^{S}\sum_{j=1}^{\infty}F^{OL}\left(p^L,i,j\right)+\sum_{p^V=1}^{S}\sum_{j=1}^{\infty}F^{OV}\left(p^V,i,j\right)\right] \\ &\leq\sum_{j=1}^{M}z_k^I(j)F^{OI}(i,j)+\sum_{p^L=1}^{S}\sum_{j=1}^{\infty}x_k^L\left(p^L,j\right)F^{OL}\left(p^L,i,j\right)+\sum_{p^V=1}^{S}\sum_{j=1}^{\infty}y_k^V\left(p^V,j\right)F^{OV}\left(p^V,i,j\right) \\ &\leq\left(z_k^O(i)\right)^u\left[\sum_{j=1}^{M}F^{OI}(i,j)+\sum_{p^L=1}^{S}\sum_{j=1}^{\infty}F^{OL}\left(p^L,i,j\right)+\sum_{p^V=1}^{S}\sum_{j=1}^{\infty}F^{OV}\left(p^V,i,j\right)\right] \\ &\qquad\qquad\forall i=1,.....,N;\forall k=1,.....,n\end{aligned} \tag{4.28}$$

Equation (4.28) can then be split in two inequalities:

$$\sum_{j=1}^{M}\left[\left(\left(z_k^O(i)\right)^l - z_k^I(j)\right)F^{OI}(i,j)\right]$$
$$+\sum_{p^L=1}^{S}\sum_{j=1}^{\infty}\left[\left(\left(z_k^O(i)\right)^l - x_k^L\left(p^L,j\right)\right)F^{OL}\left(p^L,i,j\right)\right] \qquad (4.29)$$
$$+\sum_{p^V=1}^{S}\sum_{j=1}^{\infty}\left[\left(\left(z_k^O(i)\right)^l - y_k^V\left(p^V,j\right)\right)F^{OV}\left(p^V,i,j\right)\right] \le 0 \quad ; \quad \forall i=1,...,N \quad ; \quad \forall k=1,...,n$$

$$\sum_{j=1}^{M}\left[\left(\left(z_k^O(i)\right)^u - z_k^I(j)\right)F^{OI}(i,j)\right]$$
$$+\sum_{p^L=1}^{S}\sum_{j=1}^{\infty}\left[\left(\left(z_k^O(i)\right)^u - x_k^L\left(p^L,j\right)\right)F^{OL}\left(p^L,i,j\right)\right] \qquad (4.30)$$
$$+\sum_{p^V=1}^{S}\sum_{j=1}^{\infty}\left[\left(\left(z_k^O(i)\right)^u - y_k^V\left(p^V,j\right)\right)F^{OV}\left(p^V,i,j\right)\right] \ge 0 \quad ; \quad \forall i=1,...,N; \forall k=1,...,n$$

A total capacity variable C^{tot} has been included in the model, Eq.(4.31), and has an upper bound constraint C^{ub}.

$$C^{tot} = \sum_{p^F=1}^{S}\sum_{i=1}^{\infty} C\left(p^F,i\right) \qquad (4.31)$$

Similarly, a total reactive holdup H^{tot} has been added to the model with an upper bound constraint H^{ub}, as shown in Eq.(4.32).

$$H^{tot} = \sum_{p^F=1}^{S}\sum_{i=1}^{\infty} H\left(p^F,i\right) \qquad (4.32)$$

In addition, a constraint for the total flow circulating in the network $\left(F^P\right)^{tot}$ has also been considered in this work, as shown in Eq.(4.33). This variable takes in account all flows entering the OP and has its upper bound constrained by $\left(F^P\right)^{ub}$.

$$\left(F^{P}\right)^{tot}=\sum_{p^{F}=1}^{S}\sum_{i=1}^{\infty}F^{P}\left(p^{F},i\right)=\left\{\begin{array}{l}\sum_{p^{F}=1}^{S}\sum_{i=1}^{\infty}\sum_{j=1}^{M}F^{PI}\left(p^{P},i,j\right)\\ +\sum_{p^{F}=1}^{S}\sum_{p^{L}=1}^{S}\sum_{i=1}^{\infty}\sum_{j=1}^{\infty}F^{PL}\left(p^{F},p^{L},i,j\right)\\ +\sum_{p^{F}=1}^{S}\sum_{p^{V}=1}^{S}\sum_{i=1}^{\infty}\sum_{j=1}^{\infty}F^{PL}\left(p^{F},p^{V},i,j\right)\end{array}\right\} \tag{4.33}$$

Those three last variables defined in Eq.(4.31) to Eq.(4.33) are particularly important because they can be used in the definition of the vector X presented in Eq.(4.11), with unitary coefficients, embedding the totality of holdup volume, capacity volume and system flowrate respectively.

The final general ILP formulation for the multi-pressure reactive distillation has a general objective function as showed in Eq. (4.11) subject to the constraints presented in Eqs.(4.12), (4.19), (4.20), (4.24), (4.25), (4.27), (4.29), (4.30), (4.31), (4.32), and (4.33). Since all variables represent physical quantities (flowrate, catalyst amount, stage volume), they can have only non-negative values. In addition to that, the total reactive holdup, total capacity and total flow can have their upper bound specified in the synthesis process, as shown in Eq.(4.34).

$$\begin{array}{l}F^{I}\geq 0\,;F^{O}\geq 0\,;F^{OI}\geq 0\,;F^{PI}\geq 0\,;F^{OL}\geq 0\,;F^{OV}\geq 0\,;F^{PL}\geq 0\,;F^{PV}\geq 0\,;H\geq 0\,;C\geq 0\\ 0\leq H^{tot}\leq H^{ub};\quad 0\leq C^{tot}\leq C^{ub};\quad 0\leq\left(F^{P}\right)^{tot}\leq\left(F^{P}\right)^{ub}\end{array} \tag{4.34}$$

The infimum value of an infinite linear programming cannot be solved explicitly. Nevertheless, its solution can be approximated by a series of finite linear programming of increasing size, whose sequence of optimum values converges to the infinite dimensional problem's infimum. Thus, if instead of an infinite number of dimensions one considers a finite number G, corresponding in this problem to the number of reactive flash separators available for this multi-

pressure synthesis problem, the problem formulation becomes an LP which in turns can be solved by a variety of methodologies. By allowing G to contain an ever-increasing number of reactive flash-separator units, the optimum objective function values of each LP solved forms a non-increasing sequence that converges to the ILP infimum. Taking in account this solution methodology, the general LP formulation that takes in account a finite number of units G has the following inequality form:

$$\min\ c^T X$$

s.t.

$$\left[-\sum_{i=1}^{N} F^{OI}(i,j) - \sum_{p^P=1}^{S}\sum_{i=1}^{G} F^{PI}\left(p^P,i,j\right)\right] + F^{I}(j) \le 0 \qquad \forall j = 1,...,M$$

$$\left[\sum_{i=1}^{N} F^{OI}(i,j) + \sum_{p^P=1}^{S}\sum_{i=1}^{G} F^{PI}\left(p^P,i,j\right)\right] - F^{I}(j) \le 0 \qquad \forall j = 1,...,M$$

$$\left[-\sum_{j=1}^{M} F^{OI}(i,j) - \sum_{p^L=1}^{S}\sum_{j=1}^{G} F^{OL}\left(p^L,i,j\right) - \sum_{p^V=1}^{S}\sum_{j=1}^{G} F^{OV}\left(p^V,i,j\right)\right] \le -\left(F^{O}(i)\right)^{l} \qquad \forall i = 1,.....,N$$

$$\left[\sum_{j=1}^{M} F^{OI}(i,j) + \sum_{p^L=1}^{S}\sum_{j=1}^{G} F^{OL}\left(p^L,i,j\right) + \sum_{p^V=1}^{S}\sum_{j=1}^{G} F^{OV}\left(p^V,i,j\right)\right] \le \left(F^{O}(i)\right)^{u} \qquad \forall i = 1,.....,N$$

$$\left\{\begin{array}{l} \sum_{j=1}^{M} z_k^I(j) F^{PI}\left(p^F,i,j\right) + \sum_{p^L=1}^{S}\sum_{j=1}^{G} x_k^L\left(p^L,j\right) F^{PL}\left(p^F,p^L,i,j\right) \\ \quad + \sum_{p^V=1}^{S}\sum_{j=1}^{G} y_k^V\left(p^V,j\right) F^{PV}\left(p^F,p^V,i,j\right) + R_k\left(p^F,i\right) H\left(p^F,i\right) \\ \quad - x_k^L\left(p^F,i\right)\left[\sum_{j=1}^{N} F^{OL}\left(p^F,j,i\right) + \sum_{p^P=1}^{S}\sum_{j=1}^{G} F^{PL}\left(p^P,p^F,j,i\right)\right] \\ \quad - y_k^V\left(p^F,i\right)\left[\sum_{j=1}^{N} F^{OV}\left(p^F,j,i\right) + \sum_{p^P=1}^{S}\sum_{j=1}^{G} F^{PV}\left(p^P,p^F,j,i\right)\right] \end{array}\right\} \le 0 \qquad \begin{array}{l} \forall i = 1,...,G \\ \forall k = 1,...,n \\ \forall p^F = 1,...,S \end{array}$$

$$\left\{\begin{array}{l} -\sum_{j=1}^{M} z_k^I(j) F^{PI}\left(p^F, i, j\right) - \sum_{p^L=1}^{S}\sum_{j=1}^{G} x_k^L\left(p^L, j\right) F^{PL}\left(p^F, p^L, i, j\right) \\ \quad - \sum_{p^V=1}^{S}\sum_{j=1}^{G} y_k^V\left(p^V, j\right) F^{PV}\left(p^F, p^V, i, j\right) - R_k\left(p^F, i\right) H\left(p^F, i\right) \\ \quad + x_k^L\left(p^F, i\right)\left[\sum_{j=1}^{N} F^{OL}\left(p^F, j, i\right) + \sum_{p^P=1}^{S}\sum_{j=1}^{G} F^{PL}\left(p^P, p^F, j, i\right)\right] \\ \quad + y_k^V\left(p^F, i\right)\left[\sum_{j=1}^{N} F^{OV}\left(p^F, j, i\right) + \sum_{p^P=1}^{S}\sum_{j=1}^{G} F^{PV}\left(p^P, p^F, j, i\right)\right] \end{array}\right\} \le 0 \qquad \begin{array}{l}\forall i = 1,\ldots,G \\ \forall k = 1,\ldots,n \\ \forall p^F = 1,\ldots,S\end{array}$$

$$-C\left(p^F, i\right) + H\left(p^F, i\right) \le 0 \qquad \begin{array}{l}\forall i = 1,\ldots,G \\ \forall p^F = 1,\ldots,S\end{array}$$

$$-C\left(p^F, i\right) + \tau\left[\begin{array}{c} \sum_{j=1}^{M} F^{PI}\left(p^F, i, j\right) + \sum_{p^L=1}^{S}\sum_{j=1}^{G} F^{PL}\left(p^F, p^L, i, j\right) \\ + \sum_{p^V=1}^{S}\sum_{j=1}^{G} F^{PV}\left(p^F, p^V, i, j\right) \end{array}\right] \le 0 \qquad \begin{array}{l}\forall i = 1,\ldots,G \\ \forall p^F = 1,\ldots,S\end{array}$$

$$\left[\begin{array}{l} \sum_{j=1}^{M}\left[\left(\left(z_k^O(i)\right)^l - z_k^I(j)\right) F^{OI}(i, j)\right] + \\ \quad + \sum_{p^L=1}^{S}\sum_{j=1}^{G}\left[\left(\left(z_k^O(i)\right)^l - x_k^L\left(p^L, j\right)\right) F^{OL}\left(p^L, i, j\right)\right] \\ \quad + \sum_{p^V=1}^{S}\sum_{j=1}^{G}\left[\left(\left(z_k^O(i)\right)^l - y_k^V\left(p^V, j\right)\right) F^{OV}\left(p^V, i, j\right)\right] \end{array}\right] \le 0 \qquad \begin{array}{l}\forall i = 1,\ldots,N \\ \forall k = 1,\ldots,n\end{array}$$

$$\left[\begin{array}{l} \sum_{j=1}^{M}\left[\left(z_k^I(j) - \left(z_k^O(i)\right)^u\right) F^{OI}(i, j)\right] + \\ \quad + \sum_{p^L=1}^{S}\sum_{j=1}^{G}\left[\left(x_k^L\left(p^L, j\right) - \left(z_k^O(i)\right)^u\right) F^{OL}\left(p^L, i, j\right)\right] \\ \quad + \sum_{p^V=1}^{S}\sum_{j=1}^{G}\left[\left(y_k^V\left(p^V, j\right) - \left(z_k^O(i)\right)^u\right) F^{OV}\left(p^V, i, j\right)\right] \end{array}\right] \le 0 \qquad \begin{array}{l}\forall i = 1,\ldots,N \\ \forall k = 1,\ldots,n\end{array}$$

$$\left[C^{tot} - \sum_{p^F=1}^{S}\sum_{i=1}^{G} C\left(p^F, i\right)\right] \le 0$$

$$\left[-C^{tot}+\sum_{p^F=1}^{S}\sum_{i=1}^{G}C\left(p^F,i\right)\right]\le 0$$

$$\left[H^{tot}-\sum_{p^F=1}^{S}\sum_{i=1}^{G}H\left(p^F,i\right)\right]\le 0$$

$$\left[-H^{tot}+\sum_{p^F=1}^{S}\sum_{i=1}^{G}H\left(p^F,i\right)\right]\le 0$$

$$\left[\left(F^P\right)^{tot}-\left\{\begin{array}{l}\sum_{p^F=1}^{S}\sum_{i=1}^{G}\sum_{j=1}^{M}F^{PI}\left(p^P,i,j\right)+\sum_{p^F=1}^{S}\sum_{p^L=1}^{S}\sum_{i=1}^{G}\sum_{j=1}^{G}F^{PL}\left(p^F,p^L,i,j\right)\\ \quad+\sum_{p^F=1}^{S}\sum_{p^V=1}^{S}\sum_{i=1}^{G}\sum_{j=1}^{G}F^{PL}\left(p^F,p^V,i,j\right)\end{array}\right\}\right]\le 0$$

$$\left[-\left(F^P\right)^{tot}+\left\{\begin{array}{l}\sum_{p^F=1}^{S}\sum_{i=1}^{\infty}\sum_{j=1}^{M}F^{PI}\left(p^P,i,j\right)+\sum_{p^F=1}^{S}\sum_{p^L=1}^{S}\sum_{i=1}^{G}\sum_{j=1}^{G}F^{PL}\left(p^F,p^L,i,j\right)\\ \quad+\sum_{p^F=1}^{S}\sum_{p^V=1}^{S}\sum_{i=1}^{G}\sum_{j=1}^{G}F^{PL}\left(p^F,p^V,i,j\right)\end{array}\right\}\right]\le 0$$

$$F^I\ge 0;\ F^{OI}\ge 0;F^{PI}\ge 0;F^{OL}\ge 0;F^{OV}\ge 0;F^{PL}\ge 0;F^{PV}\ge 0;H\ge 0;C\ge 0;$$

$$0\le C^{tot}\le C^{ub};\ 0\le H^{tot}\le H^{ub};\ 0\le\left(F^P\right)^{tot}\le\left(F^P\right)^{ub}$$

Next, the proposed IDEAS framework is illustrated on a case study involving a dual-pressure reactive separation of a ternary azeotropic mixture.

4.5. Case study: MTBE production through dual-pressure reactive distillation

MTBE (Methyl-tert-butyl ether) is an important chemical compound used as an antiknock agent in unleaded gasoline. Although MTBE was banned in the United States in 2005 and in several other countries after that, it is still largely used as fuel oxygenate worldwide, including by countries in Europe and Asia [55]. China consumed 7.3 million tons of MTBE in 2015, blended in gasoline for road use [56]. MTBE production through reactive distillation has also

been investigated as a potential route for separating the C_4 by-product mixture from oil refining, aiming to recover pure isobutene [57].

MTBE is synthesized from the reaction between isobutene and methanol, as shown in Eq.(4.35).

$$i-C_4H_8 + MeOH \rightleftarrows MTBE \tag{4.35}$$

For the acid-catalyzed reaction, the traditional reactor-followed-by-distillation concept is particularly complex since the ternary mixture leaving the reactor forms two minimum boiling binary azeotropes. The utilization of single pressure reactive distillation on the MTBE production has been studied for several authors [58,16,59–63] and the obtained results from this technology are shown to be close to 100% conversion. On the other hand, it is also known that the MTBE minimum boiling azeotropes are pressure-dependent, and that reaction constants are dependent on the temperature of the mixture, defined by its pressure. Therefore, the investigation of a multi-pressure influence in the reactive distillation for MTBE production is highly desired.

The kinetics for the MTBE reaction can be found on the literature [16]. The thermodynamic equilibrium constant as a function of the reaction temperature and the reaction rate constant are shown in Eq.(4.36) and Eq.(4.37).

$$\ln\left(K_{eq}\right) = \frac{6,820.0}{T} - 16.33 \tag{4.36}$$

$$k_f = 74.40\, e^{-3,187.0/T} \tag{4.37}$$

The constants for the Antoine's equation, Eq.(4.10), and the binary interaction parameters for the Wilson model, Eq.(4.8) and Eq.(4.9), are shown in Table 4.4 in the appendix.

Based on the kinetic parameters for MTBE reaction from isobutene and methanol, the system of modeling equations for the reactive flash can be solved for any liquid molar fraction vector in a given operational pressure $\left\{P, x_{IB}^{L}, x_{MOH}^{L}, x_{MTBE}^{L}\right\}$. Each species' molar fraction in the ternary mixture can take values in the interval $0 \le x_i^L \le 1$ and the sum over all species must be equal one. Therefore, an infinite number of combinations are possible for each pressure. To solve the proposed finite LP, the composition domain must be discretized in a finite number of triplets $x_{IB}^{L}, x_{MOH}^{L}, x_{MTBE}^{L}$ for each operational pressure, forming a G number of available units for the IDEAS finite LP on this synthesis procedure. Several sets of discretized liquid molar fraction triplets were then generated from the available domain considering a constant interval size on the interval $x_j \in \mathbb{R} : x_j = \left\{0 \le x \le 1\right\}$, as shown in Table 4.5 in the appendix.

As a design parameter, a minimum of 95% purity for MTBE has been selected as the production goal for the system. Based on this target, each set G of reactive distillation flashes is tested to determine if they could deliver MTBE with the selected purity. To proceed with this verification, the IDEAS finite LP was run with three inlets $\left(M = 3\right)$ containing isobutene, methanol, and MTBE respectively, all at 100% purity, and one process outlet $\left(N = 1\right)$. In the process outlet, the upper bound for MTBE molar fraction at the outlet was set to 0.95 and the exit flow to be 1.0 kmol/h. A single-pressure system $\left(S = 1\right)$ operating at 1 bar was considered in the evaluation of the discretized sets. The objective function maximizes the MTBE content in the system outlet, reflecting the production goal for each set of reactive flash separators as shown in Eq.(4.38).

$$\max \sum_{j=1}^{G} x_k^L\left(j\right) F^{OL}\left(i,j\right) + y_k^V\left(j\right) F^{OV}\left(i,j\right) \qquad ; \qquad i = 1 \; ; \; k = MTBE \qquad (4.38)$$

The constraints were implemented as presented in the finite IDEAS-LP. What this procedure accomplishes is that, if the set for a given discretization is not able to deliver 1 kmol/h with 95% MTBE purity, a flow from the inlet to the outlet containing 100% MTBE enriches the mixture so that the specified purity target is reached at the exit. Therefore, this problem has always a feasible solution and the sets can be tested until the inlet MTBE flow is equal zero. From this procedure, the 1/20 discretization was found to be the largest discretization interval (which generates the smallest reactive distillation set) that is able to produce MTBE with 95% purity from pure isobutene and pure methanol. Figure 4.4 shows the pure MTBE flow required to meet the desired specification of (95% MTBE in the output) as a function of the number of reactive flash separators.

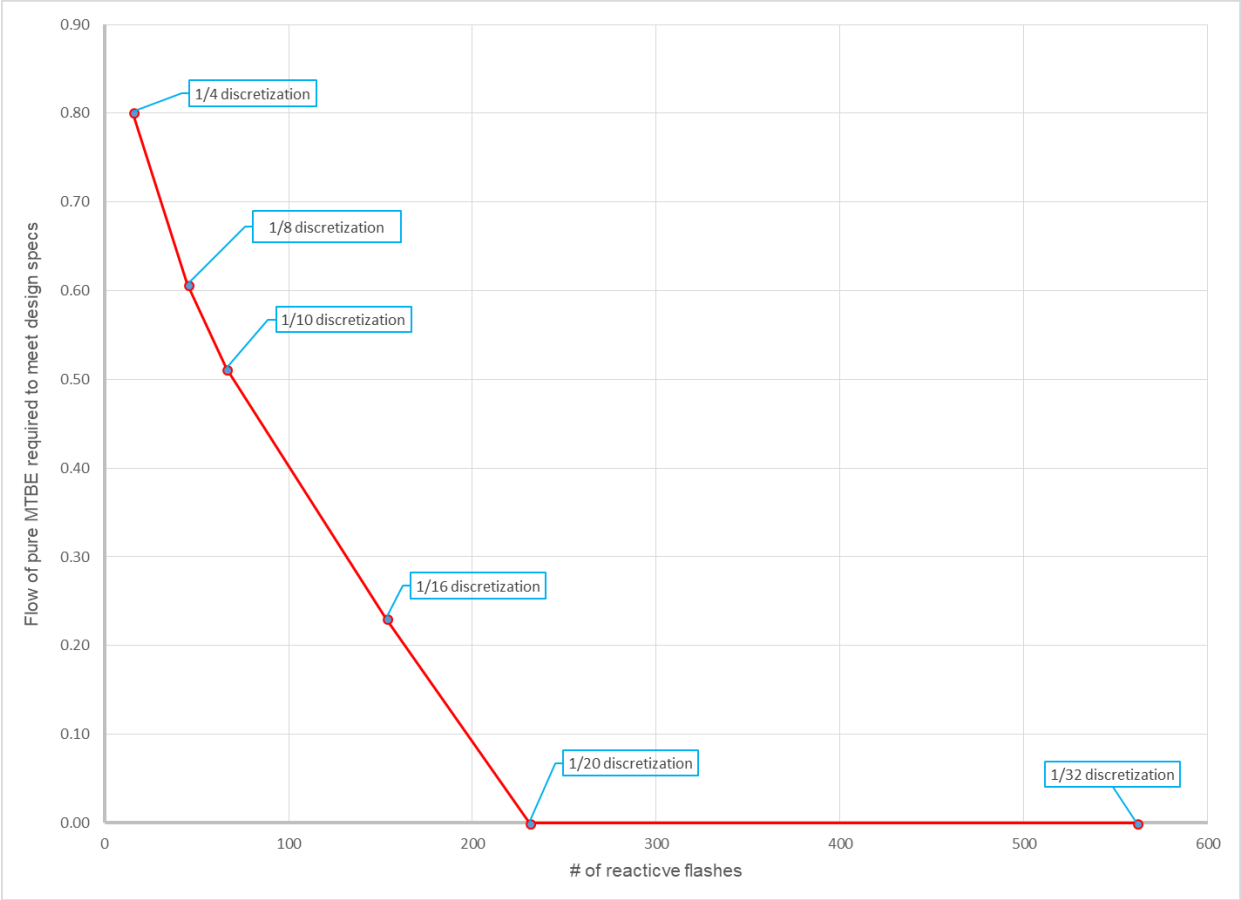

Figure 4.4 - MTBE flow required as a function of the number of reactive flashes

Now that the feasibility of the problem was verified, a variety of optimization problems can be addressed. For the dual-pressure reactive separation system, the objective is finding the global minimum total reactive holdup, the global minimum total capacity, the global minimum total flow in the network, and how those three characteristics of the system behaves in a dual-pressure system when compared with the respective single pressure systems. The objective function for those cases are presented in Eq.(4.39) to Eq.(4.41). The total reactive holdup is considered a surrogate for capital costs associated with reactors, particularly the amount of catalyst used in the process to carry out the reaction [64,65]. The system's total capacity is a surrogate for capital costs associated with vessels (flashes/stages), and is also a surrogate for

operating costs, as one of its components is proportional to the total flowrate. In addition, the system's total flowrate per se is a surrogate for the reactive separation system's energy consumption, as higher energy consumption results in higher material flows within the network [64,65].

$$\min H^{tot} \tag{4.39}$$

$$\min C^{tot} \tag{4.40}$$

$$\min \left(F^{P} \right)^{tot} \tag{4.41}$$

As shown in the test of the discretized sets, the use of sets with discretization intervals smaller than 1/20 guarantees the feasibility of the synthesis procedure. Thus, only two inlet feeds are required $(M = 2)$, each containing pure isobutene and pure methanol respectively. The IDEAS-ILP globally optimal solution approximation is obtained through a sequence of solutions from LP1 of an ever-increasing number of reactive flash separator units G in the OP. In other words, the optimal solution for the finite LP converges to the global optimal solution of the ILP when $G \to \infty$. To test the IDEAS convergence, the single-pressure $(S = 1)$ globally minimum reactive holdup problem was solved for a variety of reactive flash separators discretized sets operating at 1 bar. The convergence plot for the minimum holdup global optimum is shown in Fig.4.5.

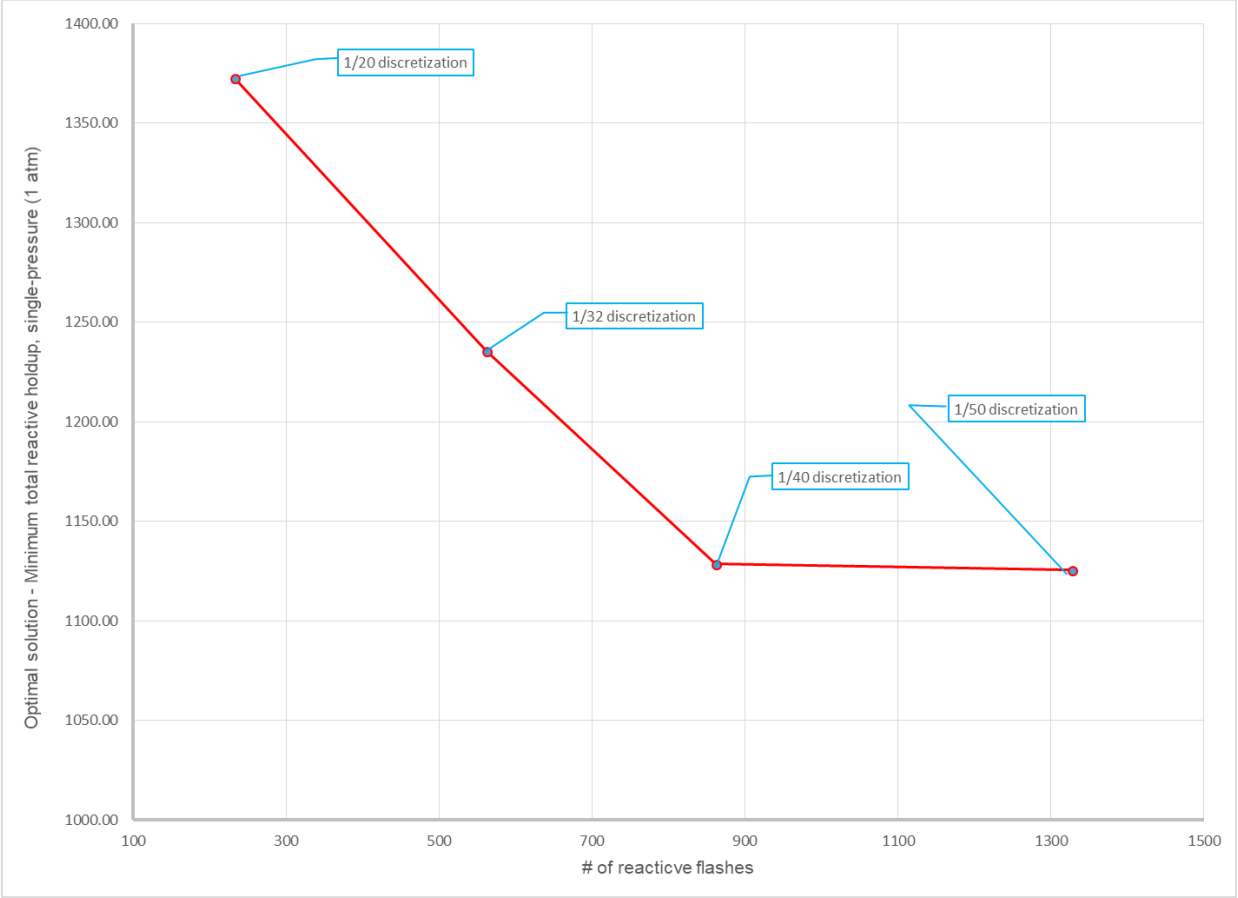

Figure 4.5 - IDEAS convergence plot for single-pressure minimum total holdup

The minimum holdup synthesis problem was solved considering a design capable to produce 2,350 bpsd (barrel per stream day) of MTBE at 95% purity, which is equivalent to a production of 130 kmol/h. In order to compare the effect of the operating pressure, two different simulations were implemented first, producing MTBE at 1.0 bar and 5.0 bar respectively in two independent single-pressure systems. Then, minimum holdup was pursued in one unique dual-pressure system, with two sets of reactive flash separators available to the synthesis procedure, one operating at 1.0 bar and the other at 5.0 bar. Those optimization problems were solved for a 1/64 discretization considering a variety of different upper limits on the system's total flowrate. The complete list of design parameters is shown in Table 4.1:

Table 4.1. Design parameters used in the MTBE production case study.

System identification	P1	P5	P1/P5
Pressure levels available for RD	Single	Single	Dual
Production output (kmol/h)	130.00	130.00	130.00
Residence Time (s)	60	60	60
Operating pressure (bar)	1.0	5.0	1.0 and 5.0
Inlet molar fractions			
Inlet 1			
Isobutene	1.0000	1.0000	1.0000
Methanol	0.0000	0.0000	0.0000
Inlet 2			
Isobutene	0.0000	0.0000	0.0000
Methanol	1.0000	1.0000	1.0000
Outlet molar fraction target bounds			
MTBE	0.950 - 1.000	0.950 - 1.000	0.950 - 1.000
Isobutene	0.000 - 0.050	0.000 - 0.050	0.000 - 0.050
Methanol	0.000 - 0.050	0.000 - 0.050	0.000 - 0.050

For the specified conditions, the IDEAS solution for the single and double-pressure systems were found and are presented in Table 4.2. The minimum total flow in the network is obtained in a lower operating pressure (1 bar), although this limiting condition requires an extremely large value for the total reactive holdup. In its turns, the minimum reactive holdup happens at a higher operating pressure (5 bar), requiring a large total flow in the network. This apparent tradeoff between reactive holdup and total flow in the network is a manifestation of the separation needs for this process. If a small amount of catalyst is used, i.e., in a minimum reactive holdup state, the synthesis process must assure that separation occurs almost exclusively via flow interchanges amongst the VLE separators, and that the flow in the network is high

enough to meet the design output of MTBE in an environment of low reactivity. If the flow is to be small, i.e., in a minimum total flow situation, very few reactive flash separators are allocated by the synthesis process and the separation and specs are met almost exclusively through reaction. The dual-pressure system can emulate both scenarios since it contains the reactive flash separators for both 1 and 5 bar operating pressures.

Table 4.2. Optimal values for different objective functions in each RD system.

Objective function	Single-pressure at 1 bar (P1)	Single-pressure at 5 bar (P5)	Dual-pressure at 1 bar and 5 bar (P1/P5)
Min Total Flow	**24735**	**74670**	**24735**
Min Reactive Holdup	**152423**	**27669**	**27669**

To better understand the correlation between minimum total flow and minimum reactive holdup, the optimal value for reactive holdup was evaluated considering a variety of upper-bound values for the total flow in the network, such that range between the global optimal reactive holdup and the global optimal total flow is covered in its totality for all the different systems studied. Such exercise led to the values presented in Table 4.3.

Table 4.3. Reactive Holdup optimal values for different total flow upper bounds for single and dual-pressure systems

Total flow upper bound (kg/h)	Optimal reactive holdup (H*) for P1 (kg)	Optimal reactive holdup (H*) for P5 (kg)	Optimal reactive holdup (H*) for P1/P5 (kg)
Unbounded	27669	152423	27669
5000000	38044	169363	28328
3000000	43656	214793	29071
2000000	47543	239737	30547
1000000	55381	288159	41667
900000	56711	297597	45159
800000	58214	309139	48741
700000	59937	323018	52402
600000	61972	339882	56252
500000	64646	360782	60686
400000	68228	386994	66212
300000	73479	422866	73368
200000	86792	489937	86382
150000	108445	551003	104398
125000	138023	602435	130066
100000	233903	689929	177736
90000	380166	751095	231559
80000	863946	834928	342622
76962	1575210	870555	384405
60000	Infeasible	1170220	674899
50000	Infeasible	1487820	963535
30000	Infeasible	7837900	7837900
26000	Infeasible	19154000	19154000
24735	Infeasible	31395900	31395900

The effects of the dual-pressure system in relation with either one of the single-pressure operating systems occurs in a transition region in which both reactive holdup and total flow in the network have low but not optimal values. The region in which the dual-pressure system has a more prominent advantage over any of the respective single-pressure ones is shown in Fig. 4.6.

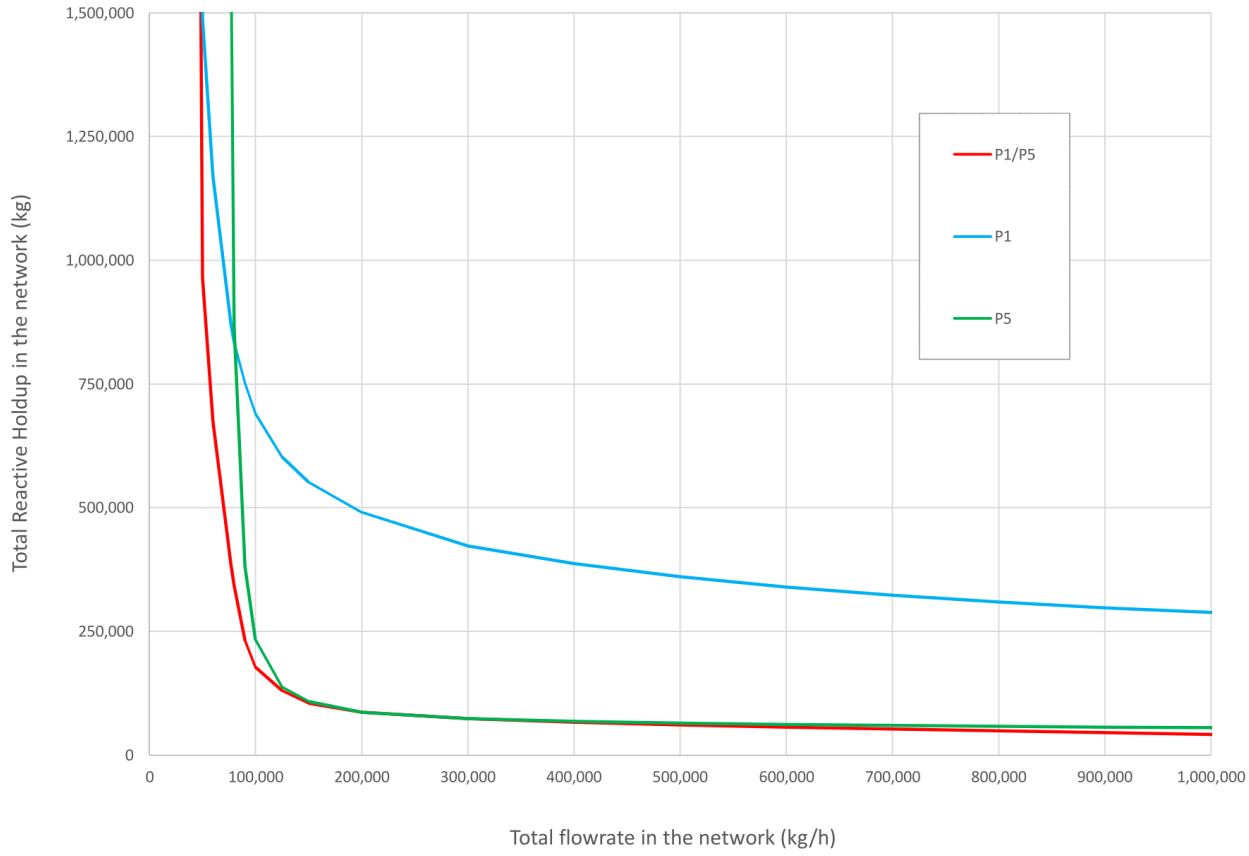

Figure 4.6 - Single and dual-pressure optimal reactive holdups as function of the total flowrate in the network

In the region between 80,000 and 120,000 kg/h of total flow there the dual-pressure system can deliver feasible designs with less reactive holdup for the same flowrate when compared to either P1 or P5 systems. The access to this feasible region through an RD system that operates in two different pressure levels indicates that dual-pressure RD systems may deliver better results in terms of catalyst use than single pressure systems under specific conditions. In addition, by enabling a feasible design with reduced values of reactive holdup and total flowrate, the overall size of the dual-pressure RD system is proportionally smaller than its single-pressure peers, which indicates its potential to further intensify the RD processes.

To better understand how the dual-pressure system delivers better results, the main process connections for a system featuring 100,000 kg/h of total flow in the network is shown in Fig.4.7. For this system, reaction occurs exclusively at the high-pressure system (P5), and the first five stages function as reactor only since no phase separation occurs.

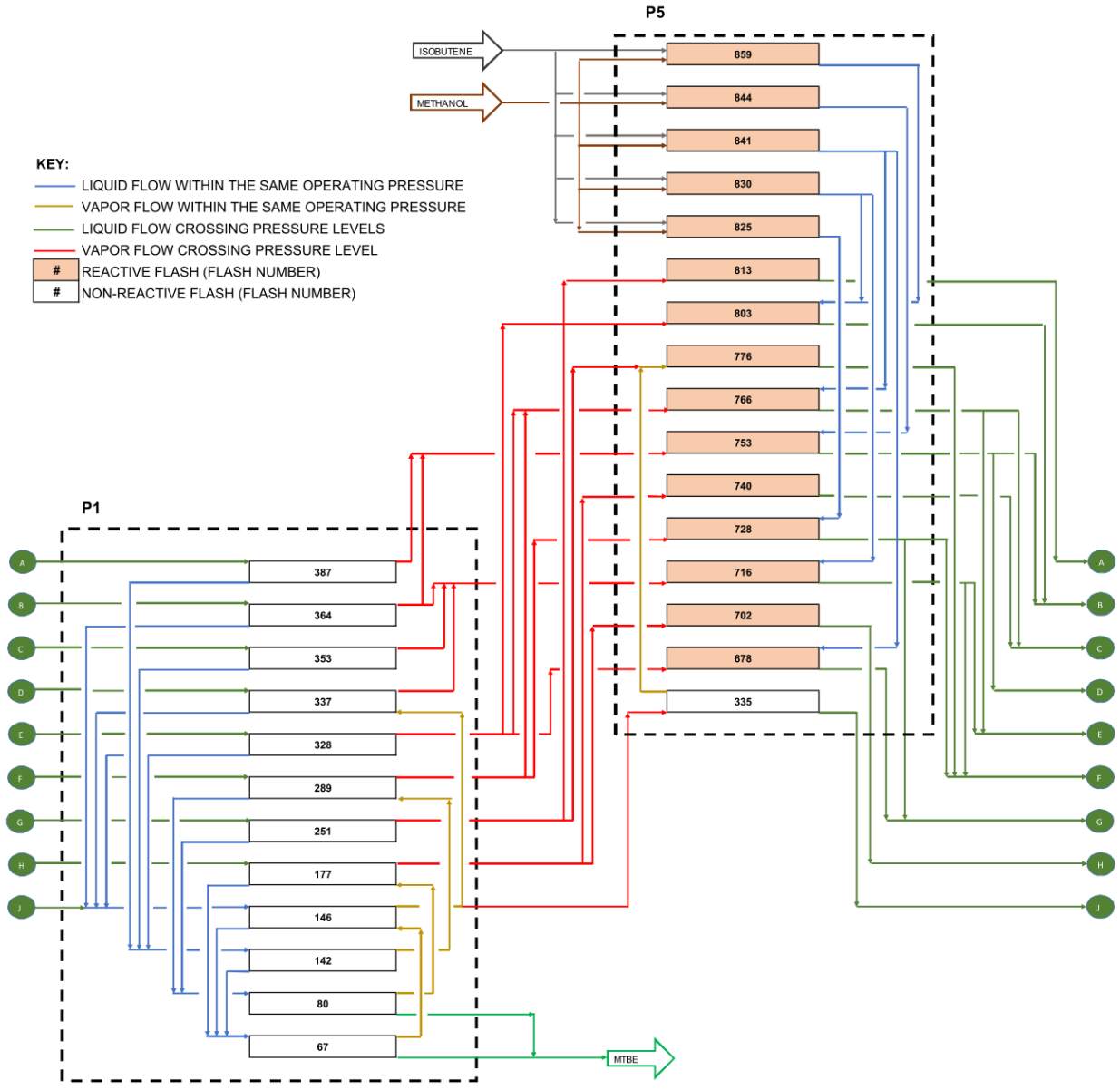

Figure 4.7 - Synthesis result for the dual-pressure system featuring 100,000 kg/h of the total flowrate in the network

Phase separation occurs mostly in the low-pressure side (P1), and some of the vapor flows are sent to the high-pressure side to mix and further react. From the interconnection among stages within this dual-pressure system, one can argue that an RD system that combines high-pressure reactive systems with low-pressure separative systems can have a reduced value in both catalyst use and total flow requirements than a traditional RD solution. This fact is captured by finding the minimum capacity value for the three systems studied (P1, P5, and P1/P5), as shown in Fig.4.8. The dual-pressure RD system shows better results than its single-pressure peers, reducing the system capacity in 78.35% and 14.91%, when compared with similar RD systems for MTBE production operating at 1 bar and 5 bar respectively.

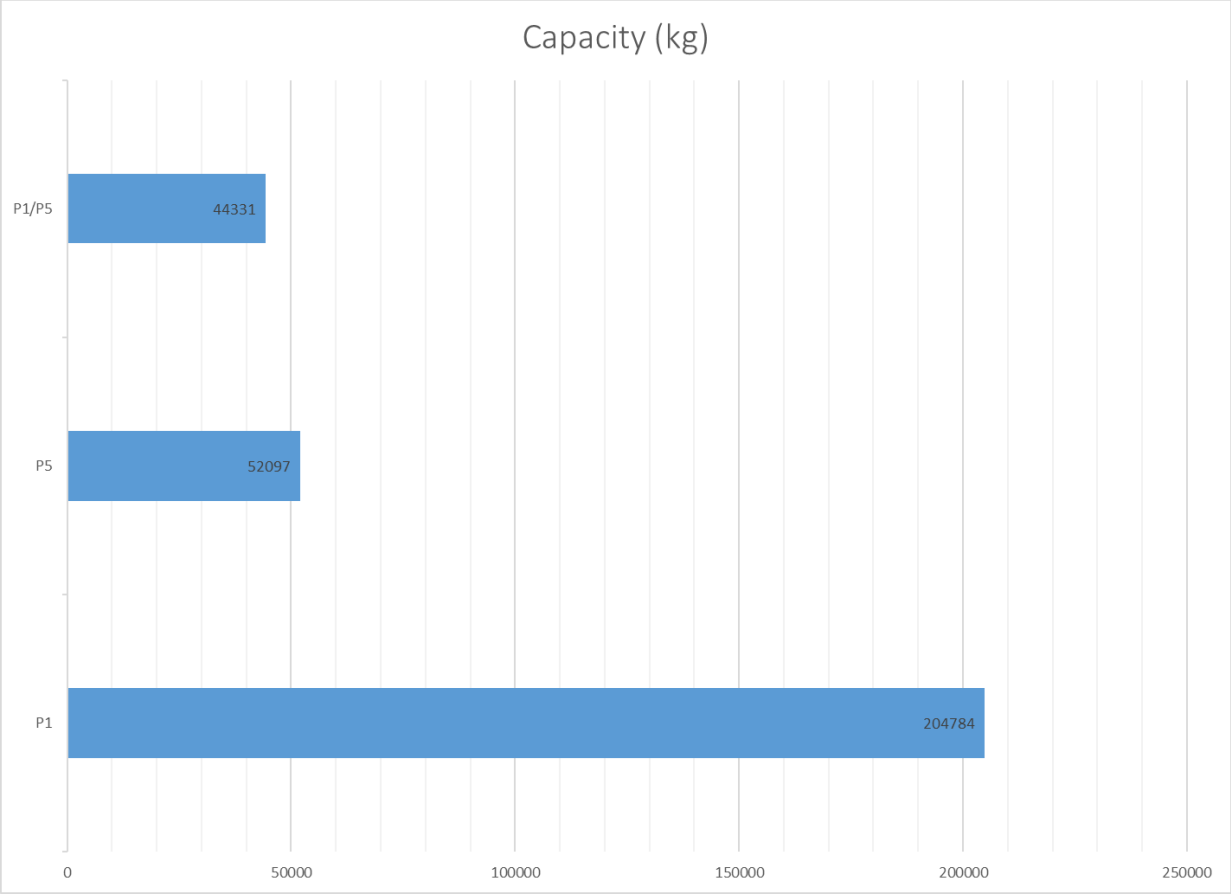

Figure 4.8 - Minimum (globally optimized) capacity value for the single-pressure systems and for the dual-pressure system

4.6. Conclusions

The effect of simultaneous reactive distillation (RD) and pressure swing distillation (PSD) were studied in this work through the application of IDEAS framework. IDEAS basic concepts and features were first reviewed and then its applicability to the multi-pressure reactive distillation was proved. A convex, infinite linear programming (ILP) was derived and the approximate solution of this IDEAS generated ILP was pursued through the solution of a number of finite dimensional linear programs (FLP) of ever-increasing size, whose optimum values form a sequence that converges to the ILP's infimum.

The methyl tert-butyl ether (MTBE) production was used as study case and a minimum discretized set on the MTBE, isobutene and ethanol molar fraction space was found to a production target of 95% pure MTBE. The minimum required set had a discretization of 1/20. Any finer discretization on the molar fraction space could reach the design constraints.

The globally optimal value for minimum total reactive holdup and minimum total flow in the system was then calculated.

From these results, it is possible to verify that IDEAS generates an RD process network for the minimum total flow problem, and a PSD process network for the minimum total reactive holdup problem. In the minimum total flow case, the separation of the azeotropic mixture is executed by reactions only, making the optimal network dense in terms of catalyst use. For the minimum reactive holdup case, azeotropic separation is being processed by constant changes in the available pressure levels, leading to a network dense in terms of reactive flash units and consequently in terms of mass flowing between these units.

The set of optimal solutions separating these two extreme cases has always a hybrid solution, showing the potential for the joint application of RD and PSD processing methods. A look into the solution for the dual-pressure system operating at 100,000 kg/h of total flow in the network indicates that an RD system that combines high-pressure reactive systems with low-pressure separative systems can have a reduced value in both catalyst use and total flow requirements than a traditional RD solution. Lastly, considering the defined variable capacity as a measure of the system's overall size, the dual-pressure RD system shows better results than its single-pressure peers, reducing the system capacity in 78.35% and 14.91%, when compared with similar RD systems for MTBE production operating at 1 bar and 5 bar respectively. Thus, for the cases of minimum capacity, the multi-pressure reactive distillation design shows a better performance than the application of any RD or PSD isolated process.

4.7. Notation

Thermodynamic Variables*:*

P	Flash unit pressure
T	Flash unit temperature
$y_k^V(i)$	k^{th} Species equilibrium vapor composition leaving the i^{th} unit
$x_k^L(i)$	k^{th} Species equilibrium liquid composition leaving the i^{th} unit
$P_k^{sat}(T)$	k^{th} Species temperature dependent saturated vapor pressure

$\phi_k\left(\left\{y_l^V\right\}_{l=1}^n, T, P\right)$ k^{th} Species non-ideal fugacity coefficient

$\gamma_k\left(\left\{x_l^L\right\}_{l=1}^n, T\right)$ k^{th} Species non-ideal liquid activity coefficient

$\Lambda_{k,j}\left(T\right)$ Wilson equation temperature dependent parameters

$A_{i,j}$ Wilson equation interaction parameters between i^{th} and j^{th} species

$A_k, B_k, C_k, D_k, E_k, F_k$ Antoine equation k^{th} species parameters

$V_k\left(V_j\right)$ $k^{th}\left(j^{th}\right)$ species molar volume

R Universal gas constant

K_{eq} Reaction equilibrium constant

k_f Reaction rate constant

IDEAS Variables*:*

$F^I\left(i\right)$ i^{th} DN inlet stream

$F^O\left(i\right)$ i^{th} DN outlet stream

$F^L\left(i\right)$ i^{th} OP liquid outlet

$F^{V}(i)$ i^{th} OP vapor outlet

$F^{OI}(i,j)$ j^{th} DN inlet stream to i^{th} DN outlet

$F^{PI}(p^{P},i,j)$ i^{th} OP (operating at pressure p^{P}) inlet stream from j^{th} DN network inlet

$F^{OL}(p^{L},i,j)$ i^{th} DN outlet stream from j^{th} OP (operating at pressure p^{L}) liquid outlet

$F^{OV}(p^{V},i,j)$ i^{th} DN outlet stream from j^{th} OP (operating at pressure p^{V}) vapor outlet

$F^{PL}(p^{P},p^{L},i,j)$ i^{th} OP (operating at pressure p^{P}) inlet stream from j^{th} OP (operating at pressure p^{L}) liquid outlet

$F^{PV}(p^{P},p^{V},i,j)$ i^{th} OP (operating at pressure p^{P}) inlet stream from j^{th} OP (operating at pressure p^{V}) vapor outlet

$z_{k}^{I}(i)$ k^{th} species, i^{th} DN inlet stream composition

$z_{k}^{O}(i)$ k^{th} species, i^{th} DN outlet stream composition

$\left(z_{k}^{O}(i)\right)^{l}, \left(z_{k}^{O}(i)\right)^{u}$ k^{th} species, i^{th} DN outlet stream composition vector, lower bound, upper bound

$x_{k}^{L}(p^{L},i)$ k^{th} species, i^{th} OP (operating at pressure p^{L}) liquid outlet composition

$y_k^V\left(p^V,i\right)$ k^{th} species, i^{th} OP (operating at pressure p^V) vapor outlet composition

$R_k\left(p^P,i\right)$ k^{th} species, i^{th} OP (operating at pressure p^P) reaction rate

$H\left(p^P,i\right)$ i^{th} OP (operating at pressure p^P) reactive holdup

G Total number of flashes generated in all pressure universes, for different discretizations

M Number of IDEAS network inlets

N Number of IDEAS network outlets

4.8. Appendix

4.8.1. Constants for Antoine's equation and Wilson equation parameters

The constants used to solve Antoine's equation and Wilson equation parameters are presented in Table 4.4 [16,61].

Table 4.4: Antoine equation's constants and Wilson equation's parameters

	Antoine Equation Constants			*Wilson Equation Parameters*			
Component	*A*	*B*	*C*	A_{X1}	A_{X2}	A_{X3}	$V_i\left(m^3/mol\right)$
Isobutene (*IB*)	9.132635	–2125.74886	–33.16	0.0	169.9953	−60.1022	93.33×10^{-6}
Methanol (*MOH*)	11.986965	–3643.31362	–33.434	2576.853	0.0	1483.248	44.44×10^{-6}
MTBE	9.203235	–2571.5846	–48.406	271.5669	–406.39	0	118.8×10^{-6}

4.8.2. Reactive flash separation sets according to the discretization size.

The discretization of the composition domain through a finite number of triplets $x_{IB}^{L}, x_{MOH}^{L}, x_{MTBE}^{L}$, defined for each operational pressure and considering a constant interval size on the interval $x_j \in \mathbb{R} : x_j = \{0 \le x \le 1\}$, result in the sets presented in Table 4.5.

Table 4.5: Reactive flash separator sets according to the discretization size

Discretization	**Low-pressure RD flash separators**	**High-pressure RD flash separators**	**Total number of RD flash separators** G
1/4	15	15	30
1/8	45	45	90
1/16	153	153	306
1/20	231	231	462
1/32	561	561	1122
1/40	861	861	1722
1/50	1326	1326	2652

4.9. References

(1) Stankiewicz, A. I.; Moulijn, J. A. Process Intensification: Transforming Chemical Engineering. *Chemical Engineering Progress* **2000**, *96* (1), 22–34.

(2) Stankiewicz, A. Reactive Separations for Process Intensification: An Industrial Perspective. *Chemical Engineering and Processing: Process Intensification* **2003**, *42* (3), 137–144. https://doi.org/10.1016/S0255-2701(02)00084-3.

(3) Van Gerven, T.; Stankiewicz, A. Structure, Energy, Synergy, Time—The Fundamentals of Process Intensification. *Ind. Eng. Chem. Res.* **2009**, *48* (5), 2465–2474. https://doi.org/10.1021/ie801501y.

(4) Górak, A.; Olujic, Z. *Distillation: Equipment and Processes*; Academic Press, 2014.

(5) Siirola, J. J. Industrial Applications of Chemical Process Synthesis. In *Advances in Chemical Engineering*; Anderson, J. L., Ed.; Academic Press, 1996; Vol. 23, pp 1–62.

(6) Doherty, M. F.; Malone, M. F. *Conceptual Design of Distillation Systems*; McGraw-Hill, 2001.

(7) Knapp, J. P.; Doherty, M. F. A New Pressure-Swing-Distillation Process for Separating Homogeneous Azeotropic Mixtures. *Industrial & engineering chemistry research* **1992**, *31* (1), 346–357.

(8) Luyben, W. L. Comparison of Pressure-Swing and Extractive-Distillation Methods for Methanol-Recovery Systems in the TAME Reactive-Distillation Process. *Ind. Eng. Chem. Res.* **2005**, *44* (15), 5715–5725. https://doi.org/10.1021/ie058006q.

(9) Barbosa, D.; Doherty, M. F. Design and Minimum-Reflux Calculations for Single-Feed Multicomponent Reactive Distillation Columns. *Chemical Engineering Science* **1988**, *43* (7), 1523–1537. https://doi.org/10.1016/0009-2509(88)85144-3.

(10) Barbosa, D.; Doherty, M. F. Design and Minimum-Reflux Calculations for Double-Feed Multicomponent Reactive Distillation Columns. *Chemical Engineering Science* **1988**, *43* (9), 2377–2389. https://doi.org/10.1016/0009-2509(88)85172-8.

(11) Bessling, B.; Schembecker, G.; Simmrock, K. H. Design of Processes with Reactive Distillation Line Diagrams. *Ind. Eng. Chem. Res.* **1997**, *36* (8), 3032–3042. https://doi.org/10.1021/ie960727p.

(12) Chadda, N.; Malone, M. F.; Doherty, M. F. Feasible Products for Kinetically Controlled Reactive Distillation of Ternary Mixtures. *AIChE J.* **2000**, *46* (5), 923–936. https://doi.org/10.1002/aic.690460507.

(13) Huss, R. S.; Chen, F.; Malone, M. F.; Doherty, M. F. Computer-Aided Tools for the Design of Reactive Distillation Systems. *Computers & Chemical Engineering* **1999**, *23*, S955–S962. https://doi.org/10.1016/S0098-1354(99)80230-0.

(14) Okasinski, M. J.; Doherty, M. F. Design Method for Kinetically Controlled, Staged Reactive Distillation Columns. *Industrial & Engineering Chemistry Research* **1998**, *37* (7), 2821–2834. https://doi.org/10.1021/ie9708788.

(15) Ung, S.; Doherty, M. F. Vapor-Liquid Phase Equilibrium in Systems with Multiple Chemical Reactions. *Chemical Engineering Science* **1995**, *50* (1), 23–48. https://doi.org/10.1016/0009-2509(94)00180-Y.

(16) Venimadhavan, G.; Buzad, G.; Doherty, M. F.; Malone, M. F. Effect of Kinetics on Residue Curve Maps for Reactive Distillation. *AIChE J.* **1994**, *40* (11), 1814–1824. https://doi.org/10.1002/aic.690401106.

(17) Buzad, G.; Doherty, M. F. New Tools for the Design of Kinetically Controlled Reactive Distillation Columns for Ternary Mixtures. *Computers & Chemical Engineering* **1995**, *19* (4), 395–408. https://doi.org/10.1016/0098-1354(94)00068-Y.

(18) Buzad, G.; Doherty, M. F. Design of Three-Component Kinetically Controlled Reactive Distillation Columns Using Fixed-Points Methods. *Chemical Engineering Science* **1994**, *49* (12), 1947–1963. https://doi.org/10.1016/0009-2509(94)80079-0.

(19) Daza, O. S.; Pérez-Cisneros, E. S.; Bek-Pedersen, E.; Gani, R. Graphical and Stage-to-Stage Methods for Reactive Distillation Column Design. *AIChE Journal* **2003**, *49* (11), 2822–2841. https://doi.org/10.1002/aic.690491115.

(20) Mansouri, S. S.; Huusom, J. K.; Gani, R.; Sales-Cruz, M. Systematic Integrated Process Design and Control of Binary Element Reactive Distillation Processes. *AIChE Journal* **2016**, *62* (9), 3137–3154. https://doi.org/10.1002/aic.15322.

(21) Cardoso, M. F.; Salcedo, R. L.; de Azevedo, S. F.; Barbosa, D. Optimization of Reactive Distillation Processes with Simulated Annealing. *Chemical Engineering Science* **2000**, *55* (21), 5059–5078. https://doi.org/10.1016/S0009-2509(00)00119-6.

(22) Ciric, A. R.; Gu, D. Synthesis of Nonequilibrium Reactive Distillation Processes by MINLP Optimization. *AIChE J.* **1994**, *40* (9), 1479–1487. https://doi.org/10.1002/aic.690400907.

(23) Seferlis, P.; Grievink, J. Optimal Design and Sensitivity Analysis of Reactive Distillation Units Using Collocation Models. *Ind. Eng. Chem. Res.* **2001**, *40* (7), 1673–1685. https://doi.org/10.1021/ie0005093.

(24) Wilson, S.; Manousiouthakis, V. IDEAS Approach to Process Network Synthesis: Application to Multicomponent MEN. *AIChE J.* **2000**, *46* (12), 2408–2416. https://doi.org/10.1002/aic.690461209.

(25) Drake, J. E.; Manousiouthakis, V. IDEAS Approach to Process Network Synthesis: Minimum Utility Cost for Complex Distillation Networks. *Chemical Engineering Science* **2002**, *57* (15), 3095–3106. https://doi.org/10.1016/S0009-2509(02)00159-8.

(26) Drake, J. E.; Manousiouthakis, V. IDEAS Approach to Process Network Synthesis: Minimum Plate Area for Complex Distillation Networks with Fixed Utility Cost. *Industrial & Engineering Chemistry Research* **2002**, *41* (20), 4984–4992. https://doi.org/10.1021/ie010735s.

(27) Justanieah, A. M.; Manousiouthakis, V. IDEAS Approach to the Synthesis of Globally Optimal Separation Networks: Application to Chromium Recovery from Wastewater. *Advances in Environmental Research* **2003**, *7* (2), 549–562. https://doi.org/10.1016/S1093-0191(02)00026-6.

(28) Martin, L. L.; Manousiouthakis, V. I. Globally Optimal Power Cycle Synthesis via the Infinite-DimEnsionAl State-Space (IDEAS) Approach Featuring Minimum Area with Fixed Utility. *Chemical Engineering Science* **2003**, *58* (18), 4291–4305. https://doi.org/10.1016/S0009-2509(02)00526-2.

(29) Holiastos, K.; Manousiouthakis, V. Infinite-Dimensional State-Space (IDEAS) Approach to Globally Optimal Design of Distillation Networks Featuring Heat and Power Integration. *Ind. Eng. Chem. Res.* **2004**, *43* (24), 7826–7842. https://doi.org/10.1021/ie010434i.

(30) Takase, H.; Hasebe, S. Synthesis of Ternary Distillation Process Structures Featuring Minimum Utility Cost Using the IDEAS Approach. *AIChE Journal* **2018**, *64* (4), 1285–1294. https://doi.org/10.1002/aic.16023.

(31) Burri, J. F.; Manousiouthakis, V. I. Global Optimization of Reactive Distillation Networks Using IDEAS. *Computers & Chemical Engineering* **2004**, *28* (12), 2509–2521. https://doi.org/10.1016/j.compchemeng.2004.06.014.

(32) da Cruz, F. E.; Manousiouthakis, V. I. Process Intensification of Reactive Separator Networks through the IDEAS Conceptual Framework. *Comput. Chem. Eng.* **2017**, *105*, 39–55. https://doi.org/10.1016/j.compchemeng.2016.12.006.

(33) Burri, J. F.; Wilson, S. D.; Manousiouthakis, V. I. Infinite DimEnsionAl State-Space Approach to Reactor Network Synthesis: Application to Attainable Region Construction. *Computers & Chemical Engineering* **2002**, *26* (6), 849–862. https://doi.org/10.1016/S0098-1354(02)00008-X.

(34) Manousiouthakis, V. I.; Justanieah, A. M.; Taylor, L. A. The Shrink–Wrap Algorithm for the Construction of the Attainable Region: An Application of the IDEAS Framework. *Computers & Chemical Engineering* **2004**, *28* (9), 1563–1575. https://doi.org/10.1016/j.compchemeng.2003.12.005.

(35) Zhou, W.; Manousiouthakis, V. I. Non-Ideal Reactor Network Synthesis through IDEAS: Attainable Region Construction. *Chemical Engineering Science* **2006**, *61* (21), 6936–6945. https://doi.org/10.1016/j.ces.2006.07.002.

(36) Zhou, W.; Manousiouthakis, V. I. Variable Density Fluid Reactor Network Synthesis—Construction of the Attainable Region through the IDEAS Approach. *Chemical Engineering Journal* **2007**, *129* (1–3), 91–103. https://doi.org/10.1016/j.cej.2006.11.004.

(37) Zhou, W.; Manousiouthakis, V. I. Pollution Prevention through Reactor Network Synthesis: The IDEAS Approach. *International Journal of Environment and Pollution* **2007**, *29* (1–3), 206–231. https://doi.org/10.1504/IJEP.2007.012804.

(38) Posada, A.; Manousiouthakis, V. Multi-Feed Attainable Region Construction Using the Shrink–Wrap Algorithm. *Chemical Engineering Science* **2008**, *63* (23), 5571–5592. https://doi.org/10.1016/j.ces.2008.07.026.

(39) Zhou, W.; Manousiouthakis, V. I. Global Capital/Total Annualized Cost Minimization of Homogeneous and Isothermal Reactor Networks. *Ind. Eng. Chem. Res.* **2008**, *47* (10), 3771–3782. https://doi.org/10.1021/ie060653+.

(40) Zhou, W.; Manousiouthakis, V. I. On Dimensionality of Attainable Region Construction for Isothermal Reactor Networks. *Computers & Chemical Engineering* **2008**, *32* (3), 439–450. https://doi.org/10.1016/j.compchemeng.2007.02.013.

(41) Zhou, W.; Manousiouthakis, V. I. Automating the AR Construction for Non-Isothermal Reactor Networks. *Computers & Chemical Engineering* **2009**, *33* (1), 176–180. https://doi.org/10.1016/j.compchemeng.2008.07.011.

(42) Ghougassian, P. G.; Manousiouthakis, V. Attainable Composition, Energy Consumption, and Entropy Generation Properties for Isothermal/Isobaric Reactor Networks. *Ind. Eng. Chem. Res.* **2013**, *52* (9), 3225–3238. https://doi.org/10.1021/ie301158m.

(43) Ghougassian, P. G.; Manousiouthakis, V. Globally Optimal Networks for Multipressure Distillation of Homogeneous Azeotropic Mixtures. *Industrial & Engineering Chemistry Research* **2012**, *51* (34), 11183–11200. https://doi.org/10.1021/ie300423q.

(44) Al-Husseini, Z.; Manousiouthakis, V. I. IDEAS Based Synthesis of Minimum Volume Reactor Networks Featuring Residence Time Density/Distribution Models. *Computers &*

Chemical Engineering **2014**, *60*, 124–142. https://doi.org/10.1016/j.compchemeng.2013.07.005.

(45) Ghougassian, P. G.; Manousiouthakis, V. Minimum Entropy Generation for Isothermal Endothermic/Exothermic Reactor Networks. *AIChE J.* **2015**, *61* (1), 103–117. https://doi.org/10.1002/aic.14598.

(46) Pichardo, P.; Manousiouthakis, V. I. Infinite DimEnsionAl State-Space as a Systematic Process Intensification Tool: Energetic Intensification of Hydrogen Production. *Chemical Engineering Research and Design* **2017**, *120*, 372–395. https://doi.org/10.1016/j.cherd.2017.01.026.

(47) Conner, J. A.; Manousiouthakis, V. I. Global Minimization of an Infinite Collection of Instances of the Total Annualized Cost Problem for Compressor Sequences. *Ind. Eng. Chem. Res.* **2015**, *54* (6), 1861–1875. https://doi.org/10.1021/ie503527w.

(48) Conner, J. A.; Manousiouthakis, V. I. Global Optimality Properties of Total Annualized and Operating Cost Problems for Compressor Sequences. *AIChE Journal* **2014**, *60* (12), 4134–4149. https://doi.org/10.1002/aic.14580.

(49) Davis, B. J.; Taylor, L. A.; Manousiouthakis, V. I. Identification of the Attainable Region for Batch Reactor Networks. *Ind. Eng. Chem. Res.* **2008**, *47* (10), 3388–3400. https://doi.org/10.1021/ie071664l.

(50) Conner, J. A.; Manousiouthakis, V. I. On the Attainable Region for Process Networks. *AIChE J.* **2014**, *60* (1), 193–212. https://doi.org/10.1002/aic.14257.

(51) Cerda, J.; Westerberg, A. W.; Mason, D.; Linnhoff, B. Minimum Utility Usage in Heat Exchanger Network Synthesis A Transportation Problem. *Chemical Engineering Science* **1983**, *38* (3), 373–387. https://doi.org/10.1016/0009-2509(83)80156-0.

(52) Duran, M. A.; Grossmann, I. E. Simultaneous Optimization and Heat Integration of Chemical Processes. *AIChE Journal* **1986**, *32* (1), 123–138. https://doi.org/10.1002/aic.690320114.

(53) Barnicki, S. D.; Siirola, J. J. Process Synthesis Prospective. *Computers & Chemical Engineering* **2004**, *28* (4), 441–446. https://doi.org/10.1016/j.compchemeng.2003.09.030.

(54) Urselmann, M.; Engell, S. Design of Memetic Algorithms for the Efficient Optimization of Chemical Process Synthesis Problems with Structural Restrictions. *Computers & Chemical Engineering* **2015**, *72*, 87–108. https://doi.org/10.1016/j.compchemeng.2014.08.006.

(55) Winterberg, M.; Schulte-Körne, E.; Peters, U.; Nierlich, F. Methyl Tert-Butyl Ether. In *ULLMANN'S Encyclopedia of Industrial Chemistry*; John Wiley & Sons, 2010; Vol. 1.

(56) Ma, J.; Xiong, D.; Li, H.; Ding, Y.; Xia, X.; Yang, Y. Vapor Intrusion Risk of Fuel Ether Oxygenates Methyl Tert-Butyl Ether (MTBE), Tert-Amyl Methyl Ether (TAME) and Ethyl Tert-Butyl Ether (ETBE): A Modeling Study. *Journal of Hazardous Materials* **2017**, *332*, 10–18. https://doi.org/10.1016/j.jhazmat.2017.02.057.

(57) Li, H.; Meng, Y.; Li, X.; Gao, X. A Fixed Point Methodology for the Design of Reactive Distillation Columns. *Chemical Engineering Research and Design* **2016**, *111*, 479–491. https://doi.org/10.1016/j.cherd.2016.05.015.

(58) Nijhuis, S. A.; Kerkhof, F. P. J. M.; Mak, A. N. S. Multiple Steady States during Reactive Distillation of Methyl Tert-Butyl Ether. *Ind. Eng. Chem. Res.* **1993**, *32* (11), 2767–2774. https://doi.org/10.1021/ie00023a045.

(59) Ung, S.; Doherty, M. F. Synthesis of Reactive Distillation Systems with Multiple Equilibrium Chemical Reactions. *Industrial & engineering chemistry research* **1995**, *34* (8), 2555–2565.

(60) Okasinski, M. J.; Doherty, M. F. Thermodynamic Behavior of Reactive Azeotropes. *AIChE J.* **1997**, *43* (9), 2227–2238. https://doi.org/10.1002/aic.690430909.

(61) Lísal, M.; Smith, W. R.; Nezbeda, I. Molecular Simulation of Multicomponent Reaction and Phase Equilibria in MTBE Ternary System. *AIChE Journal* **2000**, *46* (4), 866–875. https://doi.org/10.1002/aic.690460419.

(62) Qi, Z.; Kienle, A.; Stein, E.; Mohl, K.-D.; Tuchlenski, A.; Sundmacher, K. MTBE Decomposition in a Reactive Distillation Column. *Chemical Engineering Research and Design* **2004**, *82* (2), 185–191. https://doi.org/10.1205/026387604772992756.

(63) Huang, K.; Wang, S.-J. Design and Control of a Methyl Tertiary Butyl Ether (MTBE) Decomposition Reactive Distillation Column. *Ind. Eng. Chem. Res.* **2007**, *46* (8), 2508–2519. https://doi.org/10.1021/ie061204c.

(64) Biegler, L. T.; Grossmann, I. E.; Westerberg, A. W. Systematic Methods for Chemical Process Design. **1997**.

(65) Towler, G.; Sinnott, R. K. *Chemical Engineering Design: Principles, Practice and Economics of Plant and Process Design*; Elsevier, 2012.

CHAPTER 5

Synthesis of Reactive Distillation Networks through IDEAS featuring Quaternary Azeotropic Mixtures

5.1. Abstract

The Infinite DimEnsionAl State-Space (IDEAS) conceptual framework is proven to guarantee global optimality for any chemical process. For a large set of chemical engineering synthesis problems, the benefits imposed by the theoretical assumption of infinite dimensions with infinite cardinality, such as linearity and convexity, exceed the computational costs associated with the solution of large-scale linear programs (LP). Nevertheless, the application of IDEAS in problems with high dimensionality may impose computational challenges to obtain global optimal solutions during the IDEAS infinite LP infimum approximation process. To this end, the column generation (CG) procedure – used to rigorously and efficiently determine the optimal solution of a large-scale LP – is introduced in this work. The association of IDEAS framework with the column generation process was applied in a high dimensional problem involving the separation of quaternary azeotropic mixtures through an isobaric reactive distillation network. The network is comprised of vapor-liquid equilibrium trays, with liquid holdup that changes from tray to tray. Kinetically and/or equilibrium limited reactions are assumed to occur in the liquid phase. The method is demonstrated on a case study involving the isobaric reactive distillation of an acetic acid/isopropanol/isopropyl acetate/water azeotropic mixture. The IDEAS-CG results shows feasible design solutions for of isopropyl acetate with purity of 94% through reactive distillation.

5.2. Introduction

Separation studies of quaternary mixtures through reactive distillation (RD) systems has caught the attention of the scientific community due to the positive prospects of RD as an intensified process separation technology. In particular, the use of reactive distillation system in esterification processes is prospected as an alternative to increase reaction conversion – usually equilibrium limited – by continuous removal of products. Moreover, the reaction can help to break the azeotropes commonly found in those systems.

Isopropyl acetate (IPAc) is an important organic industrial chemical that is widely used in the production of varnishes, paints, printing inks, synthetic resins, and adhesive agents[1]. A common difficulty related to the separation of IPAc is the existence of a three-component azeotrope when produced using isopropanol (IPOH) and acetic acid (AA) as reactants. The existence of a reactive azeotrope in this system[2] also impacts the production of IPAc through reactive distillation. Due to these characteristics, a conventional reactive distillation column is reported to not be able to produce high purity acetate [3]. Based on the same difficulties involving the reactive separation of isopropyl acetate, Tang et al.[4] classified its production as pertaining to a type II configuration, which indicates that only the reaction and rectifying sections are present in the RD column, while further purification of acetate is carried out in a downstream stripper column. Also, in the type II configuration a decanter is necessary to recycle the organics back to the RD and Stripper. The possibility of improving this process through the use of the IDEAS conceptual framework is sought in this work.

The IDEAS conceptual framework has been successfully applied to either globally optimize or to identify the attainable region of numerous process synthesis problems. Some examples of IDEAS application involves multicomponent mass exchange networks [9], ideal distillation networks [10,11], separator networks [12], power cycles [13], heat/power integrated distillation networks [14,15], reactive distillation networks [16,17], reactor network attainable region construction [18–27], azeotropic distillation networks [28], reactor networks [29–31], compressor sequences [32,33], batch reactor networks [34], and process network attainable region [35].

All units in the OP can be used in the IDEAS framework to reach the desired process objective. A flow operator structure, the IDEAS distribution network DN, is employed to connect all inlet-outlet possibilities (i.e., process inlets to process units, process inlets to process outlets, process units to process units and process units to process outlets). Considering that the DN operations (mixing, splitting, recycling, and bypass) are linear in the flow variables, the IDEAS DN-OP representation is linear for any chemical process.

Due to IDEAS' innovative proposition for the process operations, which domain and range is considered to lie in an infinite (rather than finite) dimensional space, infinite dimensional linear programs (ILP) can be formulated for the synthesis of optimal process networks. In fact, since it is not possible to solve an ILP, its solution is approximated arbitrarily close by finite dimensional linear programs (LP) of ever-increasing size. The sequence formed by the LP optimal solutions converges to the global optimal solution of the ILP.

For a large set of chemical engineering synthesis problems, the benefits imposed by the theoretical assumption of infinite dimensions with infinite cardinality, such as linearity and convexity, exceed the computational costs associated with the solution of large-scale linear programs (LP). Nevertheless, the application of IDEAS in problems with high dimensionality,

such as the quaternary azeotropic mixture of isopropanol, acetic acid, isopropyl acetate, and water, may impose computational challenges during the IDEAS convergence procedure. To address this potential issue, a column generation procedure is implemented in this work.

Column generation (CG) procedures are used in a variety of different fields to solve large-scale optimization problems [5–8]. Column generation in general refers to the application of decomposition procedures [9–12], where additional variables (or columns) are added to a reduced LP problem, usually referred as "restricted master problem", during the iterative process solution until a defined stop criteria is reached. One of the predecessors of the column generation techniques, which falls in the same category, is called "cut generation". The cut generation procedure is applied to the dual problem, and then violated constraints (or "cuts") not present in the reduced LP problem are added to it.

The fact that all possible process flowsheets are taken into account during the IDEAS application, increase the possibility of finding a breakthrough in any process synthesis problem. In this paper, the IDEAS framework is applied on a case study involving the isobaric reactive distillation of an acetic acid/isopropanol/isopropyl acetate/water azeotropic mixture, aiming to find the maximum isopropyl acetate purity value for the system.

5.3. Mathematical formulation

5.3.1. Reactive flash separator model

The reactive flash separator model presented in previous works[13–15] has been applied to the quaternary azeotropic separation problem featured in this study, with the difference that the capacity value is not being tracked in this work. A variety of different models had been proposed

to design and optimize reactive distillation systems. Procedures based on geometrical approach such as the residue curve maps and the fixed point method have been heavily utilized to attack the problem [16–25]. In addition to the graphical approach, optimization-based methods using mixed-integer nonlinear programming (MINPL) formulations [26–33] have also contributed to the advancement of the reactive distillation process synthesis.

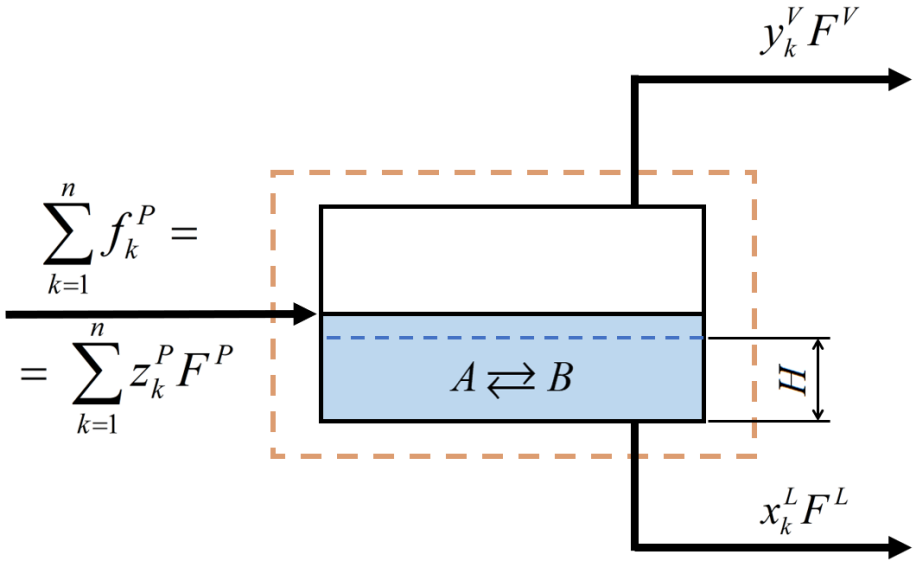

Figure 5.1 - Reactive flash separator model used in the quaternary azeotropic mixture separation problem.

The model proposed in this work (Fig.5.1) has the advantage of fully determine the outlet composition of a n component mixture with the knowledge of $n-1$ species in either the vapor or the liquid outlet. In addition, this approach has no dependence on the inlet composition. The reactive flash separator's vapor and liquid exit streams are considered to be in phase equilibrium with one another, and reactions may occur in the liquid phase, depending on the reactive volume H (the reactive holdup) of the flash separator.

This approach gives to the reactive flash the ability to account for several phenomena that can act together or isolated, depending on the necessity of the synthesis process. A fully operational reactive flash, i.e., none of the variables are equal to zero, will simultaneously act as a reactor and VLE separator. Moreover, if the reactive holdup is zero, the system acts as a VLE flash separator only; and if no separation is proceeded it is going to assume the behavior of an isolated CSTR reactor, with only one liquid flow as output. The component balance formulation for the reactive flash separator model is shown in Eq.(5.1):

$$f_k^P + R_k\left(\left\{x_j^L\right\}_{j=1}^n, T, P\right)H - x_k^L F^L - y_k^V F^V = 0 \qquad ; \qquad \forall k = 1,...,n \tag{5.1}$$

The general formulation for the phase equilibrium condition of each k^{th}-component in the mixture uses the Gamma-Phi model to relate the liquid molar fraction x_k^L with the correspondent vapor molar fraction y_k^V inside the reactive flash separator, as shown in Eq.(5.2):

$$y_k^V \phi_k\left(\left\{y_l^V\right\}_{l=1}^n, T, P\right)P = x_k^L \gamma_k\left(\left\{x_l^L\right\}_{l=1}^n, T\right)P_k^{sat}(T) \qquad \forall k = 1,...,n \tag{5.2}$$

The k^{th}-component's generation rate R_k in the reactive flash is usually given by a kinetic rate expression in the form of Eq.(5.3), although other rate forms are also possible.

$$R_k = k_f(T)\left(\prod_{reactants} a_r\left(\gamma_r, x_r\right)^{\nu_r} - \frac{1}{K_{eq}(T)}\prod_{products} a_p\left(\gamma_p, x_p\right)^{\nu_p}\right) \tag{5.3}$$

The species i activity in a multicomponent mixture is related to the activity coefficient in the liquid phase and the liquid molar fraction for the respective component as shown in Eq.(5.4).

$$a_i = \gamma_i\left(\left\{x_l^L\right\}_{l=1}^n, T\right)x_i \tag{5.4}$$

To solve the vapor-liquid equilibrium model showed in Eq.(5.2), a variety of thermodynamic models can be utilized to describe the behavior of the fugacity coefficient function $\phi_k\left(\left\{y_l^V\right\}_{l=1}^n, T, P\right)$, the activity coefficient function $\gamma_k\left(\left\{x_l^L\right\}_{l=1}^n, T\right)$ and the saturated pressure $P_k^{sat}(T)$ for the k^{th}-component in the mixture. Since vapor-liquid equilibrium is assumed in the reactive flash and considering ideal gas behavior, for each specified composition in the liquid output the specified thermodynamic models can be iteratively calculated for different temperatures until the vapor fractions sum up to the unit[13–15].

In this work, given the nonideality of the composition assumed in the study case, the NRTL model has been applied in the calculation of the activity coefficients of each species in the mixture. The Antoine equation was used to express the components' partial pressures respectively.

In the IDEAS ILP formulation, an infinite number of the aforementioned reactive flash separators are presented in the process operator (OP). The ILP formulation is presented in the next section.

5.3.2. IDEAS ILP for the reactive distillation synthesis problem

In order to consider all possible flowsheets for the reactive distillation network, the process operator OP is interfaced with a distribution network (DN) where all stream splitting, mixing and pressure adjustment occurs. Fig. 5.2 shows the resulting IDEAS framework for the reactive distillation synthesis problem.

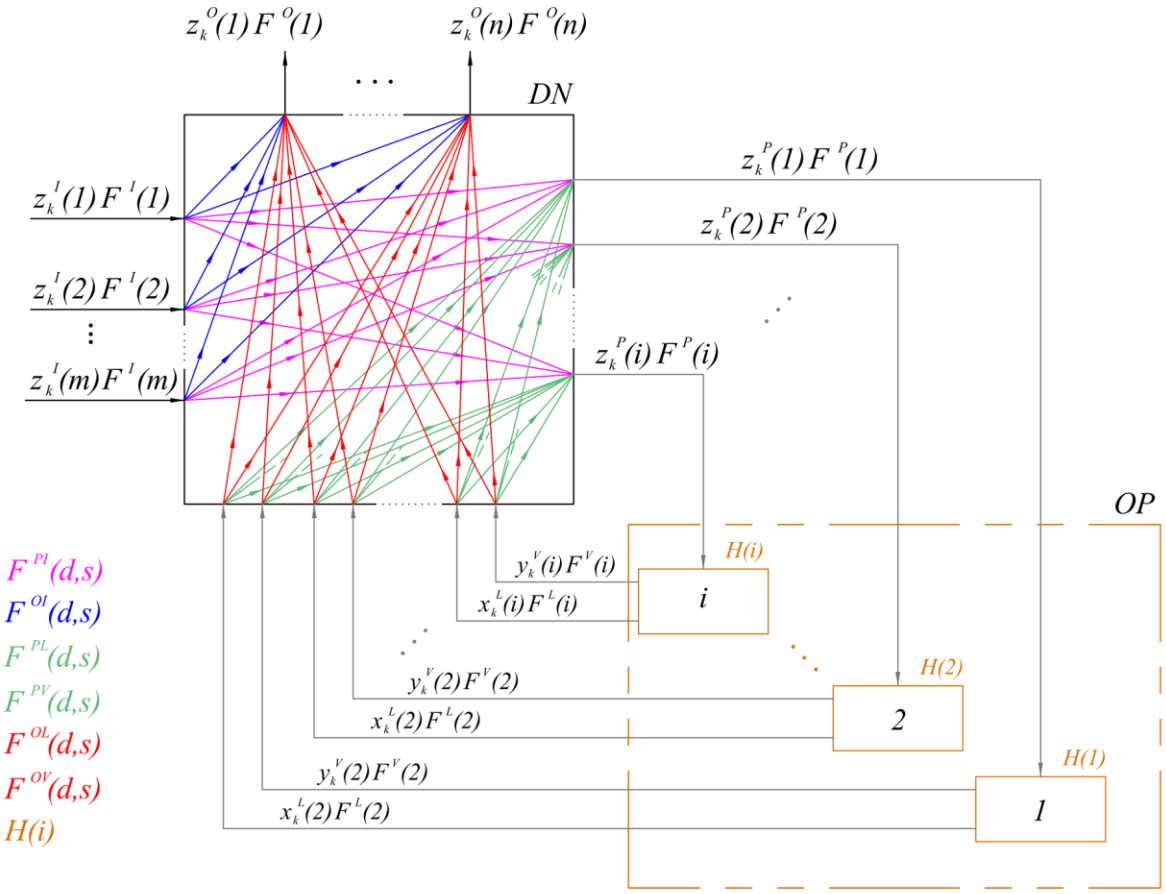

Figure 5.2 - IDEAS representation for a reactive flash separator network.

Each of the cross-flow streams in the DN is characterized by a flow rate variable, which has fixed destination and origin molar fraction conditions. The vector of flow variables are identified by a superscript that indicates their destination and source respectively: the DN inlet is identified as I, the DN outlet as O, the OP inlet as P, the liquid and vapor outputs from the OP as L and V respectively. The indexes that identify the elements of vector flow variables also follows the destination-source pair structure. The reactive holdups and the capacity are both variables associated with the elements of the OP.

Several infinite LP formulations can be derived using the IDEAS framework. In order to simplify the application on the case study, a general ILP formulation is developed can be modified for any specific case. A generic linear objective function is proposed at this point as

$$c^T F \tag{5.5}$$

where the vector F includes all flows of the DN, the inlet flows, the reactive holdups for the reactive flashes and their respective capacity. The above objective function can be used to realize a wide array of objectives, through appropriate selection of the elements of the cost vector c^T.

The development of the constraints for the ILP general formulation uses mass and component balances on the DN, and the proposed reactive flash separator model for the OP. For each inlet flow $F^I(j)$ associated with one of the M inlets of the DN, a splitting balance is written as shown in Eq.(5.6).

$$F^I(j) - \sum_{i=1}^{N} F^{OI}(i,j) - \sum_{i=1}^{\infty} F^{PI}(i,j) = 0 \quad ; \quad \forall j = 1,...,M \tag{5.6}$$

For each outlet flow $F^O(i)$ leaving the DN from one of its N outlets, a mixing balance as shown in Eq.(5.7) is considered.

$$F^O(i) - \sum_{j=1}^{M} F^{OI}(i,j) - \sum_{j=1}^{\infty} F^{OL}(i,j) - \sum_{j=1}^{\infty} F^{OV}(i,j) = 0 \quad ; \quad \forall i = 1,...,N \tag{5.7}$$

The component flow $f_k^P(i)$ that feeds the i^{th} reactive flash separator can be considered as the sum of component flows feeding that specific mixing point of the DN (component balance).

$$f_k^P(i) - \sum_{j=1}^{M} z_k^I(j) F^{PI}(i,j) - \sum_{j=1}^{\infty} x_k^L(j) F^{PL}(i,j) - \sum_{j=1}^{\infty} y_k^V(j) F^{PV}(i,j) = 0 \qquad \forall i = 1,...,\infty \ ; \ \forall k = 1,...,n \tag{5.8}$$

Thus, the total mass flow in this mixing node is represented by Eq.(5.9) below.

$$F^{P}(i)-\sum_{j=1}^{M}F^{PI}(i,j)-\sum_{j=1}^{\infty}F^{PL}(i,j)-\sum_{j=1}^{\infty}F^{PV}(i,j)=0 \quad ; \quad \forall i=1,...,\infty \tag{5.9}$$

For each $F^{L}(j)$ liquid and $F^{V}(j)$ vapor input flow entering the DN's after being processed in the OP, a splitting balance is written as:

$$F^{L}(j)-\sum_{i=1}^{N}F^{OL}(i,j)-\sum_{i=1}^{\infty}F^{PL}(i,j)=0 \quad ; \quad \forall j=1,...,\infty \tag{5.10}$$

$$F^{V}(j)-\sum_{i=1}^{N}F^{OV}(i,j)-\sum_{i=1}^{\infty}F^{PV}(i,j)=0 \quad ; \quad \forall j=1,...,\infty \tag{5.11}$$

The final products from the reactive distillation process can be found in the DN outlets. Lower and upper bounds constraints are introduced in the each of the N flow variables $F^{O}(i)$ as design parameters. The total balance for each flow exiting the DN is shown in Eq.(5.12).

$$\left(F^{O}(i)\right)^{l} \le \sum_{j=1}^{M}F^{OI}(i,j)+\sum_{j=1}^{\infty}F^{OL}(i,j)+\sum_{j=1}^{\infty}F^{OV}(i,j) \le \left(F^{O}(i)\right)^{u} \quad ; \quad \forall i=1,...,N \tag{5.12}$$

Equations (5.12) can also be expressed by two independent as shown below:

$$\left[\sum_{j=1}^{M}F^{OI}(i,j)+\sum_{j=1}^{\infty}F^{OL}(i,j)+\sum_{j=1}^{\infty}F^{OV}(i,j)\right]-\left(F^{O}(i)\right)^{l} \ge 0 \quad ; \quad \forall i=1,...,N \tag{5.13}$$

$$\left[\sum_{j=1}^{M}F^{OI}(i,j)+\sum_{j=1}^{\infty}F^{OL}(i,j)+\sum_{j=1}^{\infty}F^{OV}(i,j)\right]-\left(F^{O}(i)\right)^{u} \le 0 \quad ; \quad \forall i=1,...,N \tag{5.14}$$

The component balance at the DN's outputs, including upper and lower bounds for the product's molar fractions are represented by Eq.(5.15).

$$\left(z_k^O(i)\right)^l F^O(i) \le \left\{ \begin{array}{l} \sum_{j=1}^{M} z_k^I(j) F^{OI}(i,j) \\ +\sum_{j=1}^{\infty} x_k^L(j) F^{OL}(i,j) \\ +\sum_{j=1}^{\infty} y_k^V(j) F^{OV}(i,j) \end{array} \right\} \le \left(z_k^O(i)\right)^u F^O(i) \quad ; \quad \begin{array}{l} \forall i = 1,...,N \\ \forall k = 1,...,n \end{array} \tag{5.15}$$

Finally, the balances for the reactive flash separators in the OP are expressed as shown in Eq.(5.16).

$$f_k^P(i) + R_k(i) H(i) - x_k^L(i) F^L(i) - y_k^V(i) F^V(i) = 0 \quad ; \quad \begin{array}{l} \forall i = 1,...,\infty \\ \forall k = 1,...,n \end{array} \tag{5.16}$$

The number of variables can be reduced by substituting Eq.(5.6) to Eq.(5.8) in Eq.(5.17):

$$\begin{array}{l} R_k(i) H(i) - x_k^L(i) \left[\sum_{j=1}^{N} F^{OL}(j,i) + \sum_{j=1}^{\infty} F^{PL}(j,i) \right] \\ \quad - y_k^V(i) \left[\sum_{j=1}^{N} F^{OV}(j,i) + \sum_{j=1}^{\infty} F^{PV}(j,i) \right] + \sum_{j=1}^{M} z_k^I(j) F^{PI}(i,j) \\ \qquad + \sum_{j=1}^{\infty} x_k^L(j) F^{PL}(i,j) + \sum_{j=1}^{\infty} y_k^V(j) F^{PV}(i,j) = 0 \end{array} \quad ; \quad \begin{array}{l} \forall i = 1,...,\infty \\ \forall k = 1,...,n \end{array} \tag{5.17}$$

From Eq.(5.17), self-recycling flows are naturally eliminated from the system. This fact can lead to further simplifications as shown in Eq.(5.18):

$$
\begin{aligned}
& R_k(i)H(i)+\sum_{j=1}^{M} z_k^I(j)F^{PI}(i,j) \\
& -\sum_{j=1}^{N} x_k^L(i)F^{OL}(j,i)-\sum_{j=1}^{N} y_k^V(i)F^{OV}(j,i) \\
& \quad +\sum_{\substack{j=1 \\ j\neq i}}^{\infty}\left[x_k^L(j)F^{PL}(i,j)-x_k^L(i)F^{PL}(j,i)\right] \qquad ; \quad \begin{matrix}\forall i=1,\ldots,\infty \\ \forall k=1,\ldots,n\end{matrix} \\
& \quad +\sum_{\substack{j=1 \\ j\neq i}}^{\infty}\left[y_k^V(j)F^{PV}(i,j)-y_k^V(i)F^{PV}(j,i)\right]=0
\end{aligned}
\tag{5.18}
$$

Some variables in the component outlet bounds equations can be eliminated substituting Eq.(5.7) in Eq.(5.15):

$$
\left(z_k^O(i)\right)^l \begin{bmatrix} \sum_{j=1}^{M} F^{OI}(i,j) \\ +\sum_{j=1}^{\infty} F^{OL}(i,j) \\ +\sum_{j=1}^{\infty} F^{OV}(i,j) \end{bmatrix} \le \begin{bmatrix} \sum_{j=1}^{M} z_k^I(j)F^{OI}(i,j) \\ +\sum_{j=1}^{\infty} x_k^L(j)F^{OL}(i,j) \\ +\sum_{j=1}^{\infty} y_k^V(j)F^{OV}(i,j) \end{bmatrix} \le \left(z_k^O(i)\right)^u \begin{bmatrix} \sum_{j=1}^{M} F^{OI}(i,j) \\ +\sum_{j=1}^{\infty} F^{OL}(i,j) \\ +\sum_{j=1}^{\infty} F^{OV}(i,j) \end{bmatrix} ; \begin{matrix}\forall i=1,\ldots,N \\ \forall k=1,\ldots,n\end{matrix} \tag{5.19}
$$

Moreover, Eq.(5.19) can then be split into two inequalities:

$$
\begin{aligned}
& \sum_{j=1}^{M}\left[\left(\left(z_k^O(i)\right)^l - z_k^I(j)\right)F^{OI}(i,j)\right] \\
& +\sum_{j=1}^{\infty}\left[\left(\left(z_k^O(i)\right)^l - x_k^L(j)\right)F^{OL}(i,j)\right] \qquad ; \quad \begin{matrix}\forall i=1,\ldots,N \\ \forall k=1,\ldots,n\end{matrix} \\
& +\sum_{j=1}^{\infty}\left[\left(\left(z_k^O(i)\right)^l - y_k^V(j)\right)F^{OV}(i,j)\right] \le 0
\end{aligned}
\tag{5.20}
$$

$$
\begin{aligned}
& \sum_{j=1}^{M}\left[\left(\left(z_k^O(i)\right)^u - z_k^I(j)\right)F^{OI}(i,j)\right] \\
& +\sum_{j=1}^{\infty}\left[\left(\left(z_k^O(i)\right)^u - x_k^L(j)\right)F^{OL}(i,j)\right] \qquad ; \quad \begin{matrix}\forall i=1,\ldots,N \\ \forall k=1,\ldots,n\end{matrix} \\
& +\sum_{j=1}^{\infty}\left[\left(\left(z_k^O(i)\right)^u - y_k^V(j)\right)F^{OV}(i,j)\right] \ge 0
\end{aligned}
\tag{5.21}
$$

The final general ILP formulation for the reactive distillation network synthesis has a general objective function as showed in Eq.(5.5) subject to the constraints represented by Eqs. (5.6), (5.13), (5.14), (5.18), (5.20), and (5.21), summarized below in Eq.(5.22):

$$\nu \triangleq \inf \; c^T F \tag{5.22}$$

s.t.

$$F^I(j) - \sum_{i=1}^{N} F^{OI}(i,j) - \sum_{i=1}^{\infty} F^{PI}(i,j) = 0 \qquad \forall j = 1,...,M$$

$$\left[\sum_{j=1}^{M} F^{OI}(i,j) + \sum_{j=1}^{\infty} F^{OL}(i,j) + \sum_{j=1}^{\infty} F^{OV}(i,j)\right] - \left(F^O(i)\right)^l \geq 0 \qquad \forall i = 1,...,N$$

$$\left[\sum_{j=1}^{M} F^{OI}(i,j) + \sum_{j=1}^{\infty} F^{OL}(i,j) + \sum_{j=1}^{\infty} F^{OV}(i,j)\right] - \left(F^O(i)\right)^u \leq 0 \qquad \forall i = 1,...,N$$

$$R_k(i)H(i) + \sum_{j=1}^{M} z_k^I(j) F^{PI}(i,j) - \sum_{j=1}^{N} x_k^L(i) F^{OL}(j,i) - \sum_{j=1}^{N} y_k^V(i) F^{OV}(j,i) + \qquad \forall i = 1,...,\infty$$

$$+ \sum_{\substack{j=1 \\ j\neq i}}^{\infty} \left[x_k^L(j) F^{PL}(i,j) - x_k^L(i) F^{PL}(j,i)\right] + \sum_{\substack{j=1 \\ j\neq i}}^{\infty} \left[y_k^V(j) F^{PV}(i,j) - y_k^V(i) F^{PV}(j,i)\right] = 0 \qquad \forall k = 1,...,n$$

$$\sum_{j=1}^{M} \left[\left(\left(z_k^O(i)\right)^l - z_k^I(j)\right) F^{OI}(i,j)\right] + \sum_{j=1}^{\infty} \left[\left(\left(z_k^O(i)\right)^l - x_k^L(j)\right) F^{OL}(i,j)\right] + \qquad \forall i = 1,...,N$$

$$+ \sum_{j=1}^{\infty} \left[\left(\left(z_k^O(i)\right)^l - y_k^V(j)\right) F^{OV}(i,j)\right] \leq 0 \qquad \forall k = 1,...,n$$

$$\sum_{j=1}^{M} \left[\left(\left(z_k^O(i)\right)^u - z_k^I(j)\right) F^{OI}(i,j)\right] + \sum_{j=1}^{\infty} \left[\left(\left(z_k^O(i)\right)^u - x_k^L(j)\right) F^{OL}(i,j)\right] \qquad \forall i = 1,...,N$$

$$+ \sum_{j=1}^{\infty} \left[\left(\left(z_k^O(i)\right)^u - y_k^V(j)\right) F^{OV}(i,j)\right] \geq 0 \qquad \forall k = 1,...,n$$

$$F^I \geq 0 \,;\, F^O \geq 0 \,;\, F^{OI} \geq 0 \,;\, F^{PI} \geq 0 \,;\, F^{OL} \geq 0 \,;\, F^{OV} \geq 0 \,;\, F^{PL} \geq 0 \,;\, F^{PV} \geq 0 \,;\, H \geq 0$$

5.3.3. ILP infimum approximation by finite LPs

An infinite dimensional linear program cannot be explicitly solved. However, its solution can be approximated by a series of finite linear programs of increasing size, whose sequence of optimum values converges to the infinite dimensional problem's infimum. In particular, instead of an infinite number, consider a finite set containing G of reactive flash separators in the OP. Consequently, the aforementioned IDEAS infinite LP formulation becomes a finite LP, which is a convex problem and can be solved by any LP solver.

Considering that the finite LP can now be solved η times using an ever-increasing number G of reactive flash separators, i.e. $G(1) < G(2) < ... < G(\eta)$, the resulting finite linear programs form a non-increasing sequence of optimal values $\nu(1) > \nu(2) > ... > \nu(\eta)$, which converges to the infimum of the ILP when $\eta \to \infty$.

For a large set of chemical engineering synthesis problems, the benefits imposed by the theoretical assumption of infinite dimensions with infinite cardinality, such as linearity and convexity, exceed the computational costs associated with the solution of large-scale linear programs (LP). Nevertheless, the application of IDEAS in problems with high dimensionality may impose computational challenges to obtain global optimal solutions during the IDEAS infinite LP infimum approximation process. For the reactive distillation network synthesis ILP presented in Eq.(5.22), the total number of variables and constraints varies according to the total number of inlets (M) and outlets (N) in the IDEAS-DN, the total number of species in the system (n), and the total number of reactive flash separators $(G : G \to \infty)$ in the IDEAS-OP. The total number of variables and constraints are represented by Eq.(5.23) and (5.24), respectively.

$$M + (M \times N) + (G \times M) + 2(G \times N) + N + G + 2\left[G \times (G-1)\right] \tag{5.23}$$

$$M + 2N + (n \times G) + 2(n \times N) \tag{5.24}$$

Thus, one may note that the size of the finite IDEAS-LP for the reactive distillation problem increases quadratically (twice) with the number of units G, which invariably has the largest cardinality amongst the sets presented in this problem. For some problems, as the ones involving quaternary mixtures, the set G starts with a large number of process units for a relatively coarse discretization of the molar fraction composition domain. In order to pursue the IDEAS convergence, the discretization has to become finer each time η increases, which may compromise the ability to solve the problem under constraints of computational power, memory and time to obtain a solution. This fact is shown in Table 5.1, which presents the value of G and the number of variables for ternary and quaternary mixtures according to the discretization used.

Table 5.1. Number of variables and constraints of IDEAS-LP per discretization and system type

System	Species (*n*)	Discretization	DN-Inlets (*M*)	DN-Outlets (N)	IDEAS-OP (*G*)	Num. of variables	Num. of constraints
Ternary	3	1/8	3	2	45	4,331	154
Ternary	3	1/16	3	2	153	47,747	478
Ternary	3	1/32	3	2	561	632,819	1,702
Quaternary	4	1/8	3	2	112	25,771	355
Quaternary	4	1/16	3	2	969	1,883,747	2,926
Quaternary	4	1/32	3	2	6545	85,713,331	19,654

From the example above, it is clear that in order to obtain solutions close to the IDEAS infimum for quaternary systems, strategies for solving large-scale linear programs at reduced computational cost are required. To that end, the column generation procedure presented in the next session was applied to the solution of the IDEAS-LP for quaternary azeotropic mixtures.

5.3.4. Column Generation Procedure

A common issue that impacts the computational viability of solving a large-scale linear program is memory capacity, since the problem can be large enough to make impractical the storage of all variables and constraints at the same time. To that end, the so-called "decomposition" procedures are typically employed.

Column generation (or cut generation) techniques are decomposition procedures and have been used in the solution of different large-scale optimization problems [5–7]. A general feature of the column generation procedure is the decomposition of the optimization problem into a master problem, where the result (or approximation) for the optimal solution is pursued; and a related subproblem that contains the criteria (or heuristics) for including variables back in the master problem. Consider for example a large-scale linear program (LP) of the form presented in Eq.(5.25).

$$\begin{aligned} \nu = \max_{x} \; & c^T x \\ & s.t. \\ & Ax \le b \\ & x \ge 0 \end{aligned} \tag{5.25}$$

The respective dual problem can be written as shown in Eq.(5.26).

$$\begin{aligned} \nu = \min_{\lambda_1} \; & b^T \lambda_1 \\ & s.t. \\ & A^T \lambda_1 - \lambda_2 = c \\ & \lambda_1 \ge 0 \\ & \lambda_2 \ge 0 \end{aligned} \tag{5.26}$$

Since $\lambda_2 \geq 0$, the dual problem can be simplified as shown in Eq.(5.27).

$$\left\{\begin{array}{l} \nu = \min\limits_{\lambda_1} b^T \lambda_1 \\ \quad s.t. \\ \quad -c + A^T \lambda_1 = \lambda_2 \\ \quad \lambda_1 \geq 0 \\ \quad \lambda_2 \geq 0 \end{array}\right\} \Leftrightarrow \left\{\begin{array}{l} \nu = \min\limits_{\lambda_1} b^T \lambda_1 \\ \quad s.t. \\ \quad c + A^T \lambda_1 = \lambda_2 \geq 0 \\ \quad \lambda_1 \geq 0 \end{array}\right\} \Leftrightarrow \left\{\begin{array}{l} \nu = \min\limits_{\lambda_1} b^T \lambda_1 \\ \quad s.t. \\ \quad A^T \lambda_1 \geq c \\ \quad \lambda_1 \geq 0 \end{array}\right\} \tag{5.27}$$

Both primal and dual problems can be decomposed according to the definitions shown in Eq.(5.28).

$$x = \begin{bmatrix} x_1 \\ x_2 \end{bmatrix},\ c = \begin{bmatrix} c_1 \\ c_2 \end{bmatrix},\ A = \begin{bmatrix} A_1 & A_2 \end{bmatrix}\ ;\ \left\{\begin{array}{l} x \in \mathbb{R}^{n_1+n_2}, x_1 \in \mathbb{R}^{n_1}, x_2 \in \mathbb{R}^{n_2} \\ c \in \mathbb{R}^{n_1+n_2}, c_1 \in \mathbb{R}^{n_1}, c_2 \in \mathbb{R}^{n_2} \\ A \in \mathbb{R}^{m\times(n_1+n_2)} \\ A_1 \in \mathbb{R}^{m\times n_1} \\ A_2 \in \mathbb{R}^{m\times n_2} \\ b \in \mathbb{R}^{m} \end{array}\right. \tag{5.28}$$

Based on the notation above, the aforementioned LP (primal) and its dual can be rewritten as presented in Eq.(5.29) and (5.30), respectively.

$$\begin{array}{l} \nu = \max\limits_{x_1, x_2} c_1^{\mathrm{T}} x_1 + c_2^{\mathrm{T}} x_2 \\ \quad s.t. \\ \quad A_1 x_1 + A_2 x_2 \leq b \\ \quad x_1 \geq 0 \\ \quad x_2 \geq 0 \end{array} \tag{5.29}$$

$$\begin{array}{l} \nu = \min\limits_{\lambda} b^{\mathrm{T}} \lambda \\ \quad s.t. \\ \quad \begin{bmatrix} A_1 & A_2 \end{bmatrix}^{\mathrm{T}} \lambda \geq \begin{bmatrix} c_1 & c_2 \end{bmatrix} \\ \quad \lambda \geq 0 \end{array} \tag{5.30}$$

Consider next the definition of a reduced master problem formed by setting x_2 to zero. Then, the reduced master problem primal and its associated reduced dual are presented in Eq.(5.31) and (5.32).

$$\begin{aligned} \mu = \max_{x_1} \; & c_1^{\mathrm{T}} x_1 \\ & s.t. \\ & A_1 x_1 \le b \\ & x_1 \ge 0 \end{aligned} \tag{5.31}$$

$$\begin{aligned} \mu = \min_{\lambda} \; & b^{\mathrm{T}} \lambda \\ & s.t. \\ & A_1^T \lambda \ge c_1 \\ & \lambda \ge 0 \end{aligned} \tag{5.32}$$

Let x_1^*, λ^* be the optimal solutions of the reduced master problem's primal and dual respectively. Then, both the reduced primal and the reduced dual have the same value at the optimal solution, and all constraints of those respective problems have been satisfied, as shown in Eq.(5.33).

$$\mu = c_1^{\mathrm{T}} x_1^* = b^{\mathrm{T}} \lambda^*,\; A_1 x_1^* \le b,\; A_1^T \lambda^* \ge c_1,\; \lambda^* \ge 0,\; x_1^* \ge 0 \tag{5.33}$$

It is then clear that $\mu \le \nu$, since $x^* = \begin{bmatrix} x_1^* \\ 0 \end{bmatrix}$ is a feasible point for the primal ν. Two cases are then possible:

1- If $A_2^T \lambda^* \ge c_2$ is satisfied, then λ^* is a feasible point for the dual ν, and thus $\mu = \nu$, $x^* = \begin{bmatrix} x_1^* \\ 0 \end{bmatrix}$, is the optimal solution for the primal ν, and λ^* is the optimal solution for the dual ν.

2- If $A_2^T \lambda^* - c_2 \ge 0$ is not satisfied, then λ^* is not a feasible point for the dual ν.

In the first case, the optimization search is stopped, since the optimum of the primal ν is identified. In the second case, the optimum of the primal ν is not identified, so a criterion to include variables (columns) into the reduced master problem has to be defined. In this work, the vector $A_2^{\mathrm{T}}\lambda^* - c_2$ is evaluated at end of each interaction, so the vectors below a given tolerance $-\delta$ are then identified. Each of these entries corresponds to an entry of the vector x_2. These entries are then removed from the vector x_2 and are incorporated in the vector x_1. The new reduced primal and dual problems are then solved, and new values for x_1^*, λ^* are identified. The procedure is repeated for increasingly smaller values of $-\delta$ until case 1 is satisfied.

5.3.5. IDEAS finite LP in inequality form

The application of the aforementioned column generation procedure is based on the inequality form of the linear program to be solved. The inequality form of the finite IDEAS-LO for the quaternary reactive distillation problem is presented in Eq.(5.34).

$$\nu \triangleq \inf \; c^T F \tag{5.34}$$

s.t.

$$F^I(j) - \sum_{i=1}^{N} F^{OI}(i,j) - \sum_{i=1}^{G} F^{PI}(i,j) \le 0 \qquad \forall j = 1,\ldots,M$$

$$-F^I(j) + \sum_{i=1}^{N} F^{OI}(i,j) + \sum_{i=1}^{G} F^{PI}(i,j) \le 0 \qquad \forall j = 1,\ldots,M$$

$$R_k(i)H(i)+\sum_{j=1}^{M} z_k^I(j)F^{PI}(i,j)-\sum_{j=1}^{N} x_k^L(i)F^{OL}(j,i)-\sum_{j=1}^{N} y_k^V(i)F^{OV}(j,i)+$$
$$+\sum_{\substack{j=1\\ j\neq i}}^{G}\left[x_k^L(j)F^{PL}(i,j)-x_k^L(i)F^{PL}(j,i)\right]+\sum_{\substack{j=1\\ j\neq i}}^{G}\left[y_k^V(j)F^{PV}(i,j)-y_k^V(i)F^{PV}(j,i)\right]\le 0 \qquad \forall i=1,\ldots,G;\ \forall k=1,\ldots,n$$

$$-R_k(i)H(i)-\sum_{j=1}^{M} z_k^I(j)F^{PI}(i,j)+\sum_{j=1}^{N} x_k^L(i)F^{OL}(j,i)+\sum_{j=1}^{N} y_k^V(i)F^{OV}(j,i)+$$
$$+\sum_{\substack{j=1\\ j\neq i}}^{G}\left[-x_k^L(j)F^{PL}(i,j)+x_k^L(i)F^{PL}(j,i)\right]+\sum_{\substack{j=1\\ j\neq i}}^{G}\left[-y_k^V(j)F^{PV}(i,j)+y_k^V(i)F^{PV}(j,i)\right]\le 0 \qquad \forall i=1,\ldots,G;\ \forall k=1,\ldots,n$$

$$\sum_{j=1}^{M}\left[\left(\left(z_k^O(i)\right)^l-z_k^I(j)\right)F^{OI}(i,j)\right]+\sum_{j=1}^{G}\left[\left(\left(z_k^O(i)\right)^l-x_k^L(j)\right)F^{OL}(i,j)\right]$$
$$+\sum_{j=1}^{G}\left[\left(\left(z_k^O(i)\right)^l-y_k^V(j)\right)F^{OV}(i,j)\right]\le 0 \qquad \forall i=1,\ldots,N;\ \forall k=1,\ldots,n$$

$$\sum_{j=1}^{M}\left[\left(-\left(z_k^O(i)\right)^u+z_k^I(j)\right)F^{OI}(i,j)\right]+\sum_{j=1}^{G}\left[\left(-\left(z_k^O(i)\right)^u+x_k^L(j)\right)F^{OL}(i,j)\right]$$
$$+\sum_{j=1}^{G}\left[\left(-\left(z_k^O(i)\right)^u+y_k^V(j)\right)F^{OV}(i,j)\right]\le 0 \qquad \forall i=1,\ldots,N;\ \forall k=1,\ldots,n$$

$$\left[\sum_{j=1}^{M} F^{OI}(i,j)+\sum_{j=1}^{G} F^{OL}(i,j)+\sum_{j=1}^{G} F^{OV}(i,j)\right]\le\left(F^O(i)\right)^{ub} \qquad \forall i=1,\ldots,N$$

$$\left[-\sum_{j=1}^{M} F^{OI}(i,j)-\sum_{j=1}^{G} F^{OL}(i,j)-\sum_{j=1}^{G} F^{OV}(i,j)\right]\le-\left(F^O(i)\right)^{lb} \qquad \forall i=1,\ldots,N$$

$$\sum_{j=1}^{M}\left[z_k^I(j)F^{OI}(i,j)\right]+\sum_{j=1}^{G}\left[x_k^L(j)F^{OL}(i,j)\right]+\sum_{j=1}^{G}\left[y_k^V(j)F^{OV}(i,j)\right]-z_k^O F^O(i)\le 0 \qquad \forall i=1,\ldots,N;\ \forall k=1,\ldots,n$$

$$-\sum_{j=1}^{M}\left[z_k^I(j)F^{OI}(i,j)\right]-\sum_{j=1}^{G}\left[x_k^L(j)F^{OL}(i,j)\right]-\sum_{j=1}^{G}\left[y_k^V(j)F^{OV}(i,j)\right]+z_k^O F^O(i)\le 0 \qquad \forall i=1,\ldots,N;\ \forall k=1,\ldots,n$$

$$\left[\sum_{j=1}^{G} F^{PL}(i,j)+\sum_{j=1}^{G} F^{PV}(i,j)+\sum_{j=1}^{N} F^{OL}(i,j)+\sum_{j=1}^{N} F^{OV}(i,j)\right]-\left(F^P\right)^{tot}\le 0 \qquad \forall i=1,\ldots,G$$

$$\left[-\sum_{j=1}^{G} F^{PL}(i,j)-\sum_{j=1}^{G} F^{PV}(i,j)-\sum_{j=1}^{N} F^{OL}(i,j)-\sum_{j=1}^{N} F^{OV}(i,j)\right]+\left(F^{P}\right)^{tot}\le 0 \qquad \forall i=1,...,G$$

$$\sum_{i=1}^{G} H(i)-H^{tot}\le 0 \qquad \forall i=1,...,G$$

$$-\sum_{i=1}^{G} H(i)+H^{tot}\le 0 \qquad \forall i=1,...,G$$

$$\left(F^{P}\right)^{tot}\le\left(\left(F^{P}\right)^{tot}\right)^{ub}$$

$$H^{tot}\le\left(H^{tot}\right)^{ub}$$

$$F^{I}\ge 0\,;F^{O}\ge 0\,;F^{OI}\ge 0\,;F^{PI}\ge 0\,;F^{OL}\ge 0\,;F^{OV}\ge 0\,;F^{PL}\ge 0\,;F^{PV}\ge 0\,;H\ge 0$$

This inequality formulation and the column generation procedure described in the previous section were implemented using CPLEX in C++ to improve the purity of isopropyl acetate through reactive distillation, previously reported to have a limit of 58% purity for a single RD unit with multiple feeds [34].

5.4. Case study: Isopropyl Acetate production

5.4.1. Thermodynamic data and problem specifications

In this section, the proposed IDEAS framework formulation is applied in the design of an reactive distillation network for the production of isopropyl acetate (IPAC) from isopropanol (IPOH) and acetic acid (AA) through esterification as shown in Eq.(5.35).

$$IPOH + AA \rightleftarrows IPAc + H_2O \qquad (5.35)$$

Isopropyl acetate is an important organic industrial chemical and fine industrial solvent that are widely used in the production of varnishes, paints, printing inks, synthetic resins, and

adhesives. The interest in applying reactive distillation systems on the metathesis of 2-pentene is reflected in the recent literature [1–3,34–36].

One of the challenges related to this quaternary system is that the IPAc exhibit nonideal phase behavior, has four azeotropes, and one reactive azeotrope. In order to accurately represent the phase equilibriums of the process, the selection of the form of the thermodynamic model and the determination of the parameters are essential. The nonidealities of the liquid phase were modeled using the NRTL equation, Eq.(5.36). The binary interaction parameters for the NRTL equation used to calculate the activity coefficient for each component are shown in Table 5.2.

$$\ln\left(\gamma_i\right)=\frac{\sum_{j=1}^{n}\tau_{ji}x_j g_{ji}}{\sum_{k=1}^{n}x_k g_{ki}}+\sum_{j=1}^{n}\left[\frac{x_j g_{ij}}{\sum_{k=1}^{n}x_k g_{kj}}\left(\tau_{ij}\frac{\sum_{m=1}^{n}\tau_{mj}x_m g_{mj}}{\sum_{k=1}^{n}x_k g_{kj}}\right)\right] \tag{5.36}$$

$$g_{ij}=e^{\left[-\tau_{ij}\alpha_{ij}\right]}\quad;\quad \tau_{ij}=\frac{\left(a_{ij}+b_{ij}T\right)}{RT}$$

Table 5.2. NRTL coefficients for Acetic acid(1), Isopropanol(2), Isopropyl acetate(3), water(4)[19].

	$j=AA(1)$	$j=IPOH(2)$	$j=IPAc(3)$	$j=H_2O(4)$
a_{ij}				
$i=AA(1)$	0.0	-281.4482	141.0082	-219.7238
$i=IPOH(2)$	81.3926	0.0	269.9609	39.8541
$i=IPAc(3)$	154.7885	140.0972	0.0	1165.709
$i=H_2O(4)$	842.6081	1655.255	1270.2036	0.0
α_{ij}				
$i=AA(1)$	0.0	0.3048	0.3014	0.2997
$i=IPOH(2)$	0.3048	0.0	0.3009	0.3255
$i=IPAc(3)$	0.3014	0.3009	0.0	0.33
$i=H_2O(4)$	0.2997	0.3255	0.33	0.0

Note: All the $b_{ij}=0$.

The kinetics of this system is represented by the homogeneous model [34] shown in Eq.(5.37), where k is constant over the temperature range of interest, i.e., $k_f \big/ \left(k_{f,ref}\right) = 1$. The respective reaction equilibrium constant is shown in Eq.(5.38).

$$R = k_f \left(a_{IPOH} a_{AA} - \frac{a_{IPAc}\ a_{H_2O}}{K_{eq}} \right) \tag{5.37}$$

$$K_{eq} = 8.7 \tag{5.38}$$

The saturated pressure of the mixture is calculated by using Antoine's equation, Eq.(5.39), which coefficients can be found in Table 5.3 for T in K and P in Pa.

$$\ln P_k^{sat}\left(i\right) = A_{1,k} + \frac{A_{2,k}}{\left(T\left(i\right) + A_{3,k}\right)} \quad ; \quad \forall k = AA, IPOH,\ IPAc, H_2O \tag{5.39}$$

Table 5.3. Antoine coefficients for Acetic acid(1), Isopropanol(2), Isopropyl acetate(3), water(4)[19].

	$k = AA(1)$	$k = IPOH\left(2\right)$	$k = IPAc\left(3\right)$	$k = H_2O\left(4\right)$
$A_{1,k}$	23.3618	25.3358	21.7798	23.4776
$A_{2,k}$	−4457.83	−4628.96	−3307.73	−3984.92
$A_{3,k}$	−14.699	−20.514	−39.485	−39.724

In order to perform the reactive distillation process, the distribution network of IDEAS is set to have three inlet streams, containing pure acetic acid, isopropanol, and water, respectively. Also, two outlets streams are considered according to the specifications for the final products presented in Table 5.4.

Table 5.4. Specifications for the isopropyl acetate reactive distillation example.

Feed Flow (kmol/h)	200
Outlet Flow 1 (Distillate) (kmol/h)	100
Outlet Flow 2 (Bottom) (kmol/h)	100
Operating pressure (bar)	1
Inlet molar fractions	
Isopropanol (IPOH)	1.0000
Acetic Acid (AA)	1.0000
Water (H_2O)	1.0000
Purity target (lower - upper bounds)	
Outlet Flow 1	
Isopropanol (IPOH)	0.0000 - 1.0000
Acetic Acid (AA)	0.0000 - 1.000
Isopropyl Acetate (IPAc)	0.2500 - 1.0000
Water (H_2O)	0.0000 - 1.0000
Outlet Flow 2	
Isopropanol (IPOH)	0.0000 - 1.0000
Acetic Acid (AA)	0.0000 - 1.000
Isopropyl Acetate (IPAc)	0.0000 - 0.2500
Water (H_2O)	0.0000 - 1.0000

5.4.2. Objective function and discretization procedure

For this reactive separation system, the objective function was selected to push the purity of the isopropyl acetate to the maximum possible, since relatively low values of purity in a single distillation system were reported previously as the maximum possible [34]. Since IDEAS considers all the possible process flowsheets for a given technology, it becomes of interest to either confirm the maximum purity reported or to surpass, if possible, under the conditions reported in this work. The objective function of the IDEAS' finite LP is shown in Eq.(5.40).

$$\max \sum_{i=1}^{G} x_{IPAc}^{L}(i)F^{OL}(1,i) + y_{IPAc}^{L}(i)F^{OV}(1,i)$$
$$\text{s.t.} \qquad (5.40)$$
$$\text{Eq.(5.6), (5.13), (5.14), (5.18), (5.20) and (5.21)}$$
$$\text{All variables} \geq 0$$

The procedure applied in this system uses the IDEAS convergence method presented previously. The LP in Eq.(1.36) is solved several times with an increasingly larger sets G until no further improvement in the isopropyl acetate purity is observed, or until the purity of this component reaches 100%.

This problem was processed in the UCLA Hoffman2 Cluster operated by the Institute of Digital Research and Education (IDRE). The average computational cost found for this problem in terms of memory allocation was 1.724 Megabytes per 1000 variables. Since the Hoffman2 cluster has a maximum limit of 98,304 Megabytes per user, the maximum problem size for the quaternary azeotropic distillation that can be processed through in this server should contain 57 million variables at most. As one could recall from Table 5.1, the quaternary problem would not be processable for the 1/32 discretization (with constant discretization step sizes) when this computational limitation is considered.

As previously observed in other works[13], one strategy to obtain meaningful results in reactive distillation systems while keeping the cardinality of the set G under reasonable values is the use of different discretization step sizes in different regions of the molar liquid composition space. For most distillation systems, the addition of states close to the high purity edges of the composition space can improve the separation problem convergence when compared to the addition of states in regions far from the high purity points. This is physically expected since it is energetically expensive to achieve further separation for systems that already present high values

of purity. Following that, a non-modular discretization is applied in the generation of the set of reactive flash separator units for the IDEAS OP. The quaternary mixture's liquid molar fraction domain was divided into three regions as shown in Fig.5.3. Different discretization levels are allowed in each of the proposed regions, which edges specified by the molar fractions α and β. Note that the usually three-dimensional quaternary domain is represented as a plan in four different ternary mixture spaces.

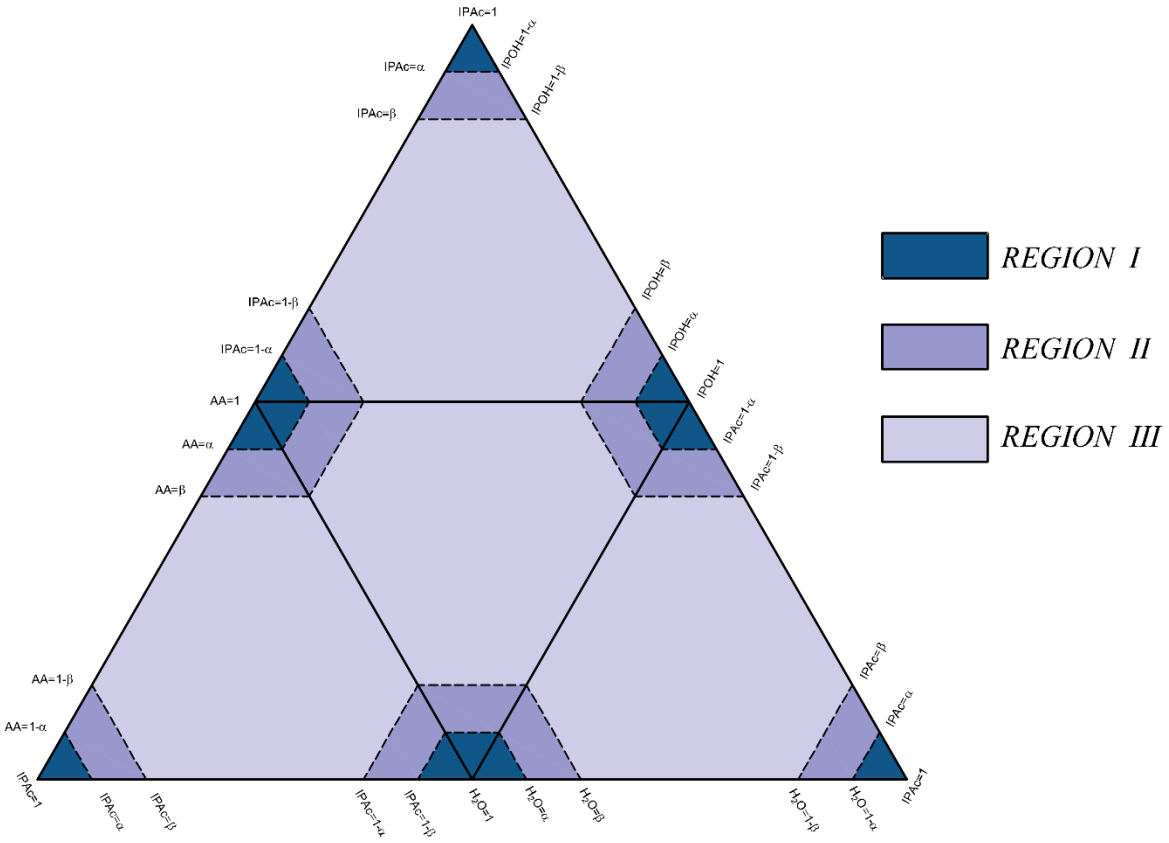

Figure 5.3 - Different discretization regions in the quaternary mixture liquid molar fraction domain for the isopropyl acetate production problem.

5.4.3. IDEAS results

The purity limit of the isopropyl acetate problem through reactive distillation is investigated by solving the optimization problem described in Eq.(5.40). Different values of α

and β have been specified in the determination of the reactive flash separator set used by the IDEAS-OP. These values, as well as discretization step in each region and respective number of reactive flash separators in the set G are presented in Table 5.5.

Table 5.5 – Results for the IDEAS quaternary reactive separation problem for max. IPAc purity.

Set #	α	β	Discretization step size			#Flashes G	# of variables	Max IPAc purity
			Region I	Region II	Region III			
1	0.75	0.5	1/8	1/8	1/8	112	25,892	**0.25**
2	0.75	0.5	1/16	1/8	1/8	234	111,170	**0.25**
3	0.75	0.5	1/8	1/16	1/8	560	631,140	**0.474353**
4	0.75	0.5	1/8	1/8	1/16	533	571,929	**0.582854**
5	0.75	0.5	1/16	1/16	1/8	682	935,042	**0.474353**
6	0.75	0.5	1/16	1/16	1/16	969	1,884,725	**0.635987**
7	0.75	0.5	1/32	1/16	1/16	1,489	4,444,685	**0.8125**
8	0.75	0.5	1/16	1/32	1/16	3,665	26,890,125	**0.8125**
9	0.75	0.5	1/16	1/16	1/32	3,329	22,187,805	**0.6875**
10	0.75	0.5	1/32	1/32	1/16	4,185	35,057,765	**0.84375**
11	0.75	0.5	1/32	1/16	1/32	3,849	29,656,565	**0.84375**
12	0.75	0.5	1/32	1/32	1/32	6,545	85,719,885	**0.84375**
13	0.75	0.5	1/50	1/16	1/16	2,709	14,052,965	**0.9**
14	0.75	0.5	1/50	1/32	1/16	5,345	57,175,485	**0.9**
15	0.75	0.5	1/64	1/16	1/16	4,705	44,307,005	**0.921875**
16	0.96875	0.75	1/128	1/32	1/16	1,613	5,214,849	**0.84375**
17	0.96875	0.75	1/128	1/64	1/16	4,805	46,209,705	**0.921875**
18	0.96875	0.5	1/128	1/32	1/16	4,309	37,165,145	**0.84375**
19	0.9	0.75	1/100	1/50	1/16	3,434	23,608,770	**0.94**

The column generation procedure was used to solve the runs highlighted in blue in table above. Although the memory limit given by the computational cluster would support some of those runs to be solved directly (without the use of column generation), in practice the scheduling procedure used by the cluster administration adds queue waiting time to the total processing time for users submitting memory intensive processing jobs. Thus, column generation was used in any version of the problem containing more than 30 million variables.

From the results, one may observe that the convergence to the infimum of the IDEAS ILP optimal is not a function of the cardinality G only, but also depends on the location in the composition space where the increase in the number of units happens. Thus, different IDEAS convergence plots can be drawn according to the use of a finer discretization in each specific region for the same value of α and β. When the set are organized according to the use of smaller discretization steps in each region, the IDEAS convergence plot shown in Fig.5.4 captures how the convergence evolves with the growth of the total number of flashes in each region. It is interesting to observe that increases in region III can lead to faster convergence for low purities of IPAc.

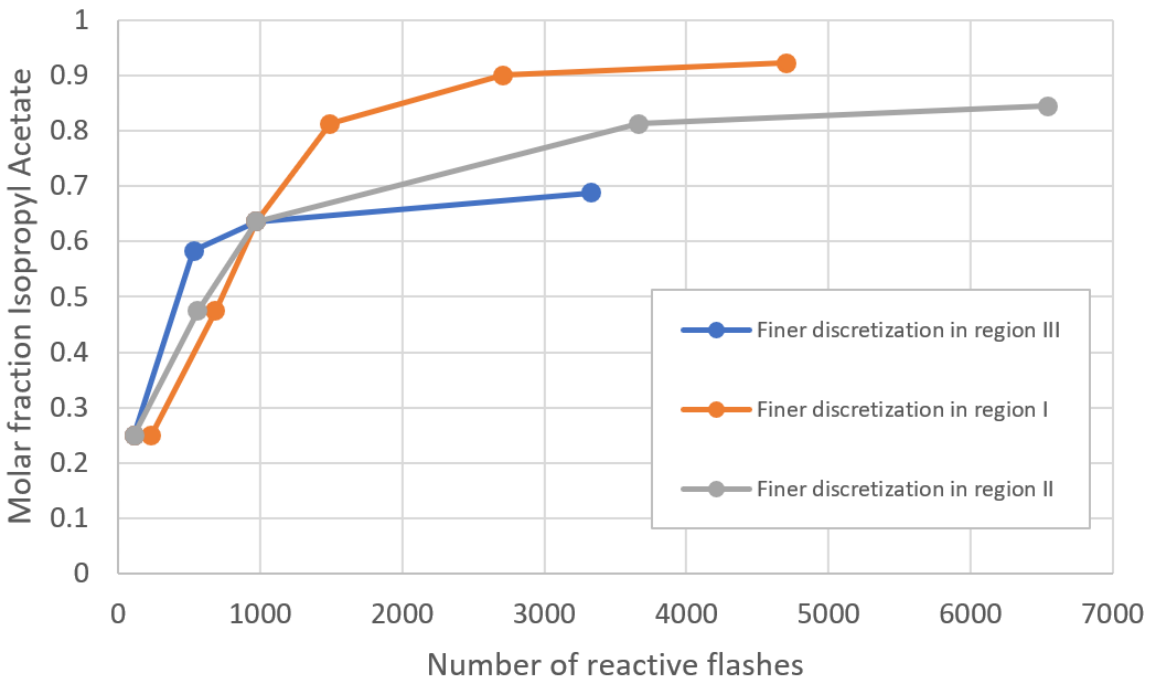

Figure 5.4 - IDEAS convergence evolution for the maximum IPAc at output 1 according to changes in the discretization of regions I, II, and III.

Another interesting feature observed in Table 5.5 is that it shows a dependence on the value of α in order to obtain high purity. A comparison between sets 15 and 17, for instance, shows that a finer discretization in region I did not affect the purity of the product. Although they have different values of α and β, sets 15 and 17 are exactly the same for molar fraction below 0.96875, and set 17 shows a finer discretization in the composition space above that value, between 0.96875 and 1. This discretization increase in the high purity was ineffective mainly because the best output purity composition from set 15 is out of reach for the newly included reactive flashes in region I of set 17.

Considering the above, an improved version of set 13 (which has reached 90% purity) is presented in set 19. Discretization is set to become finer for isopropyl acetate molar fractions

above 0.9 in this set, which means that set 13 can take advantage from the newly added reactive separation states from the point it found the maximum. This procedure resulted in an increased purity of 94%, given to this run the maximum purity for isopropyl acetate obtained in this work. The combination of this procedure with the behavior of the convergence curve seen previously indicates that is possible to develop a heuristic model for the column generation procedure that considers the location of the purity position in the composition space and generates a finer discretization around that point, so that one could obtain faster convergence.

The maximum purity obtained by IDEAS is higher than the value of 58% for a similar system[34], reported as the maximum attainable purity for the RD system under the conditions presented. The between those values is shown in Fig.5.5.

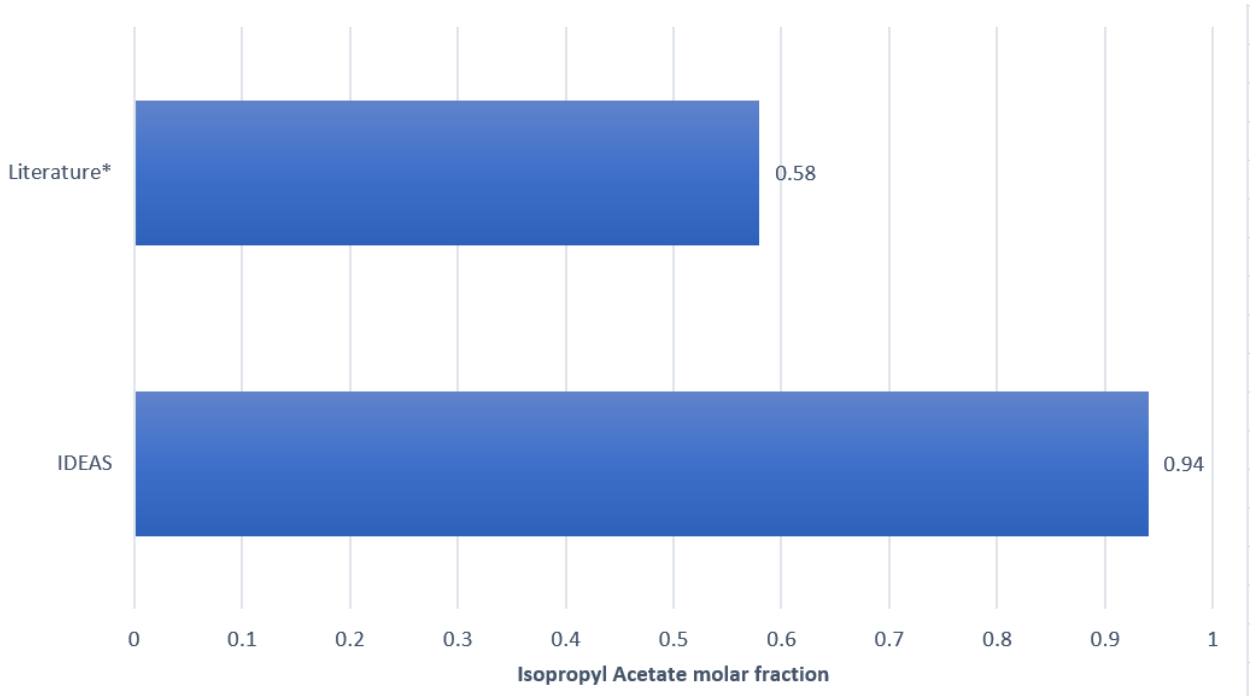

* Chadda, N.; Malone, M. F.; Doherty, M. F. Feasibility and Synthesis of Hybrid Reactive Distillation Systems. AIChE J. 2002, 48 (12), 2754–2768.

Figure 5.5 - Maximum isopropyl acetate purity for a reactive distillation column and through the use of the IDEAS framework

5.5. Conclusions

The Infinite DimEnsionAl State-Space (IDEAS) conceptual framework was applied to the synthesis of reactive distillation networks featuring quaternary azeotropic mixtures. The network is comprised of vapor-liquid equilibrium reactive flashes, with liquid holdup that is free to change in each flash individually. A model for the study of reactive separation systems is developed and applied in through the IDEAS approach. Kinetically and/or equilibrium limited reactions are assumed to occur in the liquid phase. A column generation procedure where the main LP problem is decomposed and solved iteratively was introduced and implemented in this work. This procedure overcomes memory limitations by reducing the number of variables included in the problem during the solution procedure. The method is demonstrated on a case study involving the isobaric reactive distillation of an acetic acid/isopropanol/isopropyl acetate/water azeotropic mixture. The objective function of IDEAS for this reactive separation system was selected to push the purity of the isopropyl acetate to the maximum possible. A nonmodular discretization strategy was used in this problem, enabling different proportions of reactive flash separators in the liquid molar fraction composition space. Results for this problem show that the rate of approximation to the IDEAS infimum is dependent not only on the number of units in the IDEAS-OP, but also on the location of the newly added units. This result indicates that is possible to develop a heuristic model for the column generation procedure that considers the location of the purity position in the composition space and generates a finer discretization around that point, so that one could obtain faster convergence. The IDEAS-CG results shows feasible design solutions for of isopropyl acetate with purity of 94% through reactive distillation,

compared with 58% previously reported as the limiting attainable for this system through a reactive distillation column.

5.6. Notation

Thermodynamic Variables*:*

P	Reactive flash separator pressure (Pa)
T	Reactive flash separator temperature (K)
$y_k^V(i)$	k^{th} Species equilibrium vapor composition leaving the i^{th} unit $(\dim)$
$x_k^L(i)$	k^{th} Species equilibrium liquid composition leaving the i^{th} unit $(\dim)$
$P_k^{sat}(T)$	k^{th} Species temperature dependent saturated vapor pressure (Pa)
$\phi_k\left(\left\{y_l^V\right\}_{l=1}^n, T, P\right)$	k^{th} Species non-ideal fugacity coefficient
$\gamma_k\left(\left\{x_l^L\right\}_{l=1}^n, T\right)$	k^{th} Species non-ideal liquid activity coefficient
a_k	Activity of the k^{th} species $(\dim)$
$A_{j,k}$	Antoine equation j^{th} parameter of the k^{th} species $(\dim)$
K_{eq}	Reaction equilibrium constant $(\dim)$

k_f	Forward reaction rate constant $(1/\text{h})$

IDEAS Variables*:*

$F^I(i)$	i^{th} DN inlet stream
$F^O(i)$	i^{th} DN outlet stream
$F^L(i)$	i^{th} OP liquid outlet
$F^V(i)$	i^{th} OP vapor outlet
$F^{OI}(i,j)$	j^{th} DN inlet stream to i^{th} DN outlet
$F^{PI}(i,j)$	i^{th} OP inlet stream from j^{th} DN network inlet
$F^{OL}(i,j)$	i^{th} DN outlet stream from j^{th} OP liquid outlet
$F^{OV}(i,j)$	i^{th} DN outlet stream from j^{th} OP vapor outlet
$F^{PL}(i,j)$	i^{th} OP inlet stream from j^{th} OP liquid outlet
$F^{PV}(i,j)$	i^{th} OP inlet stream from j^{th} OP vapor outlet
$H(i)$	Reactive holdup of the i^{th} reactive flash separator unit in the OP

$z_k^I(i)$	k^{th} species, i^{th} DN inlet stream composition
$z_k^O(i)$	k^{th} species, i^{th} DN outlet stream composition
$\left(z_k^O(i)\right)^l$	k^{th} species, i^{th} DN outlet stream composition vector, lower bound
$\left(z_k^O(i)\right)^u$	k^{th} species, i^{th} DN outlet stream composition vector, upper bound
$x_k^L(i)$	k^{th} species, i^{th} OP liquid outlet composition
$y_k^V(i)$	k^{th} species, i^{th} OP vapor outlet composition
G	Total number of reactive flashes in the OP
M	Number of IDEAS network inlets
N	Number of IDEAS network outlets

5.7. References

(1) Zhang, B. J.; Yang, W. S.; Hu, S.; Liang, Y. Z.; Chen, Q. L. A Reactive Distillation Process with a Sidedraw Stream to Enhance the Production of Isopropyl Acetate. *Chem. Eng. Process. Process Intensif.* **2013**, *70*, 117–130. https://doi.org/10.1016/j.cep.2013.04.011.

(2) Song, W.; Huss, R. S.; Doherty, M. F.; Malone, M. F. Discovery of a Reactive Azeotrope. *Nature* **1997**, *388* (6642), 561–563. https://doi.org/10.1038/41515.

(3) Lee, H.-Y.; Lai, I.-K.; Huang, H.-P.; Chien, I.-L. Design and Control of Thermally Coupled Reactive Distillation for the Production of Isopropyl Acetate. *Ind. Eng. Chem. Res.* **2012**, *51* (36), 11753–11763. https://doi.org/10.1021/ie300647h.

(4) Tang, Y.-T.; Chen, Y.-W.; Huang, H.-P.; Yu, C.-C.; Hung, S.-B.; Lee, M.-J. Design of Reactive Distillations for Acetic Acid Esterification. *AIChE J.* **2005**, *51* (6), 1683–1699. https://doi.org/10.1002/aic.10519.

(5) Demiriz, A.; Bennett, K. P.; Shawe-Taylor, J. Linear Programming Boosting via Column Generation. *Mach. Learn.* **2002**, *46* (1), 225–254. https://doi.org/10.1023/A:1012470815092.

(6) Gamache, M.; Soumis, F.; Marquis, G.; Desrosiers, J. A Column Generation Approach for Large-Scale Aircrew Rostering Problems. *Oper. Res.* **1999**, *47* (2), 247–263. https://doi.org/10.1287/opre.47.2.247.

(7) Vance, P. H.; Barnhart, C.; Johnson, E. L.; Nemhauser, G. L. Solving Binary Cutting Stock Problems by Column Generation and Branch-and-Bound. *Comput. Optim. Appl.* **1994**, *3* (2), 111–130. https://doi.org/10.1007/BF01300970.

(8) Gilbert, M.; Tyas, A. Layout Optimization of Large-scale Pin-jointed Frames. *Eng. Comput.* **2003**, *20* (8), 1044–1064. https://doi.org/10.1108/02644400310503017.

(9) Dantzig, G. B.; Wolfe, P. Decomposition Principle for Linear Programs. *Oper. Res.* **1960**, *8* (1), 101–111. https://doi.org/10.1287/opre.8.1.101.

(10) Dantzig, G. B.; Wolfe, P. The Decomposition Algorithm for Linear Programs. *Econometrica* **1961**, *29* (4), 767–778. https://doi.org/10.2307/1911818.

(11) Geoffrion, A. M. Generalized Benders Decomposition. *J. Optim. Theory Appl.* **1972**, *10* (4), 237–260. https://doi.org/10.1007/BF00934810.

(12) Benders, J. F. Partitioning Procedures for Solving Mixed-Variables Programming Problems. *Comput. Manag. Sci.* **2005**, *2* (1), 3–19. https://doi.org/10.1007/s10287-004-0020-y.

(13) da Cruz, F. E.; Manousiouthakis, V. I. Process Intensification of Reactive Separator Networks through the IDEAS Conceptual Framework. *Comput. Chem. Eng.* **2017**, *105*, 39–55. https://doi.org/10.1016/j.compchemeng.2016.12.006.

(14) Burri, J. F.; Manousiouthakis, V. I. Global Optimization of Reactive Distillation Networks Using IDEAS. *Comput. Chem. Eng.* **2004**, *28* (12), 2509–2521. https://doi.org/10.1016/j.compchemeng.2004.06.014.

(15) Ghougassian, P. G.; Manousiouthakis, V. Globally Optimal Networks for Multipressure Distillation of Homogeneous Azeotropic Mixtures. *Ind. Eng. Chem. Res.* **2012**, *51* (34), 11183–11200. https://doi.org/10.1021/ie300423q.

(16) Barbosa, D.; Doherty, M. F. The Simple Distillation of Homogeneous Reactive Mixtures. *Chem. Eng. Sci.* **1988**, *43* (3), 541–550. https://doi.org/10.1016/0009-2509(88)87015-5.

(17) Venimadhavan, G.; Buzad, G.; Doherty, M. F.; Malone, M. F. Effect of Kinetics on Residue Curve Maps for Reactive Distillation. *AIChE J.* **1994**, *40* (11), 1814–1824. https://doi.org/10.1002/aic.690401106.

(18) Siirola, J. J. Industrial Applications of Chemical Process Synthesis. In *Advances in Chemical Engineering*; Anderson, J. L., Ed.; Academic Press, 1996; Vol. 23, pp 1–62.

(19) Okasinski, M. J.; Doherty, M. F. Design Method for Kinetically Controlled, Staged Reactive Distillation Columns. *Ind. Eng. Chem. Res.* **1998**, *37* (7), 2821–2834. https://doi.org/10.1021/ie9708788.

(20) Malone, M. F.; Doherty, M. F. Reactive Distillation. *Ind. Eng. Chem. Res.* **2000**, *39* (11), 3953–3957. https://doi.org/10.1021/ie000633m.

(21) Chen, F.; Huss, R. S.; Malone, M. F.; Doherty, M. F. Simulation of Kinetic Effects in Reactive Distillation. *Comput. Chem. Eng.* **2000**, *24* (11), 2457–2472. https://doi.org/10.1016/S0098-1354(00)00609-8.

(22) Barnicki, S. D.; Hoyme, C. A.; Siirola, J. J. Separations Process Synthesis. In *Kirk-Othmer Encyclopedia of Chemical Technology*; John Wiley & Sons, Inc., 2000.

(23) Jiménez, L.; Wanhschafft, O. M.; Julka, V. Analysis of Residue Curve Maps of Reactive and Extractive Distillation Units. *Comput. Chem. Eng.* **2001**, *25* (4–6), 635–642. https://doi.org/10.1016/S0098-1354(01)00644-5.

(24) Huss, R. S.; Chen, F.; Malone, M. F.; Doherty, M. F. Reactive Distillation for Methyl Acetate Production. *Comput. Chem. Eng.* **2003**, *27* (12), 1855–1866. https://doi.org/10.1016/S0098-1354(03)00156-X.

(25) Li, H.; Meng, Y.; Li, X.; Gao, X. A Fixed Point Methodology for the Design of Reactive Distillation Columns. *Chem. Eng. Res. Des.* **2016**, *111*, 479–491. https://doi.org/10.1016/j.cherd.2016.05.015.

(26) Ciric, A. R.; Gu, D. Synthesis of Nonequilibrium Reactive Distillation Processes by MINLP Optimization. *AIChE J.* **1994**, *40* (9), 1479–1487. https://doi.org/10.1002/aic.690400907.

(27) Papalexandri, K. P.; Pistikopoulos, E. N. Generalized Modular Representation Framework for Process Synthesis. *AIChE J.* **1996**, *42* (4), 1010–1032. https://doi.org/10.1002/aic.690420413.

(28) Jackson, J. R.; Grossmann, I. E. A Disjunctive Programming Approach for the Optimal Design of Reactive Distillation Columns. *Comput. Chem. Eng.* **2001**, *25* (11–12), 1661–1673. https://doi.org/10.1016/S0098-1354(01)00730-X.

(29) Georgiadis, M. C.; Schenk, M.; Pistikopoulos, E. N.; Gani, R. The Interactions of Design Control and Operability in Reactive Distillation Systems. *Comput. Chem. Eng.* **2002**, *26* (4–5), 735–746. https://doi.org/10.1016/S0098-1354(01)00774-8.

(30) Cardoso, M. F.; Salcedo, R. L.; de Azevedo, S. F.; Barbosa, D. Optimization of Reactive Distillation Processes with Simulated Annealing. *Chem. Eng. Sci.* **2000**, *55* (21), 5059–5078. https://doi.org/10.1016/S0009-2509(00)00119-6.

(31) Hoffmaster, W. R.; Hauan, S. Using Feasible Regions to Design and Optimize Reactive Distillation Columns with Ideal VLE. *AIChE J.* **2006**, *52* (5), 1744–1753. https://doi.org/10.1002/aic.10765.

(32) Avami, A.; Marquardt, W.; Saboohi, Y.; Kraemer, K. Shortcut Design of Reactive Distillation Columns. *Chem. Eng. Sci.* **2012**, *71*, 166–177. https://doi.org/10.1016/j.ces.2011.12.021.

(33) Urselmann, M.; Engell, S. Design of Memetic Algorithms for the Efficient Optimization of Chemical Process Synthesis Problems with Structural Restrictions. *Comput. Chem. Eng.* **2015**, *72*, 87–108. https://doi.org/10.1016/j.compchemeng.2014.08.006.

(34) Chadda, N.; Malone, M. F.; Doherty, M. F. Feasibility and Synthesis of Hybrid Reactive Distillation Systems. *AIChE J.* **2002**, *48* (12), 2754–2768. https://doi.org/10.1002/aic.690481206.

(35) Qi, W.; Malone, M. F. Semibatch Reactive Distillation for Isopropyl Acetate Synthesis. *Ind. Eng. Chem. Res.* **2011**, *50* (3), 1272–1277. https://doi.org/10.1021/ie100354x.

(36) Venimadhavan, G.; Malone, M. F.; Doherty, M. F. Bifurcation study of kinetic effects in reactive distillation. *AIChE J.* **1999**, *45* (3), 546–556. https://doi.org/10.1002/aic.690450311.